Universidad Miguel Hernández de Elche

Los genes *DESIGUAL* modulan la simetría bilateral en las hojas de Arabidopsis

David Wilson Sánchez

Elche, 2016

Los genes *DESIGUAL* modulan la simetría bilateral en las hojas de Arabidopsis

Trabajo realizado por el Licenciado David Wilson Sánchez, en la Unidad de Genética del Instituto de Bioingeniería de la Universidad Miguel Hernández de Elche, para optar al grado de Doctor.

Elche, 19 de abril de 2016

JOSÉ LUIS MICOL MOLINA, Catedrático de Genética de la Universidad Miguel Hernández de Elche, y

SARA JOVER GIL, Profesora Asociada de Genética de la Universidad Miguel Hernández de Elche,

HACEMOS CONSTAR:

Que el presente trabajo ha sido realizado bajo nuestra dirección y recoge fielmente la labor desarrollada por el Licenciado David Wilson Sánchez para optar al grado de Doctor. Las investigaciones reflejadas en esta Tesis se han desarrollado íntegramente en la Unidad de Genética del Instituto de Bioingeniería de la Universidad Miguel Hernández de Elche.

José Luis Micol Molina Sara Jover Gil

Elche, 19 de abril de 2016

Instituto de Bioingeniería
Universidad Miguel Hernández

Avenida de la Universidad s/n
03202 ELCHE (Alicante)
Telf: 96 591 8817 - Fax: 96 522 2033
e-mail: bioingenieria@umh.es

A quien corresponda:

Eugenio Vilanova Gisbert, Catedrático de Toxicología y Director del Instituto de Bioingeniería,

HACE CONSTAR:

Que da su conformidad a la lectura de la Tesis Doctoral presentada por Don **David Wilson Sánchez**, titulada **"Los genes *DESIGUAL* modulan la simetría bilateral en las hojas de Arabidopsis"**, que se ha desarrollado dentro del Programa de Doctorado en Bioingeniería de este Instituto, bajo la dirección de los profesores Dr. José Luis Micol Molina y Dra. Sara Jover Gil.

Lo que firmo en Elche, a instancias del interesado y a los efectos oportunos, a diecinueve de abril de dos mil dieciséis.

Eugenio Vilanova Gisbert
Catedrático de Toxicología
Director del Instituto de Bioingeniería

A mi familia y amigos

ÍNDICE DE MATERIAS

ÍNDICE DE FIGURAS

I.- PREFACIO

I.- PREFACIO

Este documento se ha elaborado siguiendo la normativa de la Universidad Miguel Hernández de Elche para la "Presentación de Tesis Doctorales con un conjunto de publicaciones", y se ha dividido en las partes siguientes:

1.- Un apartado de *Resumen y Conclusiones*.

2.- Una *Introducción*, en la que se presenta el tema de la Tesis y los antecedentes y objetivos del trabajo realizado.

3.- Una *Bibliografía de la Introducción*.

4.- Un apartado de *Publicaciones,* que contiene las tres siguientes (se indica en su caso el factor de impacto [FI] de 2014).

Muñoz-Nortes, T., Wilson-Sánchez, D., Candela, H., y Micol, J.L. (2014). Symmetry, asymmetry and the cell cycle in plants: known knowns and some known unknowns. *Journal of Experimental Botany* **65**, 2645-2655. (FI: 5,526).

Wilson-Sánchez, D., Rubio-Díaz, S., Muñoz-Viana, R., Pérez-Pérez, J.M., Jover-Gil, S., Ponce, M.R., y Micol, J.L. (2014). Leaf phenomics: a systematic reverse genetic screen for Arabidopsis leaf mutants. *Plant Journal* **79**, 878-891. (FI: 5,972).

Wilson-Sánchez, D., Martínez-López, S., Jover-Gil, S., y Micol, J.L. Role of *DESIGUAL1* and auxin in bilateral symmetry of Arabidopsis leaves. Pendiente de aceptación.

5.- Un anexo que incorpora 18 comunicaciones a congresos: 9 nacionales y 9 internacionales.

La introducción de esta Tesis no incluye un apartado de Materiales y Métodos, que están descritos en las publicaciones. Este documento incorpora varias bibliografías: las de cada uno de los tres artículos y la de la introducción. Todas las citas que se intercalan en la introducción de esta memoria se corresponden con referencias que aparecen en la bibliografía del mismo apartado; algunas de dichas citas se repiten en las bibliografías de uno o varios de los artículos.

Durante mi periodo como doctorando también he publicado un artículo que no se incluye en esta Tesis:

Szakonyi, D., Van Landeghem, S., Bärenfaller, K., Baeyens, L., Blomme, J., Casanova-Sáez, R., De Bodt, S., Esteve-Bruna, D., Fiorani, F., Gonzalez, N., Grønlund, J., Immink, R.G.H., Jover-Gil, S., Kuwabara, A., Muñoz-Nortes, T., Van Dijk, A.-J., Wilson-Sánchez, D., Buchanan-Wollaston, V., Angenent, G.C., Van de Peer, Y., Inzé, D., Micol, J.L., Gruissem, W., Walsh, S., y Hilson, P. (2015). The KnownLeaf literature curation system captures knowledge about *Arabidopsis* leaf growth and development and facilitates integrated data mining. *Current Plant Biology* **2**, 1-11.

II.- RESUMEN Y CONCLUSIONES

II.- RESUMEN Y CONCLUSIONES

La hoja es el órgano más visible y fácilmente manipulable de la planta modelo *Arabidopsis thaliana* (en adelante, Arabidopsis). La inducción y caracterización de mutaciones que alteran su morfología permite identificar genes específicamente implicados en su organogénesis. Los mutantes foliares también sirven para esclarecer los mecanismos de proliferación, organización espacial y diferenciación que las células de la hoja comparten con las de otros órganos de las plantas.

Aunque se han descrito centenares de mutantes de Arabidopsis que manifiestan alteraciones en la morfología de la hoja, se acepta generalmente que no se dispone de alelos de todos los genes implicados en el desarrollo de este órgano. Con el fin de identificar nuevos genes necesarios para el desarrollo foliar o de la planta en su conjunto, hemos sometido a escrutinio una colección preexistente de dominio público: la de mutantes portadores de inserciones de ADN-T en homocigosis que se obtuvo en el Salk Institute.

Hemos analizado 19.850 líneas Salk, aislando 706 mutantes con fenotipo foliar, que se manifiesta en 98 de ellos con penetrancia incompleta. Hemos mejorado el vocabulario ontológico existente para sistematizar la descripción fenotípica de nuestros mutantes y facilitar su clasificación y la integración de la información obtenida en las bases de datos. Dado que la colección Salk está indexada, hemos intentado confirmar la presencia de las inserciones anotadas en 553 de los mutantes analizados, consiguiéndolo en el 78% de ellos. Hemos llevado a cabo búsquedas en bases de datos, ensayos de alelismo y análisis de cosegregación de las inserciones anotadas y los fenotipos observados. Hemos establecido relaciones causales inequívocas entre el 47% de las inserciones anotadas y los fenotipos mutantes a estudio. También hemos desarrollado un procedimiento sencillo y robusto para la identificación de inserciones de ADN-T no anotadas, basado en el análisis de las lecturas derivadas de la secuenciación masiva del genoma de los mutantes a estudio.

Hemos puesto nuestros resultados a disposición de la comunidad científica implementando para ello una aplicación web (PhenoLeaf; http://genetics.umh.es/phenoleaf) que recoge la información genotípica y fenotípica obtenida en nuestro escrutinio. Hemos donado a los centros de distribución de germoplasma de Arabidopsis semillas de las líneas que hemos estudiado. Como prueba de concepto de la utilidad de PhenoLeaf, hemos identificado y caracterizado parcialmente dos genes representados entre los mutantes que hemos aislado: At1g77600, que parece requerirse para la proliferación celular responsable del crecimiento proximodistal de la hoja, y At3g62870, que codifica una proteína del ribosoma citoplásmico necesaria para la proliferación celular y la función del cloroplasto.

La simetría bilateral es una propiedad estructural compartida por muchos seres vivos, y uno de los rasgos más visibles de las hojas de muchas plantas. Es sorprendente que sus alteraciones hayan brillado por su ausencia entre los mutantes Salk: solo hemos encontrado uno con hojas asimétricas, al que hemos llamado *desigual1-1* (*deal1-1*). Hemos identificado en otras colecciones públicas otros dos alelos de insuficiencia de función del gen *DEAL1* (*deal1-2* y *deal1-3*) y uno de cada uno de sus parálogos más cercanos, *DEAL2* (*deal2-1*) y *DEAL3* (*deal3-1*). El fenotipo foliar de los mutantes *deal1* se manifiesta con penetrancia incompleta; su severidad es mayor en las hojas adultas que en las juveniles, y en la región basal del limbo que en la apical. La asimetría foliar de estos mutantes se ve respectivamente incrementada o reducida mediante tratamiento con un inhibidor del transporte polar de auxina, el ácido 1-N-naftilftalámico, o una auxina sintética, el ácido naftalenacético; también es más severa en los triples mutantes *deal1 deal2 deal3*.

El margen de las hojas vegetativas de la estirpe silvestre Col-0 de Arabidopsis es dentado, alternándose lóbulos e indentaciones dispuestos simétricamente a ambos lados de la vena primaria. Este patrón se altera en los mutantes *deal1*, que muestran regiones lobadas de posición aleatoria, que contienen senos y lóbulos ectópicos. Estas aberraciones morfológicas son visibles muy poco después de que los primordios foliares se manifiesten, y se deben a excesos y defectos de la proliferación celular. Concuerda con esta observación el comportamiento de la fusión transcripcional $DEAL1_{pro}$*:GUS*, que se expresa intensamente en la fase de proliferación celular del desarrollo foliar.

Autores anteriores han propuesto que la forma del margen foliar de Arabidopsis se debe fundamentalmente a la existencia de dominios alternos en los que se concentran de manera excluyente CUP-SHAPED COTYLEDON2 (CUC2, un regulador transcripcional) o la auxina; esto último depende a su vez de la polarización de PIN-FORMED1 (PIN1, el transportador de eflujo de auxina) en uno de los lados de las células que se coordinan para conseguir una canalización de la hormona y generar así máximos de concentración en puntos concretos del margen. Hemos demostrado que *DEAL1* interacciona genéticamente con *PIN1* y que las mutaciones *deal1* alteran espacial y cuantitativamente la expresión de *CUC2*. La asimetría de los mutantes *deal1* parece deberse a una incorrecta distribución de los máximos de auxina en el margen foliar. Hemos obtenido una fusión traduccional $35S_{pro}$*:DEAL1:CFP* y realizado un ensayo de doble híbrido de la levadura para proteínas de membrana por el método de la ubiquitina dividida, concluyendo que DEAL1 es una proteína de la membrana del retículo endoplásmico cuyos extremos amino y carboxilo están orientados hacia el citoplasma. Nuestros resultados sugieren que los genes *DEAL* participan en el control de la proliferación celular durante el desarrollo foliar.

III.- INTRODUCCIÓN

III.- INTRODUCCIÓN

III.1.- Consideraciones sobre la Biología del Desarrollo

III.1.1.- El análisis causal del desarrollo

La Biología del Desarrollo estudia las transformaciones sucesivas que sufre el cigoto —una entidad unicelular— hasta convertirse en un organismo pluricelular adulto, que incluye órganos y tejidos especializados (Gilbert, 2003). En el siglo XIX, la Biología del Desarrollo se fundamentó casi exclusivamente en la Embriología y la Anatomía Comparada, cuyos abordajes no explicaron satisfactoriamente los mecanismos que gobiernan la ontogenia.

La Genética del Desarrollo nace a principios del siglo XX como resultado de la confluencia entre la Embriología Experimental y la Genética y se basa en el postulado de que los genes son responsables de la morfología de los seres vivos y de su diversidad (García-Bellido, 1986; Campos-Ortega, 1994; Slack, 2012). Durante décadas, sus principales herramientas han sido los mutantes morfológicos, cuya inducción, aislamiento y caracterización permiten inferir la función de los genes mutados merced al análisis de los fenotipos causados por la ausencia, la insuficiencia o la presencia ectópica de sus productos génicos (Wilkins, 1993; St Johnston, 2002).

El análisis genético y molecular de la mosca *Drosophila melanogaster* (Celniker y Rubin, 2003), el nematodo *Caenorhabditis elegans* (Lee *et al.*, 2004) y el teleósteo *Brachydanio rerio* (el pez cebra; Grunwald y Eisen, 2002) ha hecho formidables contribuciones a la comprensión del desarrollo animal. Se han identificado en estos sistemas modelo muchos genes implicados en el control del desarrollo, concluyéndose que su número es relativamente bajo, que interaccionan entre sí de forma jerárquica y que la mayoría de sus productos son factores de transcripción o componentes de rutas de transducción de señales (Davidson, 1994; Li y Davidson, 2009). Una disciplina relativamente nueva, la Biología de Sistemas, intenta integrar mediante modelos matemáticos la gran cantidad de información acumulada acerca del desarrollo, a fin de comprenderlo (Kholodenko y Herbert, 2005; Kalve *et al.*, 2014).

III.1.2.- Particularidades del desarrollo vegetal

El estudio del desarrollo de las plantas es valioso tanto por su contribución al conocimiento de los procesos que son específicos del reino vegetal y lo distinguen del animal, como por sus eventuales aplicaciones prácticas a la mejora de las especies cultivadas (Meyerowitz y Pruitt, 1985; Meyerowitz, 2002; Somerville y Koornneef, 2002;

Walbot y Evans, 2003). Las células animales y vegetales han evolucionado a partir del mismo conjunto inicial de genes, presente en su último ancestro común, un eucariota unicelular. Sin embargo, los análisis comparativos de los genomas y de los mecanismos de desarrollo indican que las plantas y los animales evolucionaron independientemente durante más de 1.500 millones de años (Hedges *et al.*, 2004). Aunque la lógica subyacente a muchos procesos de desarrollo es similar en estos dos reinos, la gran mayoría de las moléculas protagonistas no están relacionadas, ello a pesar de que algunos factores de transcripción animales y vegetales son reorganizaciones distintas de los mismos dominios ancestrales. Las plantas, por tanto, constituyen un elemento imprescindible en cualquier análisis comparativo del desarrollo de los seres vivos (Meyerowitz, 2002).

Las diferencias entre el desarrollo de las plantas y los animales son consecuencia de sus distintos modos de vida. Conviene tener en cuenta a este respecto que las plantas son sésiles y dependen de la captación de la luz solar y la incorporación de los nutrientes del medio. De ahí que su plan corporal sea necesariamente distinto y más simple que el de los animales (Alberts *et al.*, 1994). Las plantas cuentan con unos 40 histotipos, mientras que en los animales superiores se distinguen más de 100 (Lyndon, 1990; Holwell, 1998). Para adaptarse sin moverse a los cambios en la disponibilidad de luz y determinadas sustancias, las plantas han optado por un modelo de desarrollo fundamentalmente postembrionario, a diferencia de los animales, cuya embriogénesis termina con la generación de un embrión que manifiesta el plan corporal final. En las plantas, el desarrollo postembrionario ocurre a partir de dos poblaciones de células indiferenciadas de proliferación rápida: el meristemo apical del tallo, que da lugar al tallo, las hojas y la inflorescencia, y el de la raíz, que genera el sistema radicular (Sachs, 1991; Holwell, 1998). Al ser postembrionario, el desarrollo vegetal está muy influido por el ambiente, ya que se supedita a la adaptación de las plantas a su entorno (Twyman, 2001). Muchas células vegetales son totipotentes (Gilbert, 2003), por lo que en el desarrollo vegetal no hay decisiones irreversibles: se puede modificar el destino de cualquier célula, excepto el de aquellas en las que el núcleo se pierde o degrada. Los mecanismos de adaptación de las plantas y la modularidad de su arquitectura corporal propician el estudio de mutaciones con efectos severos sobre el desarrollo que resultarían letales en un animal (Townsley y Sinha, 2012).

La proliferación, la expansión y la migración celular son las principales fuerzas motrices del desarrollo animal. El de las plantas está condicionado por la presencia de la pared celular, que impide cualquier migración. En consecuencia, contribuyen exclusivamente a la forma de los órganos vegetales el ritmo y los planos de la división

celular, además del tamaño final de las células, que a su vez depende del volumen de la vacuola (Twyman, 2001).

III.1.3.- Arabidopsis como sistema modelo del desarrollo de las plantas

Se denomina sistema modelo a cualquier organismo experimental en cuyo estudio se haya concentrado un colectivo amplio de grupos de investigación, con el fin de obtener conclusiones que puedan ser aplicables a otras especies (Bolker, 1995). La adopción de *Arabidopsis thaliana* (en adelante, Arabidopsis) como sistema modelo para el estudio del desarrollo se debió a su pequeño tamaño, a su ciclo de vida corto y numerosa descendencia, y a su mantenimiento simple y económico en el laboratorio (Meyerowitz, 1987; Somerville y Koornneef, 2002). Posteriormente se comprobó que presenta otras características útiles para su manipulación genética, como su fácil transformación por infección con la bacteria *Agrobacterium tumefaciens* (Koornneef y Meinke, 2010) o un genoma más pequeño y con menos ADN repetitivo que los de otras plantas. Se han generado muchos recursos y herramientas, como la secuencia de los genomas de centenares de accesos (Weigel y Mott, 2009), que facilitan el estudio de la biología de Arabidopsis.

Las singulares características de Arabidopsis han facilitado la disección de numerosos procesos de su desarrollo, cuyas conclusiones han iluminado la ontogenia vegetal. Por ejemplo, su raíz tiene un desarrollo y una organización celular muy reproducibles, que han permitido comprender cómo se forman las de otras especies (Scheres y Wolkenfelt, 1998). Arabidopsis también ha servido para establecer el papel de ciertos genes homeóticos en la especificación de los órganos florales de las plantas (Coen y Meyerowitz, 1991). La estructura de las hojas de Arabidopsis es simple, resultando especialmente apropiadas para el estudio de muchos aspectos de su desarrollo (Beemster *et al.*, 2006), como el establecimiento de la dorsoventralidad de sus tejidos (Eshed *et al.*, 2004; Ha *et al.*, 2007) o la morfogénesis del margen del limbo (Bilsborough *et al.*, 2011). *Cardamine hirsuta* es una especie modelo emergente para el estudio de la disyuntiva entre hojas simples y compuestas; su íntimo parentesco con Arabidopsis posibilita análisis comparativos genéticos y fenotípicos entre las dos especies (Hay *et al.*, 2014).

III.2.- Los mutantes como herramientas genéticas

III.2.1.- Anotación funcional del genoma de Arabidopsis

Arabidopsis posee una dotación haploide de 5 cromosomas nucleares (Laibach, 1943), que totalizan 119 Mb de ADN (The Arabidopsis Genome Initiative, 2000). La

secuenciación de este genoma ha permitido la anotación de casi todos sus genes. Según la base de datos TAIR (The Arabidopsis Information Resource; http://www.arabidopsis.org/portals/genAnnotation/gene_structural_annotation/annotation_data.jsp), el genoma de Arabidopsis contiene 27.411 genes que codifican proteínas, 4.827 pseudogenes y transposones, y 1.359 genes de ARN no codificante. En noviembre de 2010 se disponía de información acerca del proceso biológico en el que participa el 56% de los genes de Arabidopsis (http://www.arabidopsis.org/portals/genAnnotation/genome_snapshot.jsp). No pocas de estas anotaciones carecen de base experimental en Arabidopsis, ya que son predicciones basadas en la homología con genes de otras especies. Lloyd y Meinke (2012) elaboraron una lista de 2.400 genes de Arabidopsis cuya función ha sido estudiada experimentalmente gracias a sus alelos mutantes.

III.2.2.- Disección mutacional de la función de los genes

La forma más habitual y directa para comprender la función de un gen es su mutación seguida del estudio del fenotipo resultante (Parinov y Sundaresan, 2000; Page y Grossniklaus, 2002). Existen dos abordajes experimentales distintos para este propósito. Por un lado, se ha dado en llamar genética inversa a la que parte del conocimiento de la secuencia del gen a estudio para modificarla y establecer a continuación sus consecuencias fenotípicas. La más moderna de las variantes de este abordaje es la que se basa en la introducción de mutaciones mediante el sistema CRISPR/Cas9 (Sander y Joung, 2014). Por el contrario, se habla de genética clásica o directa para referirse a los casos en los que se realiza una mutagénesis al azar, desconociendo los genes que serán dañados por el mutágeno, para aislar mutantes que manifiesten perturbaciones en el proceso a estudio. En cada uno de estos mutantes es necesario identificar después el gen causante del fenotipo de interés (Ostergaard y Yanofsky, 2004). A la genética inversa ha contribuido sustancialmente la disponibilidad de las secuencias completas de los genomas de las especies modelo (Lloyd y Meinke, 2012), que ha facilitado la creación de colecciones de mutaciones indexadas, cuyas posiciones en el genoma son conocidas (Alonso y Ecker, 2006).

III.2.3.- Colecciones de mutantes indexados de Arabidopsis

No existen técnicas eficientes y baratas para inducir a gran escala mutaciones dirigidas y crear así colecciones de mutantes indexados en Arabidopsis. No obstante, se han empleado como mutágenos el ADN-T y algunos transposones, que se insertan mediante recombinación ilegítima en posiciones aleatorias del genoma (O'Malley y Ecker,

2010). La secuencia de estos elementos insercionales es conocida, por lo que señalizan al gen que interrumpen (Feldmann, 1991; Mathur *et al.*, 1998; Alonso y Ecker, 2006). Una de las muchas técnicas efectivas para determinar la posición de una inserción de ADN-T es la denominada PCR mediante ligación de un adaptador (*Adapter ligation-mediated PCR*; O'Malley *et al.*, 2007). En este método el ADN genómico a estudio es digerido con restrictasas y se ligan a los extremos de los fragmentos de restricción obtenidos oligonucleótidos sintéticos a los que se denomina adaptadores. Se realiza a continuación una amplificación mediante PCR utilizando un cebador que hibrida con el ADN-T y otro que lo hace con un adaptador. El producto de amplificación es después secuenciado, y la secuencia así obtenida es finalmente alineada con la del genoma de la estirpe silvestre de referencia a fin de determinar la identidad del gen portador de la inserción.

El ADN-T es un mutágeno eficaz dado que su inserción en un gen lo interrumpe, alterando necesariamente su actividad (Feldmann *et al.*, 1989; Marks y Feldmann, 1989; Koncz *et al.*, 1990). Durante la infección por *Agrobacterium tumefaciens* pueden suceder varios eventos de inserción de ADN-T por genoma haploide (Sessions *et al.*, 2002; Alonso *et al.*, 2003; Rosso *et al.*, 2003), lo que dificulta el establecimiento de una relación causal entre una de ellas y el fenotipo mutante observado (Azpiroz-Leehan y Feldmann, 1997; Ostergaard y Yanofsky, 2004; Ulker *et al.*, 2008). Las colecciones indexadas disponibles totalizan más de 500.000 líneas, siendo las más numerosas las denominadas Salk (ya que se obtuvo en el laboratorio de Joseph Ecker, en el Salk Institute for Biological Studies) y SAIL (Syngenta Arabidopsis Insertion Library) (Galbiati *et al.*, 2000; Samson *et al.*, 2002; Sessions *et al.*, 2002; Alonso *et al.*, 2003; Rosso *et al.*, 2003; Woody *et al.*, 2007; O'Malley y Ecker, 2010). Las semillas de estas colecciones están disponibles en los centros de conservación y distribución de estirpes y clones de ADN de Arabidopsis, entre los que cabe destacar el norteamericano ABRC (Arabidopsis Biological Resource Center) y el europeo NASC (Nottingham Arabidopsis Stock Centre).

III.2.4.- Colecciones de mutantes fenotipados de Arabidopsis

Las colecciones de mutaciones indexadas facilitan el análisis de los efectos de la disfunción de centenares o miles de genes, pudiendo alcanzarse la saturación del genoma (O'Malley y Ecker, 2010). En estas colecciones pueden analizarse los efectos de cada mutación en diferentes facetas de la biología del organismo a estudio. Se han obtenido colecciones de mutantes de Arabidopsis a los que se ha caracterizado a dos niveles: de algunos de sus rasgos fenotípicos y del gen mutado que los causa. Cada una de estas colecciones está documentada en una base de datos que permite hacer escrutinios *in silico*

empleando como criterios de búsqueda genes o fenotipos particulares (Alonso y Ecker, 2006). Una de estas bases de datos incluye mutaciones en las regiones codificantes de 4.000 genes e información sobre sus efectos en varias etapas del ciclo de vida de la planta (Kuromori *et al*., 2006). En otra colección se analizaron los efectos sobre la fotosíntesis de más de 5.000 mutaciones en genes nucleares que codifican proteínas del cloroplasto (Ajjawi *et al.*, 2010). El objetivo de dichas colecciones es la anotación funcional de muchos genes, lo que conlleva la acumulación de grandes cantidades de texto e imágenes (http://rarge.psc.riken.jp/phenome; http://bioinfo.bch.msu.edu/2010_LIMS). La disponibilidad de sistemas robotizados de fenotipado de mutantes a gran escala permitirá realizar escrutinios masivos, a los que se denomina fenómicos, que incluyen rasgos fenotípicos moleculares, celulares, tisulares y de morfología y fisiología general del organismo a estudio (Carpenter y Sabatini, 2004; Finkel, 2009; Micol, 2009).

III.2.5.- Uso de la secuenciación masiva para identificar mutaciones

Se denomina secuenciación masiva a la lectura simultánea de millones de fragmentos de un genoma, cada uno de ellos de decenas o centenares de nucleótidos. Existen diversas tecnologías masivamente paralelas (Metzker, 2010; Reuter *et al.*, 2015), todas las cuales rinden una gran cantidad de información a un coste muy bajo por nucleótido. La secuenciación masiva se ha convertido en la herramienta de elección preferente para la identificación de mutaciones (Schneeberger, 2014; Candela *et al.*, 2015), tanto insercionales (Williams-Carrier *et al.*, 2010; Mourier *et al.*, 2015) como puntuales (Arnold *et al.*, 2011; Austin *et al.*, 2011), en mutantes individuales o agrupados. El objetivo del proyecto SALKseq, por ejemplo, es saturar el genoma de Arabidopsis en inserciones de ADN-T, dado que son varios centenares los genes de los que aún no se dispone de alelos insercionales (http://signal.salk.edu/).

Se han desarrollado infraestructuras y programas informáticos para gestionar y analizar las grandes cantidades de datos que rinden las tecnologías de secuenciación masiva (Goecks *et al.*, 2010; Minevich *et al.*, 2012). Algunos de estos programas facilitan la identificación de mutaciones mediante el alineamiento de las lecturas obtenidas y la secuencia de la estirpe parental del mutante; otros identifican y listan todas sus diferencias y permiten filtrarlas según diversos criterios y predecir sus consecuencias en las secuencias de las correspondientes proteínas (Nielsen *et al.*, 2011).

III.2.6.- Descripción ontológica de fenotipos mutantes

La descripción de la parte relevante del genotipo de un mutante es simple y objetiva.

La de su fenotipo, sin embargo, puede ser compleja y es siempre subjetiva en mayor o menor medida, ya que un mismo rasgo fenotípico es habitualmente descrito de diferentes formas por distintos investigadores. Para resolver este problema se han desarrollado ontologías: vocabularios controlados que se han estandarizado para describir las enfermedades humanas y los efectos fenotípicos de las mutaciones en los organismos modelo (Mabee *et al.*, 2007; Washington *et al.*, 2009). Estas ontologías son conjuntos de términos descriptivos organizados jerárquicamente, a cada uno de los cuales se ha asignado un código único y una definición. Una ontología de uso muy extendido es la denominada PATO (Phenotype, Attribute and Trait Ontology; Smith *et al.*, 2007; http://obofoundry.org/wiki/index.php/PATO:Main_Page). Los términos de PATO se clasifican en tres categorías: entidad, atributo y valor, que son, respectivamente, la estructura biológica que se está analizando, la cualidad de la entidad que se describe y el estado de un atributo. Por ejemplo, en el estudio fenotípico de la hoja, la entidad de interés puede ser el sistema vascular, el atributo, su densidad, y el valor, una densidad reducida.

Una descripción ontológica permite un acceso fácil y rápido a la información disponible, empleando para ello palabras clave. Se están desarrollando protocolos para que las descripciones de los fenotipos en las publicaciones científicas se hagan mediante ontologías para su incorporación a bases de datos públicas. En el caso de Arabidopsis, la base de datos TAIR permite hacerlo así, pero aún no es posible realizar consultas empleando términos ontológicos como criterios de búsqueda para obtener una lista de genes asociados a un rasgo fenotípico (Sozzani y Benfey, 2011). También se ha intentado extraer de manera semiautomatizada la información de las descripciones fenotípicas de la literatura científica, que se ha hecho tradicionalmente en lenguaje natural, y convertirla a formatos que permitan consultas basadas en palabras clave (Szakonyi *et al.*, 2015).

III.3.- Evolución y desarrollo de las hojas de las plantas

III.3.1.- Filogenia de la hoja

La arquitectura corporal de las plantas presenta una simetría fundamentalmente radial, con dos polos, cada uno de los cuales es un meristemo apical: una estructura de origen embrionario indiferenciada y pluripotente. Los meristemos apicales de la raíz y el tallo generan respectivamente todas las partes subterráneas y aéreas de la planta, incluidos los órganos laterales como las hojas y las flores (Lyndon, 1990).

En las primeras plantas vasculares terrestres, que aparecieron hace 440-410 millones de años, todas las estructuras generadas por el meristemo apical del tallo eran radiales. Los primeros órganos laterales, las hojas, aparecieron hace 410-360 millones de

años (Cronk, 2001), cuando lo permitió el descenso de la concentración del CO_2 atmosférico (Osborne *et al.*, 2004; Beerling, 2005). En efecto, el alto nivel de CO_2 en la atmósfera de nuestro planeta en el Paleozoico medio dificultaba el desarrollo de los estomas, ya que hubiera limitado el enfriamiento por evaporación, conduciendo a un calentamiento letal de las hojas, que absorben grandes cantidades de energía solar.

Desde un punto de vista evolutivo, las hojas pueden ser micrófilas, estructuralmente simples y con un tejido vascular no ramificado, o megáfilas, que presentan una organización definida sobre el tallo (filotaxia) y crecimiento determinado, están vascularizadas (pudiendo tener ramificaciones) y muestran dorsoventralidad y una forma laminar (Micol, 2009; Tomescu, 2009). Las hojas de Arabidopsis son megáfilas según estos criterios. El registro fósil indica que la estructura ancestral a partir de la que evolucionaron las hojas estaba ramificada tridimensionalmente y presentaba crecimiento indeterminado (Tomescu, 2009). Una de sus modificaciones críticas fue necesariamente la de dotarse de un mecanismo para interrumpir el crecimiento de manera programada. Se acepta generalmente que algunos genes de la familia KNOTTED1-LIKE HOMEOBOX (KNOX) de la clase I son los responsables últimos del mantenimiento de la pluripotencia celular y del crecimiento indeterminado del meristemo apical del tallo (Endrizzi *et al.*, 1996). A su vez, se considera responsables del crecimiento determinado de las hojas a los factores de transcripción del grupo ARP (ASYMMETRIC LEAVES, ROUGH SHEATH y PHANTASTICA, de Arabidopsis, el maíz y *Antirrhinum majus*, respectivamente). Estos genes ortólogos se expresan en los primordios foliares y reprimen específicamente a *SHOOT MERISTEMLESS* (*STM*; Cronk, 2001; Boyce, 2010), un gen *KNOX* de la clase I que también codifica un factor de transcripción.

Otra innovación crucial durante la evolución de las hojas fue la adquisición de su forma laminar a fin de maximizar la relación entre su superficie y su masa, optimizando así la función fotosintética. Este cambio morfológico sucedió aparentemente como consecuencia de la actividad antagónica de los factores de transcripción de las familias KANADI (KAN) y HOMEODOMAIN-LEUCINE ZIPPER de la clase III (HD-ZIP III; Yamaguchi *et al.*, 2012). Los genes de estas dos familias ya estaban presentes en los genomas de las plantas sin hojas, en cuyos tallos creaban la polaridad central-periférica (Boyce, 2010). El análisis de los alelos mutantes de estos genes ha demostrado que son necesarios tanto para la disposición relativa del xilema y el floema como para la generación de la forma laminar de las hojas. Se ha propuesto que la diferenciación del limbo tiene como prerrequisito la yuxtaposición de células con características dorsales y ventrales (Waites y Hudson, 1995), cuya especificación depende de los genes de las familias HD-

ZIP III y KANADI, que asumieron estas funciones durante la evolución de las plantas terrestres (Emery *et al.*, 2003).

III.3.2.- Morfología de la hoja de Arabidopsis

Las hojas de Arabidopsis presentan tres ejes de polaridad, cada uno de los cuales define dos regiones (Figura 1A): el proximodistal, el peciolo y el limbo, que corresponden a las partes más próximas y alejadas al tallo; el dorsoventral, los tejidos adaxiales y abaxiales, cuya manifestación externa es el haz y el envés, respectivamente; y el mediolateral, los tejidos vascular y fotosintético, y el margen (Byrne *et al.*, 2001). Algunos autores hablan de dos ejes mediolaterales enfrentados para resaltar la simetría bilateral del limbo (Palmer, 2004).

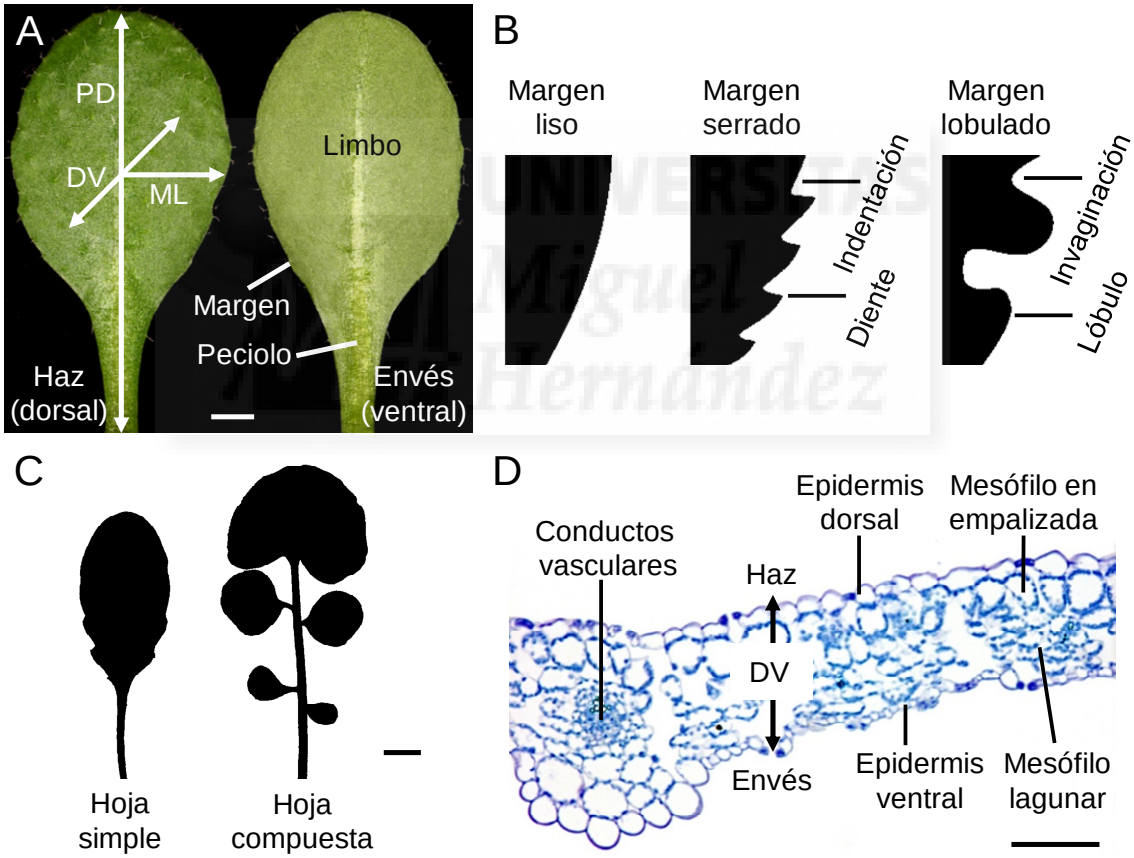

Figura 1.- Morfología e histología de la hoja vegetativa de Arabidopsis. (A) Morfología externa. Se muestran el haz (izquierda) y el envés (derecha) de una hoja del tercer nudo. PD: eje proximodistal. ML: eje mediolateral. DV: eje dorsoventral. (B) Algunos tipos de márgenes característicos de las hojas y denominación que reciben las estructuras que los forman. (C) Siluetas de una hoja simple (izquierda) y una compuesta (derecha), de Arabidopsis y *Cardamine hirsuta*, respectivamente. (D) Corte transversal de una hoja vegetativa del primer nudo. (A, D) Tomado de Jover-Gil (2005). Las barras de escala indican (A) 1 mm, (C) 4 mm y (D) 100 µm.

La morfología foliar en el plano determinado por sus ejes proximodistal y mediolateral es uno de los rasgos más diversos de las dicotiledóneas (Malinowski, 2013; Wang y Chen, 2014). Existe una gran variedad natural en la forma del margen foliar, probablemente porque modula las relaciones hídricas en la hoja, que influyen en la adaptación de las plantas a diferentes hábitats (Nicotra *et al.*, 2011). El margen de las hojas puede ser liso, cuando es totalmente convexo, como en Arabidopsis, y serrado o lobulado, cuando presenta segmentos cóncavos y convexos intercalados, como en *Arabidopsis lyrata* (Figura 1B). Por otra parte, las hojas pueden ser simples (Figura 1C), con un único limbo, como en Arabidopsis, o compuestas, con varios limbos no conectados directamente entre sí (foliolos), como en *Cardamine hirsuta* o en el tomate (*Solanum lycopersicum*; Champagne y Sinha, 2004; Blein *et al.*, 2010).

Son varios los clados del reino vegetal en los que a lo largo de la evolución han ocurrido interconversiones entre las formas simples y compuestas de las hojas (Piazza *et al.*, 2010; Vlad *et al.*, 2014). Se han descrito casos en los que la modificación de uno o unos pocos genes basta para convertir una hoja simple en compuesta, o a la inversa. La insuficiencia de la función de *REDUCED COMPLEXITY* (*RCO*), cuyo producto es un factor de transcripción con homeodominio que se expresa en el margen foliar de *Cardamine hirsuta*, o de *ENTIRE* (*E*) en el tomate, que codifica una proteína de respuesta a auxina de la familia Aux/IAA, es suficiente para producir hojas simples (Zhang *et al.*, 2007; Koenig *et al.*, 2009; Vlad *et al.*, 2014). Por otro lado, varias combinaciones dobles mutantes de alelos de ganancia de función de los genes *CUP-SHAPED COTYLEDON2* (*CUC2*), *WUSCHEL-RELATED HOMEOBOX9* (*WOX9*) y *JAGGED AND WAVY* (*JAW*) rinden hojas compuestas en Arabidopsis (Blein *et al.*, 2013). *CUC2* y *WOX9* codifican factores de transcripción, y *JAW*, un microARN; estos tres genes están implicados en el control de la proliferación celular (Palatnik *et al.*, 2003; Wu *et al.*, 2007). El estudio de estos genes indica que la diversidad morfológica de las hojas depende al menos en parte de la modulación del desarrollo de sus márgenes (Blein *et al.*, 2008). Además, la morfología del margen es muy plástica, y algunas especies pueden producir hojas con diferente configuración marginal en respuesta a diferentes condiciones ambientales durante su desarrollo (Royer *et al.*, 2009).

III.3.3.- Histología foliar

Las hojas de las plantas son histológicamente simples (Figura 1D). La epidermis es la capa de células que aísla a la planta de su entorno y regula el intercambio de sustancias con el exterior (Becraft, 1999); en la hoja de Arabidopsis envuelve a otras cinco capas de tejidos internos y está constituida mayoritariamente por células pavimentosas, aunque

también incluye otros histotipos que son componentes de estructuras especializadas como los tricomas y los estomas. La morfología de las células pavimentosas es irregular, excepto en el peciolo y el margen del limbo, y junto a la vena primaria, en donde son alargadas y estrechas. La superficie de la epidermis adaxial es relativamente lisa, mientras que la abaxial es rugosa y sus células son más pequeñas que las del haz. El tamaño de las células pavimentosas de la epidermis se corresponde con su nivel de ploidía, que oscila entre 2C y 16C (Melaragno *et al.*, 1993).

La epidermis adaxial se yuxtapone al mesófilo en empalizada, formado por una o dos capas de células fotosintéticas alargadas y densamente empaquetadas. Existen otras cuatro capas de mesófilo, denominado esponjoso o lagunar, entre el mesófilo en empalizada y la epidermis abaxial; sus células son heterogéneas en tamaño y están separadas por amplios espacios intercelulares, que facilitan la difusión de los gases.

El sistema vascular de Arabidopsis, como el de otras plantas, sirve para el transporte de sustancias y proporciona soporte mecánico a la hoja (Braybrook y Kuhlemeier, 2010). Está formado por dos tipos de tejidos: el floema, que conduce los hidratos de carbono, y el xilema, que transporta agua y solutos (Turner y Sieburth, 2002). Los haces vasculares transcurren a través del mesófilo lagunar, ocupando el xilema la parte adaxial y el floema, la abaxial. El patrón de venación de las hojas de Arabidopsis es broquidódromo —según la clasificación de Hickey (1979)— y está formado por una vena primaria central de la que surgen las secundarias formando bucles. Las areolas (regiones intervasculares del limbo) de Arabidopsis son irregulares en su forma, tamaño y orientación. El patrón de venación de las hojas de Arabidopsis se ha descrito en detalle (Candela *et al.*, 1999; Dhondt *et al.*, 2012), así como la distribución de los hidatodos, unas estructuras asociadas a los conductos vasculares a través de las que sucede la gutación o secreción de agua líquida.

III.3.4.- Algunas facetas del desarrollo foliar

III.3.4.1.- Establecimiento

La zona central del meristemo apical del tallo se divide continuamente durante el desarrollo vegetativo de una planta. Las células recién generadas van desplazando del ápice a las precedentes, que a su vez contribuyen según su posición a la formación del tallo o de las hojas. Se denomina primordio foliar al grupo de células precursoras de una hoja, cuya formación es inducida por la acumulación de auxina, que es a su vez consecuencia de la actividad de los transportadores AUXIN RESISTANT1 (AUX1) y PIN-FORMED1 (PIN1; Bayer *et al.*, 2009; Guenot *et al.*, 2012). La auxina que se acumula en

los flancos del meristemo regula negativamente a los genes *KNOX* de la clase I, induciendo la pérdida de pluripotencia celular y la iniciación del primordio. La identidad de las células del primordio es perpetuada por los factores de transcripción ARP, que se expresan en el primordio y mantienen la represión de los genes *KNOX* de la clase I (Long *et al.*, 1996; Byrne *et al.*, 2002; Hay y Tsiantis, 2006).

La expansión foliar es el proceso por el que, una vez adquirida la identidad foliar, el primordio crece hasta alcanzar el tamaño final de la hoja madura (De Veylder *et al.*, 2001; Bogre *et al.*, 2008; Breuninger y Lenhard, 2010). Durante su primera fase, conocida como de proliferación celular, las células son similares y relativamente pequeñas, incrementándose su número mediante divisiones mitóticas (Donnelly *et al.*, 1999) que contribuyen solo moderadamente al crecimiento del órgano. En la segunda fase, llamada de expansión celular, el aumento del volumen de las células hace crecer exponencialmente a la hoja. La transición entre estas dos fases, que coexisten durante parte de la organogénesis foliar, ocurre primero en el ápice y se propaga en dirección basípeta (Donnelly *et al.*, 1999; Nath *et al.*, 2003). En Arabidopsis, la expansión celular está asociada a la endorreduplicación, en la que la replicación del ADN no conlleva citocinesis (Beemster *et al.*, 2005). Durante la fase de expansión celular las células también se diferencian (Gonzalez *et al.*, 2012). El tamaño final de las hojas puede modularse variando el ritmo de la división o la expansión celular (Cho y Cosgrove, 2000; Rojas *et al.*, 2009) y su duración (Kurepa *et al.*, 2009; Lee *et al.*, 2009; Sonoda *et al.*, 2009).

III.3.4.2.- Morfogénesis

Se llama morfogénesis a la adquisición de la forma en un ser vivo (Gilbert, 2003). Se denomina patrón a la distribución no aleatoria de las distintas partes de un órgano o de un organismo (Spemann, 1938; Child, 1941; Sinnot, 1963; Wolpert, 1971; Twyman, 2001). Una hoja madura no es uniforme a nivel tisular o morfológico, ya que muestra patrones específicos. Su forma final depende de la regulación espacial y temporal de la proliferación y la expansión celular, que a su vez dependen de la expresión de determinados genes (Gifford y Foster, 1989; Sachs, 1991; Kuchen *et al.*, 2012). La gran diversidad de formas de las hojas en el plano definido por sus ejes proximodistal y mediolateral es consecuencia de la variación conjunta de dos parámetros: el patrón de crecimiento del margen y su duración (Blein *et al.*, 2013). A la morfogénesis foliar contribuye más la proliferación que la expansión celular (Blein *et al.*, 2008), aunque esta última también es importante (Pien *et al.*, 2001). A pesar de que la forma de las hojas de las plantas de una especie dada es reproducible, el número y la orientación de sus divisiones celulares no es fijo, lo que sugiere

la existencia de algún tipo de control supracelular sobre la morfogénesis foliar (Ichihashi *et al.*, 2011).

Para que la formación de patrones suceda es necesario que las células conozcan su linaje o su posición con respecto a los ejes de la estructura de la que forman parte. A esta información se le denomina posicional (Wolpert, 1969). En el siglo pasado se formularon dos hipótesis al respecto de cómo las células vegetales adquirían su información posicional. Las descripciones de linajes celulares y los resultados de la manipulación quirúrgica indicaron que algunas células solo rendían un tipo concreto de progenie, lo que sugería que su destino dependía de su linaje. En otros casos no era fácil correlacionar el destino y el linaje de las células, muchas de las cuales, en particular las de órganos en desarrollo, lo cambiaban tras ser transferidas a un nuevo contexto espacial. Esta última observación indicaba que el destino de las células también depende de su posición (Scheres, 2001). Se acepta generalmente en nuestros días que la información posicional es más determinante que el linaje celular durante el desarrollo vegetal (Pallakies y Simon, 2010). En el caso particular de la hoja, el análisis clonal ha demostrado que las tres regiones concéntricas en que se subdivide el meristemo —denominadas de fuera adentro L1, L2 y L3— son las precursoras de los tejidos epidérmicos, subepidérmicos y vasculares de la hoja, respectivamente. Sin embargo, durante el desarrollo foliar se dan divisiones periclinales que hacen que alguna de estas capas sea invadida por células de otra, que pasan a comportarse según su nueva posición (Stewart y Derman, 1975; Poethig, 1989; Pallakies y Simon, 2010).

III.3.4.3.- Información posicional durante el desarrollo foliar

Las células en desarrollo obtienen su información posicional mediante señales distribuidas heterogéneamente en su contexto tisular, que pueden ser exógenas o endógenas. Se denomina morfógenos a estas señales en los animales: moléculas difusibles cuya concentración modula el comportamiento de las células durante el desarrollo (Wolpert, 1969). En las plantas, se llama moléculas señalizadoras a las que muestran actividad morfogenética, que son de naturaleza y función diversas (Braybrook y Kuhlemeier, 2010; Pallakies y Simon, 2010). Se describen a continuación algunos ejemplos de este tipo de moléculas y el modo en que confieren información posicional a las células durante el desarrollo foliar.

Cabe mencionar en primer lugar a los sistemas ligando-receptor, constituidos por un péptido pequeño que es secretado al medio extracelular en el que difunde pasivamente formando un gradiente de concentración, y una proteína localizada en la membrana

plasmática, que se une específicamente al péptido y transduce la señal de este al medio intracelular (Matsubayashi, 2003). Pertenecen a este grupo los ligandos EPIDERMAL PATTERNING FACTOR 1 (EPF1) y EPF2 y los receptores ERECTA (ER) y TOO MANY MOUTHS (TMM), que contribuyen al correcto espaciamiento de los estomas. Las células precursoras de los estomas producen EPF1 y EPF2, que al difundirse inhiben la diferenciación de las células adyacentes (Torii, 2012).

Los ARN pequeños móviles son moléculas cortas y difusibles, que forman gradientes reprimiendo postranscripcionalmente a sus genes diana de forma no autónoma celular (Skopelitis *et al.*, 2012). El microARN166 (miR166), por ejemplo, se expresa en el polo abaxial de los primordios foliares, desde donde se difunde hacia el adaxial, formando un gradiente de silenciamiento de los transcritos del gen *PHABULOSA* (*PHB*), que otorga identidad adaxial a las células (Waites y Hudson, 1995; McConnell y Barton, 1998; McConnell *et al.*, 2001; Emery *et al.*, 2003; Eshed *et al.*, 2004; Kidner y Martienssen, 2004).

Por último, merecen comentario las fitohormonas, que pueden conferir información posicional al ser transportadas activamente o difundir pasivamente (Holder, 1979; Pallakies y Simon, 2010). Un ejemplo de ello es la auxina, que participa en la especificación del patrón vascular y la determinación de la forma del margen foliar mediante su distribución heterogénea en el limbo, tal como se discute en el apartado siguiente (Hay *et al.*, 2006; Scarpella *et al.*, 2010; Bilsborough *et al.*, 2011).

III.3.4.4.- Papel de la auxina en el desarrollo foliar

La auxina regula muchos aspectos del desarrollo vegetal. Suele distribuirse en gradientes de concentración o en puntos discretos, habitualmente llamados máximos. Estos gradientes y máximos cambian dinámicamente durante el desarrollo, modulando el efecto de la hormona. Existen opiniones contrapuestas acerca de si la auxina es un morfógeno en sentido estricto (Bhalerao y Bennett, 2003). Algunos autores consideran que, en ciertos aspectos del desarrollo, la auxina puede considerarse un “disparador morfogenético” (Dubrovsky *et al.*, 2008): un factor que se distribuye de manera no homogénea, induciendo nuevos destinos de desarrollo en células inicialmente iguales a sus vecinas (Benkova *et al.*, 2009). La mayor parte de la auxina de una planta se sintetiza en el tallo y llega a las hojas mediante transporte activo, mediado por proteínas de las familias PIN-FORMED (PIN) y AUXIN RESISTANT (AUX). La ubicación de estos transportadores en la membrana de las células foliares cambia en respuesta a señales exógenas y endógenas con el fin de canalizar la auxina en una dirección determinada (Tanaka *et al.*, 2006; Teale *et al.*, 2006; Benkova *et al.*, 2009; Vanneste y Friml, 2009).

La auxina es un determinante del desarrollo del margen foliar (Reinhardt *et al.*, 2003; de Reuille *et al.*, 2006; Jonsson *et al.*, 2006; Smith *et al.*, 2006; Barkoulas *et al.*, 2008; Bilsborough *et al.*, 2011). Los primordios foliares de Arabidopsis presentan inicialmente un margen liso en el que se forman progresivamente dientes y lóbulos, cuyas posiciones dependen del transporte polar de auxina. El transportador PIN1 (Hay *et al.*, 2006) y el factor de transcripción CUC2 (Nikovics *et al.*, 2006) forman máximos de auxina (Figura 2). Estos

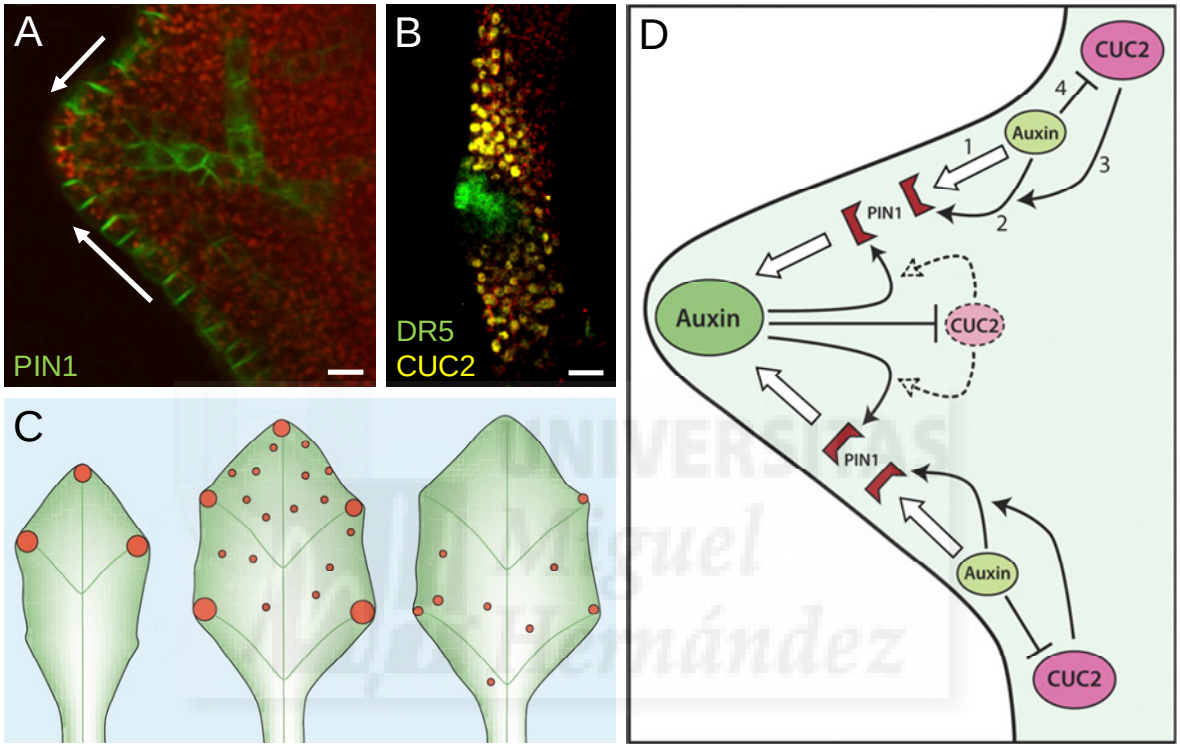

Figura 2.- Papel de la auxina en el desarrollo del margen foliar de Arabidopsis. (A) Visualización mediante microscopía confocal de la polarización de la proteína de fusión PIN1:GFP en la membrana de las células del margen. Las flechas indican la dirección del transporte de auxina que forma un máximo de la hormona. Se aprecia claramente la acumulación de PIN1 en uno de los lados de cada célula, perpendicularmente a la dirección del transporte. (B) Acumulación de auxina, visualizada indirectamente mediante la fusión transcripcional *DR5$_{pro}$:GFP* (en verde; DR5 es un promotor sintético que responde a auxina) en un máximo situado entre dos dominios de expresión de la proteína de fusión CUC2:VENUS (en amarillo). (C) Formación de máximos de auxina (círculos) en sucesivos estadios (de izquierda a derecha) del desarrollo de un primordio foliar. (D) Relaciones entre la auxina, PIN1 y CUC2 en el margen foliar. La acumulación de la auxina causada por su transporte polar por PIN1 influye en la expresión y polarización de esta última proteína, lo que estabiliza el máximo. CUC2 también influye en la orientación de PIN1 para estabilizar dicho máximo, mientras que la auxina, a su vez, inhibe la expresión de CUC2. Los símbolos → y ⊣ indican regulación positiva y negativa, respectivamente. GFP: proteína verde fluorescente. VENUS: variante de la YFP (proteína amarilla fluorescente, que es a su vez una variante de la GFP). Modificado a partir de (A, B, D) Bilsborough *et al.* (2011) y (C) Teale *et al.* (2006). Las barras de escala indican 10 µm.

máximos coinciden con regiones del limbo que crecen más que las adyacentes, formando un diente o un lóbulo. Los dominios en los que se expresa *CUC2*, por el contrario, crecen menos (Figura 2D; Bilsborough *et al.*, 2011). Los importadores de auxina de la familia AUX también son necesarios para la formación de los máximos de auxina en el margen foliar (Kasprzewska *et al.*, 2015). Se desconoce la naturaleza molecular de la relación entre el transporte de auxina y CUC2.

La auxina también es necesaria para la formación de los foliolos de las hojas compuestas (Koenig *et al.*, 2009) y para iniciar la diferenciación de las venas (Scarpella *et al.*, 2006; Wenzel *et al.*, 2007; Scarpella *et al.*, 2010). Tras la formación de cada máximo de auxina en el margen foliar, PIN1 canaliza la auxina hacia la región medial del limbo. Así, las venas secundarias tienen su origen en los dientes y lóbulos del margen, y desembocan en la vena primaria.

III.4.- Antecedentes y objetivos

III.4.1.- Generación de la simetría bilateral en los seres vivos

La simetría bilateral es una propiedad morfológica de gran importancia para la mayoría de los seres vivos, y ha aparecido varias veces en la evolución de los animales y las plantas para satisfacer necesidades diversas. En el caso de los animales, un plan corporal con simetría bilateral permite una movilidad más eficiente, esencial para su supervivencia (Finnerty, 2003). Las plantas son sésiles y la mayoría de sus estructuras, como la raíz, el tallo, y muchas flores y frutos presentan simetría radial. Solo la mayoría de las hojas y algunas flores son bilateralmente simétricas como consecuencia de la dorsoventralidad que han adquirido durante su evolución para la captación de luz y el intercambio de gases, y para la polinización, respectivamente (Hudson, 2000; Preston y Hileman, 2009; Endress, 2012).

Los órganos con simetría radial, como el tallo, presentan solo dos ejes de polaridad: el proximodistal, desde la base al ápice de la planta, y el mediolateral, que cruza diferentes capas de tejidos concéntricos (Figura 3A, en la página 21). En los organismos y los órganos bilaterales existe un tercer eje, el dorsoventral, que es perpendicular al proximodistal y genera la partición del eje mediolateral (Figura 3A; Bowman *et al.*, 2002; Husbands *et al.*, 2009).

Se dispone de un gran número de mutantes morfológicos de *Antirrhinum majus*, cuyo análisis ha revelado que la expresión asimétrica de uno o pocos genes basta para

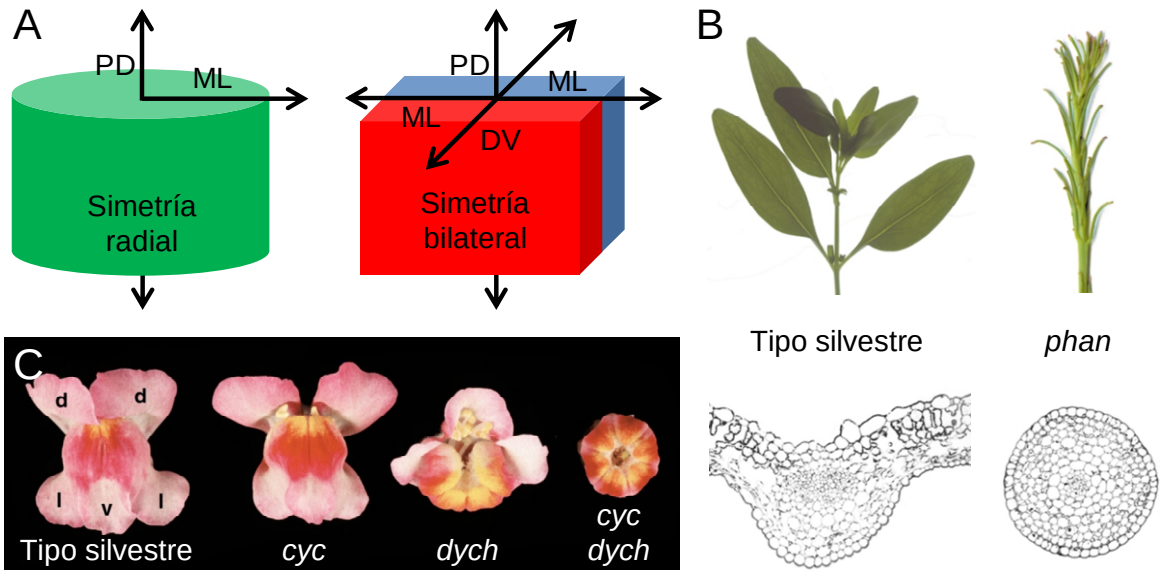

Figura 3.- Relación entre la simetría radial y la bilateral en *Antirrhinum majus*. (A) Ejes de polaridad en estructuras tridimensionales que manifiestan simetría radial (izquierda) y bilateral (derecha). PD, ML y DV: eje proximodistal, mediolateral y dorsoventral, respectivamente. (B) Morfología general (arriba) y cortes histológicos transversales (abajo) de las hojas del tipo silvestre y un mutante *phan* de *Antirrhinum majus*. La dorsoventralidad de la hoja silvestre se pierde en la mutante, que está radializada. (C) Transición de la simetría bilateral de la flor zigomorfa silvestre de *Antirrhinum majus* a mutantes actinomorfas. *cyc*: *cycloidea*. *dych*: *dychotoma*. d, l y v: pétalos dorsales, laterales y ventral, respectivamente. (B) y (C) se han tomado de Bowman *et al.* (2002).

especificar un nuevo eje de polaridad, como el dorsoventral. En efecto, la insuficiencia de la función del gen *Phantastica* (*Phan*), que se expresa en las células foliares adaxiales, causa la radialización de las hojas (Figura 3B; Waites y Hudson, 1995). A una conclusión similar conduce el fenotipo del doble mutante *cycloidea dichotoma* (*cyc dich*), que presenta flores con simetría radial y pérdida de identidad dorsal (Figura 3C; Luo *et al.*, 1996; Hileman y Baum, 2003; Hileman, 2014). Estos y otros fenotipos de radialización foliar o floral suelen estar asociados a alelos mutantes de genes que codifican factores de transcripción que se expresan desigualmente en los territorios dorsal y ventral de los órganos afectados (Waites y Hudson, 1995; McConnell y Barton, 1998; McConnell *et al.*, 2001; Galego y Almeida, 2002; Emery *et al.*, 2003; Eshed *et al.*, 2004; Kidner y Martienssen, 2004; Corley *et al.*, 2005). Los factores de transcripción CYC y DICH, de la familia TCP (por los genes *teosinte branched1*, *CYCLOIDEA*, *PROLIFERATING CELL FACTOR1* y *2*) controlan la polaridad floral regulando a genes efectores de la proliferación y la expansión celular (Martín-Trillo y Cubas, 2010). Otros autores han propuesto que para generar la dorsoventralidad, CYC y DICH también deben controlar a otros genes que confieran direccionalidad al crecimiento de los órganos florales (Green *et al.*, 2010; Kennaway *et al.*, 2011).

III.4.2.- Desviaciones de la simetría bilateral en los seres vivos

Se han definido varios tipos de desviaciones de la simetría bilateral (Ludwig, 1932; Bock y Marsh, 1991). Se ha dado en llamar asimetría fluctuante a la desviación sutil y aleatoria de la simetría bilateral que se atribuye al ambiente y al polimorfismo genético en las poblaciones (Palmer, 1996; Hosken *et al.*, 2000; Palmer, 2004; Lin *et al.*, 2012). Se denomina asimetría conspicua a las diferencias reproducibles y controladas genéticamente entre las dos mitades de un órgano u organismo completo, distinguiéndose dos tipos: asimetría direccional, si la manifiestan de igual modo todos los individuos de una especie dada, y antisimetría, si coexisten dos tipos especulares en la población. Se cree que la antisimetría se debe a la influencia del ambiente sobre ciertos genes durante el desarrollo (Palmer, 2004). El cangrejo *Homarus americanus*, cuya pinza más utilizada durante el desarrollo se hipertrofia, constituye un ejemplo de antisimetría (Govind y Pearce, 1989).

Es tan sorprendente como cierto que no se conocen genes responsables de la simetría bilateral. Sin embargo, sí se han descrito numerosas estructuras biológicas, tanto animales como vegetales, que manifiestan una asimetría bilateral que está controlada por genes concretos (Vandenberg y Levin, 2013). En el embrión de *Drosophila melanogaster*, los ejes anteroposterior y dorsoventral son especificados por productos de genes maternos en función de la posición del oocito en el folículo ovárico (Gilbert, 2003); sin embargo, se desconoce la existencia de mecanismos responsables de la definición de los polos izquierdo y derecho. De hecho, se han buscado sin éxito mutantes de *Drosophila melanogaster* con pérdida de la simetría bilateral en diversas estructuras corporales (Smith y Sondhi, 1960; Purnell y Thompson, 1973; Coyne, 1987; Tuinstra *et al.*, 1990). Se ha concluido de lo anterior que la unidad básica de la estructura corporal de *Drosophila melanogaster* es cualquiera de sus dos mitades, izquierda o derecha, y que la simetría bilateral se consigue combinándolas especularmente (Palmer, 2004). El animal, en consecuencia, presenta dos ejes mediolaterales.

III.4.3.- La simetría bilateral en las hojas de las plantas

El polo proximal del eje proximodistal y el dorsal del eje dorsoventral de un primordio foliar se especifican en función de la posición de este último en el meristemo apical del tallo. En otras palabras, el primordio usa una estructura preexistente como referencia espacial (Hudson, 2000). Aunque todas las hojas manifiestan asimetría bilateral fluctuante, las de algunas plantas pueden considerarse bilateralmente simétricas mientras que las de otras especies manifiestan asimetría conspicua. Dado que todas las especies con hojas asimétricas muestran una filotaxia espiral, se ha propuesto que esta última causa la

asimetría (Chitwood *et al.*, 2012b). Algunos ejemplos de plantas con hojas asimétricas son Arabidopsis y el tomate, cuyo grado de asimetría es pequeño pero reproducible, o especies de los géneros *Aglaonema* y *Calathea*, en las que la asimetría es mayor (Chitwood *et al.*, 2012b). Se ha demostrado en Arabidopsis y el tomate que la causa de la asimetría es una distribución asimétrica de la auxina en el primordio, impuesta por la propia arquitectura espiral del meristemo (Chitwood *et al.*, 2012a). En efecto, cada primordio emergente compite por la auxina más con el siguiente (que al ser más joven consume más auxina de los tejidos vecinos) que con el anterior (que al ser más viejo es capaz de sintetizar su propia auxina). Esta disponibilidad asimétrica de auxina para el primordio emergente causa un crecimiento asimétrico de la hoja (Figura 4). Se deriva de lo anterior que la simetría en la distribución de la auxina es fundamental para la simetría foliar.

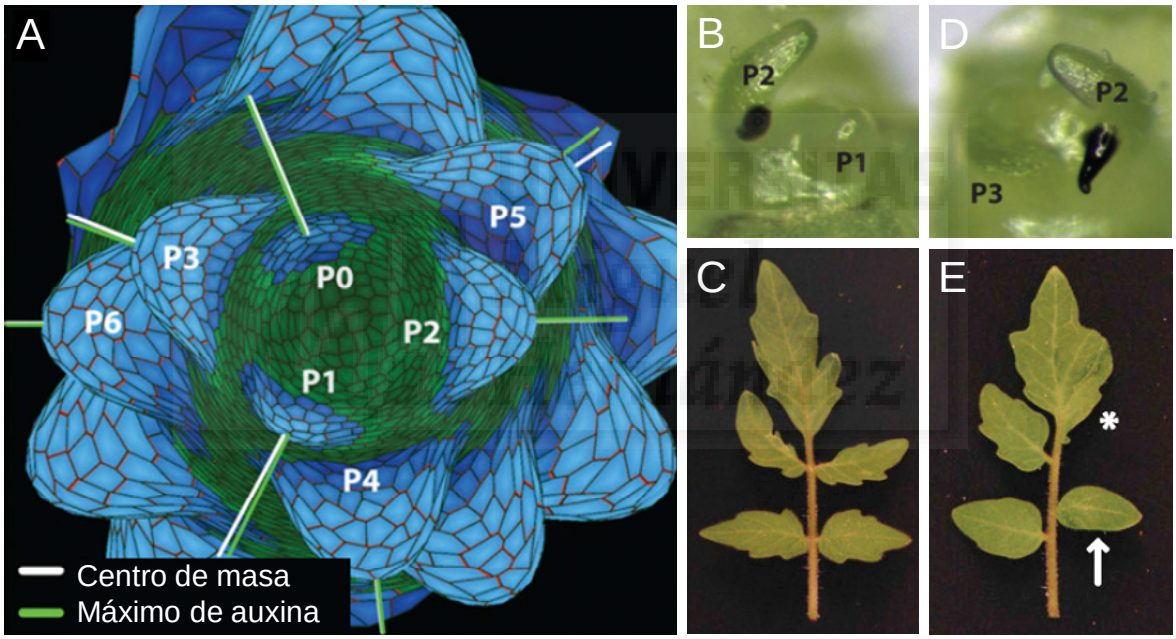

Figura 4.- Efectos de la auxina sobre la simetría bilateral de las hojas del tomate, una planta con filotaxia espiral. (A) Distribución espacial de los centros de masa (ejes proximodistales) de los primordios foliares y de los máximos de auxina en un meristemo apical del tallo del tomate. Nótese que los máximos de auxina están desviados lateralmente respecto a los centros de masa. Los polígonos verdes y azules representan las células epidérmicas del meristemo y los primordios foliares, respectivamente. Los primordios están numerados (P0 a P6) en orden inverso al de su aparición. (B-E) Efectos de la aplicación asimétrica de lanolina (B-C) sin y (D-E) con ácido indolacético sobre la simetría en la hoja compuesta del tomate. (B, D) Posición de aplicación de la lanolina (manchas oscuras). (C, E) Hojas resultantes de los tratamientos. Nótese en (E) que la aplicación de auxina causa el desplazamiento distal de un foliolo lateral (flecha) y la aparición de un lóbulo ectópico en el foliolo terminal (asterisco). Tomado de Chitwood *et al.* (2012a).

En Arabidopsis —como en *Drosophila melanogaster*— no se han encontrado mutantes cuyas hojas manifiesten asimetría direccional o antisimetría propiamente dichas. Se han descrito mutantes con asimetría aleatoria, en los que las hojas de una misma planta son diferentes entre sí, lo que sugiere que sus mutaciones intensifican la asimetría fluctuante intrínseca del tipo silvestre (Hosken *et al.*, 2000; Townsley y Sinha, 2012).

A continuación se describen algunos mutantes de Arabidopsis cuyas hojas manifiestan algún grado de asimetría bilateral (Figura 2 de Muñoz-Nortes *et al.* [2014], en la página 42 de esta Tesis). Los factores de transcripción AS1 (ASYMMETRIC LEAVES1) y AS2 y las proteínas BOP1 (BLADE-ON-PETIOLE1) y BOP2, que presentan dominios BTB/POZ y repeticiones de anquirina, contribuyen a la diferenciación foliar reprimiendo en la hoja a genes que codifican factores de transcripción de la familia KNOX de la clase I (*KNOTTED-LIKE FROM ARABIDOPSIS THALIANA1* [*KNAT1]*, *KNAT2* y *KNAT6*) y a dos de la familia YABBY (*YAB3* y *FILAMENTOUS FLOWER* [*FIL*]). En los mutantes simples *as1*, *as2* y *bop1* y en el doble mutante *bop1 bop2* aparecen lóbulos asimétricos en la región basal de la hoja (Byrne *et al.*, 2000; Semiarti *et al.*, 2001; Ha *et al.*, 2007; Ha *et al.*, 2010).

El factor de transcripción JAGGED (JAG) es necesario para la transición entre la proliferación y la diferenciación en los órganos laterales y se requiere para que adquieran su forma silvestre; los mutantes *jag* presentan pérdida aleatoria de la simetría foliar y defectos morfológicos en los órganos florales (Dinneny *et al.*, 2004). *TRN1* (*TORNADO1*) y *TRN2* participan en el establecimiento del eje mediolateral en la raíz y en la expansión lateral del limbo en las hojas. Los alelos nulos de *TRN1* y *TRN2* causan la pérdida de la simetría bilateral foliar (Cnops *et al.*, 2000; Cnops *et al.*, 2006). Las proteínas BAM1 (BARELY ANY MERISTEM1), BAM2, BAM3 y STRUBBELIG (SUB) son presuntos receptores con actividad tirosina quinasa. Los genes *BAM* participan en el desarrollo de diversas estructuras vegetales, entre ellas la hoja, y sus alelos mutantes alteran la simetría foliar (DeYoung *et al.*, 2006). El gen *SUB* regula el ritmo y la orientación de los planos de la división celular, así como la transición a la fase de expansión y diferenciación (Chevalier *et al.*, 2005); sus alelos mutantes presentan hojas antisimétricas (Lin *et al.*, 2012).

III.4.4.- Objetivos de esta Tesis

Las hojas de las plantas capturan eficientemente la luz solar, retiran CO_2 de la atmósfera, producen el oxígeno que respiramos y constituyen la fuente directa o indirecta de casi todos los alimentos que consumimos (Micol, 2009). La comprensión de los mecanismos que determinan el número de hojas de una planta, así como su forma, tamaño y estructura interna, debería permitir la manipulación genética de especies vegetales para

satisfacer mejor las necesidades de la humanidad y del planeta en su conjunto. A pesar de todo ello, se dispone de muy poca información acerca de los procesos genéticos que subyacen al crecimiento y la morfogénesis de las hojas.

Los abordajes genéticos han sido los más fructíferos en el análisis del desarrollo foliar, gracias a la obtención de mutantes que manifiestan anomalías en la morfología de las hojas. Con el objetivo de contribuir a la disección genética del desarrollo de este órgano en Arabidopsis se iniciaron en 1993 en el laboratorio de J.L. Micol varias búsquedas de mutantes que manifestasen alteraciones en la arquitectura foliar. Se identificaron así 153 mutantes inducidos mediante EMS y 28 por bombardeo con neutrones rápidos. También se estudiaron 56 mutantes pertenecientes a una colección de dominio público, la del Arabidopsis Information Service (AIS). Su análisis de complementación demostró que correspondían a 94, 8 y 14 genes, respectivamente (Berná *et al.*, 1999; Serrano-Cartagena *et al.*, 1999). Se han identificado desde entonces 55 de estos genes —inicialmente mediante clonación posicional, y más recientemente, por secuenciación masiva—, que han sido caracterizados genética y molecularmente en el laboratorio de J.L. Micol, en algunos casos en colaboración con otros grupos (Micol, 2009; Pérez-Pérez *et al.*, 2009).

El número medio de alelos obtenidos de los genes a estudio en el laboratorio de J. L. Micol indicaba claramente que no se había alcanzado la saturación del genoma (Berná *et al.*, 1999; Pérez-Pérez *et al.*, 2009). De ahí que se decidiera en 2007 analizar la colección Salk de mutantes de ADN-T (Alonso *et al.*, 2003), año en el que el ABRC había empezado a agrupar en grandes lotes las líneas de la colección Salk, para facilitar las búsquedas a gran escala, haciéndolas asequibles para muchos laboratorios medianos.

Los objetivos iniciales de esta Tesis incluían (1) completar en la medida de lo posible el escrutinio de mutantes foliares en la colección Salk, previamente iniciado, (2) realizar una caracterización genotípica y fenotípica preliminar de los mutantes foliares encontrados, y (3) estudiar con un mayor grado de detalle aquellos que se considerasen de especial interés. El rasgo fenotípico que se consideró más importante *a priori* fue la perturbación de la simetría bilateral, por haber sido muy poco estudiado y estar muy poco representado en las poblaciones de mutantes disponibles, ello a pesar de que esta propiedad morfológica es una de las más conspicuas de los seres vivos en general y de las hojas de las plantas en particular. Solo uno de los mutantes foliares identificados mostró hojas con asimetría bilateral: la línea SALK_047972, cuya caracterización ha constituido el grueso del trabajo realizado en esta Tesis, que ha incluido la confirmación de la identidad del gen causante de su fenotipo mutante, al que hemos llamado *DESIGUAL1* (*DEAL1*), y su análisis genético, filogenético y molecular. Hemos definido el número de miembros de la familia

génica a la que pertenece *DEAL1*, obtenido sus alelos mutantes y estudiado sus interacciones genéticas intra y extrafamiliares. Nuestro objetivo último era proponer un modelo que explicase el fenotipo de los mutantes *deal* y en particular la contribución de los genes de la familia DEAL al desarrollo de la hoja de Arabidopsis y eventualmente, de la planta en su conjunto.

IV.- BIBLIOGRAFÍA DE LA INTRODUCCIÓN

IV.- BIBLIOGRAFÍA DE LA INTRODUCCIÓN

Ajjawi, I., Lu, Y., Savage, L.J., Bell, S.M., y Last, R.L. (2010). Large-scale reverse genetics in Arabidopsis: case studies from the Chloroplast 2010 Project. *Plant Physiology* **152,** 529-540.

Alberts, B., Bray, D., Lewis, J., Raff, M., Roberts, K., y Watson, J.D. (1994). *Molecular Biology of the Cell, 3rd edition*. Garland Publishing.

Alonso, J.M., Stepanova, A.N., Leisse, T.J., Kim, C.J., Chen, H., Shinn, P., Stevenson, D.K., Zimmerman, J., Barajas, P., Cheuk, R., Gadrinab, C., Heller, C., Jeske, A., Koesema, E., Meyers, C.C., Parker, H., Prednis, L., Ansari, Y., Choy, N., Deen, H., Geralt, M., Hazari, N., Hom, E., Karnes, M., Mulholland, C., Ndubaku, R., Schmidt, I., Guzman, P., Aguilar-Henonin, L., Schmid, M., Weigel, D., Carter, D.E., Marchand, T., Risseeuw, E., Brogden, D., Zeko, A., Crosby, W.L., Berry, C.C., y Ecker, J.R. (2003). Genome-wide insertional mutagenesis of *Arabidopsis thaliana. Science* **301,** 653-657.

Alonso, J.M., y Ecker, J.R. (2006). Moving forward in reverse: genetic technologies to enable genome-wide phenomic screens in *Arabidopsis. Nature Reviews Genetics* **7,** 524-536.

Arnold, C.N., Xia, Y., Lin, P., Ross, C., Schwander, M., Smart, N.G., Muller, U., y Beutler, B. (2011). Rapid identification of a disease allele in mouse through whole genome sequencing and bulk segregation analysis. *Genetics* **187,** 633-641.

Austin, R.S., Vidaurre, D., Stamatiou, G., Breit, R., Provart, N.J., Bonetta, D., Zhang, J., Fung, P., Gong, Y., Wang, P.W., McCourt, P., y Guttman, D.S. (2011). Next-generation mapping of Arabidopsis genes. *Plant Journal* **67,** 715-725.

Azpiroz-Leehan, R., y Feldmann, K.A. (1997). T-DNA insertion mutagenesis in *Arabidopsis*: going back and forth. *Trends in Genetics* **13,** 152-156.

Barkoulas, M., Hay, A., Kougioumoutzi, E., y Tsiantis, M. (2008). A developmental framework for dissected leaf formation in the *Arabidopsis* relative *Cardamine hirsuta. Nature Genetics* **40,** 1136-1141.

Bayer, E.M., Smith, R.S., Mandel, T., Nakayama, N., Sauer, M., Prusinkiewicz, P., y Kuhlemeier, C. (2009). Integration of transport-based models for phyllotaxis and midvein formation. *Genes and Development* **23,** 373-784.

Becraft, P.W. (1999). Development of the leaf epidermis. *Current Topics in Developmental Biology* **45,** 1-40.

Beemster, G.T., De Veylder, L., Vercruysse, S., West, G., Rombaut, D., Van Hummelen, P., Galichet, A., Gruissem, W., Inzé, D., y Vuylsteke, M. (2005). Genome-wide analysis of gene expression profiles associated with cell cycle transitions in growing organs of Arabidopsis. *Plant Physiology* **138,** 734-743.

Beemster, G.T., Vercruysse, S., De Veylder, L., Kuiper, M., e Inzé, D. (2006). The *Arabidopsis* leaf as a model system for investigating the role of cell cycle regulation in organ growth. *Journal of Plant Research* **119,** 43-50.

Beerling, D.J. (2005). Leaf evolution: gases, genes and geochemistry. *Annals of Botany* **96,** 345-352.

Benkova, E., Ivanchenko, M.G., Friml, J., Shishkova, S., y Dubrovsky, J.G. (2009). A morphogenetic trigger: is there an emerging concept in plant developmental biology? *Trends in Plant Science* **14,** 189-193.

Berná, G., Robles, P., y Micol, J.L. (1999). A mutational analysis of leaf morphogenesis in *Arabidopsis thaliana. Genetics* **152,** 729-742.

Bhalerao, R.P., y Bennett, M.J. (2003). The case for morphogens in plants. *Nature Cell Biology* **5,** 939-943.

Bilsborough, G.D., Runions, A., Barkoulas, M., Jenkins, H.W., Hasson, A., Galinha, C., Laufs, P., Hay, A., Prusinkiewicz, P., y Tsiantis, M. (2011). Model for the regulation of *Arabidopsis*

thaliana leaf margin development. *Proceedings of the National Academy of Sciences of the USA* **108,** 3424-3429.

Blein, T., Pulido, A., Vialette-Guiraud, A., Nikovics, K., Morin, H., Hay, A., Johansen, I.E., Tsiantis, M., y Laufs, P. (2008). A conserved molecular framework for compound leaf development. *Science* **322,** 1835-1839.

Blein, T., Hasson, A., y Laufs, P. (2010). Leaf development: what it needs to be complex. *Current Opinion in Plant Biology* **13,** 75-82.

Blein, T., Pautot, V., y Laufs, P. (2013). Combinations of mutations sufficient to alter *Arabidopsis* leaf dissection. *Plants* **2,** 230-247.

Bock, G.R., y Marsh, J. (1991). *Biological asymmetry and handedness*. John Wiley & Sons.

Bogre, L., Magyar, Z., y Lopez-Juez, E. (2008). New clues to organ size control in plants. *Genome Biology* **9,** 226.

Bolker, J.A. (1995). Model systems in developmental biology. *BioEssays* **17,** 451-455.

Bowman, J.L., Eshed, Y., y Baum, S.F. (2002). Establishment of polarity in angiosperm lateral organs. *Trends in Genetics* **18,** 134-141.

Boyce, C.K. (2010). The evolution of plant development in a paleontological context. *Current Opinion in Plant Biology* **13,** 102-107.

Braybrook, S.A., y Kuhlemeier, C. (2010). How a plant builds leaves. *Plant Cell* **22,** 1006-1018.

Breuninger, H., y Lenhard, M. (2010). Control of tissue and organ growth in plants. *Current Topics in Developmental Biology* **91,** 185-220.

Byrne, M., Timmermans, M., Kidner, C., y Martienssen, R. (2001). Development of leaf shape. *Current Opinion in Plant Biology* **4,** 38-43.

Byrne, M.E., Barley, R., Curtis, M., Arroyo, J.M., Dunham, M., Hudson, A., y Martienssen, R.A. (2000). *asymmetric leaves1* mediates leaf patterning and stem cell function in Arabidopsis. *Nature* **408,** 967-971.

Byrne, M.E., Simorowski, J., y Martienssen, R.A. (2002). *ASYMMETRIC LEAVES1* reveals *knox* gene redundancy in *Arabidopsis. Development* **129,** 1957-1965.

Campos-Ortega, J.A. (1994). *Evolución histórica de la Biología del desarrollo*. En *Descifrar la vida.* Casadesús, J., y Ruiz Berraquero, F. (eds.). Universidad de Sevilla.

Candela, H., Martínez-Laborda, A., y Micol, J.L. (1999). Venation pattern formation in *Arabidopsis thaliana* vegetative leaves. *Developmental Biology* **205,** 205-216.

Candela, H., Casanova-Sáez, R., y Micol, J.L. (2015). Getting started in mapping-by-sequencing. *Journal of Integrative Plant Biology* **57,** 606-612.

Carpenter, A.E., y Sabatini, D.M. (2004). Systematic genome-wide screens of gene function. *Nature Reviews Genetics* **5,** 11-22.

Celniker, S.E., y Rubin, G.M. (2003). The *Drosophila melanogaster* genome. *Annual Review of Genomics and Human Genetics* **4,** 89-117.

Cnops, G., Wang, X., Linstead, P., Van Montagu, M., Van Lijsebettens, M., y Dolan, L. (2000). *TORNADO1* and *TORNADO2* are required for the specification of radial and circumferential pattern in the *Arabidopsis* root. *Development* **127,** 3385-3394.

Cnops, G., Neyt, P., Raes, J., Petrarulo, M., Nelissen, H., Malenica, N., Luschnig, C., Tietz, O., Ditengou, F., Palme, K., Azmi, A., Prinsen, E., y Van Lijsebettens, M. (2006). The *TORNADO1* and *TORNADO2* genes function in several patterning processes during early leaf development in *Arabidopsis thaliana. Plant Cell* **18,** 852-866.

Coen, E.S., y Meyerowitz, E.M. (1991). The war of the whorls: genetic interactions controlling flower development. *Nature* **353,** 31-37.

Corley, S.B., Carpenter, R., Copsey, L., y Coen, E. (2005). Floral asymmetry involves an interplay between TCP and MYB transcription factors in *Antirrhinum. Proceedings of the National Academy of Sciences of the USA* **102,** 5068-5073.

Coyne, J.A. (1987). Lack of response to selection for directional asymmetry in *Drosophila melanogaster*. *Journal of Heredity* **78,** 119.

Cronk, Q.C. (2001). Plant evolution and development in a post-genomic context. *Nature Reviews Genetics* **2,** 607-619.

Champagne, C., y Sinha, N. (2004). Compound leaves: equal to the sum of their parts? *Development* **131,** 4401-4412.

Chevalier, D., Batoux, M., Fulton, L., Pfister, K., Yadav, R.K., Schellenberg, M., y Schneitz, K. (2005). *STRUBBELIG* defines a receptor kinase-mediated signaling pathway regulating organ development in *Arabidopsis. Proceedings of the National Academy of Sciences of the USA* **102,** 9074-9079.

Child, C.M. (1941). *Patterns and problems of development*. University of Chicago Press.

Chitwood, D.H., Headland, L.R., Ranjan, A., Martínez, C.C., Braybrook, S.A., Koenig, D.P., Kuhlemeier, C., Smith, R.S., y Sinha, N.R. (2012a). Leaf asymmetry as a developmental constraint imposed by auxin-dependent phyllotactic patterning. *Plant Cell* **24,** 2318-2327.

Chitwood, D.H., Naylor, D.T., Thammapichai, P., Weeger, A.C., Headland, L.R., y Sinha, N.R. (2012b). Conflict between intrinsic leaf asymmetry and phyllotaxis in the resupinate leaves of *Alstroemeria psittacina. Frontiers in Plant Science* **3,** Article 182.

Cho, H.T., y Cosgrove, D.J. (2000). Altered expression of expansin modulates leaf growth and pedicel abscission in *Arabidopsis thaliana. Proceedings of the National Academy of Sciences of the USA* **97,** 9783-9788.

Davidson, E.H. (1994). Molecular biology of embryonic development: how far have we come in the last ten years? *BioEssays* **16,** 603-615.

de Reuille, P.B., Bohn-Courseau, I., Ljung, K., Morin, H., Carraro, N., Godin, C., y Traas, J. (2006). Computer simulations reveal properties of the cell-cell signaling network at the shoot apex in *Arabidopsis. Proceedings of the National Academy of Sciences of the USA* **103,** 1627-1632.

De Veylder, L., Beeckman, T., Beemster, G.T., Krols, L., Terras, F., Landrieu, I., van der Schueren, E., Maes, S., Naudts, M., e Inzé, D. (2001). Functional analysis of cyclin-dependent kinase inhibitors of Arabidopsis. *Plant Cell* **13,** 1653-1668.

DeYoung, B.J., Bickle, K.L., Schrage, K.J., Muskett, P., Patel, K., y Clark, S.E. (2006). The CLAVATA1-related BAM1, BAM2 and BAM3 receptor kinase-like proteins are required for meristem function in *Arabidopsis. Plant Journal* **45,** 1-16.

Dhondt, S., Van Haerenborgh, D., Van Cauwenbergh, C., Merks, R.M., Philips, W., Beemster, G.T., e Inzé, D. (2012). Quantitative analysis of venation patterns of Arabidopsis leaves by supervised image analysis. *Plant Journal* **69,** 553-563.

Dinneny, J.R., Yadegari, R., Fischer, R.L., Yanofsky, M.F., y Weigel, D. (2004). The role of *JAGGED* in shaping lateral organs. *Development* **131,** 1101-1110.

Donnelly, P.M., Bonetta, D., Tsukaya, H., Dengler, R.E., y Dengler, N.G. (1999). Cell cycling and cell enlargement in developing leaves of *Arabidopsis. Developmental Biology* **215,** 407-419.

Dubrovsky, J.G., Sauer, M., Napsucialy-Mendivil, S., Ivanchenko, M.G., Friml, J., Shishkova, S., Celenza, J., y Benkova, E. (2008). Auxin acts as a local morphogenetic trigger to specify lateral root founder cells. *Proceedings of the National Academy of Sciences of the USA* **105,** 8790-8794.

Emery, J.F., Floyd, S.K., Alvarez, J., Eshed, Y., Hawker, N.P., Izhaki, A., Baum, S.F., y Bowman, J.L. (2003). Radial patterning of *Arabidopsis* shoots by class III *HD-ZIP* and *KANADI* genes. *Current Biology* **13,** 1768-1774.

Endress, P.K. (2012). The immense diversity of floral monosymmetry and asymmetry across angiosperms. *Botanical Review* **78,** 345-397.

Endrizzi, K., Moussian, B., Haecker, A., Levin, J.Z., y Laux, T. (1996). The *SHOOT MERISTEMLESS* gene is required for maintenance of undifferentiated cells in *Arabidopsis* shoot and floral meristems and acts at a different regulatory level than the meristem genes *WUSCHEL* and *ZWILLE. Plant Journal* **10,** 967-979.

Eshed, Y., Izhaki, A., Baum, S.F., Floyd, S.K., y Bowman, J.L. (2004). Asymmetric leaf development and blade expansion in *Arabidopsis* are mediated by KANADI and YABBY activities. *Development* **131,** 2997-3006.

Feldmann, K.A., Marks, M.D., Christianson, M.L., y Quatrano, R.S. (1989). A dwarf mutant of *Arabidopsis* generated by T-DNA insertion mutagenesis. *Science* **243,** 1351-1354.

Feldmann, K.A. (1991). T-DNA insertion mutagenesis in *Arabidopsis*: mutational spectrum. *Plant Journal* **1,** 71-82.

Finkel, E. (2009). Imaging. With 'phenomics', plant scientists hope to shift breeding into overdrive. *Science* **325,** 380-381.

Finnerty, J.R. (2003). The origins of axial patterning in the metazoa: how old is bilateral symmetry? *International Journal of Developmental Biology* **47,** 523-529.

Galbiati, M., Moreno, M.A., Nadzan, G., Zourelidou, M., y Dellaporta, S.L. (2000). Large-scale T-DNA mutagenesis in *Arabidopsis* for functional genomic analysis. *Functional and Integrative Genomics* **1,** 25-34.

Galego, L., y Almeida, J. (2002). Role of *DIVARICATA* in the control of dorsoventral asymmetry in *Antirrhinum* flowers. *Genes and Development* **16,** 880-891.

García-Bellido, A. (1986). *Genetic analysis of morphogenesis*. En *Genetics, development and evolution*. Gustafson, J.P., Stebbins, G.L., y Ayala, F.J. (eds.). Plenum Publishing Corporation.

Gifford, E., y Foster, A. (1989). *Morphology and evolution of vascular plants*. W.H. Freeman & Co.

Gilbert, S.F. (2003). *Developmental Biology, 7th edition*. Sinauer Associates.

Goecks, J., Nekrutenko, A., y Taylor, J. (2010). Galaxy: a comprehensive approach for supporting accessible, reproducible, and transparent computational research in the life sciences. *Genome Biology* **11,** R86.

Gonzalez, N., Vanhaeren, H., e Inzé, D. (2012). Leaf size control: complex coordination of cell division and expansion. *Trends in Plant Science* **17,** 332-340.

Govind, C.K., y Pearce, J. (1989). Critical period for determining claw asymmetry in developing lobsters. *Development and Cellular Biology* **249,** 31-35.

Green, A.A., Kennaway, J.R., Hanna, A.I., Bangham, J.A., y Coen, E. (2010). Genetic control of organ shape and tissue polarity. *PLOS Biology* **8,** e1000537.

Grunwald, D.J., y Eisen, J.S. (2002). Headwaters of the zebrafish — emergence of a new model vertebrate. *Nature Reviews Genetics* **3,** 717-724.

Guenot, B., Bayer, E., Kierzkowski, D., Smith, R.S., Mandel, T., Zadnikova, P., Benkova, E., y Kuhlemeier, C. (2012). PIN1-independent leaf initiation in Arabidopsis. *Plant Physiology* **159,** 1501-1510.

Ha, C.M., Jun, J.H., Nam, H.G., y Fletcher, J.C. (2007). *BLADE-ON-PETIOLE1* and *2* control Arabidopsis lateral organ fate through regulation of LOB domain and adaxial-abaxial polarity genes. *Plant Cell* **19,** 1809-1825.

Ha, C.M., Jun, J.H., y Fletcher, J.C. (2010). Control of Arabidopsis leaf morphogenesis through regulation of the *YABBY* and *KNOX* families of transcription factors. *Genetics* **186,** 197-206.

Hay, A., Barkoulas, M., y Tsiantis, M. (2006). ASYMMETRIC LEAVES1 and auxin activities converge to repress *BREVIPEDICELLUS* expression and promote leaf development in *Arabidopsis*. *Development* **133,** 3955-3961.

Hay, A., y Tsiantis, M. (2006). The genetic basis for differences in leaf form between *Arabidopsis thaliana* and its wild relative *Cardamine hirsuta*. *Nature Genetics* **38,** 942-947.

Hay, A.S., Pieper, B., Cooke, E., Mandakova, T., Cartolano, M., Tattersall, A.D., Ioio, R.D., McGowan, S.J., Barkoulas, M., Galinha, C., Rast, M.I., Hofhuis, H., Then, C., Plieske, J., Ganal, M., Mott, R., Martínez-García, J.F., Carine, M.A., Scotland, R.W., Gan, X., Filatov, D.A., Lysak, M.A., y Tsiantis, M. (2014). *Cardamine hirsuta*: a versatile genetic system for comparative studies. *Plant Journal* **78,** 1-15.

Hedges, S.B., Blair, J.E., Venturi, M.L., y Shoe, J.L. (2004). A molecular timescale of eukaryote evolution and the rise of complex multicellular life. *BMC Evolutionary Biology* **4,** 2.

Hickey, L.J. (1979). *A revised classification of the architecture of dicotyledonous leaves*. En *Anatomy of the dicotyledons, 2nd edition.* Metcalfe, C.R., y Chalk, L. (eds.). Clarendon Press.

Hileman, L.C., y Baum, D.A. (2003). Why do paralogs persist? Molecular evolution of *CYCLOIDEA* and related floral symmetry genes in *Antirrhineae* (*Veronicaceae*). *Molecular Biology and Evolution* **20,** 591-600.

Hileman, L.C. (2014). Bilateral flower symmetry — how, when and why? *Current Opinion in Plant Biology* **17,** 146-152.

Holder, N. (1979). Positional information and pattern formation in plant morphogenesis and a mechanism for the involvement of plant hormones. *Journal of Theoretical Biology* **77,** 195-212.

Holwell, S.H. (1998). *Leaf development*. En *Molecular Genetics of Plant Development.* Howell, S.H. (ed.). Cambridge University Press.

Hosken, D.J., Blanckenhorn, W.U., y Ward, P.I. (2000). Developmental stability in yellow dung flies (*Scathophaga stercoraria*): Fluctuating asymmetry, heterozygosity and environmental stress. *Journal of Evolutionary Biology* **13,** 919-926.

Hudson, A. (2000). Development of symmetry in plants. *Annual Review of Plant Physiology and Plant Molecular Biology* **51,** 349-370.

Husbands, A.Y., Chitwood, D.H., Plavskin, Y., y Timmermans, M.C. (2009). Signals and prepatterns: new insights into organ polarity in plants. *Genes and Development* **23,** 1986-1997.

Ichihashi, Y., Kawade, K., Usami, T., Horiguchi, G., Takahashi, T., y Tsukaya, H. (2011). Key proliferative activity in the junction between the leaf blade and leaf petiole of Arabidopsis. *Plant Physiology* **157,** 1151-1162.

Jonsson, H., Heisler, M.G., Shapiro, B.E., Meyerowitz, E.M., y Mjolsness, E. (2006). An auxin-driven polarized transport model for phyllotaxis. *Proceedings of the National Academy of Sciences of the USA* **103,** 1633-1638.

Jover-Gil, S. (2005). Caracterización de genes implicados en la organogénesis foliar en *Arabidopsis thaliana*. Tesis Doctoral. Universidad Miguel Hernández de Elche.

Kalve, S., De Vos, D., y Beemster, G.T. (2014). Leaf development: a cellular perspective. *Frontiers in Plant Science* **5,** 362.

Kasprzewska, A., Carter, R., Swarup, R., Bennett, M., Monk, N., Hobbs, J.K., y Fleming, A. (2015). Auxin influx importers modulate serration along the leaf margin. *Plant Journal* **83,** 705-718.

Kennaway, R., Coen, E., Green, A., y Bangham, A. (2011). Generation of diverse biological forms through combinatorial interactions between tissue polarity and growth. *PLOS Computational Biology* **7,** e1002071.

Kholodenko, B.N., y Herbert, M. (2005). *Systems Biology: Definitions and Perspectives*. En *Topics in Current Genetics.* Alberghina, L., y Westerhoff, H.V. (eds.). Springer-Verlag.

Kidner, C.A., y Martienssen, R.A. (2004). Spatially restricted microRNA directs leaf polarity through ARGONAUTE1. *Nature* **428,** 81-84.

Koenig, D., Bayer, E., Kang, J., Kuhlemeier, C., y Sinha, N. (2009). Auxin patterns *Solanum lycopersicum* leaf morphogenesis. *Development* **136,** 2997-3006.

Koncz, C., Mayerhofer, R., Koncz-Kalman, Z., Nawrath, C., Reiss, B., Redei, G.P., y Schell, J. (1990). Isolation of a gene encoding a novel chloroplast protein by T-DNA tagging in *Arabidopsis thaliana. EMBO Journal* **9,** 1337-1346.

Koornneef, M., y Meinke, D. (2010). The development of Arabidopsis as a model plant. *Plant Journal* **61,** 909-921.

Kuchen, E.E., Fox, S., de Reuille, P.B., Kennaway, R., Bensmihen, S., Avondo, J., Calder, G.M., Southam, P., Robinson, S., Bangham, A., y Coen, E. (2012). Generation of leaf shape through early patterns of growth and tissue polarity. *Science* **335,** 1092-1096.

Kurepa, J., Wang, S., Li, Y., Zaitlin, D., Pierce, A.J., y Smalle, J.A. (2009). Loss of 26S proteasome function leads to increased cell size and decreased cell number in Arabidopsis shoot organs. *Plant Physiology* **150,** 178-189.

Kuromori, T., Wada, T., Kamiya, A., Yuguchi, M., Yokouchi, T., Imura, Y., Takabe, H., Sakurai, T., Akiyama, K., Hirayama, T., Okada, K., y Shinozaki, K. (2006). A trial of phenome analysis using 4000 *Ds*-insertional mutants in gene-coding regions of Arabidopsis. *Plant Journal* **47,** 640-651.

Laibach, F. (1943). *Arabidopsis thaliana* (L.) Heynh. als objekt für genetische und entwicklungsphysiologische Untersuchungen. *Botanische Archiv* **44,** 439-455.

Lee, B.H., Ko, J.H., Lee, S., Lee, Y., Pak, J.H., y Kim, J.H. (2009). The Arabidopsis *GRF-INTERACTING FACTOR* gene family performs an overlapping function in determining organ size as well as multiple developmental properties. *Plant Physiology* **151,** 655-668.

Lee, J., Nam, S., Hwang, S.B., Hong, M., Kwon, J.Y., Joeng, K.S., Im, S.H., Shim, J., y Park, M.C. (2004). Functional genomic approaches using the nematode *Caenorhabditis elegans* as a model system. *Journal of Biochemistry and Molecular Biology* **37,** 107-113.

Li, E., y Davidson, E.H. (2009). Building developmental gene regulatory networks. *Birth Defects Research* **87,** 123-130.

Lin, L., Zhong, S.H., Cui, X.F., Li, J., y He, Z.H. (2012). Characterization of temperature-sensitive mutants reveals a role for receptor-like kinase SCRAMBLED/STRUBBELIG in coordinating cell proliferation and differentiation during Arabidopsis leaf development. *Plant Journal* **72,** 707-720.

Long, J.A., Moan, E.I., Medford, J.I., y Barton, M.K. (1996). A member of the KNOTTED class of homeodomain proteins encoded by the *STM* gene of *Arabidopsis. Nature* **379,** 66-69.

Ludwig, W. (1932). *Das rechts-links problem im tierreich und beim menschen*. Springer.

Luo, D., Carpenter, R., Vincent, C., Copsey, L., y Coen, E. (1996). Origin of floral asymmetry in *Antirrhinum. Nature* **383,** 794-799.

Lyndon, R.F. (1990). *Plant Development*. Unwin Hyman.

Lloyd, J., y Meinke, D. (2012). A comprehensive dataset of genes with a loss-of-function mutant phenotype in Arabidopsis. *Plant Physiology* **158,** 1115-1129.

Mabee, P.M., Ashburner, M., Cronk, Q., Gkoutos, G.V., Haendel, M., Segerdell, E., Mungall, C., y Westerfield, M. (2007). Phenotype ontologies: the bridge between genomics and evolution. *Trends in Ecology and Evolution* **22,** 345-350.

Malinowski, R. (2013). Understanding of leaf development — the science of complexity. *Plants* **2,** 396-415.

Marks, M.D., y Feldmann, K.A. (1989). Trichome development in *Arabidopsis thaliana*. I. T-DNA tagging of the *GLABROUS1* gene. *Plant Cell* **1,** 1043-1050.

Martín-Trillo, M., y Cubas, P. (2010). TCP genes: a family snapshot ten years later. *Trends in Plant Science* **15,** 31-39.

Mathur, J., Szabados, L., Schaefer, S., Grunenberg, B., Lossow, A., Jonas-Straube, E., Schell, J., Koncz, C., y Koncz-Kalman, Z. (1998). Gene identification with sequenced T-DNA tags generated by transformation of *Arabidopsis* cell suspension. *Plant Journal* **13,** 707-716.

Matsubayashi, Y. (2003). Ligand-receptor pairs in plant peptide signaling. *Journal of Cell Science* **116,** 3863-3870.

McConnell, J.R., y Barton, M.K. (1998). Leaf polarity and meristem formation in *Arabidopsis. Development* **125,** 2935-2942.

McConnell, J.R., Emery, J., Eshed, Y., Bao, N., Bowman, J., y Barton, M.K. (2001). Role of *PHABULOSA* and *PHAVOLUTA* in determining radial patterning in shoots. *Nature* **411,** 709-713.

Melaragno, J.E., Mehrotra, B., y Coleman, A.W. (1993). Relationship between endopolyploidy and cell size in epidermal tissue of Arabidopsis. *Plant Cell* **5,** 1661-1668.

Metzker, M.L. (2010). Sequencing technologies — the next generation. *Nature Reviews Genetics* **11,** 31-46.

Meyerowitz, E.M., y Pruitt, R.E. (1985). *Arabidopsis thaliana* and Plant Molecular Genetics. *Science* **229,** 1214-1218.

Meyerowitz, E.M. (1987). *Arabidopsis thaliana. Annual Review of Genetics* **21,** 93-111.

Meyerowitz, E.M. (2002). Plants compared to animals: the broadest comparative study of development. *Science* **295,** 1482-1485.

Micol, J.L. (2009). Leaf development: time to turn over a new leaf? *Current Opinion in Plant Biology* **12,** 9-16.

Minevich, G., Park, D.S., Blankenberg, D., Poole, R.J., y Hobert, O. (2012). CloudMap: a cloud-based pipeline for analysis of mutant genome sequences. *Genetics* **192,** 1249-1269.

Mourier, T., Mollerup, S., Vinner, L., Hansen, T.A., Kjartansdottir, K.R., Guldberg Froslev, T., Snogdal Boutrup, T., Nielsen, L.P., Willerslev, E., y Hansen, A.J. (2015). Characterizing novel endogenous retroviruses from genetic variation inferred from short sequence reads. *Scientific Reports* **5,** 15644.

Nath, U., Crawford, B.C., Carpenter, R., y Coen, E. (2003). Genetic control of surface curvature. *Science* **299,** 1404-1407.

Nicotra, A.B., Leigh, A., Boyce, K., Jones, C.S., Niklas, K.J., Royer, D.L., y Tsukaya, H. (2011). The evolution and functional significance of leaf shape in the angiosperms. *Functional Plant Biology* **38,** 535-552.

Nielsen, R., Paul, J.S., Albrechtsen, A., y Song, Y.S. (2011). Genotype and SNP calling from next-generation sequencing data. *Nature Reviews Genetics* **12,** 443-451.

Nikovics, K., Blein, T., Peaucelle, A., Ishida, T., Morin, H., Aida, M., y Laufs, P. (2006). The balance between the *MIR164A* and *CUC2* genes controls leaf margin serration in *Arabidopsis. Plant Cell* **18,** 2929-2945.

O'Malley, R.C., Alonso, J.M., Kim, C.J., Leisse, T.J., y Ecker, J.R. (2007). An adapter ligation-mediated PCR method for high-throughput mapping of T-DNA inserts in the *Arabidopsis* genome. *Nature Protocols* **2,** 2910-2917.

O'Malley, R.C., y Ecker, J.R. (2010). Linking genotype to phenotype using the Arabidopsis unimutant collection. *Plant Journal* **61,** 928-940.

Osborne, C.P., Beerling, D.J., Lomax, B.H., y Chaloner, W.G. (2004). Biophysical constraints on the origin of leaves inferred from the fossil record. *Proceedings of the National Academy of Sciences of the USA* **101,** 10360-10362.

Ostergaard, L., y Yanofsky, M.F. (2004). Establishing gene function by mutagenesis in *Arabidopsis thaliana. Plant Journal* **39,** 682-696.

Page, D.R., y Grossniklaus, U. (2002). The art and design of genetic screens: *Arabidopsis thaliana. Nature Reviews Genetics* **3,** 124-136.

Palatnik, J.F., Allen, E., Wu, X., Schommer, C., Schwab, R., Carrington, J.C., y Weigel, D. (2003). Control of leaf morphogenesis by microRNAs. *Nature* **425,** 257-263.

Palmer, A.R. (1996). From symmetry to asymmetry: phylogenetic patterns of asymmetry variation in animals and their evolutionary significance. *Proceedings of the National Academy of Sciences of the USA* **93,** 14279-14286.

Palmer, A.R. (2004). Symmetry breaking and the evolution of development. *Science* **306,** 828-833.

Pallakies, H., y Simon, R. (2010). *Positional information in plant development*. En *Encyclopedia of Life Sciences*. John Wiley & Sons.

Parinov, S., y Sundaresan, V. (2000). Functional genomics in *Arabidopsis*: large-scale insertional mutagenesis complements the genome sequencing project. *Current Opinion in Plant Biology* **11,** 157-161.

Pérez-Pérez, J.M., Candela, H., Robles, P., Quesada, V., Ponce, M.R., y Micol, J.L. (2009). Lessons from a search for leaf mutants in *Arabidopsis thaliana. International Journal of Developmental Biology* **53,** 1623-1634.

Piazza, P., Bailey, C.D., Cartolano, M., Krieger, J., Cao, J., Ossowski, S., Schneeberger, K., He, F., de Meaux, J., Hall, N., Macleod, N., Filatov, D., Hay, A., y Tsiantis, M. (2010). *Arabidopsis thaliana* leaf form evolved via loss of *KNOX* expression in leaves in association with a selective sweep. *Current Biology* **20,** 2223-2228.

Pien, S., Wyrzykowska, J., McQueen-Mason, S., Smart, C., y Fleming, A. (2001). Local expression of expansin induces the entire process of leaf development and modifies leaf shape. *Proceedings of the National Academy of Sciences of the USA* **98,** 11812-11817.

Poethig, S. (1989). Genetic mosaics and cell lineage analysis in plants. *Trends in Genetics* **5,** 273-277.

Preston, J.C., y Hileman, L.C. (2009). Developmental genetics of floral symmetry evolution. *Trends in Plant Science* **14,** 147-154.

Purnell, D.J., y Thompson, J.N.J. (1973). Selection for asymmetrical bias in a behavioral character of *Drosophila melanogaster*. *Heredity* **31,** 401-405.

Reinhardt, D., Pesce, E.R., Stieger, P., Mandel, T., Baltensperger, K., Bennett, M., Traas, J., Friml, J., y Kuhlemeier, C. (2003). Regulation of phyllotaxis by polar auxin transport. *Nature* **426,** 255-260.

Reuter, J.A., Spacek, D.V., y Snyder, M.P. (2015). High-throughput sequencing technologies. *Molecular Cell* **58,** 586-597.

Rojas, C.A., Eloy, N.B., Lima Mde, F., Rodrigues, R.L., Franco, L.O., Himanen, K., Beemster, G.T., Hemerly, A.S., y Ferreira, P.C. (2009). Overexpression of the *Arabidopsis* anaphase promoting complex subunit CDC27a increases growth rate and organ size. *Plant Molecular Biology* **71,** 307-318.

Rosso, M.G., Li, Y., Strizhov, N., Reiss, B., Dekker, K., y Weisshaar, B. (2003). An *Arabidopsis thaliana* T-DNA mutagenized population (GABI-Kat) for flanking sequence tag-based reverse genetics. *Plant Molecular Biology* **53,** 247-259.

Royer, D.L., Meyerson, L.A., Robertson, K.M., y Adams, J.M. (2009). Phenotypic plasticity of leaf shape along a temperature gradient in *Acer rubrum*. *PLOS One* **4,** e7653.

Sachs, T. (1991). *Pattern formation in plant tissues*. Cambridge University Press.

Samson, F., Brunaud, V., Balzergue, S., Dubreucq, B., Lepiniec, L., Pelletier, G., Caboche, M., y Lecharny, A. (2002). FLAGdb/FST: a database of mapped flanking insertion sites (FSTs) of *Arabidopsis thaliana* T-DNA transformants. *Nucleic Acids Research* **30,** 94-97.

Sander, J.D., y Joung, J.K. (2014). CRISPR-Cas systems for editing, regulating and targeting genomes. *Nature Biotechnology* **32,** 347-355.

Scarpella, E., Marcos, D., Friml, J., y Berleth, T. (2006). Control of leaf vascular patterning by polar auxin transport. *Genes and Development* **20,** 1015-1027.

Scarpella, E., Barkoulas, M., y Tsiantis, M. (2010). Control of leaf and vein development by auxin. *Cold Spring Harbor Perspectives in Biology* **2,** a001511.

Scheres, B., y Wolkenfelt, H. (1998). The *Arabidopsis* root as a model to study plant development. *Plant Physiology and Biochemistry* **63,** 21-32.

Scheres, B. (2001). Plant cell identity. The role of position and lineage. *Plant Physiology* **125,** 112-114.

Schneeberger, K. (2014). Using next-generation sequencing to isolate mutant genes from forward genetic screens. *Nature Reviews Genetics* **15,** 662-676.

Semiarti, E., Ueno, Y., Tsukaya, H., Iwakawa, H., Machida, C., y Machida, Y. (2001). The *ASYMMETRIC LEAVES2* gene of *Arabidopsis thaliana* regulates formation of a symmetric lamina, establishment of venation and repression of meristem-related homeobox genes in leaves. *Development* **128,** 1771-1783.

Serrano-Cartagena, J., Robles, P., Ponce, M.R., y Micol, J.L. (1999). Genetic analysis of leaf form mutants from the *Arabidopsis* Information Service collection. *Molecular and General Genetics* **261,** 725-739.

Sessions, A., Burke, E., Presting, G., Aux, G., McElver, J., Patton, D., Dietrich, B., Ho, P., Bacwaden, J., Ko, C., Clarke, J.D., Cotton, D., Bullis, D., Snell, J., Miguel, T., Hutchison, D., Kimmerly, B., Mitzel, T., Katagiri, F., Glazebrook, J., Law, M., y Goff, S.A. (2002). A high-throughput Arabidopsis reverse genetics system. *Plant Cell* **14,** 2985-2994.

Sinnot, E.W. (1963). *The problem of organic form*. Yale University Press.

Skopelitis, D.S., Husbands, A.Y., y Timmermans, M.C. (2012). Plant small RNAs as morphogens. *Current Opinion in Cell Biology* **24,** 217-224.

Slack, J.M.W. (2012). *Essential Developmental Biology, 3rd edition*. Wiley-Blackwell.

Smith, B., Ashburner, M., Rosse, C., Bard, J., Bug, W., Ceusters, W., Goldberg, L.J., Eilbeck, K., Ireland, A., Mungall, C.J., Leontis, N., Rocca-Serra, P., Ruttenberg, A., Sansone, S.A., Scheuermann, R.H., Shah, N., Whetzel, P.L., y Lewis, S. (2007). The OBO Foundry: coordinated evolution of ontologies to support biomedical data integration. *Nature Biotechnology* **25,** 1251-1255.

Smith, J.M., y Sondhi, K.C. (1960). The genetics of a pattern. *Genetics* **45,** 1039-1050.

Smith, R.S., Guyomarc'h, S., Mandel, T., Reinhardt, D., Kuhlemeier, C., y Prusinkiewicz, P. (2006). A plausible model of phyllotaxis. *Proceedings of the National Academy of Sciences of the USA* **103,** 1301-1306.

Somerville, C., y Koornneef, M. (2002). A fortunate choice: the history of *Arabidopsis* as a model plant. *Nature Reviews Genetics* **3,** 883-889.

Sonoda, Y., Sako, K., Maki, Y., Yamazaki, N., Yamamoto, H., Ikeda, A., y Yamaguchi, J. (2009). Regulation of leaf organ size by the Arabidopsis RPT2a 19S proteasome subunit. *Plant Journal* **60,** 68-78.

Sozzani, R., y Benfey, P.N. (2011). High-throughput phenotyping of multicellular organisms: finding the link between genotype and phenotype. *Genome Biology* **12,** 219.

Spemann, H. (1938). *Embryonic development and induction*. Yale University Press.

St Johnston, D. (2002). The art and design of genetic screens: *Drosophila melanogaster*. *Nature Reviews Genetics* **3,** 176-188.

Stewart, R., y Derman, H. (1975). Flexibility in ontogeny as shown by the contribution of the shoot apical layers to leaves of periclinal chimeras. *American Journal of Botany* **62,** 935-947.

Szakonyi, D., Van Landeghem, S., Bärenfaller, K., Baeyens, L., Blomme, J., Casanova-Sáez, R., De Bodt, S., Esteve-Bruna, D., Fiorani, F., Gonzalez, N., Grønlund, J., Immink, R.G.H., Jover-Gil, S., Kuwabara, A., Muñoz-Nortes, T., Van Dijk, A.-J., Wilson-Sánchez, D., Buchanan-Wollaston, V., Angenent, G.C., Van de Peer, Y., Inzé, D., Micol, J.L., Gruissem, W., Walsh, S., y Hilson, P. (2015). The KnownLeaf literature curation system captures knowledge about *Arabidopsis* leaf growth and development and facilitates integrated data mining. *Current Plant Biology* **2,** 1-11.

Tanaka, H., Dhonukshe, P., Brewer, P.B., y Friml, J. (2006). Spatiotemporal asymmetric auxin distribution: a means to coordinate plant development. *Cellular and Molecular Life Sciences* **63,** 2738-2754.

Teale, W.D., Paponov, I.A., y Palme, K. (2006). Auxin in action: signalling, transport and the control of plant growth and development. *Nature Reviews Genetics* **7,** 847-859.

The Arabidopsis Genome Initiative (2000). Analysis of the genome sequence of the flowering plant *Arabidopsis thaliana*. *Nature* **408,** 796-815.

Tomescu, A.M. (2009). Megaphylls, microphylls and the evolution of leaf development. *Trends in Plant Science* **14,** 5-12.

Torii, K.U. (2012). Mix-and-match: ligand-receptor pairs in stomatal development and beyond. *Trends in Plant Science* **17,** 711-719.

Townsley, B.T., y Sinha, N.R. (2012). A new development: evolving concepts in leaf ontogeny. *Annual Review of Plant Biology* **63,** 535-562.

Tuinstra, E.J., De Jong, G., y Scharloo, W. (1990). Lack of response to family selection for directional asymmetry in *Drosophila melanogaster*: Left and right are not distinguished in development. *Proceedings of the Royal Society: Biological Sciences* **241,** 146-152.

Turner, S., y Sieburth, L.E. (2002). *Vascular patterning*. En *The Arabidopsis Book*. American Society of Plant Biologists.

Twyman, R.M. (2001). *Developmental Biology*. Bios Scientific Publishers.

Ulker, B., Peiter, E., Dixon, D.P., Moffat, C., Capper, R., Bouche, N., Edwards, R., Sanders, D., Knight, H., y Knight, M.R. (2008). Getting the most out of publicly available T-DNA insertion lines. *Plant Journal* **56,** 665-677.

Vandenberg, L.N., y Levin, M. (2013). A unified model for left-right asymmetry? Comparison and synthesis of molecular models of embryonic laterality. *Developmental Biology* **379,** 1-15.

Vanneste, S., y Friml, J. (2009). Auxin: a trigger for change in plant development. *Cell* **136,** 1005-1016.

Vlad, D., Kierzkowski, D., Rast, M.I., Vuolo, F., Dello Ioio, R., Galinha, C., Gan, X., Hajheidari, M., Hay, A., Smith, R.S., Huijser, P., Bailey, C.D., y Tsiantis, M. (2014). Leaf shape evolution through duplication, regulatory diversification, and loss of a homeobox gene. *Science* **343,** 780-783.

Waites, R., y Hudson, A. (1995). *phantastica*: a gene required for dorsoventrality of leaves in *Antirrhinum majus*. *Development* **121,** 2143-2154.

Walbot, V., y Evans, M.M. (2003). Unique features of the plant life cycle and their consequences. *Nature Reviews Genetics* **4,** 369-379.

Wang, Y., y Chen, R. (2014). Regulation of compound leaf development. *Plants* **3,** 1-17.

Washington, N.L., Haendel, M.A., Mungall, C.J., Ashburner, M., Westerfield, M., y Lewis, S.E. (2009). Linking human diseases to animal models using ontology-based phenotype annotation. *PLOS Biology* **7,** e1000247.

Weigel, D., y Mott, R. (2009). The 1001 genomes project for *Arabidopsis thaliana. Genome Biology* **10,** 107.

Wenzel, C.L., Schuetz, M., Yu, Q., y Mattsson, J. (2007). Dynamics of *MONOPTEROS* and PIN-FORMED1 expression during leaf vein pattern formation in *Arabidopsis thaliana. Plant Journal* **49,** 387-398.

Wilkins, A.S. (1993). *Genetic analysis of animal development, 2nd edition*. John Wiley and Sons.

Williams-Carrier, R., Stiffler, N., Belcher, S., Kroeger, T., Stern, D.B., Monde, R.A., Coalter, R., y Barkan, A. (2010). Use of Illumina sequencing to identify transposon insertions underlying mutant phenotypes in high-copy *Mutator* lines of maize. *Plant Journal* **63,** 167-177.

Wolpert, L. (1969). Positional information and the spatial pattern of cellular differentiation. *Journal of Theoretical Biology* **25,** 1-47.

Wolpert, L. (1971). Positional information and pattern formation. *Current Topics in Developmental Biology* **6,** 183-224.

Woody, S.T., Austin-Phillips, S., Amasino, R.M., y Krysan, P.J. (2007). The *WiscDsLox* T-DNA collection: an Arabidopsis community resource generated by using an improved high-throughput T-DNA sequencing pipeline. *Journal of Plant Research* **120,** 157-165.

Wu, X., Chory, J., y Weigel, D. (2007). Combinations of *WOX* activities regulate tissue proliferation during *Arabidopsis* embryonic development. *Developmental Biology* **309,** 306-316.

Yamaguchi, T., Nukazuka, A., y Tsukaya, H. (2012). Leaf adaxial-abaxial polarity specification and lamina outgrowth: evolution and development. *Plant and Cell Physiology* **53,** 1180-1194.

Zhang, J., Chen, R., Xiao, J., Qian, C., Wang, T., Li, H., Ouyang, B., y Ye, Z. (2007). A single-base deletion mutation in *SlIAA9* gene causes tomato (*Solanum lycopersicum*) *entire* mutant. *Journal of Plant Research* **120,** 671-678.

V.- PUBLICACIONES

Journal of Experimental Botany, Vol. 65, No. 10, pp. 2645–2655, 2014
doi:10.1093/jxb/ert476 Advance Access publication 28 January, 2014

Journal of Experimental Botany
www.jxb.oxfordjournals.org

REVIEW PAPER

Symmetry, asymmetry, and the cell cycle in plants: known knowns and some known unknowns

Tamara Muñoz-Nortes, David Wilson-Sánchez, Héctor Candela and José Luis Micol*

Instituto de Bioingeniería, Universidad Miguel Hernández, Campus de Elche, 03202 Elche, Spain

* To whom correspondence should be adddressed. E-mail: jlmicol@umh.es

Received 24 October 2013; Revised 12 December 2013; Accepted 13 December 2013

Abstract

The body architectures of most multicellular organisms consistently display both symmetry and asymmetry. Here, we discuss some of the available knowledge and open questions on how symmetry and asymmetry appear in several conspicuous plant cells and tissues. We focus, where possible, on the role of genes that participate in the maintenance or the breaking of symmetry and that are directly or indirectly related to the cell cycle, under an organ-centric point of view and with an emphasis on the leaf.

Key words: *Arabidopsis*, asymmetric cell divisions, bilateral symmetry, laterality, symmetry, symmetry breaking.

Introduction

Most living beings exhibit some form of symmetry; examples are all bilaterian animals and many plant leaves, which show bilateral or mirror symmetry, and adult echinoderms and many flowers, which show radial or rotational symmetry. In Biology, however, symmetry is usually imperfect from a geometric perspective, and in not a few cases has been dramatically broken by evolution at the cell, tissue, organ, or whole-body levels. Prototypical examples of both symmetry and symmetry breaking in animal development are provided by vertebrates, whose bodies exhibit a bilaterally symmetrical exterior whereas their internal architecture includes asymmetrically positioned heart and visceral organs (Vandenberg and Levin, 2013), the latter phenomenon being termed developmental chirality, left–right asymmetry, or laterality. The consistent symmetries and asymmetries found in many body plans raise fundamental biological questions on their underlying molecular mechanisms; these questions include the extent of their evolutionary conservation across kingdoms and their causal relationship, if any, with the known symmetries and asymmetries that cells display in shape, movement, outgrowth, and internal distribution of organelles and molecules.

Two of the above-mentioned questions have been addressed in a recent study focused on the functional importance of tubulins in symmetry breaking in distinct and phylogenetically distant biological systems (Lobikin *et al.*, 2012). Tubulins are the proteins that make up and/or contribute to the arrangement of microtubules, one of the most important components of the cytoskeleton. Left-handed helical growth is caused by the *lefty1* and *lefty2* dominant-negative alleles of the *Arabidopsis* genes encoding α-tubulin and Tubgcp2 (a γ-tubulin-associated protein), respectively (Hashimoto, 2002; Thitamadee *et al.*, 2002; Abe *et al.*, 2004). When the same mutations were induced in the *Caenorhabditis elegans*, *Xenopus*, and human orthologues of the above-mentioned genes, these mutations altered very early steps of left–right patterning in nematode and frog embryos, as well as the chirality of cultured human neutrophils (Lobikin *et al.*, 2012), indicating that the origin of laterality is cytoplasmic, ancient, and highly conserved across widely divergent phyla.

Asymmetric cell divisions and the cell cycle in plants

In plants, symmetry breaking can occur at the molecular, subcellular, tissue, organ, and body levels (Li and Bowerman, 2010). At the cellular level, asymmetry exists in cell shapes, cell functions,

and subcellular protein distributions, which together contribute to cell polarity (Nelson, 2003). Asymmetry is also evident in the so-called asymmetric or formative divisions, in which an initial cell divides into two daughter cells that acquire unequal fates (Gunning *et al.*, 1978; Weimer *et al.*, 2012; Smolarkiewicz and Dhonukshe, 2013). Two sister cells can acquire divergent fates as a result of extrinsic factors, such as interactions with neighbouring cells and environmental signals, or of intrinsic cell factors that are inherited unequally. The latter type of asymmetric cell divisions require that organelles and other intracellular components are organized in an asymmetric manner in the mother cell (Horvitz and Herskowitz, 1992; Petricka *et al.*, 2009). The molecular mechanisms that control the asymmetry of cell divisions have been hypothesized to be tightly coupled to cell cycle timing and progression (Zhong, 2008), as asymmetric divisions often depend on cell cycle regulators and are essential for normal plant development and reproduction (De Smet and Beeckman, 2011).

The development of multicellular plants and animals initiates with multiple asymmetric divisions of an initial cell, the zygote, and the subsequent specification and differentiation of distinct cell types in the embryo (Scheres and Benfey, 1999). While cell migration plays an essential role in animal embryos, the rigid walls of plant cells make cell migration impossible. For this reason, the generation of plant tissues and organs relies on the control of the asymmetry and orientation of cell divisions, cell differentiation, and cell expansion (Abrash and Bergmann, 2009; Petricka *et al.*, 2009).

Asymmetric divisions in the zygote and early embryo

In higher plants, the first division of the zygote is asymmetric (Fig. 1A), giving rise to an apical cell, which will form most of the embryo proper, and a basal cell, which will give rise to the hypophysis and the suspensor, the structure that connects the embryo with the maternal tissues (Jürgens, 2001). The correct orientation and asymmetry of the first zygotic division is controlled in *Arabidopsis* by the *GNOM* (*GN*) gene, which encodes an ADP ribosylation factor-GDP/GTP exchange factor (ARF-GEF) that regulates the formation of vesicles in membrane trafficking. The GNOM protein is specifically involved in the endosomal recycling of the auxin-efflux carrier PIN-FORMED1 (PIN1) (Richter *et al.*, 2010). In *gn* mutants, the first division of the zygote is symmetric and the subsequent divisions are also altered (Mayer *et al.*, 1993). In *Arabidopsis*, the *YODA* (*YDA*) gene encodes a mitogen-activated protein kinase kinase kinase (MAPKKK). In loss-of-function *yda* mutants, the zygote also divides symmetrically, and some derivatives of the basal cell become part of the embryo, instead of the suspensor. Conversely, gain of *YDA* function causes excessive proliferation of the suspensor (Lukowitz *et al.*, 2004). Therefore, *GN* and *YDA* are essential in breaking zygote symmetry in *Arabidopsis*. Additional asymmetric cell divisions are important for the establishment of the basic body plan at early stages of embryo development, including the divisions that initiate the formation of epidermal, ground, and vascular tissues (Jürgens, 1995).

Asymmetric divisions in root and shoot development

Establishment of the primary root apical meristem requires the asymmetric division of the hypophysis, the uppermost cell of the suspensor (De Smet *et al.*, 2010), and the formation of lateral roots starts with several asymmetric divisions of pericycle cells (De Smet *et al.*, 2008). The importance of asymmetric divisions in the *Arabidopsis* root is also illustrated

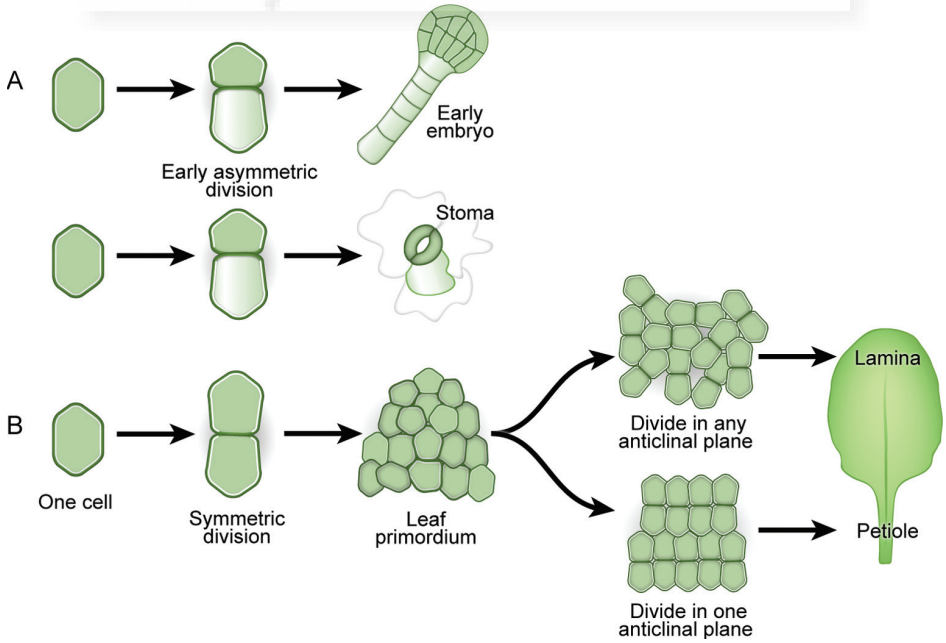

Fig. 1. Two models for the establishment of developmental asymmetry through cell division in plants. The asymmetric architecture of an organ or whole body can be achieved either (A) by one or few very early asymmetric cell divisions (i.e. as in the embryo or the stomatal lineages) or (B) later on by an asymmetrically distributed division property (i.e. division plane orientation in leaf primordia). Drawings are not to scale.

by the cell divisions that lead to the formation of cortical and endodermal cell files, the two lineages that constitute the root ground tissue. In the root meristem, the cortex/endodermal initial cell (CEI) experiences a transverse asymmetric division that gives rise to one stem cell and a cortex/endodermal initial cell daughter (CEID). The CEID subsequently divides asymmetrically in the longitudinal plane to produce two different cell types, the endodermal and cortical cells (Dolan *et al.*, 1993; Walker *et al.*, 2007).

Mutations in the *SHORT-ROOT* (*SHR*) and *SCARECROW* (*SCR*) genes, which encode transcription factors, disrupt the CEID longitudinal asymmetric division, resulting in a single layer of ground tissue. *SHR* seems to be required for the specification of endodermal cells, because the cells derived from the CEID only exhibit cortical properties in *shr* mutants (Benfey *et al.*, 1993). However, in *scr* mutants, the cells derived from the abnormal CEID exhibit traits from both cell types, suggesting that SCR controls the asymmetric division of the CEID rather than the specification of endodermal or cortical identity (Di Laurenzio *et al.*, 1996). *SHR* and *SCR* regulate the spatiotemporal activation of components of the cell cycle network during the asymmetric divisions that initiate the cortical and endodermal root lineages. At the time of CEID periclinal division, SHR and SCR are bound to the promoter of a D-type cyclin, CYCD6;1, indicating that this cyclin is a direct target of these genes. In addition, CEID periclinal divisions are diminished in *cycd6;1* mutants, suggesting that the activation of *CYCD6;1* through the SHR/SCR network is required for the asymmetric divisions giving rise to the cortical and endodermal root lineages (Sozzani *et al.*, 2010).

Other cell cycle genes are regulated by SHR and SCR during lateral root formation. Two cyclin-dependent kinases, CDKB2;1 and CDKB2;2, are expressed in CEI cells (De Smet *et al.*, 2008). Ectopic expression of the *CDKB2;1* and *CDKB2;2* genes in ground tissue causes an increase in endodermal cell divisions, and partially rescues the division defects of *shr* mutants, suggesting that these kinases act downstream of *SHR* and *SCR* in the regulation of asymmetric divisions during lateral root formation (Sozzani *et al.*, 2010).

A recent study of *fewer roots* (*fwr*), a novel recessive allele of the above-mentioned *GN* gene, strongly suggests that *GN* is required for the establishment of the auxin response maximum for lateral root initiation, probably through the regulation of local and global auxin distribution in the root (Okumura *et al.*, 2013). Additional observations suggest a link between auxin, lateral root initiation, and the cell cycle. A CDK inhibitor, *KIP-RELATED PROTEIN2* (*KRP2*), which is expressed specifically in the asymmetrically divided pericycle cells, seems to regulate the G_1 to S transition in an auxin-dependent manner. In the absence of an auxin signal, *KRP2* prevents the cell cycle induction of pericycle cells. Conversely, when auxin is present, the down-regulation of *KRP2* makes the G_1 to S transition of these cells possible (Himanen *et al.*, 2002).

A common mechanism that controls formative divisions in the root and shoot of *Arabidopsis* relies on the activity of CDKA;1, a homologue of the human A-type cyclin-dependent kinase Cdk1. High CDKA;1 levels are required for asymmetric cell divisions in root and shoot tissues (Weimer *et al.*, 2012). RETINOBLASTOMA RELATED1 (RBR1) is an essential target of CDKA;1. Phosphorylation of RBR1 by CDKA;1 inhibits RBR1 and regulates the entry into S phase, allowing asymmetric cell divisions. Two B-type cyclin-dependent kinases, CDKB1;1 and CDKB1;2, seem to be functionally redundant with CDKA;1 (Nowack *et al.*, 2012; Pusch *et al.*, 2012).

Asymmetric divisions in stomatal patterning

Stomatal patterning, both in monocotyledonous and in dicotyledonous plants, initiates with the asymmetric division of an epidermal cell (Fig. 1A) (Larkin *et al.*, 1997; Facette and Smith, 2012). In maize, this symmetry breaking gives rise to the so-called guard mother cell (GMC), which divides symmetrically to produce a pair of guard cells and induces the division of contiguous cells to form the subsidiary cells (Sack and Chen, 2009). In *Arabidopsis*, a protodermal cell divides asymmetrically to yield the meristemoid mother cell (MMC). The MMC divides asymmetrically, giving rise to a larger spacer pavement cell and a smaller meristemoid cell, which in turn can experience additional asymmetric spacing divisions or become a GMC. Like in maize, the subsequent symmetric division of the GMC produces a guard cell pair (Barton, 2007; Bergmann and Sack, 2007).

In *Arabidopsis*, the plant-specific protein BREAKING OF ASYMMETRY IN THE STOMATAL LINEAGE (BASL) regulates asymmetric divisions and accumulates at the cell periphery before the MMC divides asymmetrically. *basl* loss-of-function alleles cause a loss of asymmetry in these divisions, so that the two daughter cells frequently express meristemoid fate markers (Dong *et al.*, 2009). Other mutations that alter the asymmetric divisions characteristic of wild-type stomatal development include *too many mouths* (*tmm*), *speechless* (*spch*), and *yda*. *TMM* encodes a transmembrane leucine repeat-containing receptor-like protein. *tmm* mutants exhibit an increased number of leaf stomata, many of which form clusters of adjacent guard cells, which suggests a defect in the oriented asymmetric divisions that lead to the spacing of stomata in the leaves (Geisler *et al.*, 2000; Bergmann and Sack, 2007). *SPCH* encodes a basic helix–loop–helix (bHLH) transcription factor. In *spch* mutants, the protodermal cell divides symmetrically. The *MUTE* gene also encodes a bHLH protein that acts downstream of *SPCH*, and *mute* alleles promote asymmetric divisions in the MMC stage, forming excessive pavement cells. As a consequence, differentiation to GMC does not occur, and *mute* mutants fail to generate guard cells (MacAlister *et al.*, 2007; Pillitteri *et al.*, 2007). *YDA* represses stomatal initiation in response to spacing regulators. In *yda* mutants, the asymmetry of the spacing divisions of meristemoids is altered, giving rise to clusters of adjacent stomata (Bergmann *et al.*, 2004).

The sequence of asymmetric divisions that leads to the spacing of stomata and the surrounding pavement cells is related to cell cycle progression. The expression of the CDK inhibitor *KIP-RELATED PROTEIN1* (*KRP1*) under the control of the *TMM* promoter produces a reduction in

asymmetric divisions, resulting in enlarged pavement cells (Weinl *et al.*, 2005). The final stage of stomatal development is also related to changes in the timing of the cell cycle. When the GMC divides symmetrically to form a pair of guard cells, the cell cycle in these daughter cells is arrested in the G_1 stage or they exit the cell cycle (G_0) (Bergmann and Sack, 2007). The FOUR LIPS (FLP), MYB88, and FAMA transcription factors are responsible for the end of cell cycling during later steps of stomatal lineage differentiation. *FLP* is expressed before GMC mitosis, and *flp* mutants produce clusters of guard cells because GMC cell cycling continues, instead of guard cell differentiation (Lai *et al.*, 2005).

Several cell cycle regulators have been related to stomatal development. *CDKB1;1* promotes stomatal production by positively regulating mitosis in GMCs (Boudolf *et al.*, 2004a, b). The cyclin-dependent protein kinase *CDT1* and *CELL DIVISION CONTROL 6* (*CDC6*) are expressed in stomatal precursor cells and decide which cells will replicate their DNA. Overexpression of these genes increases the number of stomata in *Arabidopsis* leaves (Castellano *et al.*, 2004). The *Arabidopsis* D-type cyclin CYCD4 controls cell division in the stomatal lineage of the hypocotyl epidermis, and its overexpression increases the generation of stomata (Kono *et al.*, 2007). Another cell cycle regulator, the RBR1 protein, appears to be involved in asymmetric divisions of the stomatal lineage. RBR1 inhibits the activity of E2F-DP, a heterodimeric transcription factor that activates *CDKB1;1*. Inactivation of RBR1 or overexpression of E2F-DP leads to an increased number of asymmetric divisions in the stomatal lineage (Desvoyes *et al.*, 2006). Furthermore, virus-induced silencing of *RBR1* generates stomatal clusters similar to those of *tmm* mutants, suggesting that *TMM* regulates asymmetric cell divisions through the RBR1/E2F-DP pathway (Park *et al.*, 2005).

Asymmetric divisions in pollen development

In male gametophyte development, microspores undergo an asymmetric division that is called pollen mitosis I (PMI), which generates a small generative cell (GC) and a large vegetative cell (VC). The GC divides symmetrically and gives rise to two sperm cells, whereas the VC yields the pollen tube (Mccormick, 1993). Both the *gemini pollen* (*gem*) and *sidecar pollen* (*scp*) mutations alter the asymmetric division that gives rise to GC and VC (PMI), but with different consequences. In the *gem* mutants, both daughter cells express typical VC markers (Twell *et al.*, 1998). *SCP* encodes a LATERAL ORGAN BOUNDARIES DOMAIN/ASYMMETRIC LEAVES 2-like (LBD/ASL) protein (Oh *et al.*, 2010, 2011), whose mutations cause the division of the microspore to be symmetric. As a result, one daughter cell becomes a VC and the other experiences a normal asymmetric division, generating pollen grains with two VCs and one GC (Chen and McCormick, 1996). In addition, *scp* mutants show delayed entry into mitosis (Borg *et al.*, 2009).

The regulation of cell cycle progression is crucial for male gametogenesis in *Arabidopsis*. It has been demonstrated that CDKA;1 also participates in the generation of the GC, and is repressed by the cell cycle inhibitors KRP6 and KRP7 in the VC (Iwakawa *et al.*, 2006). The degradation of KRP6 and KRP7 via SKP1-cullin 1–FBL17 (SCF^{FBL17}) releases CDKA;1 in the GC and allows cell cycle progression (Kim *et al.*, 2008). Moreover, the R2R3 MYB transcription factor DUO POLLEN 1 activates CYCB1;1, the regulatory subunit of CDKA;1 (Brownfield *et al.*, 2009).

Conserved and non-conserved ways of breaking symmetry

A regulatory module that appears to play an important and highly conserved role in asymmetric cell divisions along several eukaryotic model organisms involves the cell division control 42 (Cdc42) protein (Li and Bowerman, 2010). Cdc42 is a GTPase that belongs to the Rho GTPase family, which was first discovered in *Saccharomyces cerevisiae* (Adams *et al.*, 1990). This protein is called Cdc42 or Rac in metazoans and fungi, and RHO-RELATED PROTEIN FROM PLANTS (ROP) in plants (Johnson *et al.*, 2011). Rho GTPases regulate processes such as gene expression, cell polarity, and the cell cycle (Jaffe and Hall, 2005).

Several symmetry-breaking processes are regulated by ROP GTPases in plants (Yang and Lavagi, 2012). In *Arabidopsis*, all Rho-related GTPases belong to the ROP subfamily, and six of the 11 *Arabidopsis* ROPs participate in cell polarity (Yang, 2008). ROP1 participates in the growth of pollen tube tips. ROP1 generates an apical cap in the plasma membrane that is regulated by two feedback mechanisms: a positive feedback that allows the lateral spreading of active ROP1, and a negative feedback that restricts the presence of active ROP1 to the apical cap (Hwang *et al.*, 2010). This apical ROP cap has also been found at the tip of root hairs, suggesting that the mechanism of ROP-mediated polarization is shared by pollen tubes and root hairs (Molendijk *et al.*, 2001). Plant ROP proteins are also involved in the generation of the characteristic shape of pavement epidermal cells through the regulation of the cytoskeleton (Qian *et al.*, 2009). It seems that polarized domains in the plasma membrane of pavement cells have a ROP-based regulation. The activation of a ROP2 effector, ROP-INTERACTIVE CRIB MOTIF-CONTAINING PROTEIN 4 (RIC4), promotes the accumulation of F-actin in the lobes, whereas ROP6 is activated in the indentations, and activates RIC1 to promote microtubule organization. ROP2 inhibits the ROP6–MT pathway, whereas microtubules inhibit ROP2 activation. Thus, these two pathways are mutually exclusive, leading to the formation of the characteristic puzzle-shaped pavement cells (Fu *et al.*, 2005, 2009). Another example of ROP-based regulation is related to the above-mentioned *BASL* gene. Overexpression of *BASL* in petiole and hypocotyl epidermal cells generates cellular outgrowths. There is evidence that the generation of these outgrowths requires the action of ROP GTPases (Dong *et al.*, 2009; Facette and Smith, 2012).

Other symmetry-breaking mechanisms are not conserved in higher plants. Septins are a family of GTPases that form

higher order structures adequate for the control and maintenance of cell asymmetry (Spiliotis and Gladfelter, 2012), and have long been known to play roles in animal and fungal cytokinesis. Four septin genes (*CDC3*, *CDC10*, *CDC11*, and *CDC12*) were identified in yeast in the screen for cell division mutants performed by Lee Hartwell >40 years ago (Hartwell, 1971). Septin genes seem to have been lost in the Plantae lineage, exceptions being some algae: septin homologues have only been found in diatoms and green algae, but not in glaucophytes, red algae, and land plants (Yamazaki *et al.*, 2013). Why septins have been lost and which proteins have taken their role in higher plants remain open questions.

Another interesting question is to what extent different symmetry-breaking mechanisms are conserved across the different plant tissues. Some genes are known to control different asymmetric cell divisions in different tissues. For instance, *YDA* is required for asymmetric divisions in both the zygote and stomatal lineages. In the first case, it enforces the asymmetry of the first zygote division, whereas, in the stomata, it promotes the meristemoid asymmetric division that leads to the spacing of stomata. Another example is *GN*, which is required for the first asymmetric division of the zygote, and also for the asymmetric divisions of pericycle cells during lateral root formation. Some cell cycle regulators are necessary for asymmetric divisions, including CDKA;1, which is required for root and shoot formative divisions, and also for the asymmetric division that forms a GC during pollen development.

Organ symmetry and the cell cycle in plants

In the following sections, we evaluate how changes in the cell cycle can affect the shape and symmetry of plant organs. Altering cell cycle progression in plants might be expected to alter whole-organ morphology, but the relationship between symmetry and the cell cycle does not seem straightforward. Evidence shows that organ shape can be modified by altering the cell proliferation rate or the timing of transition from proliferation to differentiation, but not as much when division plane orientation is impaired. The functions of several genes that link the cell cycle to the acquisition of shape and symmetry in plant organs are discussed.

Leaf bilateral symmetry

Numerous components of the molecular machinery that controls the cell cycle in plant leaves have homologues among animals and fungi. However, the coordination of cell proliferation required to achieve leaf patterning must be controlled by a unique gene regulatory network, since leaves are organs with no counterparts outside the plant kingdom (Townsley and Sinha, 2012). Leaves are determinate organs that develop in a coordinated pattern from leaf primordia in the flank of the shoot apical meristem (SAM). Cells within a primordium continue to divide for a limited period of time, with no fixed patterns of cell division. Cells cease to divide according to a stochastic gradient of termination of cell division, and cell expansion accounts for the final enlargement of the leaf (Donnelly *et al.*, 1999). Chitwood *et al.* (2012) have recently reported a slight, but reproducible deviation from bilateral symmetry in the leaves of tomato and *Arabidopsis*, which the authors attribute to differences between the right and left sides of the primordium at the time of leaf initiation. These differences correlate with the direction of the phyllotactic pattern, emphasizing the impact of an asymmetric distribution of auxin in the meristem on the growth patterns of plant leaves.

Mutations in several genes are known to alter dramatically the bilateral symmetry of *Arabidopsis* leaves (Fig. 2). In wild-type plants, the activity of the class I *knotted1-like homeobox* (*knox1*) genes *KNOTTED-LIKE FROM ARABIDOPSIS 2* (*KNAT2*), *BREVIPEDICELLUS* (*BP*/*KNAT1*), and *KNAT6* is confined to the SAM, where they promote cell division and prevent differentiation (Chuck *et al.*, 1996; Belles-Boix *et al.*, 2006). Genes such as *ASYMMETRIC LEAVES 1* (*AS1*) and *AS2* normally repress the expression of *knox1* genes in the leaves (Byrne *et al.*, 2002). *AS1* and *AS2* encode nuclear proteins with a MYB domain (Byrne *et al.*, 2000; Sun *et al.*, 2002) and a plant-specific AS2/LOB domain (Iwakawa *et al.*, 2002; Shuai *et al.*, 2002), respectively. Both proteins have been reported to form a complex that binds to the *BP* promoter (Xu *et al.*, 2003; Yang *et al.*, 2008), limiting cell proliferation at the leaf base. Failure to limit this cell proliferation in *as1* and *as2* mutants causes the formation of asymmetric lobes in the leaf lamina. In addition to their role in the meristems, *knox1* genes are also important for cell proliferation during the development of compound leaves in *Arabidopsis suecica* and *Arabidopsis halleri*, as shown by the suppression of leaf dissection caused by an artificial microRNA targeting the homologues of the *knox1* gene *SHOOT MERISTEMLESS* in these species (Piazza *et al.*, 2010).

The *BLADE-ON-PETIOLE 1* (*BOP1*) and *BOP2* genes promote lateral organ fate and polarity, and are necessary to maintain a balance between both sides of the leaf. They encode BTB/POZ domain- and ankyrin repeat-containing proteins, suggesting that they play a role in protein–protein interactions (Norberg *et al.*, 2005). BOP1 and BOP2 control leaf morphogenesis through regulation of the *knox1*, *YABBY3* (*YAB3*), and *FILAMENTOUS FLOWER* (*FIL*) genes (Ha *et al.*, 2007, 2010). Indeed, the petiole of *bop1 bop2* double mutants shows ectopic lamina tissue that can be progressively suppressed by eliminating several *knox1* genes, *YAB3*, and *FIL*. This suppression is uneven along the petiole, resulting in asymmetric development. The extent of suppression is dosage dependent, revealing that wild-type symmetry is achieved by tuning the amount of several gene products, some of which regulate cell proliferation activity. BOP1 and BOP2 also repress *JAGGED* (see below), therefore widening the role of these proteins to timing the shift from cell proliferation to differentiation (Norberg *et al.*, 2005).

The *CLAVATA 1* (*CLV1*)-related *BARELY ANY MERISTEM 1* (*BAM1*), *BAM2*, and *BAM3* genes encode receptor-like kinases that are required for several

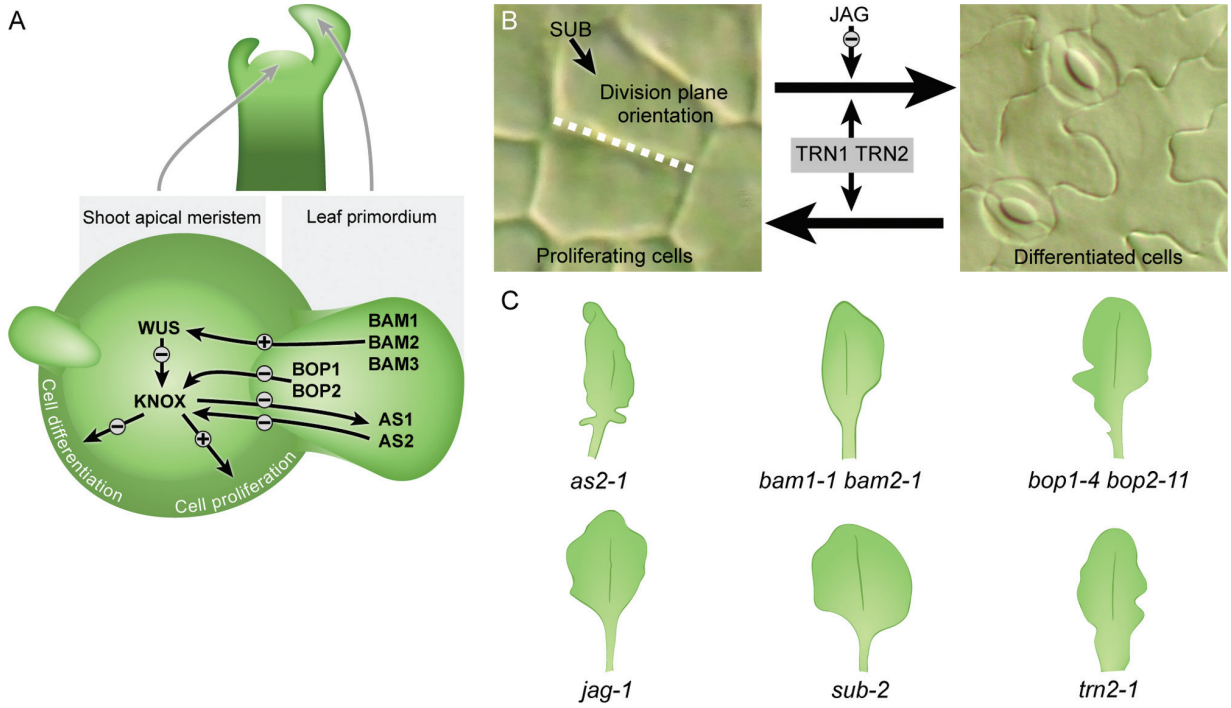

Fig. 2. Genes that control cell proliferation and are required for achieving bilateral symmetry in leaves. (A) Diagram of a shoot apical meristem and emerging leaf primordia, showing genes involved in cell cycling regulation and their functional relationship. (B) Diagram representing several genes necessary to regulate the leaf developmental transition from a proliferating to a differentiated tissue. (A, B) When known, (+) and (–) symbols denote enhancement and repression of activity, respectively. (C) Leaf diagrams of single and double mutants affected in the genes shown in (A) and (B), exhibiting bilateral asymmetry. Drawings are not to scale.

developmental processes, including the control of leaf symmetry. These genes regulate the pool of SAM stem cells, in a way opposite to that of *CLV1*. In the *bam* mutants, growth is unequal at the basal region of the lamina, rendering an asymmetric leaf. Since expression of the *BAM* genes is not restricted to the SAM, the *bam* mutants exhibit a pleiotropic phenotype (DeYoung *et al.*, 2006).

After the establishment of a leaf primordium, proliferation continues until cells differentiate, producing an organ with a high degree of bilateral symmetry. Mutations that alter the correct progression of these events result in loss of symmetry. Such is the case for the *Arabidopsis jagged* loss-of-function mutants. *JAGGED* encodes a protein with a single C2H2 zinc-finger domain that prevents premature differentiation of tissues in a position-dependent manner in lateral organs (Dinneny *et al.*, 2004). Symmetry is also lost in the *tornado* (*trn*) mutants, which present narrow and asymmetric leaf laminae because of a severe reduction of cell number caused by an imbalance between cell proliferation and cell differentiation. *TRN1* and *TRN2* are expressed in the SAM and young leaf primordia and encode proteins involved in signalling (Cnops *et al.*, 2006). TRN1 encodes a protein of unknown function with high similarity to nucleotide-binding oligomerization domain- leucine-rich repeat (NOD-LRR) proteins and is predicted to be cytoplasmic. *TRN1* is a homologue of *DAPK1* (*DEATH-ASSOCIATED PROTEIN KINASE1*). However, the kinase domain is not present, as occurs in the genes required for cellular communication *CLAVATA2* and *TOO MANY MOUTHS* (Nadeau and Sack, 2003). TRN2 belongs to the tetraspanin family, a group of proteins that participate in diverse communication processes, such as cell proliferation, differentiation, and virus and toxin recognition (Hemler, 2003). Genetic analyses revealed that both genes act in the same pathway (Cnops *et al.*, 2006).

Temperature-sensitive mutant alleles of the *STRUBBELIG* (*SUB*) gene develop asymmetric leaves when grown at 30 °C (Lin *et al.*, 2012). *SUB* encodes a receptor-like kinase that is required in some tissues for the orientation of the mitotic division plane (Chevalier *et al.*, 2005). Expression pattern analyses and temperature shift experiments suggest that *SUB* probably mediates a developmental stage-specific signal for early leaf patterning (Lin *et al.*, 2012).

Leaf asymmetry along the proximal–distal axis

Leaf primordia exhibit polarity along three axes: proximal–distal (base–apex), dorsal–ventral (adaxial–abaxial), and medial–lateral (midvein–margin). How asymmetry is generated along the proximal–distal axis is poorly understood, partly because the leaf, unlike the embryo, does not derive from a single cell. Leaf proximal–distal axis establishment seems to occur at the leaf initiation stage, as leaf primordia first grow in the proximal–distal direction. This complicates the identification of the genes responsible for the generation of the proximal–distal axis, since their loss of function is likely to prevent the normal emergence of the organ (Hudson, 2000).

After leaf initiation, a proliferative zone in the primordium produces the cells that will develop into the petiole and the

lamina (Ichihashi *et al.*, 2011). This meristem-like region harbours asymmetric cell divisions in the anticlinal plane perpendicular to the proximal–distal axis. The daughter cells originated from these divisions that fall on the petiole side will undergo more divisions in the same anticlinal plane, whereas the daughter cells that are in the blade side will divide in all anticlinal planes (Fig. 1B).

Several developmental processes do not occur evenly across the lamina, revealing that functional asymmetry exists, which can contribute to explain its proximal–distal morphological asymmetry. One such process is the transition from cell proliferation to cell expansion. This is coupled with the entry into the endoreduplication cycle and occurs basipetally. Donnelly *et al.* (1999) used a *cyc1At$_{pro}$:GUS* reporter construct to monitor cell division at different time points, and found that cell division arrests first at the apex and later at the base of the lamina. The shift from cell proliferation to cell growth might be triggered by the exposure of cells of the leaf primordia to light, which occurs progressively from the tip to the base (Andriankaja *et al.*, 2012). These authors found that genes involved in the retrograde (from chloroplast to nucleus) signalling were differentially expressed during this transition, and also that proliferating primordia treated with norflurazon, a chemical inhibitor of retrograde signalling, have inhibited onset of cell expansion.

Another process that is differentially distributed is endoreduplication, a cell cycle variant in which DNA replicates repeatedly but cytokinesis does not occur, resulting in polyploid cells. Since mitotic cell division and endoreduplication are not simultaneous processes along the leaf, the distribution of cycling and endoreduplicating cells is not homogeneous. In fact, the transition from cell division to endoreduplication proceeds basipetally (Donnelly *et al.*, 1999), making the leaf an asymmetric organ in terms of cell cycle progression along the proximal–distal axis.

Supracellular control of cell division

An impaired division plane orientation during the proliferative phase of leaf development may result in the accumulation of many incorrectly oriented divisions over time and therefore break bilateral symmetry. This assumption comes from the general belief that a strict control of division plane alignment is a prerequisite for ordered spatial development in plants. However, several cases are known of mutants with altered planes of cell division throughout the plant, yet their organ morphology remains unaffected. An example is provided by the *tangled1* (*tan1*) mutation, which alters cell division orientations throughout maize leaf development without altering leaf shape or bilateral symmetry, suggesting that the generation of shape is controlled at a supracellular level, independently from the initial orientation of the new cell walls (Smith *et al.*, 1996). The maize *Tan1* gene encodes a highly basic protein that directly binds to microtubule-containing cytoskeletal structures that are misoriented in dividing *tan1* mutant cells, which suggests that the TAN1 protein participates in the orientation of these cytoskeletal structures (Smith *et al.*, 2001). A cortical ring of microtubules and F-actin—the pre-prophase band (PPB)— is formed in most plant cells during S or G_2 phase, at the future division plane, and persists throughout prophase (Mineyuki, 1999). AtTAN, the *Arabidopsis* orthologue of maize TAN1, co-localizes with the PPB and persists at the cell division site after PPB disassembly. Hence, AtTAN preserves the memory of the PPB throughout mitosis and cytokinesis (Walker *et al.*, 2007).

In addition, mutants in which the cell division plane is severely disrupted can still generate basic elements of plant anatomy (Traas *et al.*, 1995). Such is the case for the Arabidopsis *fass* (*fs*) and *tonneau* (*ton*) mutants. The *TON2/FS* gene encodes the B″ subunit of protein phosphatase 2A, which is essential for the control of cortical cytoskeleton organization and regulates microtubule nucleation (Camilleri *et al.*, 2002; Kirik *et al.*, 2012). Despite the cells of these mutants being unable to form the PPB, all cell types are present in their correct relative positions. Similarly, modulation of the expression of several cyclins was found to alter the plant growth rate, but with little or no impact on plant shape (Doerner *et al.*, 1996; Cockcroft *et al.*, 2000).All these data support the hypothesis that at least some aspects of plant morphogenesis can occur in a cell division-independent manner.

An interesting hypothesis is that shape acquisition, and therefore symmetry, is governed by gradients of cell division rate. Using *Arabidopsis* leaf primordia, Wyrzykowska *et al.* (2002) locally and transiently manipulated the cell division rate, and observed the outcome on leaf morphogenesis. Induction of cyclin genes increased the number of cells at the site of induction, although lamina expansion was reduced, resulting in an asymmetric lamina. Conversely, treatment with the cell cycle inhibitor roscovitine resulted in a local increase in lamina growth, again perturbing bilateral symmetry. These observations suggest that cells respond to gradients of cell cycle regulators, transducing them into gradients of cell division rate, and this response ultimately shapes the organ.

However, cell division-dependent mechanisms fail to explain completely the acquisition of shape, as regulators of cell expansion are also known to contribute to leaf morphogenesis. As an example, expansins are cell wall-loosening proteins necessary for cell growth (McQueen-Mason *et al.*, 1992; Cosgrove, 2000). Pien *et al.* (2001) successfully eliminated the bilateral symmetry of tobacco leaves by locally and transiently overexpressing the cucumber CsEx29 expansin. Auxin and cytokinin were shown to enhance synergistically the accumulation of the cytokinin-inducible soybean mRNA (Cim1) expansin in soybean cell cultures, suggesting that these hormones participate in the coordination of organ growth at the supracellular (or organ) level (Downes *et al.*, 2001).

Asymmetry in zygomorphic flowers

Symmetry is an inherent trait of several organs of flowering plants, such as leaves, roots, shoots, flowers, and fruits. Floral symmetry has attracted the attention of many researchers because of its biological significance in pollination processes. In fact, flowers have traditionally been classified into different categories depending on their symmetry. Polysymmetric or actinomorphic flowers have radial symmetry, and they are

frequently designated as 'symmetric flowers'. Monosymmetric or zygomorphic flowers have bilateral or dorsoventral symmetry, with a single symmetry plane, and are sometimes referred to as 'asymmetric flowers' (Endress, 2001; Almeida and Galego, 2005). Zygomorphy is thought to have evolved many times independently in flowering plants as an adaptation to pollinators (Cubas *et al.*, 2001; Feng *et al.*, 2006).

In *Antirrhinum majus*, flower asymmetry depends on the function of two closely related TCP-box genes, *CYCLOIDEA* (*CYC*) and *DICHOTOMA*, which activate the MYB transcription factor RADIALIS in dorsal areas of the floral meristem (Luo *et al.*, 1996, 1999; Almeida *et al.*, 1997; Corley *et al.*, 2005). Floral meristems produce five stamen primordia in *Antirrhinum*, and the *CYC* gene suppresses the development of dorsal staminodes. Cell cycle-related genes, such as *CYCD3B*, *CYCB1;1*, *CYCB2*, *CDC2C*, and *CDC2D*, are expressed at very low levels at early stages of staminode formation, reflecting reduced growth and cell division (Luo *et al.*, 1996; Gaudin *et al.*, 2000; Preston and Hileman, 2009).

Root and shoot radial symmetry

Maintenance of root and shoot radial symmetry is achieved in part by tightly controlling the orientation, frequency, and timing of cell division in their apical meristems. *MGOUN3/BRUSHY1/TONSOKU* (*MGO3/BRU1/TSK*) is one of the genes required to maintain such a radial pattern (Guyomarc'h *et al.*, 2004), as revealed by the effects of its mutant alleles, which strongly perturb meristematic cell division planes, which in turn cause fasciated shoots and split root tips (Suzuki *et al.*, 2004). The *MGO3/BRU1/TSK* gene encodes a nuclear leucine–glycine–asparagine (LGN) domain protein (Vandenberg and Levin, 2013). LGN repeats are present in animal proteins involved in asymmetric cell division (Suzuki *et al.*, 2004). Expression of *MGO3/BRU1/TSK* is cell cycle dependent and its mutant alleles cause a delayed G_2 to M transition (Suzuki *et al.*, 2005). These results suggest that *MGO3/BRU1/TSK* plays an important role in some aspects of cell cycle progression and cell division orientation, and that these processes are involved in keeping the radial symmetry of roots and shoots.

In the *fasciata1* (*fas1*) and *fas2* mutants, the SAM is radially asymmetric, and the shoot becomes fasciated. Expression of *FAS1* and *FAS2* is high in actively dividing cells (Exner *et al.*, 2006) and the perturbation of shoot radial symmetry seems to be caused by altered cell division patterns in the SAM, which in turn cause irregular SAM cell arrangement (Leyser and Furner, 1992; Kaya *et al.*, 2001). FAS1 and FAS2 are subunits of the *Arabidopsis* counterpart of the human chromatin assembly factor-1 (CAF-1), a heterotrimeric complex that participates in several aspects of cell division, such as nucleosome assembly on newly replicated DNA to reconstitute S-phase chromatin (Smith and Stillman, 1989) and homologous chromosome recombination (Kirik *et al.*, 2006). Loss of *FAS1* function results in reduced type-A CDK activity, inhibits mitotic progression, and promotes a precocious and systemic switch to the endocycle (Ramirez-Parra and Gutierrez, 2007), observations that shed light on the mechanism by which *FAS* genes contribute to proper cytokinesis in the SAM.

The *Arabidopsis TEBICHI* (*TEB*) gene is necessary for controlling cell division and differentiation in meristems. The TEB protein is homologous to *Drosophila* MUS308 and mammalian DNA polymerase θ (POLQ), which restrict DNA double-strand breaks in response to DNA damage. DNA damage responses are constitutively activated in *teb* mutants, which also show fasciated stems. The meristems of *teb* mutants show abnormal patterns of cell division and differentiation, as well as an accumulation of cells expressing *cyclinB1;1*:GUS. This accumulation suggests a defect in the G_2 to M transition triggered by DNA damage and also occurs in other fasciated mutants such as *fas2* and *mgo3/bru1/tsk* (Inagaki *et al.*, 2006).

Breaking symmetries and asymmetries: final remarks

The structural diversity and complexity of living beings, including plants, is the outcome of a complex sequence of developmental events. Complex structures require cell fate decisions that often occur as a consequence of asymmetric cell divisions. Mutants that break such asymmetries, sometimes reverting them to a symmetric condition, have allowed researchers to identify critical steps in the development of plant embryos. Plants have taken advantage of these asymmetries not only to deliver different fates to different cell lineages, but also to generate complex, often beautiful, developmental patterns, as in the spacing of the stomatal complexes of plant leaves.

The beauty and elegance of developmental symmetries is also apparent at the macroscopic, organ, and organism levels. Mutants that break such symmetries have identified cell cycle regulators, highlighting that such symmetries often emerge from the concurrent behaviour of individual cells. How individual cells proliferate and expand in a coordinated manner to produce highly symmetric organs, such as the leaves, with reproducible size and shape, remains one of the most intriguing open questions in Plant Biology.

Acknowledgements

The authors wish to thank S.B. Ingham for his help in preparing the figures, and the anonymous reviewers for their valuable comments. Research in the laboratory of JLM is supported by grants from the Ministerio de Economía y Competitividad of Spain [BFU2011-22825 and CSD2007-00057 (TRANSPLANTA)], the Generalitat Valenciana (PROMETEO/2009/112), and the European Commission [LSHG-CT-2006–037704 (AGRONOMICS)]. HC is a recipient of a Marie Curie International Reintegration Grant (PIRG03-GA-2008–231073). TM-N and DW-S hold pre-doctoral fellowships from the Val I+D program of the Generalitat Valenciana.

References

Abe T, Thitamadee S, Hashimoto T. 2004. Microtubule defects and cell morphogenesis in the *lefty1lefty2* tubulin mutant of *Arabidopsis thaliana*. *Plant and Cell Physiology* **45,** 211–220.

Abrash EB, Bergmann DC. 2009. Asymmetric cell divisions: a view from plant development. *Developmental Cell* **16,** 783–796.

Adams AEM, Johnson DI, Longnecker RM, Sloat BF, Pringle JR. 1990. *CDC42* and *CDC43*, two additional genes involved in budding and the establishment of cell polarity in the yeast *Saccharomyces cerevisiae*. *Journal of Cell Biology* **111,** 131–142.

Almeida J, Galego L. 2005. Flower symmetry and shape in *Antirrhinum*. *International Journal of Developmental Biology* **49,** 527–537.

Almeida J, Rocheta M, Galego L. 1997. Genetic control of flower shape in *Antirrhinum majus*. *Development* **124,** 1387–1392.

Andriankaja M, Dhondt S, De Bodt S, *et al*. 2012. Exit from proliferation during leaf development in *Arabidopsis thaliana*: a not-so-gradual process. *Developmental Cell* **22,** 64–78.

Barton MK. 2007. Making holes in leaves: promoting cell state transitions in stomatal development. *The Plant Cell* **19,** 1140–1143.

Belles-Boix E, Hamant O, Witiak SM, Morin H, Traas J, Pautot V. 2006. *KNAT6*: an *Arabidopsis* homeobox gene involved in meristem activity and organ separation. *The Plant Cell* **18,** 1900–1907.

Benfey PN, Linstead PJ, Roberts K, Schiefelbein JW, Hauser MT, Aeschbacher RA. 1993. Root development in *Arabidopsis*: four mutants with dramatically altered root morphogenesis. *Development* **119,** 57–70.

Bergmann DC, Lukowitz W, Somerville CR. 2004. Stomatal development and pattern controlled by a MAPKK kinase. *Science* **304,** 1494–1497.

Bergmann DC, Sack FD. 2007. Stomatal development. *Annual Review of Plant Biology* **58,** 163–181.

Borg M, Brownfield L, Twell D. 2009. Male gametophyte development: a molecular perspective. *Journal of Experimental Botany* **60,** 1465–1478.

Boudolf V, Barroco R, Engler JD, Verkest A, Beeckman T, Naudts M, Inzé D, De Veylder L. 2004a. B1-type cyclin-dependent kinases are essential for the formation of stomatal complexes in *Arabidopsis thaliana*. *The Plant Cell* **16,** 945–955.

Boudolf V, Vlieghe K, Beemster GTS, Magyar Z, Acosta JAT, Maes S, Van Der Schueren E, Inzé D, De Veylder L. 2004b. The plant-specific cyclin-dependent kinase CDKB1;1 and transcription factor E2Fa-DPa control the balance of mitotically dividing and endoreduplicating cells in *Arabidopsis*. *The Plant Cell* **16,** 2683–2692.

Brownfield L, Hafidh S, Borg M, Sidorova A, Mori T, Twell D. 2009. A plant germline-specific integrator of sperm specification and cell cycle progression. *PLoS Genetics* **5,** e1000430.

Byrne ME, Barley R, Curtis M, Arroyo JM, Dunham M, Hudson A, Martienssen RA. 2000. *Asymmetric leaves1* mediates leaf patterning and stem cell function in *Arabidopsis*. *Nature* **408,** 967–971.

Byrne ME, Simorowski J, Martienssen RA. 2002. *ASYMMETRIC LEAVES1* reveals *knox* gene redundancy in *Arabidopsis*. *Development* **129,** 1957–1965.

Camilleri C, Azimzadeh J, Pastuglia M, Bellini C, Grandjean O, Bouchez D. 2002. The *Arabidopsis TONNEAU2* gene encodes a putative novel protein phosphatase 2A regulatory subunit essential for the control of the cortical cytoskeleton. *The Plant Cell* **14,** 833–845.

Castellano MD, Boniotti MB, Caro E, Schnittger A, Gutierrez C. 2004. DNA replication licensing affects cell proliferation or endoreplication in a cell type-specific manner. *The Plant Cell* **16,** 2380–2393.

Chen YCS, McCormick S. 1996. *sidecar pollen*, an *Arabidopsis thaliana* male gametophytic mutant with aberrant cell divisions during pollen development. *Development* **122,** 3243–3253.

Chevalier D, Batoux M, Fulton L, Pfister K, Yadav RK, Schellenberg M, Schneitz K. 2005. STRUBBELIG defines a receptor kinase-mediated signaling pathway regulating organ development in *Arabidopsis*. *Proceedings of the National Academy of Sciences, USA* **102,** 9074–9079.

Chitwood DH, Headland LR, Ranjan A, Martinez CC, Braybrook SA, Koenig DP, Kuhlemeier C, Smith RS, Sinha NR. 2012. Leaf asymmetry as a developmental constraint imposed by auxin-dependent phyllotactic patterning. *The Plant Cell* **24,** 2318–2327.

Chuck G, Lincoln C, Hake S. 1996. KNAT1 induces lobed leaves with ectopic meristems when overexpressed in *Arabidopsis*. *The Plant Cell* **8,** 1277–1289.

Cnops G, Neyt P, Raes J, *et al*. 2006. The *TORNADO1* and *TORNADO2* genes function in several patterning processes during early leaf development in *Arabidopsis thaliana*. *The Plant Cell* **18,** 852–866.

Cockcroft CE, den Boer BG, Healy JM, Murray JA. 2000. Cyclin D control of growth rate in plants. *Nature* **405,** 575–579.

Corley SB, Carpenter R, Copsey L, Coen E. 2005. Floral asymmetry involves an interplay between TCP and MYB transcription factors in *Antirrhinum*. *Proceedings of the National Academy of Sciences, USA* **102,** 5068–5073.

Cosgrove DJ. 2000. Loosening of plant cell walls by expansins. *Nature* **407,** 321–326.

Cubas P, Coen E, Zapater JMM. 2001. Ancient asymmetries in the evolution of flowers. *Current Biology* **11,** 1050–1052.

De Smet I, Beeckman T. 2011. Asymmetric cell division in land plants and algae: the driving force for differentiation. *Nature Reviews Molecular Cell Biology* **12,** 177–188.

De Smet I, Lau S, Mayer U, Jürgens G. 2010. Embryogenesis—the humble beginnings of plant life. *The Plant Journal* **61,** 959–970.

De Smet I, Vassileva V, De Rybel B, *et al*. 2008. Receptor-like kinase ACR4 restricts formative cell divisions in the *Arabidopsis* root. *Science* **322,** 594–597.

Desvoyes B, Ramirez-Parra E, Xie Q, Chua NH, Gutierrez C. 2006. Cell type-specific role of the retinoblastoma/E2F pathway during *Arabidopsis* leaf development. *Plant Physiology* **140,** 67–80.

DeYoung BJ, Bickle KL, Schrage KJ, Muskett P, Patel K, Clark SE. 2006. The CLAVATA1-related BAM1, BAM2 and BAM3 receptor kinase-like proteins are required for meristem function in Arabidopsis. *The Plant Journal* **45,** 1–16.

Di Laurenzio L, WysockaDiller J, Malamy JE, Pysh L, Helariutta Y, Freshour G, Hahn MG, Feldmann KA, Benfey PN. 1996. The *SCARECROW* gene regulates an asymmetric cell division that is essential for generating the radial organization of the *Arabidopsis* root. *Cell* **86,** 423–433.

Dinneny JR, Yadegari R, Fischer RL, Yanofsky MF, Weigel D. 2004. The role of *JAGGED* in shaping lateral organs. *Development* **131,** 1101–1110.

Doerner P, Jorgensen JE, You R, Steppuhn J, Lamb C. 1996. Control of root growth and development by cyclin expression. *Nature* **380,** 520–523.

Dolan L, Janmaat K, Willemsen V, Linstead P, Poethig S, Roberts K, Scheres B. 1993. Cellular organization of the *Arabidopsis thaliana* root. *Development* **119,** 71–84.

Dong J, MacAlister CA, Bergmann DC. 2009. BASL controls asymmetric cell division in *Arabidopsis*. *Cell* **137,** 1320–1330.

Donnelly PM, Bonetta D, Tsukaya H, Dengler RE, Dengler NG. 1999. Cell cycling and cell enlargement in developing leaves of *Arabidopsis*. *Developmental Biology* **215,** 407–419.

Downes BP, Steinbaker CR, Crowell DN. 2001. Expression and processing of a hormonally regulated beta-expansin from soybean. *Plant Physiology* **126,** 244–252.

Endress PK. 2001. Evolution of floral symmetry. *Current Opinion in Plant Biology* **4,** 86–91.

Exner V, Taranto P, Schonrock N, Gruissem W, Hennig L. 2006. Chromatin assembly factor CAF-1 is required for cellular differentiation during plant development. *Development* **133,** 4163–4172.

Facette MR, Smith LG. 2012. Division polarity in developing stomata. *Current Opinion in Plant Biology* **15,** 585–592.

Feng XZ, Zhao Z, Tian ZX, *et al*. 2006. Control of petal shape and floral zygomorphy in *Lotus japonicus*. *Proceedings of the National Academy of Sciences, USA* **103,** 4970–4975.

Fu Y, Gu Y, Zheng ZL, Wasteneys G, Yang ZB. 2005. *Arabidopsis* interdigitating cell growth requires two antagonistic pathways with opposing action on cell morphogenesis. *Cell* **120,** 687–700.

Fu Y, Xu TD, Zhu L, Wen MZ, Yang ZB. 2009. A ROP GTPase signaling pathway controls cortical microtubule ordering and cell expansion in *Arabidopsis*. *Current Biology* **19,** 1827–1832.

Gaudin V, Lunness PA, Fobert PR, Towers M, Riou-Khamlichi C, Murray JAH, Coen E, Doonan JH. 2000. The expression of *D-cyclin* genes defines distinct developmental zones in snapdragon apical meristems and is locally regulated by the *cycloidea* gene. *Plant Physiology* **122,** 1137–1148.

Geisler M, Nadeau J, Sack FD. 2000. Oriented asymmetric divisions that generate the stomatal spacing pattern in *Arabidopsis* are disrupted by the *too many mouths* mutation. *The Plant Cell* **12,** 2075–2086.

Gunning BES, Hughes JE, Hardham AR. 1978. Formative and proliferative cell divisions, cell differentiation, and developmental changes in meristem of *Azolla* roots. *Planta* **143,** 121–144.

Guyomarc'h S, Vernoux T, Traas J, Zhou DX, Delarue M. 2004. *MGOUN3*, an *Arabidopsis* gene with tetratricopeptide-repeat-related motifs, regulates meristem cellular organization. *Journal of Experimental Botany* **55,** 673–684.

Ha CM, Jun JH, Fletcher JC. 2010. Control of *Arabidopsis* leaf morphogenesis through regulation of the YABBY and KNOX families of transcription factors. *Genetics* **186,** 197–206.

Ha CM, Jun JH, Nam HG, Fletcher JC. 2007. BLADE-ON-PETIOLE 1 and 2 control *Arabidopsis* lateral organ fate through regulation of LOB domain and adaxial–abaxial polarity genes. *The Plant Cell* **19,** 1809–1825.

Hartwell LH. 1971. Genetic control of the cell division cycle in yeast. IV. Genes controlling bud emergence and cytokinesis. *Experimental Cell Research* **69,** 265–276.

Hashimoto T. 2002. Molecular genetic analysis of left–right handedness in plants. *Philosophical Transactions of the Royal Society B: Biological Sciences* **357,** 799–808.

Hemler ME. 2003. Tetraspanin proteins mediate cellular penetration, invasion, and fusion events and define a novel type of membrane microdomain. *Annual Review of Cell and Developmental Biology* **19,** 397–422.

Himanen K, Boucheron E, Vanneste S, Engler JD, Inzé D, Beeckman T. 2002. Auxin-mediated cell cycle activation during early lateral root initiation. *The Plant Cell* **14,** 2339–2351.

Horvitz HR, Herskowitz I. 1992. Mechanisms of asymmetric cell division: two Bs or not two Bs, that is the question. *Cell* **68,** 237–255.

Hudson A. 2000. Development of symmetry in plants. *Annual Review of Plant Physiology and Plant Molecular Biology* **51,** 349–370.

Hwang JU, Wu G, Yan A, Lee YJ, Grierson CS, Yang ZB. 2010. Pollen-tube tip growth requires a balance of lateral propagation and global inhibition of Rho-family GTPase activity. *Journal of Cell Science* **123,** 340–350.

Ichihashi Y, Kawade K, Usami T, Horiguchi G, Takahashi T, Tsukaya H. 2011. Key proliferative activity in the junction between the leaf blade and leaf petiole of Arabidopsis. *Plant Physiology* **157,** 1151–1162.

Inagaki S, Suzuki T, Ohto MA, Urawa H, Horiuchi T, Nakamura K, Morikami A. 2006. *Arabidopsis* TEBICHI, with helicase and DNA polymerase domains, is required for regulated cell division and differentiation in meristems. *The Plant Cell* **18,** 879–892.

Iwakawa H, Shinmyo A, Sekine M. 2006. *Arabidopsis CDKA;1*, a cdc2 homologue, controls proliferation of generative cells in male gametogenesis. *The Plant Journal* **45,** 819–831.

Iwakawa H, Ueno Y, Semiarti E, *et al*. 2002. The *ASYMMETRIC LEAVES2* gene of *Arabidopsis thaliana*, required for formation of a symmetric flat leaf lamina, encodes a member of a novel family of proteins characterized by cysteine repeats and a leucine zipper. *Plant and Cell Physiology* **43,** 467–478.

Jaffe AB, Hall A. 2005. Rho GTPases: biochemistry and biology. *Annual Review of Cell and Developmental Biology* **21,** 247–269.

Johnson JM, Jin M, Lew DJ. 2011. Symmetry breaking and the establishment of cell polarity in budding yeast. *Current Opinion in Genetics and Development* **21,** 740–746.

Jürgens G. 1995. Axis formation in plant embryogenesis: cues and clues. *Cell* **81,** 467–470.

Jürgens G. 2001. Apical–basal pattern formation in *Arabidopsis* embryogenesis. *EMBO Journal* **20,** 3609–3616.

Kaya H, Shibahara KI, Taoka KI, Iwabuchi M, Stillman B, Araki T. 2001. *FASCIATA* genes for chromatin assembly factor-1 in *Arabidopsis* maintain the cellular organization of apical meristems. *Cell* **104,** 131–142.

Kim HJ, Oh SA, Brownfield L, Hong SH, Ryu H, Hwang I, Twell D, Nam HG. 2008. Control of plant germline proliferation by SCF^{FBL17} degradation of cell cycle inhibitors. *Nature* **455,** 1134–1137.

Kirik A, Ehrhardt DW, Kirik V. 2012. TONNEAU2/FASS regulates the geometry of microtubule nucleation and cortical array organization in interphase *Arabidopsis* cells. *The Plant Cell* **24,** 1158–1170.

Kirik A, Pecinka A, Wendeler E, Reiss B. 2006. The chromatin assembly factor subunit FASCIATA1 is involved in homologous recombination in plants. *The Plant Cell* **18,** 2431–2442.

Kono A, Umeda-Hara C, Adachi S, Nagata N, Konomi M, Nakagawa T, Uchimiya H, Umeda M. 2007. The *Arabidopsis* D-type cyclin CYCD4 controls cell division in the stomatal lineage of the hypocotyl epidermis. *The Plant Cell* **19,** 1265–1277.

Lai LB, Nadeau JA, Lucas J, Lee EK, Nakagawa T, Zhao LM, Geisler M, Sack FD. 2005. The *Arabidopsis* R2R3 MYB proteins FOUR LIPS and MYB88 restrict divisions late in the stomatal cell lineage. *The Plant Cell* **17,** 2754–2767.

Larkin JC, Marks MD, Nadeau J, Sack F. 1997. Epidermal cell fate and patterning in leaves. *The Plant Cell* **9,** 1109–1120.

Leyser O, Furner IJ. 1992. Characterisation of three shoot apical meristem mutants of *Arabidopsis thaliana*. *Development* **116,** 397–403.

Li R, Bowerman B. 2010. Symmetry breaking in biology. *Cold Spring Harbor Perspectives in Biology* **2,** a003475.

Lin L, Zhong SH, Cui XF, Li J, He ZH. 2012. Characterization of temperature-sensitive mutants reveals a role for receptor-like kinase SCRAMBLED/STRUBBELIG in coordinating cell proliferation and differentiation during Arabidopsis leaf development. *The Plant Journal* **72,** 707–720.

Lobikin M, Wang G, Xu J, Hsieh YW, Chuang CF, Lemire JM, Levin M. 2012. Early, nonciliary role for microtubule proteins in left–right patterning is conserved across kingdoms. *Proceedings of the National Academy of Sciences, USA* **109,** 12586–12591.

Lukowitz W, Roeder A, Parmenter D, Somerville C. 2004. A MAPKK kinase gene regulates extra-embryonic cell fate in *Arabidopsis*. *Cell* **116,** 109–119.

Luo D, Carpenter R, Copsey L, Vincent C, Clark J, Coen E. 1999. Control of organ asymmetry in flowers of *Antirrhinum*. *Cell* **99,** 367–376.

Luo D, Carpenter R, Vincent C, Copsey L, Coen E. 1996. Origin of floral asymmetry in *Antirrhinum*. *Nature* **383,** 794–799.

MacAlister CA, Ohashi-Ito K, Bergmann DC. 2007. Transcription factor control of asymmetric cell divisions that establish the stomatal lineage. *Nature* **445,** 537–540.

Mayer U, Buttner G, Jürgens G. 1993. Apical–basal pattern formation in the *Arabidopsis* embryo: studies on the role of the *gnom* gene. *Development* **117,** 149–162.

Mccormick S. 1993. Male gametophyte development. *The Plant Cell* **5,** 1265–1275.

McQueen-Mason S, Durachko DM, Cosgrove DJ. 1992. Two endogenous proteins that induce cell wall extension in plants. *The Plant Cell* **4,** 1425–1433.

Mineyuki Y. 1999. The preprophase band of microtubules: its function as a cytokinetic apparatus in higher plants. *International Review of Cytology* **187,** 1–49.

Molendijk AJ, Bischoff F, Rajendrakumar CSV, Friml J, Braun M, Gilroy S, Palme K. 2001. *Arabidopsis thaliana* Rop GTPases are localized to tips of root hairs and control polar growth. *EMBO Journal* **20,** 2779–2788.

Nadeau JA, Sack FD. 2003. Stomatal development: cross talk puts mouths in place. *Trends in Plant Science* **8,** 294–299.

Nelson WJ. 2003. Adaptation of core mechanisms to generate cell polarity. *Nature* **422,** 766–774.

Norberg M, Holmlund M, Nilsson O. 2005. The *BLADE ON PETIOLE* genes act redundantly to control the growth and development of lateral organs. *Development* **132,** 2203–2213.

Nowack MK, Harashima H, Dissmeyer N, Zhao X, Bouyer D, Weimer AK, De Winter F, Yang F, Schnittger A. 2012. Genetic framework of cyclin-dependent kinase function in *Arabidopsis*. *Developmental Cell* **22,** 1030–1040.

Oh SA, Park KS, Twell D, Park SK. 2010. The *SIDECAR POLLEN* gene encodes a microspore-specific LOB/AS2 domain protein required for the correct timing and orientation of asymmetric cell division. *The Plant Journal* **64,** 839–850.

Oh SA, Twell D, Park SK. 2011. *SIDECAR POLLEN* suggests a plant-specific regulatory network underlying asymmetric microspore division in Arabidopsis. *Plant Signaling and Behavior* **6,** 416–419.

Okumura K, Goh T, Toyokura K, Kasahara H, Takebayashi Y, Mimura T, Kamiya Y, Fukaki H. 2013. GNOM/FEWER ROOTS is required for the establishment of an auxin response maximum for arabidopsis lateral root initiation. *Plant and Cell Physiology* **54,** 406–417.

Park JA, Ahn JW, Kim YK, Kim SJ, Kim JK, Kim WT, Pai HS. 2005. Retinoblastoma protein regulates cell proliferation, differentiation, and endoreduplication in plants. *The Plant Journal* **42,** 153–163.

Petricka JJ, Van Norman JM, Benfey PN. 2009. Symmetry breaking in plants: molecular mechanisms regulating asymmetric cell divisions in *Arabidopsis*. *Cold Spring Harbor Perspectives in Biology* **1,** a000497.

Piazza P, Bailey CD, Cartolano M, *et al*. 2010. *Arabidopsis thaliana* leaf form evolved via loss of KNOX expression in leaves in association with a selective sweep. *Current Biology* **20,** 2223–2228.

Pien S, Wyrzykowska J, McQueen-Mason S, Smart C, Fleming A. 2001. Local expression of expansin induces the entire process of leaf development and modifies leaf shape. *Proceedings of the National Academy of Sciences, USA* **98,** 11812–11817.

Pillitteri LJ, Sloan DB, Bogenschutz NL, Torii KU. 2007. Termination of asymmetric cell division and differentiation of stomata. *Nature* **445,** 501–505.

Preston JC, Hileman LC. 2009. Developmental genetics of floral symmetry evolution. *Trends in Plant Science* **14,** 147–154.

Pusch S, Harashima H, Schnittger A. 2012. Identification of kinase substrates by bimolecular complementation assays. *The Plant Journal* **70,** 348–356.

Qian PP, Hou SW, Guo GQ. 2009. Molecular mechanisms controlling pavement cell shape in *Arabidopsis* leaves. *Plant Cell Reports* **28,** 1147–1157.

Ramirez-Parra E, Gutierrez C. 2007. E2F regulates *FASCIATA1*, a chromatin assembly gene whose loss switches on the endocycle and activates gene expression by changing the epigenetic status. *Plant Physiology* **144,** 105–120.

Richter S, Anders N, Wolters H, *et al*. 2010. Role of the *GNOM* gene in *Arabidopsis* apical–basal patterning—from mutant phenotype to cellular mechanism of protein action. *European Journal of Cell Biology* **89,** 138–144.

Sack FD, Chen JG. 2009. Pores in place. *Science* **323,** 592–593.

Scheres B, Benfey PN. 1999. Asymmetric cell division in plants. *Annual Review of Plant Physiology and Plant Molecular Biology* **50,** 505–537.

Shuai B, Reynaga-Pena CG, Springer PS. 2002. The lateral organ boundaries gene defines a novel, plant-specific gene family. *Plant Physiology* **129,** 747–761.

Smith LG, Gerttula SM, Han S, Levy J. 2001. Tangled1: a microtubule binding protein required for the spatial control of cytokinesis in maize. *Journal of Cell Biology* **152,** 231–236.

Smith LG, Hake S, Sylvester AW. 1996. The *tangled-1* mutation alters cell division orientations throughout maize leaf development without altering leaf shape. *Development* **122,** 481–489.

Smith S, Stillman B. 1989. Purification and characterization of CAF-I, a human cell factor required for chromatin assembly during DNA replication *in vitro*. *Cell* **58,** 15–25.

Smolarkiewicz M, Dhonukshe P. 2013. Formative cell divisions: principal determinants of plant morphogenesis. *Plant and Cell Physiology* **54,** 333–342.

Sozzani R, Cui H, Moreno-Risueno MA, Busch W, Van Norman JM, Vernoux T, Brady SM, Dewitte W, Murray JAH, Benfey PN. 2010. Spatiotemporal regulation of cell-cycle genes by SHORTROOT links patterning and growth. *Nature* **466,** 128–132.

Spiliotis ET, Gladfelter AS. 2012. Spatial guidance of cell asymmetry: septin GTPases show the way. *Traffic* **13,** 195–203.

Sun Y, Zhou Q, Zhang W, Fu Y, Huang H. 2002. *ASYMMETRIC LEAVES1*, an *Arabidopsis* gene that is involved in the control of cell differentiation in leaves. *Planta* **214,** 694–702.

Suzuki T, Inagaki S, Nakajima S, *et al*. 2004. A novel *Arabidopsis* gene *TONSOKU* is required for proper cell arrangement in root and shoot apical meristems. *The Plant Journal* **38,** 673–684.

Suzuki T, Nakajima S, Inagaki S, Hirano-Nakakita M, Matsuoka K, Demura T, Fukuda H, Morikami A, Nakamura K. 2005. *TONSOKU* is expressed in S phase of the cell cycle and its defect delays cell cycle progression in *Arabidopsis*. *Plant and Cell Physiology* **46,** 736–742.

Thitamadee S, Tuchihara K, Hashimoto T. 2002. Microtubule basis for left-handed helical growth in *Arabidopsis*. *Nature* **417,** 193–196.

Townsley BT, Sinha NR. 2012. A new development: evolving concepts in leaf ontogeny. *Annual Review of Plant Biology* **63,** 535–562.

Traas J, Bellini C, Nacry P, Kronenberger J, Bouchez D, Caboche M. 1995. Normal differentiation patterns in plants lacking microtubular preprophase bands. *Nature* **375,** 676–677.

Twell D, Park SK, Lalanne E. 1998. Asymmetric division and cell-fate determination in developing pollen. *Trends in Plant Science* **3,** 305–310.

Vandenberg LN, Levin M. 2013. A unified model for left–right asymmetry? Comparison and synthesis of molecular models of embryonic laterality. *Developmental Biology* **379,** 1–15.

Walker KL, Muller S, Moss D, Ehrhardt DW, Smith LG. 2007. Arabidopsis Tangled identifies the division plane throughout mitosis and cytokinesis. *Current Biology* **17,** 1827–1836.

Weimer AK, Nowack MK, Bouyer D, Zhao X, Harashima H, Naseer S, De Winter F, Dissmeyer N, Geldner N, Schnittger A. 2012. RETINOBLASTOMA RELATED1 regulates asymmetric cell divisions in *Arabidopsis*. *The Plant Cell* **24,** 4083–4095.

Weinl C, Marquardt S, Kuijt SJH, Nowack MK, Jakoby MJ, Hulskamp M, Schnittger A. 2005. Novel functions of plant cyclin-dependent kinase inhibitors, ICK1/KRP1, can act non-cell-autonomously and inhibit entry into mitosis. *The Plant Cell* **17,** 1704–1722.

Wyrzykowska J, Pien S, Shen WH, Fleming AJ. 2002. Manipulation of leaf shape by modulation of cell division. *Development* **129,** 957–964.

Xu L, Xu Y, Dong A, Sun Y, Pi L, Huang H. 2003. Novel *as1* and *as2* defects in leaf adaxial–abaxial polarity reveal the requirement for *ASYMMETRIC LEAVES1* and *2* and *ERECTA* functions in specifying leaf adaxial identity. *Development* **130,** 4097–4107.

Yamazaki T, Owari S, Ota S, Sumiya N, Yamamoto M, Watanabe K, Nagumo T, Miyamura S, Kawano S. 2013. Localization and evolution of septins in algae. *The Plant Journal* **74,** 605–614.

Yang JY, Iwasaki M, Machida C, Machida Y, Zhou X, Chua NH. 2008. betaC1, the pathogenicity factor of TYLCCNV, interacts with AS1 to alter leaf development and suppress selective jasmonic acid responses. *Genes and Development* **22,** 2564–2577.

Yang ZB. 2008. Cell polarity signaling in *Arabidopsis*. *Annual Review of Cell and Developmental Biology* **24,** 551–575.

Yang ZB, Lavagi I. 2012. Spatial control of plasma membrane domains: ROP GTPase-based symmetry breaking. *Current Opinion in Plant Biology* **15,** 601–607.

Zhong W. 2008. Timing cell-fate determination during asymmetric cell divisions. *Current Opinion in Neurobiology* **18,** 472–478.

the plant journal

SEB Society for Experimental Biology

The Plant Journal (2014) **79,** 878–891 doi: 10.1111/tpj.12595

RESOURCE

Leaf phenomics: a systematic reverse genetic screen for Arabidopsis leaf mutants

David Wilson-Sánchez[†], Silvia Rubio-Díaz[†], Rafael Muñoz-Viana[†,‡], José Manuel Pérez-Pérez, Sara Jover-Gil, María Rosa Ponce and José Luis Micol*

Instituto de Bioingeniería, Universidad Miguel Hernández, Campus de Elche, 03202 Elche, Spain

Received 16 August 2013; revised 7 June 2014; accepted 9 June 2014; published online 20 June 2014.
*For correspondence (e-mail jlmicol@umh.es).
[†]These authors contributed equally to this work.
[‡]Present address: Department of Plant Biology, Uppsala Biocenter, Swedish University of Agricultural Sciences, 75651 Uppsala, Sweden.

SUMMARY

The study and eventual manipulation of leaf development in plants requires a thorough understanding of the genetic basis of leaf organogenesis. Forward genetic screens have identified hundreds of Arabidopsis mutants with altered leaf development, but the genome has not yet been saturated. To identify genes required for leaf development we are screening the Arabidopsis Salk Unimutant collection. We have identified 608 lines that exhibit a leaf phenotype with full penetrance and almost constant expressivity and 98 additional lines with segregating mutant phenotypes. To allow indexing and integration with other mutants, the mutant phenotypes were described using a custom leaf phenotype ontology. We found that the indexed mutation is present in the annotated locus for 78% of the 553 mutants genotyped, and that in half of these the annotated T-DNA is responsible for the phenotype. To quickly map non-annotated T-DNA insertions, we developed a reliable, cost-effective and easy method based on whole-genome sequencing. To enable comprehensive access to our data, we implemented a public web application named PhenoLeaf (http://genetics.umh.es/phenoleaf) that allows researchers to query the results of our screen, including text and visual phenotype information. We demonstrated how this new resource can facilitate gene function discovery by identifying and characterizing At1g77600, which we found to be required for proximal–distal cell cycle-driven leaf growth, and At3g62870, which encodes a ribosomal protein needed for cell proliferation and chloroplast function. This collection provides a valuable tool for the study of leaf development, characterization of biomass feedstocks and examination of other traits in this fundamental photosynthetic organ.

Keywords: leaf development, reverse genetic screen, gene-indexed leaf mutant collection, leaf mutant database, *Arabidopsis thaliana*, resource.

INTRODUCTION

The isolation of loss-of-function alleles and examination of their phenotypic effects provides a direct and reliable way to assign a function to a gene (Parinov and Sundaresan, 2000; Page and Grossniklaus, 2002; Carpenter and Sabatini, 2004). Although forward genetics has yielded a wealth of *Arabidopsis thaliana* (hereafter Arabidopsis) mutants impaired in leaf development (Feldmann, 1991; Berná *et al.*, 1999; Serrano-Cartagena *et al.*, 1999), reverse genetics became the preferred approach after the sequencing of the Arabidopsis genome (Lloyd and Meinke, 2012). Since then, large-scale phenotyping efforts have allowed researchers to identify gene functions that contribute to the formation of leaves (Kuromori *et al.*, 2006; Ajjawi *et al.*, 2010; Myouga *et al.*, 2010, 2013; Lu *et al.*, 2011).

Efficient reverse genetics has been made possible in Arabidopsis by the availability of large, gene-indexed insertional mutant collections (Galbiati *et al.*, 2000; Samson *et al.*, 2002; Sessions *et al.*, 2002; Alonso *et al.*, 2003; Rosso *et al.*, 2003; Kuromori *et al.*, 2004; Ito *et al.*, 2005; Woody *et al.*, 2007). Together, these collections include hundreds of thousands of T-DNA or transposon insertions mapped to the Columbia-0 (Col-0) reference genome, with

30 990 genes annotated by at least one mutant allele (http://signal.salk.edu/Source/AtTOME_Data_Source.html). To date, 20 803 of these genes are represented by homozygous knockout mutants available from the stock centers. The large Salk Unimutant collection (O'Malley and Ecker, 2010) is particularly useful for reverse genetics screens since it includes two T-DNA alleles of most Arabidopsis genes (http://signal.salk.edu/cgi-bin/homozygotes.cgi).

Public gene-indexed insertional mutant collections allow systematic reverse genetics screens to test the function of all the genes in the genome, rather than a limited set of selected genes (Giaever *et al.*, 2002; Carpenter and Sabatini, 2004; Alonso and Ecker, 2006; O'Malley and Ecker, 2010; Pressman *et al.*, 2012). A systematic reverse genetic screen combines advantages from both forward and reverse genetics. First, it prevents the bias towards a particular gene or type of gene that typically limits reverse genetics; secondly, it more easily reaches saturation of the genome. Usually, the goal of a systematic reverse screen is to produce a list of gene–phenotype pairs and make these data available for the community to query either the gene or the phenotype. These gene–phenotype pairs enable other researchers to perform *in silico* screens for a particular gene or phenotype (Alonso and Ecker, 2006), saving labor and time. In Arabidopsis, several public databases gather this kind of information, including qualitative and quantitative descriptions, and digital images of the phenotype of interest. These databases include: the Chloroplast 2010 Project (http://bioinfo.bch.msu.edu/2010_LIMS; Lu *et al.*, 2011), the RIKEN Arabidopsis Phenome Information Database (http://rarge.psc.riken.jp/phenome/; Kuromori *et al.*, 2006) and the Chloroplast Function Database (http://rarge.psc.riken.jp/chloroplast/; Myouga *et al.*, 2010).

To identify the genes required for leaf development, we initiated a systematic reverse genetic screen using the Salk Unimutant collection (Alonso *et al.*, 2003). So far, 608 non-segregating mutants and 98 segregating lines have been isolated. We described their phenotypes using ontology terms and conducted a preliminary characterization of the genotypes. These data were archived in an online database named PhenoLeaf (http://genetics.umh.es/phenoleaf) to make the data publicly available. To demonstrate the usefulness of our resource data, we identified and characterized two genes not previously related to leaf development. Seeds of the leaf mutants were provided to the Arabidopsis stock centers.

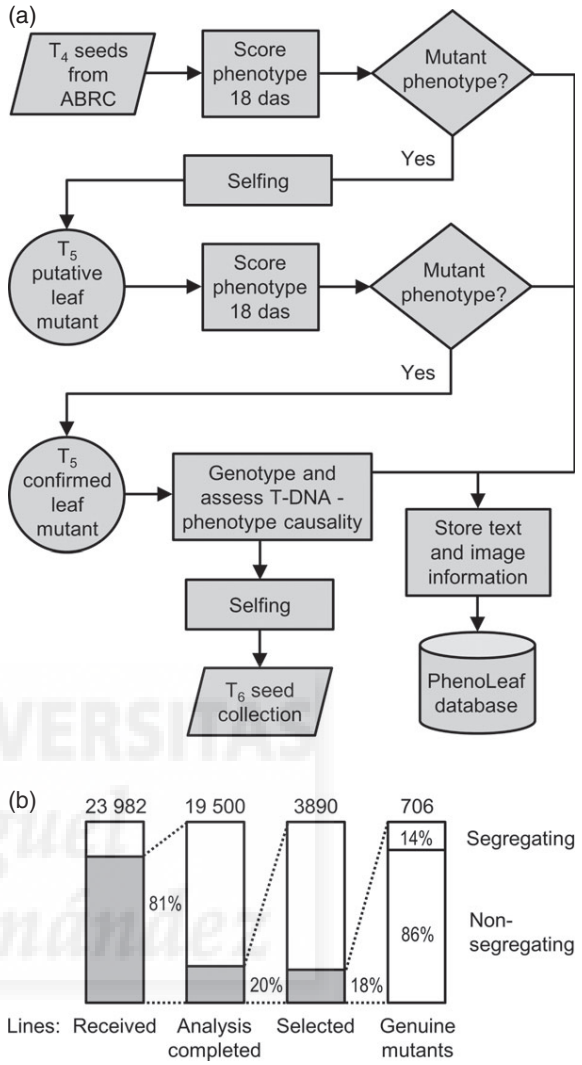

Figure 1. Systematic screen for leaf mutants.
(a) Workflow chart depicting the screening of the T-DNA lines, characterization of the leaf mutants, production of homozygous seeds and storage of the information in the PhenoLeaf database.
(b) Screen status and yield at the time of this publication. The total number of genes is 14 586, of which 6133 are represented by two alleles. Out of 23 982 lines currently available, 19 500 have already been analyzed. We selected 3890 lines because they displayed at least one non-wild-type plant, of which 706 were confirmed as genuine leaf mutants.

RESULTS

Leaf mutant screen

To conduct a comprehensive search for mutations affecting leaf morphology, we are screening all available batches of T_4 homozygous T-DNA lines from the Salk Unimutant collection from the Arabidopsis Biological Resource Center (ABRC). The workflow of our mutant screen is shown in Figure 1(a). Thirty T_4 plants from each line were analyzed because we found that some lines included plants that were not homozygous mutants at the annotated locus (Table S1), consistent with data from Ajjawi *et al.* (2010). Seedlings were grown *in vitro*, as described in Experimental Procedures. Eighteen days after stratification (das), plates were photographed, seedlings were individually analyzed and any morphological leaf abnormality was scored and added to the online database. Lines including at least one plant

with a putative leaf mutant phenotype were selected, and up to three phenotypically mutant plants were transferred into pots and allowed to self-pollinate. Sixteen T_5 seeds obtained from each selfed T_4 plant were sown *in vitro* and pictures were taken of the T_5 rosettes to test the reproducibility of the phenotype.

The screened lines were recorded in the database to document the leaf phenotypes displayed in the T_4 and T_5 generations. When all T_4 plants displayed leaf morphology indistinguishable from that of Col-0, the line was recorded as 'wild-type leaves'. When T_4 plants with leaf abnormalities were found, but we failed to see the same phenotypic traits in the T_5 generation, the line was recorded as 'putative leaf mutant'. When T_4 plants with leaf abnormalities were found, and those same traits were recovered again in the T_5 generation, the line was recorded either as 'confirmed non-segregating mutant' or 'confirmed segregating mutant', depending on the homogeneity of the phenotype across the studied T_5 plants. The putative leaf mutants correspond to lines that we were unable to confirm because their phenotype was subtle in our growth conditions and to false positives due to inferior T_4 seed quality and seedling growth (Figure S1). At the time of writing we had isolated 608 non-segregating and 98 segregating mutant lines, altogether 3.6% of the lines analyzed (Figure 1b). All confirmed non-segregating and segregating leaf mutants are included in Table S2. Non-segregating mutants, hereafter referred to as genuine leaf mutants, were subjected to a detailed phenotypic description and genotyped for the annotated T-DNA insertion (see below).

Table 1 Ontology structure

Entity	Attribute	Values
Rosette	Relative size	Equal to Col-0; increased size; decreased size
	Phyllotaxis	Normal (same as Col-0); abnormal
	Compactness	Equal to Col-0; compact; loose
	Leaf number	Equal to Col-0; increased number; decreased number
Leaf lamina	Relative size	Equal to Col-0; increased size; decreased size
	Symmetry	Symmetrical; asymmetrical
	Shape (2D)[a]	Roundish; ovate; orbicular; oblong; elliptical; lanceolate; linear; spatulate; cuneate; subulate; rhomboid; triangular; heart-shaped; reniform; arrow-shaped
	Shape (3D)[b]	Convex; flat; concave; undulate; involute; revolute; convolute; circinate; reclinate
	Surface	Smooth; rugose
	Color filling	Green; pale green; yellow green; dark green; white; yellow; purple
	Color pattern	Mono-colored; variegated; spotted; blotched; netted
Leaf margin	Shape (2D)[a]	Continuous; crenated; serrated; toothed; lobed; angular
Petiole	Relative length	Equal to Col-0; increased length; decreased length
	Relative width	Equal to Col-0; increased width; decreased width

The first value for each attribute corresponds to the wild-type line Col-0, exception being the leaf lamina entity, attribute shape (2D), where the first two values correspond to Col-0 leaves.
[a]Refers to the plane defined by the leaf proximal–distal and medial–lateral axes (2D, two dimensions).
[b]Refers to the direction defined by the leaf adaxial–abaxial axis (3D, three dimensions).

Ontological description of the genuine leaf mutants

To avoid semantic ambiguity of the phenotypic descriptions and to allow us to index and compare the mutants, their phenotypic traits were described using a controlled vocabulary (Bodenreider and Stevens, 2006). We implemented a leaf-specific ontology (Tables 1 and S3) including existing terms from Plant Ontology (PO) (Jaiswal *et al.*, 2005; http://www.plantontology.org/), Phenotype, Attribute and Trait Ontology (PATO) (Smith *et al.*, 2007; http://obofoundry.org/wiki/index.php/PATO:Main_Page) and others newly proposed and registered in PATO. Every phenotypic trait was documented following an entity–attribute–value (EAV) structure (Figure 2). The ontology descriptions of all the leaf mutants identified so far are included in Table S2 and the PhenoLeaf database.

Examination of the mutant descriptions (Figure 3) shows that we isolated mutants for all the entities and attributes initially established, indicating that we have developed a comprehensive leaf mutant collection and suggesting that many different developmental or maintenance processes that occur in the leaf were hit in our screen. We discovered mutant phenotypes very rarely found in the literature, such as asymmetric leaf laminae, mesophylls with empty patches, protruding primary veins, and leaf numbers twice as high as that in the wild type (some shown in Figure 2), indicating that our screen may have identified previously missed mutations affecting leaf development. No ontological term could be found for some of these phenotypes, which thus fell into the 'other phenotypic traits' category. Also, the different attributes considered were altered with very different frequencies. For example, some leaf traits, such as 'filling color', appeared to be easily altered by single mutations, while others, such as 'lamina symmetry', were very seldom perturbed (Figure 3).

Genotyping and characterization of annotated insertion loci in the genuine leaf mutants

As the T-DNA insertions in the Salk lines are gene indexed, we aimed to confirm whether the leaf mutants isolated in this work were homozygous for the annotated insertion. We genotyped a minimum of five T_5 seedlings obtained by

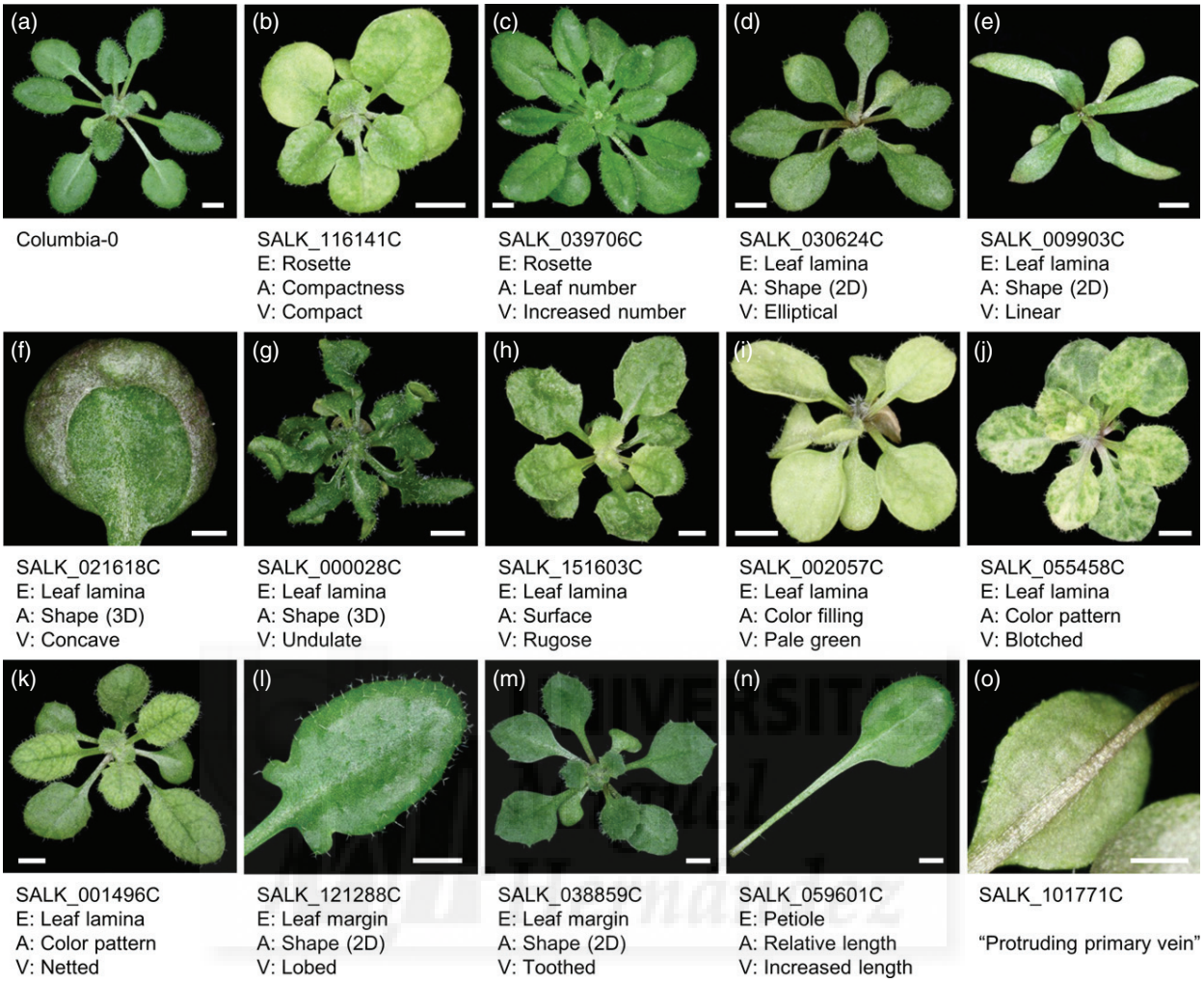

Figure 2. Rosettes and ontological descriptions of some representative leaf mutants.
The first line below each picture indicates the Salk line from which the mutant was isolated. The next three lines describe the most conspicuous trait of the mutant using our ontology. Scale bars correspond to 2 mm. E, Entity; A, Attribute; V, Value. Pictures were taken 21 days after stratification (das).
(b) Example of multiple traits in a single mutant. In addition to having a compact rosette (compactness), the leaf lamina is rounded [shape (2D)] and variegated (color pattern).
(o) Example of a mutant trait for which there is no term in our ontology. Common words are instead used to describe the phenotype.

selfing a single T_4 plant displaying a mutant leaf phenotype, and inferred the genotype of the T_4 parent from the results. Table S2 and the PhenoLeaf database include the genotype for the annotated insertion determined for each line. Seventy-eight per cent of the leaf mutants identified were homozygous for the annotated insertion (Figure 4a), consistent with the data reported by Ajjawi *et al.* (2010). Roughly three-quarters of the confirmed insertions are within transcribed regions and half affect coding sequences (Figure 4b). The abundance of insertions in the transcriptional units decreases with the distance from the transcription start site (TSS), which most likely reflects the distribution of transcript lengths in the genome. Upstream of the TSS, there was a frequency bias towards the proximal 500-bp region.

Gene–phenotype causality in the mutant collection

In the Salk collection, each line contains one annotated T-DNA insertion. However, Alonso *et al.* (2003) estimated an average of 1.5 T-DNA insertions per haploid genome and recent studies showed that T-DNA insertional lines often contain additional, non-annotated base substitutions and structural mutations (De Muyt *et al.*, 2009; Ajjawi *et al.*, 2010; Clark and Krysan, 2010; Dobritsa *et al.*, 2011). In large-scale approaches, evidence of gene–phenotype causality can only be obtained through quick methods due to constraints on resources and throughput. We used four methods to provide evidence of gene–phenotype causality: (i) multiple independent alleles with similar phenotypes, (ii) the same phenotype scored in different large-scale

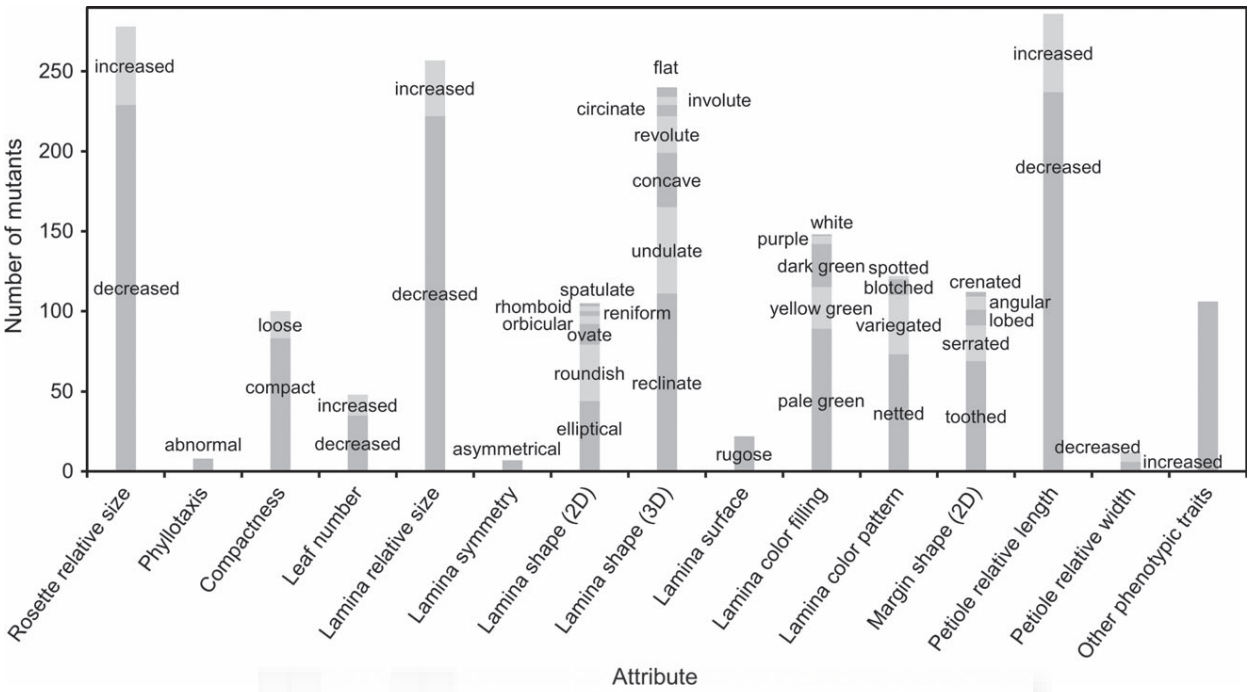

Figure 3. Classification of leaf mutant phenotypes based on ontological terms.
X-axis categories denote the leaf attributes considered. Tags on the bars indicate the terms. The number of mutants considered in this graph is 536. The total number of trait annotations is 1851 (3.5 per mutant).

projects, (iii) T-DNA insertion co-segregation with the mutant phenotype, and (iv) a non-complementation result from an allelism test. Using these methods, we gathered evidence supporting gene–phenotype causality for 42 genuine mutants from our collection, with one to three independent sources of evidence for a given line (Table S2 and the Phenoleaf database).

Additionally, we looked at gene–phenotype causality from a population perspective. The co-segregation and allelism test data were used to estimate the percentage of leaf mutants for which the annotated T-DNA insertion causes the mutant phenotype. First, we studied co-segregation in 15 randomly selected homozygotes for the annotated T-DNA insertion. Co-segregation was found between the leaf mutant phenotype and the T-DNA insertion in 47% (seven lines) of these cases. Second, we queried our mutant database to confirm homozygous leaf mutants in which the annotated insertion disrupted a gene with a previously described mutant allele (reviewed in Lloyd and Meinke, 2012) and performed allelism tests for 15 of these mutants. In 11 of these crosses (73%), the same phenotype was seen in both parental lines and their F_1 progeny, which indicated non-complementation and proved that the annotated T-DNA insertion caused the observed aberrant leaf morphology (Table S4).

Among the studied T_4 lines, about 30% of the genes were represented by two independent alleles. To find gene–phenotype causal relationships, we selected homozygous mutants and compared their phenotypes with those of the alternative allele. Negative results were obtained in many cases: the line putatively carrying the alternative allele presented a very subtle phenotype or lacked the annotated T-DNA (Savage *et al.*, 2013), making this approach unfeasible.

Rapid methods to clone non-annotated T-DNA insertions

For cases where the annotated T-DNA is not responsible for the mutant phenotype, we developed a method to clone non-annotated T-DNA insertions based on a cost-effective Illumina paired-end pooled whole-genome sequencing method coupled with a simple data analysis pipeline. First, we simulated different coverage depths *in silico* and found that 4.5× coverage depth provides enough information to detect T-DNA insertions reliably. Ten mutants were then pooled in groups and sequenced to 4.5× coverage depth per independent genome. In contrast to SNP detection, no straightforward software or protocols exist for insertions such as T-DNAs (Pabinger *et al.*, 2013), and thus we developed an easy method based on three subsequent cycles of read alignment and filtering (Figure 5 and Experimental Procedures). Each detected insertion was confirmed and traced back to the corresponding individual line in the pool by PCR. In the 10 mutants sequenced, 19 insertions were recovered (Table 2). The positions of 11 T-DNAs were already known, either because they were insertions annotated by the Ecker lab,

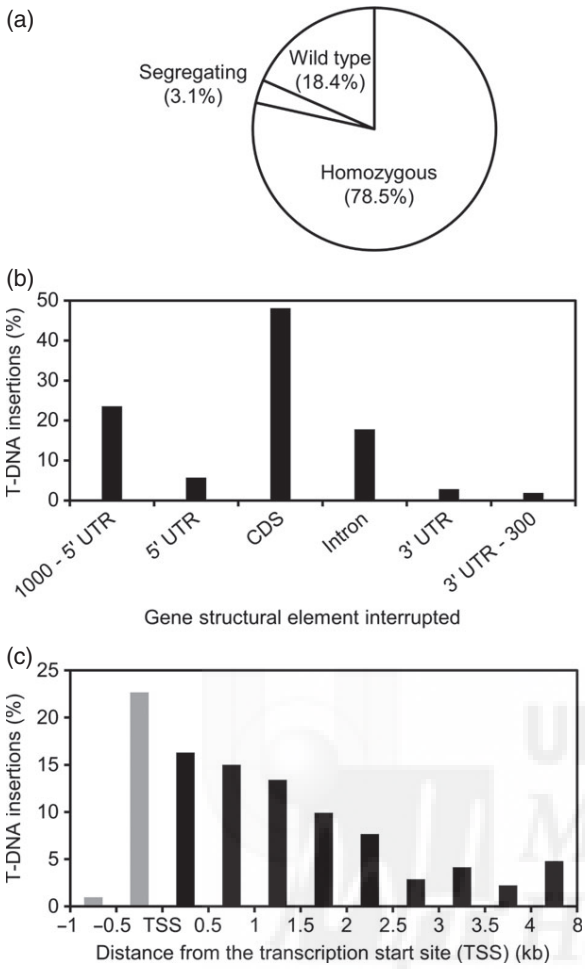

Figure 4. Leaf mutant genotyping.
(a) Percentage of lines with each of the three possible genotypes at the annotated locus (n = 553).
(b) Frequency distribution of confirmed annotated insertions, grouped according to the gene structural element they interrupt (n = 413). The category '1000-5 UTR' corresponds to the first 1000 bp upstream of the transcription start site (TSS), while the category '3′ UTR-300' denotes the first 300 bp downstream of the end of transcription. CDS, coding sequence.
(c) Frequency distribution of confirmed annotated insertions, grouped according to the distance to the TSS of the gene they interrupt (n = 413). Note that the class 4 to 8 kb from the TSS spans a region eight times greater than the rest of the classes.
In (b) and (c) T-DNA insertion to gene comparisons were made considering only the first alternative transcript (gene model) available at The Arabidopsis Information Resource. When a T-DNA interrupted more than one gene, only the closest one was considered for the calculations.

or because they had been recovered by adapter ligation-mediated PCR (AL-PCR; see below). We detected in this way all 11 known mutations, which were used as positive controls, thus validating the robustness of the method. We concluded that this method provides an efficient way to clone unknown insertions when the annotated insertion does not account for the mutant phenotype. Additionally, this experiment revealed that the average number of T-DNA insertions in the studied lines is 2.1.

Adapter ligation-mediated PCR was also used (AL-PCR; O'Malley *et al.*, 2007; Thole *et al.*, 2009), with some modifications, to obtain all possible flanking sequence tags (FSTs; see Experimental Procedures). We confirmed the insertions detected by PCR genotyping at the corresponding loci. We analyzed six T_5 lines and recovered 11 independent insertions (1.8 per line; Table 2). In these lines, 10 insertions were already known, but only 9 were recovered by AL-PCR, suggesting that this method is less reliable than whole-genome sequencing.

PhenoLeaf, an online resource for Arabidopsis researchers

To make this mutant collection available to Arabidopsis researchers we implemented a relational database that stores all the information obtained and links our phenotype and genotype data with publicly available datasets from The Arabidopsis Information Resource (TAIR; gene structural and functional annotation) and the Salk Institute Genomic Analysis Laboratory (SIGnAL) (T-DNA coordinates; Figure 6a). To enhance the usefulness of our resource data, we built PhenoLeaf, a web-based query system available through http://genetics.umh.es/phenoleaf (Figure 6b–e). In PhenoLeaf, the user can search by gene (Figure 6b) or by mutant phenotype (Figure 6c). When the query is submitted, the user is directed to a results summary page (Figure 6d). Once there, by clicking on a result record the user can see the full details of a particular line (Figure 6e). As we analyze additional lines, the results will become publicly available through the web query application. Seeds of the leaf mutants were donated to the Nottingham Arabidopsis Stock Centre (NASC). Users can search for a particular leaf mutant line using our query interface and then be redirected to the NASC website to order the corresponding seeds. Therefore, this web interface provides a comprehensive resource for the scientific community.

Using our collection for rapid identification of genes required for leaf morphogenesis

As a demonstration of the usefulness of our collection to accelerate gene study, we used our database to identify two genes not previously related to leaf morphogenesis. We queried our database for mutants that have specific traits and harbor a homozygous T-DNA insertion in a gene of unknown function. We demonstrated gene–phenotype causality, and performed a phenotypic characterization to further define the functions of the genes.

Characterization of At1g77600. We were interested in examining the differential growth rate along the proximal–distal and medial–lateral axes of leaves. We queried the database for mutants with altered two-dimensional leaf shape and found that the At1g77600 locus was represented in our database by two independent lines that both showed compact rosettes and roundish leaves (Figure 7b,

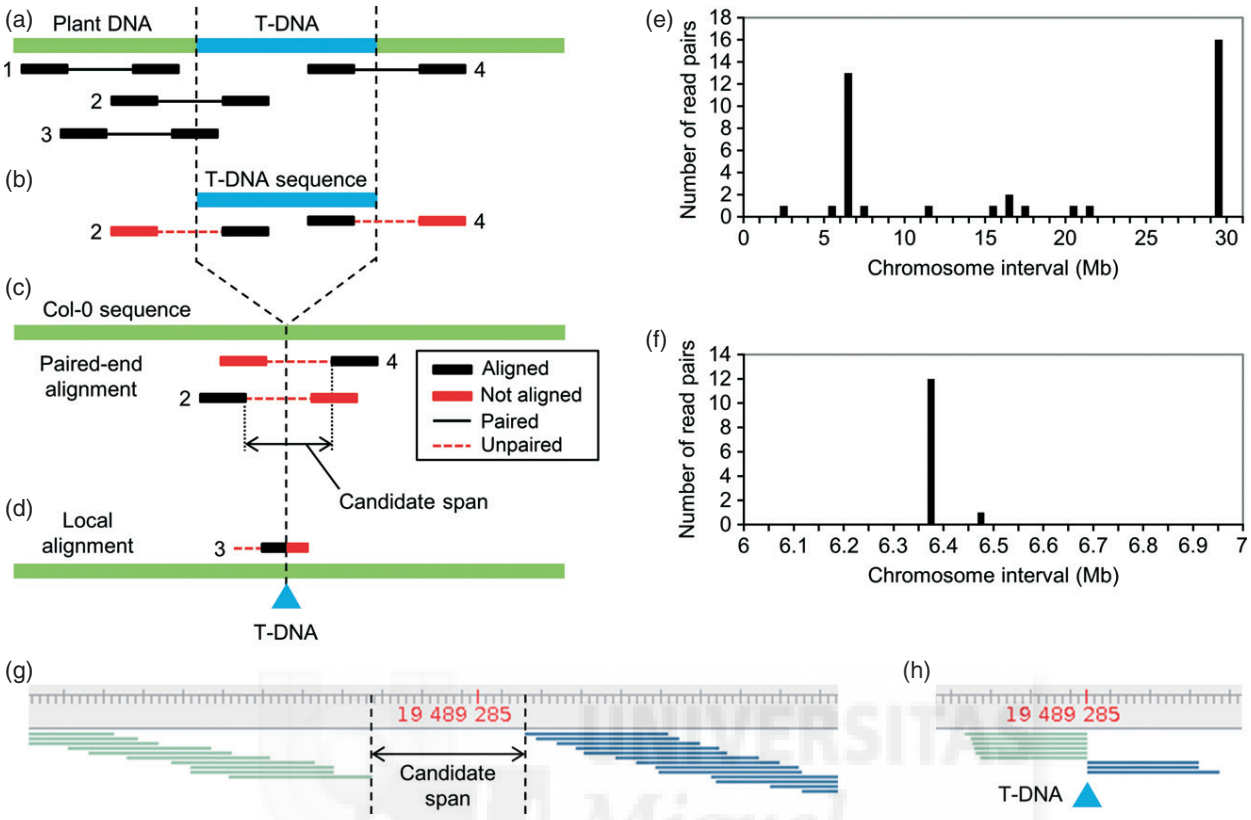

Figure 5. Mapping of T-DNA insertions using Illumina short reads.
(a) Example of paired-end reads within a genome segment encompassing a T-DNA insertion. The pairs of boxes linked by lines represent the random library fragments, the boxes being the sequenced part. Fragments 2 and 4 are used to establish a candidate span to contain the T-DNA. The reverse read of fragment 3 is used to tell the position of the T-DNA with a 1-nucleotide resolution.
(b) Paired-end full-read alignment to the T-DNA sequence (alignment 1). The figure shows that mate 2 from fragment 2 aligned to the left end of the T-DNA and mate 1 from fragment 4 aligned to the right end. The SAM file containing the output of the alignment is filtered for those pairs of reads where one mate aligned and the other did not, and then written to a new FastQ file.
(c) Filtered read pairs alignment to the Col-0 reference sequence (alignment 2). Mate 1 from fragment 2 and mate 2 from fragment 4 align at the flanks of the T-DNA position. These two reads establish the candidate span that harbors the T-DNA insertion.
(d) Local alignment to the Col-0 reference sequence (alignment 3). A local alignment allows partial alignments of reads by ignoring non-matching parts and therefore marks the exact position of a T-DNA insertion. The figure shows that the leftmost part of mate 2 from fragment 3 aligns to the reference sequence exactly up to the last base before the insertion, marking the exact T-DNA position.
(e) Overview of alignment 2 of pool #1 reads in Arabidopsis chromosome 1. Reads were grouped in 1-Mb classes. The accumulation of reads in intervals 6–7 and 29–30 Mb marks two putative insertion sites. Intervals pointed by only one read are artifacts, as confirmed by PCR genotyping the precise loci.
(f) Enlargement of interval 6–7 shown in (e), around the first putative insertion site. Out of 13 reads, 12 remain clustered in interval 6.35–6.40 and one is actually a single alignment pointing to other loci.
(g) Genome browser screenshot showing reads signaling a candidate span for an insertion. Green reads are forward reads that aligned to the left end of the T-DNA insertion. Blue reads are reverse reads that mapped to the right end of the same T-DNA insertion. Read length is 90 nucleotides.
(h) Trimmed reads pointing the exact T-DNA position. In all cases, the last read character before the trimming maps to the same position on the reference sequence.

c,f). Two additional T-DNA lines that interrupt At1g77600 also shared the same phenotype. All mutations were found to be recessive, and allelism tests showed that the mutations failed to complement each other, indicating that At1g77600 is responsible for the phenotype (Figure S2b–f). At1g77600 encodes a protein that belongs to the armadillo repeat superfamily. A morphometric characterization of the phenotype showed that the rosette of the SALK_087484 mutant is 1.5 times more compact (see Experimental Procedures) than the wild type due to a reduction in petiole and lamina length, but it retains a wild-type lamina width (Figures 7h,i and S3a,b). We next sought to determine the origin of this reduction at the cellular level. In both the lamina and the petiole the mean cell size and the cell diameter along the proximal–distal axis were not significantly different from those of Col-0, suggesting that cell expansion was not the origin of its shortened leaves (Figures 7j and S3c,d). In contrast, the number of cells from end to end of the proximal–distal axis was lower in both the lamina and the petiole of the mutant (Figures 7k and S3e), explaining the macroscopic reduction in lamina and petiole length. This trait suggests

Table 2 T-DNA insertions identified using whole-genome sequencing and adapter ligation-mediated PCR (AL-PCR)

Line	Leaf phenotype	Insertions found	Chromosome	Position (bp)	Zygosity[a]	T-DNA insertion site	Detected[b] by AL-PCR/WGS	Annotated by Ecker lab
SALK_047972C	Lobed	2	1	15 202 126	NA	Centromere	+/	
			2	13 713 831	HM	At2g32280, protein of unknown function	+/	+
SALK_086776C	Serrated, cup shaped	1	4	73 919	HM	At4g00180, *YABBY3*	+/	+
SALK_144022C	Concave, undulate	1	3	21 234 684	HM	At3g57390, *AGAMOUS-LIKE18*	+/	+
SALK_025062C	Disorganized morphology	2	2	19 333 624	HM	At2g47060, *PTO-INTERACTING1-4*	+/+	+
			5	1 954 604	HM	At5g06390, *FASCICLIN-LIKE ARABINOGALACTAN PROTEIN 17 PRECURSOR*	–/+	
SALK_026171C	Wrinkled, necrosis	4	2	8 985 786	HM	At2g20875, *EPIDERMAL PATTERNING FACTOR 1*	+/+	
			3	18 401 955	HM	223 bp downstream of the 3′ end of At3g49640, tRNA dihydrouridine synthase activity	+/+	
			3	22 662 837	HM	At3g61220, *SHORT-CHAIN DEHYDROGENASE/REDUCTASE 1*	+/+	
			4	2 696 258	HM	774 bp upstream of the 5′ end of At4g05270, ubiquitin-like superfamily protein	+/+	
SALK_101771C	Abnormal midvein	2	1	6 371 711	HM	At1g18500, *ISOPROPYLMALATE SYNTHASE 1*	+/+	+
			5	3 197 478	S	357 bp downstream of the 3′ end of At5g10180, *SULFATE TRANSPORTER 2;1*	+/+	
SALK_021618C/ SALK_047274C[c]	Small, cup shaped	2	2	19 489 183	HM	At2g47490, *ARABIDOPSIS THALIANA NAD+ TRANSPORTER 1*	/+	+
			3	1 351 590	HM	Nearest gene is 1662 bp away	/+	
SALK_040660C	Bent down	1	1	29 750 108	HM	At1g79090, protein of unknown function	/+	+
SALK_077716C	Rolled	2	4	17 583 130	HM	921 bp upstream of the 5′ end of At4g37400, *CYTOCHROME P450, FAMILY 81, SUBFAMILY F, POLYPEPTIDE 3*	/+	
			4	17 619 182	HM	79 bp upstream of the 5′ end of At4g37480, chaperone DnaJ-domain superfamily protein	/+	
SALK_113067C	Toothed, netted	4	1	1 469 427	HM	183 pb upstream of the 5′ end of At1g05100, *MITOGEN-ACTIVATED PROTEIN KINASE KINASE KINASE 18*	/+	
			2	18 513 585	HM	At2g44900, *F-BOX ARMADILLO PROTEIN 1*	/+	
			2	19 643 790	HM	465 bp upstream of the 5′ end of At2g48020, major facilitator superfamily protein	/+	
			3	80 126	HM	20 bp downstream of the 3′ end of At3g01250, unknown protein	/+	+
SALK_114083C	Small, cup shaped	1	1	2 648 512	HM	At1g08410, P-loop containing nucleoside triphosphate hydrolases superfamily protein	/+	+
SALK_121288C	Lobed	1	3	2 825 494	HM	At3g09210, *PLASTID TRANSCRIPTIONALLY ACTIVE 13*	/+	

[a]HM, homozygous; S, segregating; NA, not amplifiable by PCR using short primers because the locus contains repetitive sequences.
[b]The plus and minus signs indicate detection or not of a T-DNA insertion, respectively, determined by AL-PCR or whole-genome sequencing. The absence of a sign indicates that the corresponding technique was not used. WGS, whole-genome sequencing.
[c]Lines SALK_021618C and SALK_047274C were considered to be the same mutant, since they shared two insertions in identical positions.

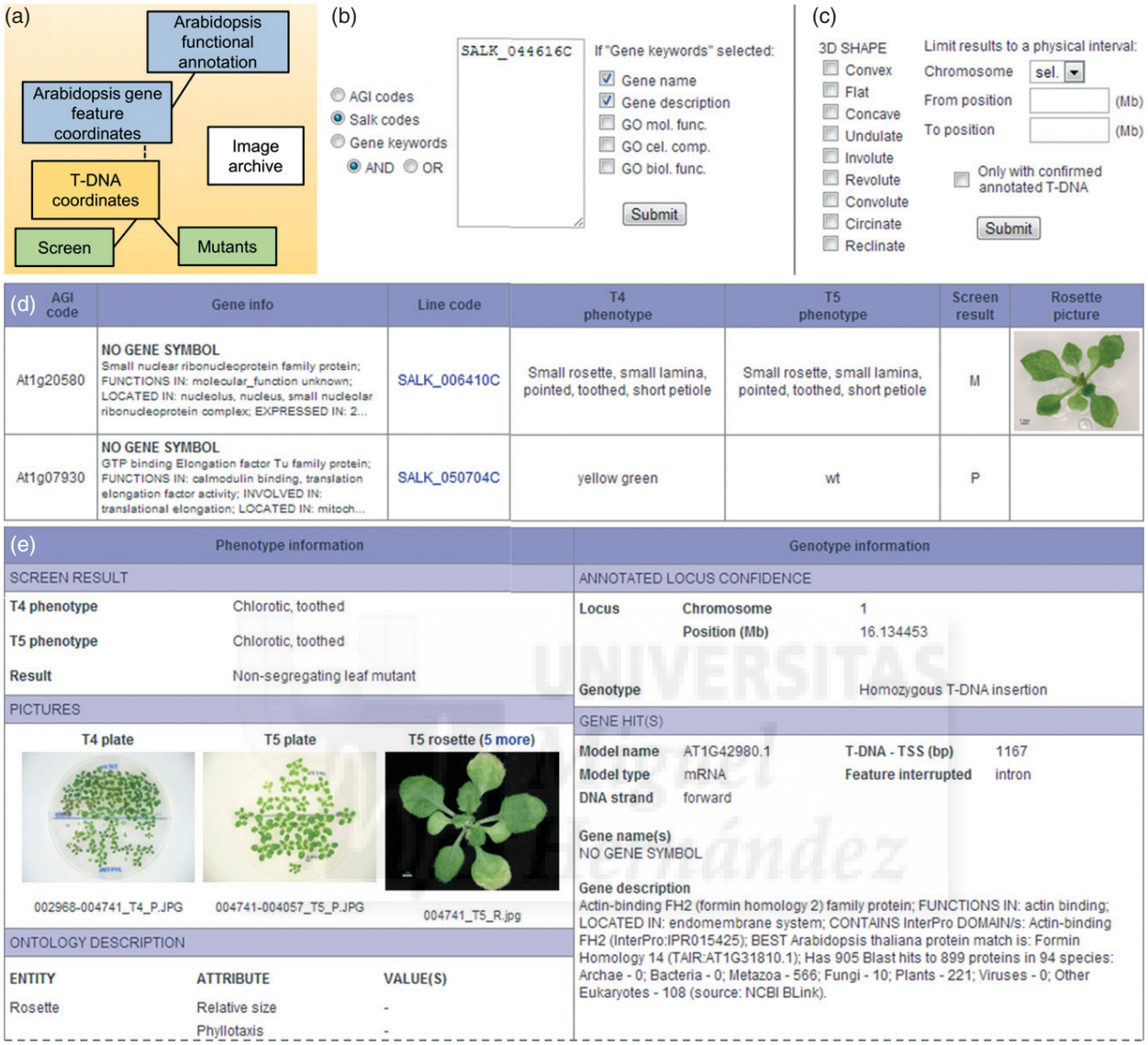

Figure 6. PhenoLeaf database and query application to perform *in silico* screens.
(a) Simplified structure of the relational database underlying the web query system. The blue rectangles represent datasets curated at The Arabidopsis Information Resource. The yellow rectangle represents a dataset produced by the Ecker laboratory. The dataset labeled 'Screen' contains all the information that is generated in the course of the screen, and the dataset 'Mutants' is a detailed description of the phenotypes and genotypes of the leaf mutants. The solid lines represent the relationship between different datasets. The application relates lines to genes and vice versa by comparing the coordinates of the T-DNAs and the genes (dashed line). The white rectangle represents the image file archive, which so far contains 16 700 JPEG files of plates and individual rosettes.
(b) Form to query by one or multiple genes of interest (*in silico* reverse screen). The user can choose between AGI codes, Salk alleles or gene keywords.
(c) Form to query by a phenotypic trait of interest (*in silico* forward screen). Multiple combinations of traits can be specified selecting different ontology terms. In addition, the query can be restricted to only genes within a physical interval and/or lines with confirmed annotated T-DNA.
(d) Table-like summary page. Each record shows a Salk line (allele), information about the gene affected and the phenotype we scored. In the records corresponding to confirmed leaf mutants, a representative picture of the phenotype is displayed.
(e) Full details of the SALK_139862C line. The left panel displays all the information related to the phenotype scored in the screen. It includes all available pictures (not all shown in the image) and a phenotype description using ontology terms. The right panel displays information about the gene mutated and the particular allele studied, such as the genotype test result and the gene structural feature interrupted by the T-DNA.

that At1g77600 is necessary for cell division-driven proximal–distal leaf growth.

Characterization of At3g62870. Our lab studies the relationship between leaf development and ribosomal protein function; mutations affecting these proteins often cause smaller, toothed and netted leaves (Horiguchi *et al.*, 2011, 2012; Casanova-Sáez *et al.*, 2014). We found in our database that the SALK_086913 mutant harbors a homozygous insertion in At3g62870, which encodes a member of

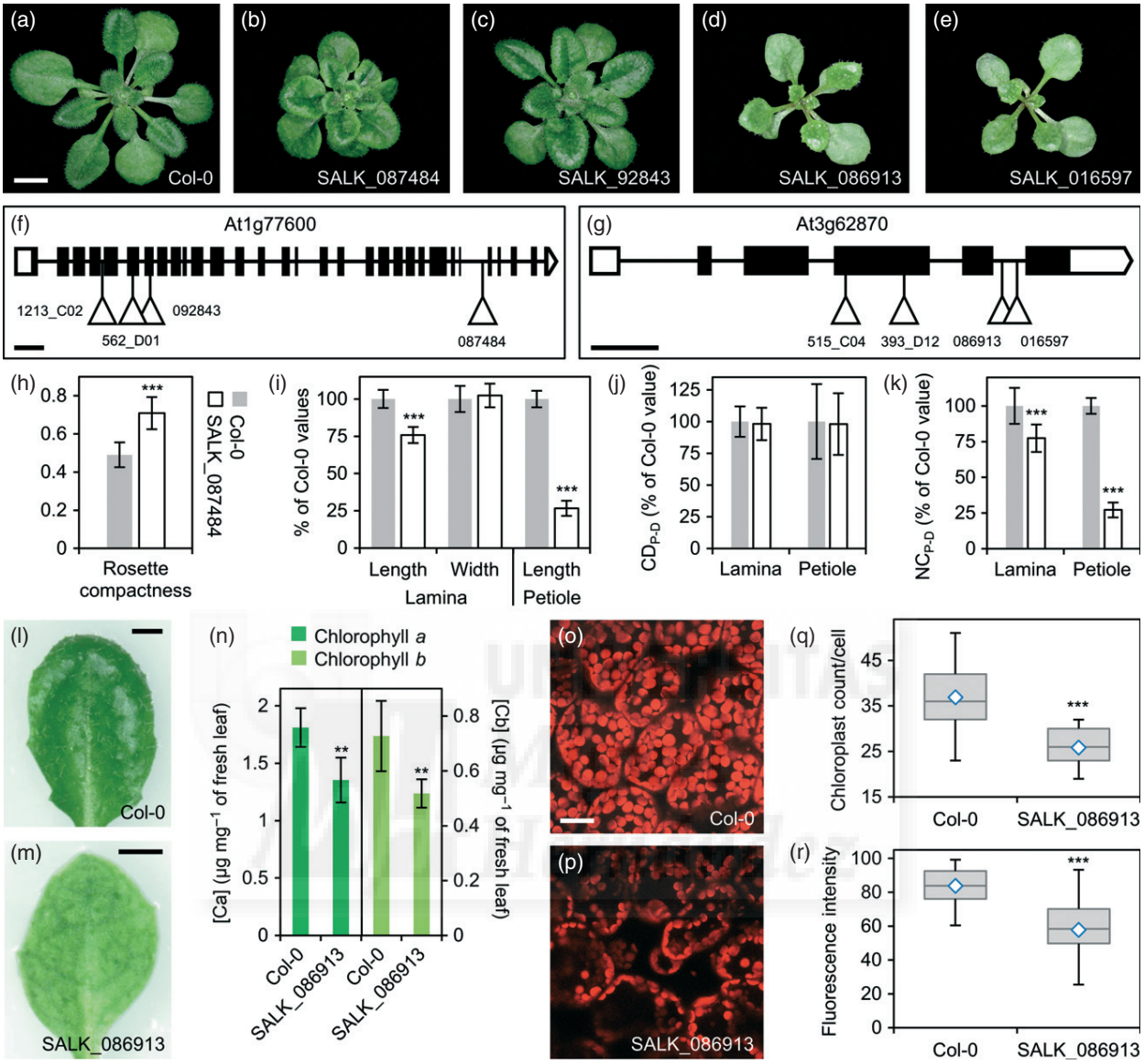

Figure 7. Identification and characterization of the genes At1g66700 and At3g62870.
(a–e) Phenotypes of Col-0 and two T-DNA mutants affected in each gene. Pictures were taken 21 das.
(f, g) Tagged genes with the position of T-DNA insertions used for gene confirmation.
(h, k) Morphometric study of the eighth-node leaves of SALK_087484C.
(j) $CD_{P\text{-}D}$: palisade mesophyll cell diameter parallel to the leaf proximal-distal axis.
(k) $NC_{P\text{-}D}$: total number of palisade mesophyll cells along the proximal-distal axis.
(l–r) Study of the photosynthetic competence of SALK_086913.
(l, m) Adaxial side of 14-das leaves showing macroscopic pigmentation.
(n) Chlorophyll concentration of 14-das plants.
(o, p) Confocal laser scanning sections of the palisade mesophyll cells of third-node leaves showing chlorophyll autofluorescence. Micrographs were taken 14 das.
(q) Boxplot distribution of chloroplast count per cell in 28-µm sections. Boxes are delimited by the first (Q1, lower hinge) and third (Q3, upper hinge) quartiles. Whiskers represent Q1 − 1.5 IQ (lower) and Q3 + 1.5·IQ (upper), where IQ = Q3–Q1. ◊, mean. –, median.
(r) Boxplot distribution of the mean chlorophyll autofluorescence intensity normalized to a 100-step range in 28-µm sections.
Scale bars: (a–e) 5 mm; (f) 1 kb; (g) 0.2 kb; (l, m) 1 mm; (o, p) 20 µm. The ** and *** symbols represent *P*-values of 0.01 and 0.001, respectively.

the L7Ae superfamily of ribosomal proteins that has not been functionally studied to date. Three additional mutations were found to share the same phenotype, and allelism tests showed that the mutants failed to complement each other (Figures 7d,e,g and S2g–k). The rosettes and leaves of SALK_086913 were significantly smaller (Figure S3a,b) because of diminished cell proliferation (Figure S3e,f). Cell expansion and density were not significantly

affected (Figure S3c,d). The protein has been detected in the cytoplasm (Chang *et al.*, 2005; Giavalisco *et al.*, 2005), although the mutant leaves appeared pale green and netted (Figure 7l,m), suggesting that chloroplast function was impaired in the mutant. Concentrations of chlorophyll *a* and *b* in the mutant were reduced to three-fourths of the wild-type levels (Figure 7n). The mutant also showed significantly fewer chloroplasts per cell and a reduced and variable chlorophyll content per chloroplast (Figure 7o–r). Despite this, the maximum efficiencies of PSII in the wild type and the mutant, measured as F_v/F_m, were 0.772 ± 0.01 and 0.774 ± 0.01, respectively, and the difference was not significant ($n = 7$, $P = 0.9$). We concluded that At3g62870 affects chloroplast biogenesis.

DISCUSSION

Our screen of the Salk Arabidopsis Unimutant collection identified 706 mutants exhibiting visible leaf phenotypes. The identification rate of mutant phenotypes was 3.6%, similar to that of Kuromori *et al.* (2006), who screened 4000 *Ds* mutants for visible mutant phenotypes. Myouga *et al.* (2010) found that of 318 Salk homozygous knockout lines of chloroplast-targeted protein-coding nuclear genes, 8.5% show a mutant phenotype. Their higher yield probably reflects the fact that they selected genes encoding chloroplast-targeted proteins and discarded non-homozygous lines prior to screening. We identified a phenotype for many genes that had no previously identified mutant phenotype, indicating that our database provides a useful resource that will help researchers to place many genes within the genetic network underlying leaf development and maintenance.

However, our screen could not capture all leaf-related genes. According to Wang (2008), 80% of T-DNA insertions within a gene transcription unit result in no protein expression; therefore, essential genes are probably underrepresented in the Unimutant collection. Functionally redundant genes are also likely to have escaped from this screen. New strategies such as screening double mutant collections (GABI-DUPLO; https://www.gabi-kat.de/duplo.html) (Bolle *et al.*, 2013) or whole-gene-family knockouts silenced by artificial microRNAs (Schwab *et al.*, 2006; Jover-Gil *et al.*, 2014) will enable additional systematic reverse genetic screens.

To increase the utility of our collection, mutant phenotypes were described using ontological terms from a controlled and widely accepted vocabulary that ensures that the description of any particular mutant can be understood by others. This also allows researchers to group, query, and compare mutants from the same or different datasets, such as public resources like TAIR (http://www.arabidopsis.org/).

A leaf mutant collection where every line has an annotated T-DNA insertion is attractive for potential users because the putative gene responsible for the phenotype is already known. However, only 78% of the leaf mutants identified contained a T-DNA insertion at the position annotated in the Salk database. Similar to our results, Ajjawi *et al.* (2010) genotyped 6673 lines from the Salk collection and concluded that 74% were homozygous, 14% were segregating and the remaining 12% lacked the annotated insertion. Myouga *et al.* (2010) genotyped 483 Salk lines and found that only 66% contained the annotated insertion. We also found that the annotated T-DNA insertion does not always account for the observed leaf phenotype. Co-segregation and allelism data were different. We believe that the co-segregation percentage (47%) provides a picture closer to reality, because the lines used in the allelism tests were not randomly selected, possibly introducing a bias in the experiment. Also, the co-segregation percentage is more similar to previously reported results. For example, Ajjawi *et al.* (2010) used the Salk collection for the Chloroplast 2010 Project and found that their observed phenotypes often were not related to the annotated T-DNA-tagged gene. De Muyt *et al.* (2009) screened the Versailles T-DNA population, plus lines from other collections, for meiotic recombination defects and found that just 43% ($n = 28$) of the mutations isolated were caused by a T-DNA insertion. Dobritsa *et al.* (2011) searched for genes involved in pollen exine production, confirming linkage between the annotated gene and the phenotype in only 30% of the 23 Salk lines checked. Genotype information displayed in our database is therefore partial, and a causal relation with the phenotype scored must be experimentally established on a case-by-case basis.

If the annotated T-DNA is missing or does not cause the phenotype of interest, researchers can map other T-DNAs in the line to try to discover genes with a role in leaf development. Here we presented a cost-effective and simple method to map the non-annotated T-DNA by a workflow that is simpler than previous methods (Korbel *et al.*, 2007; Williams-Carrier *et al.*, 2010; Polko *et al.*, 2012; Lepage *et al.*, 2013), and feasible for any plant genetics laboratory. Also, all the software tools used here have been fitted with a graphical interface and integrated in open source, cloud-based platforms for data-intensive research such as Galaxy (http://galaxyproject.org/; Goecks *et al.*, 2010) and iPlant (http://www.iplantcollaborative.org/; Oliver *et al.*, 2013), thus making computer equipment and command line knowledge dispensable. Our method also proved to be robust, detecting 11 out of 11 previously known T-DNAs in the mutants analyzed.

The database and web-based query tool developed in this work, PhenoLeaf, makes our data publicly available to scientists for leaf functional analysis. Researchers can use PhenoLeaf for *in silico* forward or reverse genetics. For example, a user interested in chloroplast function could enter a list of genes that encode chloroplast-targeted proteins, or enter the keywords 'located chloroplast', and

check our phenotypic data for these genes (*in silico* reverse genetics). The user could also search for mutants with defective pigmentation and check the genes putatively affected (*in silico* forward genetics). To demonstrate the usefulness of our resource, we used PhenoLeaf to identify two genes not previously related to leaf development. We quickly found that At1g77600 is required for proximal–distal cell proliferation by querying PhenoLeaf for mutants with roundish leaves; similarly, we assigned a chloroplast-related function to At3g62870, a member of the ribosomal protein L7Ae superfamily. In conclusion, we have generated a valuable public resource for the study of leaf development.

EXPERIMENTAL PROCEDURES

Plant material, culture conditions and crosses

Seeds of the *A. thaliana* (L.) Heynh. wild-type accession Col-0 and all Salk T-DNA insertion mutants screened in this work were obtained from ABRC. The stock numbers of the batches were CS27941, CS27951, CS27942, CS27952, CS27943, CS27953 and CS27944. Previously described alleles used for allelism tests were either purchased from NASC [*tz-1* (Li and Redei, 1969), *gls1-30* (Coschigano *et al.*, 1998), *tir1-1* (Ruegger *et al.*, 1998), *esi1-1* (Chen *et al.*, 2005), and *ddl-2* (Morris *et al.*, 2006)] or kindly provided by the authors who first described them [Hidetoshi Saze, *ibm1-4* (Saze *et al.*, 2008); Joanne Chory, *cue1-2* (Streatfield *et al.*, 1999); José Alonso, *wei8-1* (Stepanova *et al.*, 2008); Edgar Spalding, *mdr1-1* and *mdr1-3* (Noh *et al.*, 2001); Scott Poethig, *sqn-1* and *sqn-2* (Berardini *et al.*, 2001); Scott Michaels, *cdc73-1* and *cdc73-2* (Yu and Michaels, 2010); and Hiroyasu Motose, *ibo1-4* (Motose *et al.*, 2008)]. Seeds were sterilized with bleach and stratified at 4°C for 72 h. Seedlings were grown *in vitro* as described in Ponce *et al.* (1998), under continuous illumination of approximately 75 μmol m^{-2} sec^{-1}. Adult plants were grown in a 2:2:1 (volume) mixture of perlite:vermiculite:sphagnum moss in identical environmental conditions as seedlings. Crosses were performed as described in Berná *et al.* (1999).

Leaf mutant screen and phenotyping

For each Salk T_4 T-DNA line obtained, 30 seeds were grown *in vitro* as described above. Each Petri dish contained two independent lines to help eliminate phenotypic traits caused by microenvironmental variations across plates. As described in Pérez-Pérez *et al.* (2011), T_5 T-DNA lines were grown at a density of 20 plants per plate. The phenotypic analysis was done under a magnifier lamp against a white surface. Plate photographs were taken 18 das with a Panasonic DMC-FX9 digital camera (2816 × 2112 pixels; http://panasonic.net/), whereas T_5 rosette close-up images of genuine mutants were taken 21 das with a Nikon SMZ1500 stereomicroscope equipped with a Nikon DXM1200F digital camera (3840 × 3072 pixels; http://www.nikon.com/). The phenotype annotations were stored in a relational database.

Genotyping of T-DNA insertion loci

The presence of the annotated T-DNA insertions was determined by PCR, following the Salk Institute Genomic Analysis Laboratory recommendations (http://signal.salk.edu/tdnaprimers.2.html). Primers were designed either using their primer design tool (http://signal.salk.edu/tdnaprimers.2.html; Table S5), or manually for non-annotated T-DNA insertions (Table S7). The PCR reactions were performed with Phire Hot Start II DNA polymerase (Thermo Scientific, http://www.thermoscientific.com/). Template DNA was obtained by grinding one leaf of a 15- to 21-day-old rosette with three glass beads in 115 μl of distilled water. Immediately afterwards, samples were incubated at 50°C for 3 min and centrifuged at 15 870 *g* for 1 min. One microliter of supernatant was used as PCR template in 10- μl reactions.

Next-generation sequencing and analysis

Total DNA was purified from at least five T_5 siblings of a given line to capture segregating T-DNAs, using the DNeasy Plant Mini Kit (Qiagen, http://www.qiagen.com/) following the instructions of the manufacturer. Whole-genome sequencing of the samples was performed at BGI Hong Kong in an Illumina HiSeq2000 sequencer. Average insert size in the paired-end libraries generated was 500 bp, read length was 90 bp and coverage was 23× per sample. Each sample consisted of a pool of DNA from five different leaf mutants. The read data were submitted to the NCBI and are available as accession SRX473258. All the data analyses were performed on a machine equipped with Intel Core i7 X980 3.33 GHz ×12 CPU and 24 GB RAM. The reads were aligned using Bowtie 2 (Langmead and Salzberg, 2012) using the default settings in both the end-to-end and local alignments. Sequence alignment map (SAM) files were processed using custom PHP scripts. These scripts were written for comparison of alignments to the Col-0 and pBIN-pROK2 sequences, and for processing SAM alignments and writing the output to new FastQ files. To detect non-canonical T-DNA insertions, such as a vector backbone sequence next to the T-DNA, we aligned sequences against the complete sequence of pBIN-pROK2, the vector used to produce the Salk collection. Tablet viewer (Milne *et al.*, 2010) was used to visualize alignments. Primers used for confirming non-annotated insertions detected are listed in Table S7.

Adapter ligation-mediated PCR

Selective amplification of FSTs was done as described in O'Malley *et al.* (2007) and Thole *et al.* (2009) with the following modifications: 50 ng of genomic DNA was digested and ligated; a nested PCR was also performed when the *Ase*I adapter was used; when multiple PCR products were obtained, they were purified by recovering DNA from each band in the electrophoresis gel with a pipette tip and each pure DNA sample was used as a template in a subsequent PCR amplification; and amplification was attempted at both the LB and RB ends. Adapters used were those described in O'Malley *et al.* (2007). Adapter and primer sequences are shown in Table S6. Primers used for confirming non-annotated insertions detected are listed in Table S7.

Database and web query interface

The genomic coordinates of all T-DNA lines were obtained from the SIGnAL database (http://natural.salk.edu/database/tdnaexpress/). These coordinates were used for all calculations displayed in our database web interface. In the SIGnAL T-DNA Express website (http://signal.salk.edu/cgi-bin/tdnaexpress) it is considered that a T-DNA can potentially affect the function of a gene when it is located from 1000 bp upstream of the TSS to 300 bp downstream of the end of transcription. For simplicity, we adopted those values, thus creating the structural elements 1000-5′ untranslated region (UTR) and 3′UTR-300. The database is managed using MySQL software, and the programs to calculate and format the information for the user were written in PHP scripting language.

Morphology, ultrastructure and photosynthesis analyses

Leaf clearing, fixation and embedding, quantification of rosette, leaf and cellular anatomical features and observation of leaf tissues by confocal microscopy were performed as previously described (Pérez-Pérez *et al.*, 2011; Quesada *et al.*, 2011). Rosette compactness was calculated by dividing the rosette area by the area of the best-fitting ellipse containing the rosette. Mean chlorophyll autofluorescence intensity was measured from confocal images using ImageJ 1.47v (http://rsb.info.nih.gov/ij/). For chlorophyll quantification, four independent samples of 100 mg of fresh leaves from rosettes collected 14 das were pooled, frozen in liquid N_2 and homogenized with 4 ml of 80% acetone at 4°C. The samples were centrifuged for 10 min at 2350 *g* and pigment concentration in the supernatant was spectrophotometrically determined following Wellburn (1994). Photosynthetic maximum quantum yield was measured 20 das on plants dark-adapted for 30 min and after applying a 0.8-sec saturating light pulse (4000 μmol photons m^{-2} sec^{-1}). Measurements were made with a DUAL-PAM/F fluorometer and a DUAL-BA leaf positioning device (WALZ, http://www.walz.com/). Student's *t*-tests and Mann–Whitney *U*-tests for comparing distributions were done using SPSS 16.0.2 (SPSS Inc., http://www.spss.com.hk/).

ACKNOWLEDGEMENTS

The authors wish to thank H. Candela for comments on the manuscript, and the researchers who provided seeds of previously characterized mutants that we used for allelism tests (see Experimental Procedures). We especially thank D. Navarro, L. Serna and J. M. Sánchez-Larrosa for valuable help during the screening, and J. M. Serrano, F. M. Lozano, T. Trujillo, R. Sarmiento and A. Torregrosa for their excellent technical assistance. This work was supported by grants from the Ministerio de Economía y Competitividad of Spain [BFU2011-22825 and CSD2007-00057 (TRANSPLANTA)], the European Commission (LSHG–CT–2006–037704; AGRON-OMICS) and the Generalitat Valenciana (Prometeo/2009/112) to JLM. SJG held the PIRG06-GA-2009-256579 (ARABIGANS) grant from the European Commission and DWS the ACIF/2012/137 fellowship from the Generalitat Valenciana (VALi+d program).

SUPPORTING INFORMATION

Additional Supporting Information may be found in the online version of this article.

Figure S1. Seed quality and seedling growth.

Figure S2. Rosette phenotypes of the lines carrying mutant alleles of At1g77600 and At3g62870 and of the F_1 progeny of their crosses.

Figure S3. Morphometric characterization of the SALK_087484 and SALK_086913 mutants.

Table S1. Genotypes for the annotated insertion in 24 randomly chosen lines.

Table S2. Description of confirmed non-segregating and segregating mutants.

Table S3. Ontological terms and their definitions.

Table S4. Rosette phenotypes of the mutants used in allelism tests and of the F_1 progeny of their crosses.

Table S5. Primers used for the genotyping of annotated T-DNA insertions.

Table S6. Oligonucleotides used for adapter ligation-mediated PCR.

Table S7. Primers used for the genotyping of non-annotated T-DNA insertions.

REFERENCES

Ajjawi, I., Lu, Y., Savage, L.J., Bell, S.M. and Last, R.L. (2010) Large-scale reverse genetics in Arabidopsis: case studies from the Chloroplast 2010 Project. *Plant Physiol.* **152**, 529–540.

Alonso, J.M. and Ecker, J.R. (2006) Moving forward in reverse: genetic technologies to enable genome-wide phenomic screens in Arabidopsis. *Nat. Rev. Genet.* **7**, 524–536.

Alonso, J.M., Stepanova, A.N., Leisse, T.J. *et al.* (2003) Genome-wide insertional mutagenesis of *Arabidopsis thaliana*. *Science*, **301**, 653–657.

Berardini, T.Z., Bollman, K., Sun, H. and Poethig, R.S. (2001) Regulation of vegetative phase change in *Arabidopsis thaliana* by cyclophilin 40. *Science*, **291**, 2405–2407.

Berná, G., Robles, P. and Micol, J.L. (1999) A mutational analysis of leaf morphogenesis in *Arabidopsis thaliana*. *Genetics*, **152**, 729–742.

Bodenreider, O. and Stevens, R. (2006) Bio-ontologies: current trends and future directions. *Brief. Bioinform.* **7**, 256–274.

Bolle, C., Huep, G., Kleinbolting, N., Haberer, G., Mayer, K., Leister, D. and Weisshaar, B. (2013) GABI-DUPLO: a collection of double mutants to overcome genetic redundancy in *Arabidopsis thaliana*. *Plant J.* **75**, 157–171.

Carpenter, A.E. and Sabatini, D.M. (2004) Systematic genome-wide screens of gene function. *Nat. Rev. Genet.* **5**, 11–22.

Casanova-Sáez, R., Candela, H. and Micol, J.L. (2014) Combined haploinsufficiency and purifying selection drive retention of RPL36a paralogs in Arabidopsis. *Sci. Rep.* **4**, 4122.

Chang, I.F., Szick-Miranda, K., Pan, S. and Bailey-Serres, J. (2005) Proteomic characterization of evolutionarily conserved and variable proteins of Arabidopsis cytosolic ribosomes. *Plant Physiol.* **137**, 848–862.

Chen, G., Bi, Y.R. and Li, N. (2005) *EGY1* encodes a membrane-associated and ATP-independent metalloprotease that is required for chloroplast development. *Plant J.* **41**, 364–375.

Clark, K.A. and Krysan, P.J. (2010) Chromosomal translocations are a common phenomenon in *Arabidopsis thaliana* T-DNA insertion lines. *Plant J.* **64**, 990–1001.

Coschigano, K.T., Melo-Oliveira, R., Lim, J. and Coruzzi, G.M. (1998) Arabidopsis *gls* mutants and distinct Fd-GOGAT genes. Implications for photorespiration and primary nitrogen assimilation. *Plant Cell*, **10**, 741–752.

De Muyt, A., Pereira, L., Vezon, D. *et al.* (2009) A high throughput genetic screen identifies new early meiotic recombination functions in *Arabidopsis thaliana*. *PLoS Genet.* **5**, e1000654.

Dobritsa, A.A., Geanconteri, A., Shrestha, J. *et al.* (2011) A large-scale genetic screen in Arabidopsis to identify genes involved in pollen exine production. *Plant Physiol.* **157**, 947–970.

Feldmann, K.A. (1991) T-DNA insertion mutagenesis in *Arabidopsis*: mutational spectrum. *Plant J.* **1**, 71–82.

Galbiati, M., Moreno, M.A., Nadzan, G., Zourelidou, M. and Dellaporta, S.L. (2000) Large-scale T-DNA mutagenesis in *Arabidopsis* for functional genomic analysis. *Funct. Integr. Genomics* **1**, 25–34.

Giaever, G., Chu, A.M., Ni, L. *et al.* (2002) Functional profiling of the *Saccharomyces cerevisiae* genome. *Nature*, **418**, 387–391.

Giavalisco, P., Wilson, D., Kreitler, T., Lehrach, H., Klose, J., Gobom, J. and Fucini, P. (2005) High heterogeneity within the ribosomal proteins of the *Arabidopsis thaliana* 80S ribosome. *Plant Mol. Biol.* **57**, 577–591.

Goecks, J., Nekrutenko, A. and Taylor, J. (2010) Galaxy: a comprehensive approach for supporting accessible, reproducible, and transparent computational research in the life sciences. *Genome Biol.* **11**, R86.

Horiguchi, G., Mollá-Morales, A., Pérez-Pérez, J.M., Kojima, K., Robles, P., Ponce, M.R., Micol, J.L. and Tsukaya, H. (2011) Differential contributions of ribosomal protein genes to *Arabidopsis thaliana* leaf development. *Plant J.* **65**, 724–736.

Horiguchi, G., Van Lijsebettens, M., Candela, H., Micol, J.L. and Tsukaya, H. (2012) Ribosomes and translation in plant developmental control. *Plant Sci.* **191–192**, 24–34.

Ito, T., Motohashi, R., Kuromori, T., Noutoshi, Y., Seki, M., Kamiya, A., Mizukado, S., Sakurai, T. and Shinozaki, K. (2005) A resource of 5,814 *dissociation* transposon-tagged and sequence-indexed lines of *Arabidopsis* transposed from start loci on chromosome 5. *Plant Cell Physiol.* **46**, 1149–1153.

Jaiswal, P., Avraham, S., Ilic, K. *et al.* (2005) Plant Ontology (PO): a controlled vocabulary of plant structures and growth stages. *Comp. Funct. Genomics* **6**, 388–397.

Jover-Gil, S., Paz-Ares, J., Micol, J.L. and Ponce, M.R. (2014) Multi-gene silencing in Arabidopsis: a collection of artificial microRNAs targeting groups of paralogs encoding transcription factors. *Plant J.* in press.

Korbel, J.O., Urban, A.E., Affourtit, J.P. *et al.* (2007) Paired-end mapping reveals extensive structural variation in the human genome. *Science*, **318**, 420–426.

Kuromori, T., Hirayama, T., Kiyosue, Y., Takabe, H., Mizukado, S., Sakurai, T., Akiyama, K., Kamiya, A., Ito, T. and Shinozaki, K. (2004) A collection of 11,800 single-copy *Ds* transposon insertion lines in *Arabidopsis*. *Plant J.* **37**, 897–905.

Kuromori, T., Wada, T., Kamiya, A. *et al.* (2006) A trial of phenome analysis using 4000 *Ds*-insertional mutants in gene-coding regions of Arabidopsis. *Plant J.* **47**, 640–651.

Langmead, B. and Salzberg, S.L. (2012) Fast gapped-read alignment with Bowtie 2. *Nat. Methods* **9**, 357–359.

Lepage, E., Zampini, E., Boyle, B. and Brisson, N. (2013) Time- and cost-efficient identification of T-DNA insertion sites through targeted genomic sequencing. *PLoS ONE*, **8**, e70912.

Li, S.L. and Redei, G.P. (1969) Thiamine mutants of the crucifer, Arabidopsis. *Biochem. Genet.* **3**, 163–170.

Lloyd, J. and Meinke, D. (2012) A comprehensive dataset of genes with a loss-of-function mutant phenotype in Arabidopsis. *Plant Physiol.* **158**, 1115–1129.

Lu, Y., Savage, L.J., Larson, M.D., Wilkerson, C.G. and Last, R.L. (2011) Chloroplast 2010: a database for large-scale phenotypic screening of Arabidopsis mutants. *Plant Physiol.* **155**, 1589–1600.

Milne, I., Bayer, M., Cardle, L., Shaw, P., Stephen, G., Wright, F. and Marshall, D. (2010) Tablet - next generation sequence assembly visualization. *Bioinformatics*, **26**, 401–402.

Morris, E.R., Chevalier, D. and Walker, J.C. (2006) *DAWDLE*, a forkhead-associated domain gene, regulates multiple aspects of plant development. *Plant Physiol.* **141**, 932–941.

Motose, H., Tominaga, R., Wada, T., Sugiyama, M. and Watanabe, Y. (2008) A NIMA-related protein kinase suppresses ectopic outgrowth of epidermal cells through its kinase activity and the association with microtubules. *Plant J.* **54**, 829–844.

Myouga, F., Akiyama, K., Motohashi, R., Kuromori, T., Ito, T., Iizumi, H., Ryusui, R., Sakurai, T. and Shinozaki, K. (2010) The Chloroplast Function Database: a large-scale collection of Arabidopsis *Ds*/*Spm*- or T-DNA-tagged homozygous lines for nuclear-encoded chloroplast proteins, and their systematic phenotype analysis. *Plant J.* **61**, 529–542.

Myouga, F., Akiyama, K., Tomonaga, Y., Kato, A., Sato, Y., Kobayashi, M., Nagata, N., Sakurai, T. and Shinozaki, K. (2013) The Chloroplast Function Database II: a comprehensive collection of homozygous mutants and their phenotypic/genotypic traits for nuclear-encoded chloroplast proteins. *Plant Cell Physiol.* **54**, e2.

Noh, B., Murphy, A.S. and Spalding, E.P. (2001) *Multidrug resistance*-like genes of Arabidopsis required for auxin transport and auxin-mediated development. *Plant Cell*, **13**, 2441–2454.

Oliver, S.L., Lenards, A.J., Barthelson, R.A., Merchant, N. and McKay, S.J. (2013) Using the iPlant collaborative discovery environment. *Curr. Protoc. Bioinformatics* **1**, 22.

O'Malley, R.C. and Ecker, J.R. (2010) Linking genotype to phenotype using the Arabidopsis unimutant collection. *Plant J.* **61**, 928–940.

O'Malley, R.C., Alonso, J.M., Kim, C.J., Leisse, T.J. and Ecker, J.R. (2007) An adapter ligation-mediated PCR method for high-throughput mapping of T-DNA inserts in the Arabidopsis genome. *Nat. Protoc.* **2**, 2910–2917.

Pabinger, S., Dander, A., Fischer, M., Snajder, R., Sperk, M., Efremova, M., Krabichler, B., Speicher, M.R., Zschocke, J. and Trajanoski, Z. (2013) A survey of tools for variant analysis of next-generation genome sequencing data. *Brief. Bioinform.* **5**, 256–278.

Page, D.R. and Grossniklaus, U. (2002) The art and design of genetic screens: *Arabidopsis thaliana*. *Nat. Rev. Genet.* **3**, 124–136.

Parinov, S. and Sundaresan, V. (2000) Functional genomics in *Arabidopsis*: large-scale insertional mutagenesis complements the genome sequencing project. *Curr. Opin. Biotechnol.* **11**, 157–161.

Pérez-Pérez, J.M., Rubio-Díaz, S., Dhondt, S., Hernández-Romero, D., Sánchez-Soriano, J., Beemster, G.T., Ponce, M.R. and Micol, J.L. (2011) Whole organ, venation and epidermal cell morphological variations are correlated in the leaves of Arabidopsis mutants. *Plant, Cell Environ.* **34**, 2200–2211.

Polko, J.K., Temanni, M.R., van Zanten, M., van Workum, W., Iburg, S., Pierik, R., Voesenek, L.A. and Peeters, A.J. (2012) Illumina sequencing technology as a method of identifying T-DNA insertion loci in activation-tagged *Arabidopsis thaliana* plants. *Mol. Plant* **5**, 948–950.

Ponce, M.R., Quesada, V. and Micol, J.L. (1998) Rapid discrimination of sequences flanking and within T-DNA insertions in the Arabidopsis genome. *Plant J.* **14**, 497–501.

Pressman, S., Reinke, C.A., Wang, X. and Carthew, R.W. (2012) A systematic genetic screen to dissect the microRNA pathway in *Drosophila*. *G3*, **2**, 437–448.

Quesada, V., Sarmiento-Mañús, R., González-Bayón, R., Hricová, A., Pérez-Marcos, R., Gracía-Martínez, E., Medina-Ruiz, L., Leyva-Díaz, E., Ponce, M.R. and Micol, J.L. (2011) Arabidopsis *RUGOSA2* encodes an mTERF family member required for mitochondrion, chloroplast and leaf development. *Plant J.* **68**, 738–753.

Rosso, M.G., Li, Y., Strizhov, N., Reiss, B., Dekker, K. and Weisshaar, B. (2003) An *Arabidopsis thaliana* T-DNA mutagenized population (GABI-Kat) for flanking sequence tag-based reverse genetics. *Plant Mol. Biol.* **53**, 247–259.

Ruegger, M., Dewey, E., Gray, W.M., Hobbie, L., Turner, J. and Estelle, M. (1998) The TIR1 protein of Arabidopsis functions in auxin response and is related to human SKP2 and yeast grr1p. *Genes Dev.* **12**, 198–207.

Samson, F., Brunaud, V., Balzergue, S., Dubreucq, B., Lepiniec, L., Pelletier, G., Caboche, M. and Lecharny, A. (2002) FLAGdb/FST: a database of mapped flanking insertion sites (FSTs) of *Arabidopsis thaliana* T-DNA transformants. *Nucleic Acids Res.* **30**, 94–97.

Savage, L.J., Imre, K.M., Hall, D.A. and Last, R.L. (2013) Analysis of essential Arabidopsis nuclear genes encoding plastid-targeted proteins. *PLoS ONE*, **8**, e73291.

Saze, H., Shiraishi, A., Miura, A. and Kakutani, T. (2008) Control of genic DNA methylation by a jmjC domain-containing protein in *Arabidopsis thaliana*. *Science*, **319**, 462–465.

Schwab, R., Ossowski, S., Riester, M., Warthmann, N. and Weigel, D. (2006) Highly specific gene silencing by artificial microRNAs in Arabidopsis. *Plant Cell*, **18**, 1121–1133.

Serrano-Cartagena, J., Robles, P., Ponce, M.R. and Micol, J.L. (1999) Genetic analysis of leaf form mutants from the Arabidopsis Information Service collection. *Mol. Gen. Genet.* **261**, 725–739.

Sessions, A., Burke, E., Presting, G. *et al.* (2002) A high-throughput Arabidopsis reverse genetics system. *Plant Cell*, **14**, 2985–2994.

Smith, B., Ashburner, M., Rosse, C. *et al.* (2007) The OBO Foundry: coordinated evolution of ontologies to support biomedical data integration. *Nat. Biotechnol.* **25**, 1251–1255.

Stepanova, A.N., Robertson-Hoyt, J., Yun, J., Benavente, L.M., Xie, D.Y., Dolezal, K., Schlereth, A., Jurgens, G. and Alonso, J.M. (2008) TAA1-mediated auxin biosynthesis is essential for hormone crosstalk and plant development. *Cell*, **133**, 177–191.

Streatfield, S.J., Weber, A., Kinsman, E.A., Hausler, R.E., Li, J., Post-Beittenmiller, D., Kaiser, W.M., Pyke, K.A., Flugge, U.I. and Chory, J. (1999) The Phosphoenolpyruvate/Phosphate translocator is required for phenolic metabolism, palisade cell development, and plastid-dependent nuclear gene expression. *Plant Cell*, **11**, 1609–1622.

Thole, V., Alves, S.C., Worland, B., Bevan, M.W. and Vain, P. (2009) A protocol for efficiently retrieving and characterizing flanking sequence tags (FSTs) in *Brachypodium distachyon* T-DNA insertional mutants. *Nat. Protoc.* **4**, 650–661.

Wang, Y.H. (2008) How effective is T-DNA insertional mutagenesis in Arabidopsis? *J. Biochem. Tech.* **1**, 11–20.

Wellburn, A. (1994) The spectral determination of chlorophylls a and b, as well as total carotenoids, using various solvents with spectrophotometers of different resolution. *Plant Physiol.* **144**, 7.

Williams-Carrier, R., Stiffler, N., Belcher, S., Kroeger, T., Stern, D.B., Monde, R.A., Coalter, R. and Barkan, A. (2010) Use of Illumina sequencing to identify transposon insertions underlying mutant phenotypes in high-copy *Mutator* lines of maize. *Plant J.* **63**, 167–177.

Woody, S.T., Austin-Phillips, S., Amasino, R.M. and Krysan, P.J. (2007) The *WiscDsLox* T-DNA collection: an Arabidopsis community resource generated by using an improved high-throughput T-DNA sequencing pipeline. *J. Plant. Res.* **120**, 157–165.

Yu, X. and Michaels, S.D. (2010) The Arabidopsis Paf1c complex component CDC73 participates in the modification of *FLOWERING LOCUS C* chromatin. *Plant Physiol.* **153**, 1074–1084.

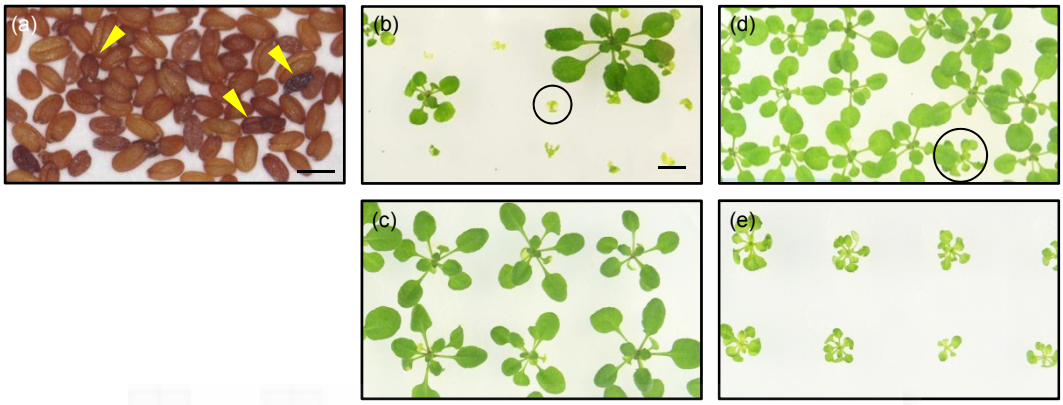

Figure S1. Seed quality and seedling growth.
(a) Appearance of the seeds from one of the lines; some of the seeds are dark and shrunken (yellow arrowheads).
(b-c) Example of (b, circle) a T4 plant with abnormal morphology that produced (c) phenotypically wild-type T5 offspring.
(d-e) Example of the isolation of (d, circle) a T4 abnormal plant whose (e) T5 offspring recapitulated the same phenotype.
Scale bars correspond to (b) 0.5 and (c-f) 10 mm.

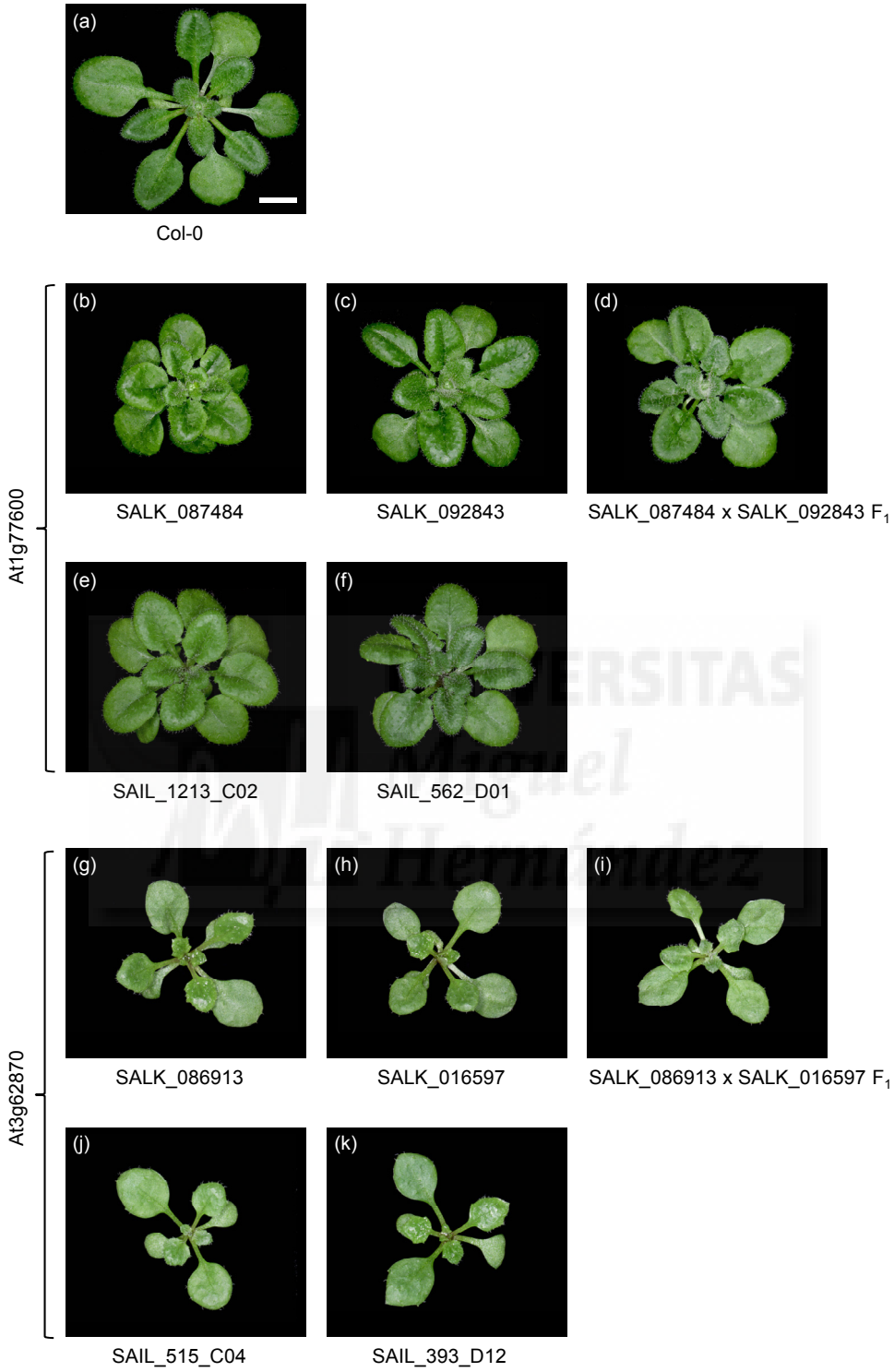

Figure S2. Rosette phenotypes of the lines carrying mutant alleles of At1g77600 and At3g62870 and of the F_1 progeny of their crosses. Pictures were taken 21 das. Scale bar: 5 mm.

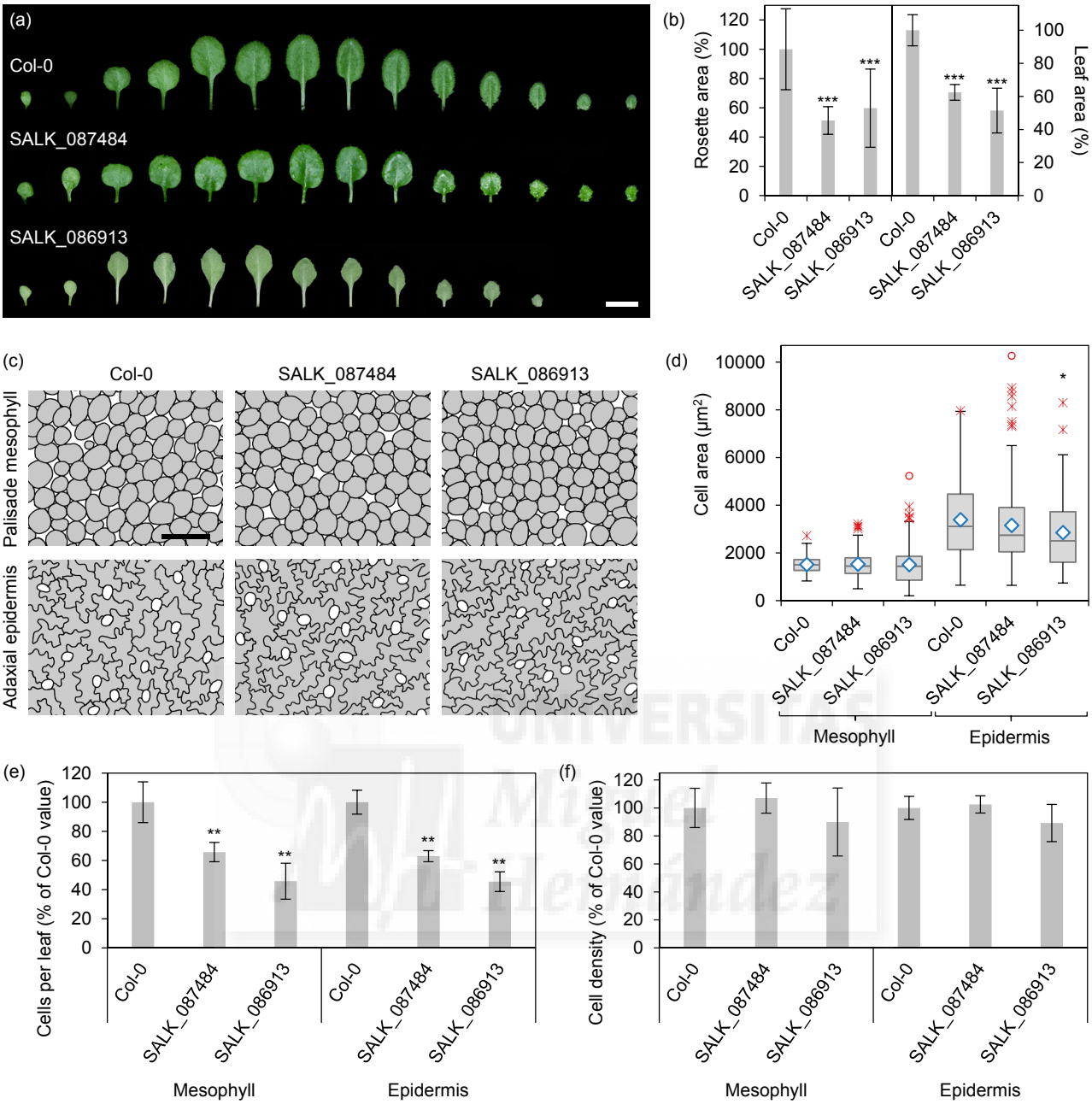

Figure S3. Morphometric characterization of the SALK_087484 and SALK_086913 mutants.
(a) Dissected rosettes of Col-0 and the mutants.
(b) Relative rosette and leaf areas.
(c) Palisade mesophyll and adaxial epidermis cell diagrams showing cell area and density.
(d) Boxplot distribution of cell sizes. Boxes are delimited by the first (Q1, lower hinge) and third (Q3, upper hinge) quartiles. Whiskers represent Q1–1.5•IQ (lower) and Q3+1.5•IQ (upper), where IQ = Q3–Q1. ⋄: Mean. –: Median. ○: Extreme maximum outlier (> [Q3+3•IQ]). ×: Maximum outlier.
(e) Relative number of cells per leaf of Col-0 and the mutants.
(f) Relative cell density of Col-0 and the mutants.
All photographs were taken 21 das. All data correspond to 3rd-node leaves.
Scale bars: (a) 5 mm and (c) 100 µm.
The symbols *, ** and *** represent, p-values of 0.05, 0.01 and 0.001, respectively.

Table S1. Genotypes for the annotated insertion in 24 randomly chosen lines

Genotypes found (5 plants per line were tested)	Number of lines
Homozygous	12
Homozygous and wild type	5
Homozygous, heterozygous and wild type	2
Heterozygous and wild type	1
Wild type	4

Table S2a. Description of confirmed non-segregating mutants

UMH identifier	Salk line (isolated from)	Annotated locus genotype[1]	Gene mutated (AGI code)[2]	Gene description[2]	Evidence in favor of or against a gene-phenotype causality	Alleles associated with evidence of a gene-phenotype causality	Previously described allele[3]	Rosette relative size	Rosette phyllotaxy	Rosette compactness	Rosette relative organ number	Leaf relative size	Leaf symmetry	Leaf 2D shape	Leaf 3D shape	Leaf surface deformation	Leaf color filling	Leaf color pattern	Margin 2D shape	Petiole relative length	Petiole relative width	Other traits[4]
1	SALK_019994C	HM	At1g55370	*NDH-DEPENDENT CYCLIC ELECTRON FLOW 5* (*NDF5*)			Yes											netted				
2	SALK_037675C	WT					N/A								reclinate							
3	SALK_110749C	WT					N/A							elliptical					toothed			
4	SALK_129037C	HM	At4g13590	Uncharacterized protein family			No	decreased		compact	decreased	decreased					pale green			decreased		
5	SALK_130499C	HM	At4g31390	Protein kinase superfamily protein			No	decreased			decreased	decreased					pale green		toothed	decreased		
6	SALK_018664C	HM	At4g09000	*GENERAL REGULATORY FACTOR 1* (*GRF1*)			No	increased				increased		roundish								
7	SALK_019044C	WT					N/A								reclinate, convolute							
8	SALK_019175C	NC	At2g31725	Eukaryotic protein of unknown function			No	decreased		compact	decreased	decreased					dark green			decreased		
9	SALK_021062C	S	At2g11110	Transposable element gene			No	decreased		compact		decreased			reclinate, revolute					decreased		
10	SALK_021217C	HM	At3g47640	*POPEYE* (*PYE*)	T-DNA insertion co-segregates with mutant phenotype		No									rugose						necrosis
11	SALK_021650C	HM	At5g21090	Leucine-rich repeat (LRR) family protein			No	decreased				decreased			undulate	rugose						
12	SALK_038240C	WT					N/A	decreased				decreased			revolute, reclinate,					decreased		
13	SALK_038804C	NC	At4g08100	Transposable element gene			No	decreased		compact		decreased		orbicular			yellow green			decreased		
14	SALK_038907C	HM	At2g28725	Protein of unknown function			No	decreased				decreased		roundish	undulate		pale green			decreased		
15	SALK_060403C	HM	At1g50770	Aminotransferase-like, plant mobile domain family protein	Same phenotype as in The Chloroplast 2010 project (Lu et al. 2011)	SALK_060403, CSHL_ET5739, SALK_123235	No	decreased			decreased	decreased					yellow	variegated		decreased		
16	SALK_067017C	HM	At5g52440	*HIGH CHLOROPHYLL FLUORESCENCE 106* (*HCF106*)	Same phenotype as in The Chloroplast 2010 project (Lu et al. 2011)	SALK_067017, SALK_044421	No	decreased				decreased		roundish	flat		pale green		toothed			
17	SALK_110684C	ND	At1g50575	Putative lysine decarboxylase family protein			No			compact				roundish	reclinate					decreased		
18	SALK_129352C	HM	At3g30180	*BRASSINOSTEROID-6-OXIDASE 2* (*BR6OX2*)			Yes							reniform			dark green					
19	SALK_061494C	HM	At5g35220	*ETHYLENE-DEPENDENT GRAVITROPISM-DEFICIENT AND YELLOW-GREEN 1* (*EGY1*)	No complementation in allelism test, Same phenotype as in The Chloroplast Function Database (Myouga et al., 2010)	*egy1-1*, WiscDsLox293-296inv.L15	Yes			compact				roundish			pale green			decreased		
20	SALK_020801C	HM	At2g01450	*MAP KINASE 17* (*MPK17*)			No						asymmetrical			rugose		blotched				
21	SALK_001364C	NC	At2g22090	*UBP1-ASSOCIATED PROTEIN 1A* (*UBA1A*)			No															many trichomes, purple petiole and midvein
22	SALK_001004C	HM	At2g30810	Gibberellin-regulated family protein			No											netted				
23	SALK_036097C	HM	At1g50270	Pentatricopeptide repeat (PPR) superfamily protein			No	decreased		compact		decreased		roundish			adaxial: dark green, abaxial: purple		toothed	decreased		
24	SALK_001496C	HM	At1g62430	*CDP-DIACYLGLYCEROL SYNTHASE 1* (*CDS1*)			No											netted				
25	SALK_032946C	ND	At1g03020	Thioredoxin superfamily protein			No	decreased			decreased	decreased					pale green			decreased		
26	SALK_072705C	NC	At5g62800	Protein with RING/U-box and TRAF-like domains			No			compact										decreased		
27	SALK_072771C	HM	At2g07540	Transposable element gene			No								concave, undulate							
28	SALK_075797C	HM	At5g51770	Protein kinase superfamily protein			No								concave							
29	SALK_126818C	WT					N/A											netted				
30	SALK_127430C	NC	At2g20580	*26S PROTEASOME REGULATORY SUBUNIT S2 1A* (*RPN1A*)			Yes	decreased				decreased					yellow green			decreased		slow development
31	SALK_030786C	HM	At3g46790	*CHLORORESPIRATORY REDUCTION 2* (*CRR2*)			Yes											netted				
32	SALK_151239C	HM	At5g57690	*DIACYLGLYCEROL KINASE 4* (*DGK4*)			No	decreased		compact		decreased			undulate					decreased		
33	SALK_130961C	HM	At2g47650	*UDP-XYLOSE SYNTHASE 4* (*UXS4*)			No	decreased		compact		decreased		roundish	reclinate					decreased		
34	SALK_150644C	HM	At3g22590	*PLANT HOMOLOGOUS TO PARAFIBROMIN* (*PHP*)	No complementation in allelism test	*cdc73-1*, *cdc73-2*	Yes	increased		loose		increased		ovate						increased		
35	SALK_152782C	HM	At3g44200	*NIMA (NEVER IN MITOSIS, GENE A)-RELATED 6* (*NEK6*)	No complementation in allelism test	*lbo1-4*	Yes			compact										decreased		
36	SALK_150306C	NC	At4g35650	*ISOCITRATE DEHYDROGENASE III* (*IDH-III*)			No	decreased				decreased			reclinate, convolute					decreased		
37	SALK_001994C	ND	At5g10990	SAUR-like auxin-responsive protein family			No											netted				
38	SALK_007854C	HM	At4g11120	Translation elongation factor Ts (EF-Ts), putative			No			compact					undulate		pale green			decreased		
39	SALK_030624C	HM	At5g61050	Histone deacetylase-related / HD-related			No	decreased				decreased		elliptical						decreased	decreased	
40	SALK_030930C	HM	At4g19570	Chaperone DnaJ-domain superfamily protein			No	decreased				decreased		elliptical	concave					decreased	decreased	
41	SALK_075970C	HM	At3g16650	Transducin/WD40 repeat-like superfamily protein			No	increased				increased								increased		
42	SALK_106720C	S	At1g78010	tRNA modification GTPase, putative			No							reniform								
43	SALK_107544C	HM	At4g23060	*IQ-DOMAIN 22* (*IQD22*)			No	decreased				decreased						netted		decreased		
44	SALK_108010C	WT					N/A										pale green	netted				
45	SALK_108337C	HM	At2g19790	*SNARE-like superfamily protein*			No								reclinate, revolute							
46	SALK_057986C	WT					N/A	decreased				decreased					pale green		toothed	decreased		
47	SALK_151603C	HM	At3g62980	*TRANSPORT INHIBITOR RESPONSE 1* (*TIR1*)	Complementation in allelism test	*tir1-1*	Yes	decreased				decreased				rugose	yellow green		toothed	decreased		
48	SALK_089798C	HM	At3g25520	*RIBOSOMAL PROTEIN L5* (*ATL5*)	T-DNA insertion co-segregates with mutant phenotype		Yes	decreased				decreased		elliptical					toothed	decreased		
49	SALK_113836C	WT					N/A	decreased		compact	decreased	decreased		reniform	circinate, undulate		dark green			decreased		
50	SALK_065118C	HM	At1g53140	*DYNAMIN RELATED PROTEIN 5A* (*DRP5A*)			No	decreased		compact		decreased		orbicular	undulate					decreased		
51	SALK_048175C	HM	At1g30450	*CATION-CHLORIDE CO-TRANSPORTER 1* (*CCC1*)			Yes	decreased				decreased			circinate		adaxial dark green, abaxial purple			decreased		purple abaxial lamina surface
52	SALK_054681C	HM	At5g46115	Protein of unknown function			No															glabrous
53	SALK_048627C	NC	At3g57810	Cysteine proteinases superfamily protein			No	decreased				decreased					dark green			decreased		
54	SALK_055458C	HM	At1g14040	*EXS* (*ERD1/XPR1/SYG1*) family protein			No	decreased				decreased		roundish				variegated, blotched	toothed	decreased		
55	SALK_064931C	ND	At2g47840	*TRANSLOCON AT THE INNER ENVELOPE MEMBRANE OF CHLOROPLASTS 20-II* (*TIC20-II*)			No	decreased				decreased					white			decreased		albino
56	SALK_082482C	WT					N/A	decreased			decreased	decreased			concave				toothed	decreased		

Table S2a. Description of confirmed non-segregating mutants

UMH identifier	Salk line (isolated from)	Annotated locus genotype[1]	Gene mutated (AGI code)[2]	Gene description[2]	Evidence in favor of or against a gene-phenotype causality	Alleles associated with evidence of a gene-phenotype causality	Previously described allele[3]	Rosette relative size	Rosette phyllotaxy	Rosette compactness	Rosette relative organ number	Leaf relative size	Leaf symmetry	Leaf 2D shape	Leaf 3D shape	Leaf surface deformation	Leaf color filling	Leaf color pattern	Margin 2D shape	Petiole relative length	Petiole relative width	Other traits[4]
57	SALK_083333C	HM	At5g62660	F-box and associated interaction domains-containing protein			No												serrated			
58	SALK_086240C	WT					N/A		abnormal					roundish	concave, undulate							trichomes are short and twisted, juvenile leaf petioles grow upright and laminae are stuck toghether
59	SALK_086630C	HM	At3g50400	GDSL-like Lipase/Acylhydrolase superfamily protein			No	decreased			increased	decreased			reclinate, undulate		dark green					
60	SALK_086690C	HM	At3g23970	F-box family protein			No	decreased				decreased		elliptical	undulate				serrated	decreased		
61	SALK_111394C	HM	At4g09350	*NADH DEHYDROGENASE-LIKE COMPLEX T (NdhT)*			No	increased				increased						netted				
62	SALK_145086C	HM	At1g13740	*ABI FIVE BINDING PROTEIN 2 (AFP2)*			No	decreased				decreased		roundish			yellow green	netted	angular	decreased	decreased	
63	SALK_120077C	WT					N/A	increased				increased								increased		
64	SALK_059985C	ND	At5g28845	Transposable element gene			No	decreased				decreased			reclinate		pale green			decreased		
65	SALK_119457C	HM	At4g30410	Sequence-specific DNA binding transcription factor	T-DNA insertion co-segregates with mutant phenotype		No	decreased				decreased			reclinate		dark green			decreased		hirsute
66	SALK_133751C	HM	At5g43950	Plant protein of unknown function			No	decreased		compact	decreased	decreased					adaxial: dark green, abaxial: purple			decreased		
67	SALK_133963C	HM	At1g33080	MATE efflux family protein			No	decreased			decreased	decreased		elliptical			dark green			decreased		
68	SALK_141603C	WT					N/A								reclinate							purple petioles
69	SALK_142112C	HM	At1g74940	Protein of unknown function			No	decreased				decreased					pale green		angular	decreased		
70	SALK_145158C	WT					N/A	decreased				decreased							toothed	decreased		
71	SALK_145983C	HM	At4g09340	SPla/RYanodine receptor (SPRY) domain-containing protein			No								reclinate, revolute							
72	SALK_147068C	HM	At5g48120	ARM repeat superfamily protein			No								undulate		pale green					
73	SALK_144264C	HM	At3g19510	Member of the PHD-finger homeodomain protein family			No	decreased				decreased	asymmetrical			rugose	pale green	variegated	angular	decreased		
74	SALK_133805C	ND	At4g30580	*LYSOPHOSPHATIDIC ACID ACYLTRANSFERASE 1 (LPAT2)*			Yes	decreased		compact		decreased					pale green		toothed	decreased	decreased	
75	SALK_139862C	HM	At3g56170	*CA-2+ DEPENDENT NUCLEASE (CAN)*			No	decreased				decreased			reclinate					decreased		
76	SALK_138430C	ND	At5g46050	*PEPTIDE TRANSPORTER 3 (PTR3)*			No							elliptical			pale green					
77	SALK_147805C	HM	At2g31870	*SANSKRIT FOR 'BRIGHT' (TEJ)*			Yes	decreased		compact		decreased		roundish						decreased		
78	SALK_080188C	HM	At5g58970	*UNCOUPLING PROTEIN 2 (UCP2)*			No											netted				
79	SALK_124393C	WT					N/A											netted				some plants are very small and have bent-down leaves
80	SALK_139777C	HM	At5g54540	Uncharacterised conserved protein			No								reclinate, convolute							
81	SALK_125189C	HM	At1g61310	LRR and NB-ARC domains-containing disease resistance protein			No	decreased				decreased			undulate					decreased		forked leaves
82	SALK_138229C	HM	At1g54840	HSP20-like chaperones superfamily protein			No								concave							
83	SALK_143422C	HM	At2g44650	*CHLOROPLAST CHAPERONIN 10 (CHL-CPN10)*			No												serrated			
84	SALK_144022C	NC	At3g57390	*AGAMOUS-LIKE 18 (AGL18)*	T-DNA insertion does not co-segregate with mutant phenotype		No								concave							
85	SALK_125416C	WT					N/A											variegated				
86	SALK_136507C	HM	At1g78020	Protein of unknown function			No	decreased		compact	decreased	decreased		orbicular			yellow green			decreased		
87	SALK_138474C	HM	At5g42690	Protein of unknown function			No	decreased		compact	decreased	decreased			circinate, undulate					decreased		
88	SALK_138650C	HM	At2g36480	ENTHV HS family protein			No				increased				reclinate							
89	SALK_148403C	HM	At5g61950	Ubiquitin carboxyl-terminal hydrolase-related protein			No												serrated			
90	SALK_126071C	HM	At1g04730	*CHROMOSOME TRANSMISSION FIDELITY 18 (CTF18)*			No				increased											
91	SALK_009120C	NC	At4g36870	*BEL1-LIKE HOMEODOMAIN 2 (BLH2)*			No	decreased			decreased	decreased		roundish	concave		pale green			decreased		
92	SALK_008088C	HM	At1g10200	Member of the Arabidopsis LIM proteins			No	increased			increased	increased								increased		
93	SALK_010406C	WT					N/A	decreased				decreased				rugose		variegated		decreased		
94	SALK_026289C	HM	At2g24090	Ribosomal protein L35	Same phenotype as in The Chloroplast Function Database (Myouga et al., 2010)	SALK_026289.23.35.x	No	decreased			decreased	decreased		roundish			yellow green	variegated				
95	SALK_045623C	HM	At5g65050	*AGAMOUS-LIKE 31 (AGL31)*			Yes															early flowering
96	SALK_053198C	HM	At5g24470	*PSEUDO-RESPONSE REGULATOR 5 (PRR5)*			Yes	increased				increased								increased		
97	SALK_106689C	HM	At2g28450	Zinc finger (CCCH-type) family protein			No	decreased				decreased			involute, reclinate			netted		decreased		interveinal leaf lamina is darker than the veins
98	SALK_151478C	S	At5g05620	*GAMMA-TUBULIN COMPLEX PROTEIN 2 (GCP2)*			No	decreased		compact		decreased		roundish	flat		yellow green	variegated		decreased		
99	SALK_016311C	HM	At3g19360	Zinc finger (CCCH-type) family protein	T-DNA insertion does not co-segregate with mutant phenotype		No	decreased				decreased					dark green			decreased		hirsute
100	SALK_045619C	NC	At5g65640	*BETA HLH PROTEIN 93 (bHLH093)*			No															clockwise twisted petioles
101	SALK_022117C	HM	At2g01290	*RIBOSE-5-PHOSPHATE ISOMERASE 2 (RPI2)*			Yes							roundish			pale green	variegated				
102	SALK_060871C	WT					N/A	decreased		compact	decreased	decreased		orbicular			adaxial: dark green, abaxial: purple			decreased		
103	SALK_148633C	HM	At4g20450	Leucine-rich repeat protein kinase family protein			No											netted				
104	SALK_040079C	HM	At5g27570	*CELL DIVISION CYCLE 20.5 (CDC20.5)*	T-DNA insertion co-segregates with mutant phenotype		No	decreased				decreased					yellow green	netted, spotted	angular	decreased		hirsute
105	SALK_054336C	WT					N/A															
106	SALK_019359C	HM	At4g10920	Transcriptional co-activator that forms homodimers or heterodimers with the KIWI protein			No	increased				increased								increased		
107	SALK_025598C	HM	At2g46970	*PHYTOCHROME INTERACTING FACTOR 3-LIKE 1 (PIL1)*			Yes	increased				increased								increased		
108	SALK_069422C	WT					N/A													increased		
109	SALK_151354C	ND	At4g32780	Phosphoinositide binding			No	increased				increased								increased		
110	SALK_063595C	HM	At1g20640	Plant regulator RWP-RK family protein			No	decreased				decreased					pale green			decreased		
111	SALK_038835C	HM	At3g62440	*SECONDARY WALL THICKENING-ASSOCIATED F-BOX 1 (SAF1)*			No	increased				increased								increased		
112	SALK_143087C	WT					N/A															

Table S2a. Description of confirmed non-segregating mutants

UMH identifier	Salk line (isolated from)	Annotated locus genotype[1]	Gene mutated (AGI code)[2]	Gene description[2]	Evidence in favor of or against a gene-phenotype causality	Alleles associated with evidence of a gene-phenotype causality	Previously described allele[3]	Rosette relative size	Rosette phyllotaxy	Rosette compactness	Rosette relative organ number	Leaf relative size	Leaf symmetry	Leaf 2D shape	Leaf 3D shape	Leaf surface deformation	Leaf color filling	Leaf color pattern	Margin 2D shape	Petiole relative length	Petiole relative width	Other traits[4]
113	SALK_039212C	NC	At3g03150	Protein of unknown function			No	increased				increased								increased		
114	SALK_033511C	HM	At2g15790	*SQUINT* (*SQN*)	No complementation in allelism test	*sqn-1*, *sqn-2*	Yes												serrated			first two leaves are bigger than wild type
115	SALK_014243C	HM	At3g52105	Protein of unknown function			No			loose										increased	decreased	dark green petioles
116	SALK_018321C	HM	At5g52660	Homeodomain-like superfamily protein			No	decreased				decreased			reclinate		pale green			decreased		early flowering
117	SALK_063956C	HM	At5g38450	*CYTOCHROME P450, FAMILY 735, SUBFAMILY A, POLYPEPTIDE 1* (*CYP735A1*)			No										pale green	netted				
118	SALK_038138C	HM	At3g12020	P-loop containing nucleoside triphosphate hydrolases superfamily protein			No	increased				increased		elliptical	reclinate					increased		
119	SALK_037549C	HM	At2g23220	*CYTOCHROME P450, FAMILY 81, SUBFAMILY D, POLYPEPTIDE 6* (*CYP81D6*)			No								reclinate							clockwise twisted petioles
120	SALK_024759C	HM	At1g48950	C3HC zinc finger-like			No							elliptical	revolute							
121	SALK_048174C	HM	At4g11540	Cysteine/Histidine-rich C1 domain family protein			No				decreased						pale green	netted				
122	SALK_075661C	HM	At3g13228	RING/U-box superfamily protein			No	decreased				decreased					pale green	netted	toothed	decreased		
123	SALK_142184C	WT					N/A												lobed			
124	SALK_119925C	WT					N/A											netted				
125	SALK_035676C	HM	At1g10050	Putative glycosyl hydrolase family 10 protein (xylanase).			No	decreased				decreased				rugose	pale green	netted		decreased		
126	SALK_037023C	WT					N/A	decreased				decreased					yellow green			decreased		
127	SALK_014499C	WT					N/A	decreased				decreased						netted	toothed	decreased		
128	SALK_018660C	ND	At5g51540	Zincin-like metalloproteases family protein			No	decreased				decreased								decreased		some plants accumulate pigments
129	SALK_124232C	ND	At1g11790	*AROGENATE DEHYDRATASE 1* (*ADT1*)	Same phenotype as in The Chloroplast 2010 project (Lu et al. 2011)	SALK_124232, SALK_067937, SALK_138343	No	decreased		compact		decreased		oblong			dark green			decreased		some plants show necrosis in the lamina apex
130	SALK_009370C	NC	At5g05190	Protein of unknown function			No							roundish	undulate							
131	SALK_000028C	S	At3g48160	*DP-E2F-LIKE 1* (*DEL1*)			Yes								undulate							
132	SALK_013273C	WT					N/A							oblong								
133	SALK_026667C	HM	At5g28250	Transposable element gene			No								reclinate		dark green					
134	SALK_098395C	WT					N/A	decreased		compact		decreased			undulate					decreased		
135	SALK_012836C	HM	At3g21640	*TWISTED DWARF 1* (*TWD1*)	Two independent alleles found with similar phenotypes	SALK_086834C	Yes	decreased		compact		decreased			circinate					decreased		
136	SALK_076935C	HM	At4g11300	Protein of unknown function			No								reclinate							
137	SALK_008429C	HM	At1g65310	*XYLOGLUCAN ENDOTRANSGLUCOSYLASE/HYDROLASE 17* (*XTH17*)	Complementation in allelism test	*xth17-1*	Yes															shrunken lamina apex
138	SALK_003954C	ND	At2g33450	Ribosomal L28 family			No	decreased		compact		decreased						variegated		decreased		
139	SALK_017254C	HM	At2g40750	*WRKY DNA-BINDING PROTEIN 54* (*WRKY54*)			No								undulate							variable expressivity
140	SALK_148614C	ND	At3g01670	Protein of unknown function			No	decreased				decreased					yellow green			decreased		
141	SALK_002057C	HM	At2g22460	Protein of unknown function			No										pale green					
142	SALK_012771C	HM	At4g25410	Basic helix-loop-helix (bHLH) DNA-binding superfamily protein			No										pale green					
143	SALK_012970C	HM	At1g48750	Bifunctional inhibitor/lipid-transfer protein/seed storage 2S albumin superfamily protein			No	decreased				decreased		elliptical			dark green		toothed	decreased		
144	SALK_032963C	HM	At5g16270	*SISTER CHROMATID COHESION 1 PROTEIN 4* (*SYN4*)			Yes	increased				increased										
145	SALK_145203C	HM	At4g08540	DNA-directed RNA polymerase II protein			No	increased				increased					pale green					
146	SALK_151530C	ND	At1g50900	*GRANA DEFICIENT CHLOROPLAST 1* (*GDC1*)			Yes	decreased		compact	decreased	decreased			reclinate	rugose	yellow green			decreased		
147	SALK_077716C	WT					N/A	decreased				decreased			circinate					decreased		
148	SALK_146865C	HM	At4g16990	*RESISTANCE TO LEPTOSPHAERIA MACULANS 3* (*RLM3*)			Yes	decreased				decreased					pale green			decreased		
149	SALK_077422C	HM	At3g19680	Protein of unknown function	Same phenotype as in The Chloroplast 2010 project (Lu et al. 2011)	SALK_077422, SALK_090249	No								undulate, revolute							
150	SALK_147685C	HM	At3g33142	Transposable element gene			No								undulate, revolute							
151	SALK_057033C	WT					N/A	decreased				decreased			reclinate		dark green			decreased		
152	SALK_027152C	WT					N/A	decreased		compact		decreased					pale green			decreased		
153	SALK_051100C	HM	At2g20560	DNAJ heat shock family protein			No	decreased				decreased		spatulate					toothed	decreased	increased	
154	SALK_044496C	WT					N/A	decreased				decreased								decreased		
155	SALK_044145C	WT					N/A								reclinate							
156	SALK_000901C	HM	At3g47750	*ATP-BINDING CASSETTE A4* (*ABCA4*)			No								flat							
157	SALK_041437C	HM	At5g11160	*ADENINE PHOSPHORIBOSYLTRANSFERASE 5* (*APT5*)			No	increased				increased							lobed	increased		
158	SALK_048133C	ND	At2g38330	MATE efflux family protein			No															early flowering
159	SALK_050137C	HM	At3g13610	2-oxoglutarate (2OG) and Fe(II)-dependent oxygenase superfamily protein			No												serrated			
160	SALK_102810C	ND	At3g47833	*SUCCINATE DEHYDROGENASE 7* (*SDH7*)			No											blotched				
161	SALK_121961C	HM	At2g20270	Thioredoxin superfamily protein			No								reclinate, revolute							
162	SALK_077069C	HM	At2g47390	Prolyl oligopeptidase family protein			No											netted				some leaves show chlorotic patches
163	SALK_114679C	HM	At1g52120	Mannose-binding lectin superfamily protein			No	decreased				decreased					pale green			decreased		
164	SALK_110242C	HM	At3g48780	*SERINE PALMITOYLTRANSFERASE 1* (*SPT1*)			No															heterogeneous leaf size
165	SALK_037483C	HM	At2g41140	*CDPK-RELATED KINASE 1* (*CRK1*)			No								undulate, revolute							
166	SALK_076314C	ND	At5g22480	ZPR1 zinc-finger domain protein			No								undulate							
167	SALK_033307C	HM	At2g02000	*GLUTAMATE DECARBOXYLASE 3* (*GAD3*)			No										yellow green					
168	SALK_044415C	HM	At2g44950	*HISTONE MONO-UBIQUITINATION 1* (*HUB1*)	Complementation in allelism test	*ang4-1*	Yes										yellow green		serrated			

Table S2a. Description of confirmed non-segregating mutants

UMH identifier	Salk line (isolated from)	Annotated locus genotype[1]	Gene mutated (AGI code)[2]	Gene description[2]	Evidence in favor of or against a gene-phenotype causality	Alleles associated with evidence of a gene-phenotype causality	Previously described alleles[3]	Rosette relative size	Rosette phyllotaxy	Rosette compactness	Rosette relative organ number	Leaf relative size	Leaf symmetry	Leaf 2D shape	Leaf 3D shape	Leaf surface deformation	Leaf color filling	Leaf color pattern	Margin 2D shape	Petiole relative length	Petiole relative width	Other traits[4]
169	SALK_020957C	HM	At5g65420	*CYCLIN D4.1* (*CYCD4.1*)			Yes	increased		loose		increased								increased		
170	SALK_072930C	HM	At2g22540	*SHORT VEGETATIVE PHASE* (*SVP*)			Yes	increased			decreased	increased								increased		early flowering
171	SALK_039030C	HM	At5g14620	*DOMAINS REARRANGED METHYLTRANSFERASE 2* (*DRM2*)			No											netted	toothed			
172	SALK_032511C	WT					N/A											netted	toothed			
173	SALK_043149C	HM	At3g15950	Similar to *TSK-ASSOCIATING PROTEIN 1* (*TSA1*)			Yes			compact					reclinate					decreased		some petioles grow upright
174	SALK_044018C	WT					N/A	decreased				decreased					yellow green			decreased		
175	SALK_103278C	HM	At4g32105	Beta-1,3-N-Acetylglucosaminyltransferase family protein			No	decreased				decreased						netted		decreased	decreased	
176	SALK_040739C	WT					N/A	decreased		compact		decreased			reclinate					decreased		early flowering
177	SALK_060822C	WT					N/A	increased				increased					pale green					
178	SALK_015251C	WT					N/A			compact										decreased		
179	SALK_040244C	HM	At4g27060	*TORTIFOLIA 1* (*TOR1*)	Two independent alleles found with similar phenotypes. Same phenotype as in The RIKEN Arabidopsis Phenome Information Database (Kuromori et al. 2006)	SALK_094291C, RIKEN: 15-1038-1	Yes															clockwise twisted petioles
181	SALK_021488C	ND	At5g66020	*SUPPRESSOR OF ACTIN 1B* (*ATSAC1B*)			No	decreased				decreased								decreased		
182	SALK_062605C	NC	At5g47550	Cystatin/monellin superfamily protein			No	decreased				decreased								decreased		
183	SALK_006729C	ND	At3g49190	O-acyltransferase (WSD1-like) family protein			No	decreased		compact		decreased			cincinate		dark green			decreased		
184	SALK_012907C	ND	At1g51830	Leucine-rich repeat protein kinase family protein			No											netted				
185	SALK_008125C	ND	At1g15790	Protein of unknown function			No								reclinate							shrunken lamina apex
186	SALK_021171C	HM	At1g07650	Leucine-rich repeat transmembrane protein kinase			No	decreased				decreased					purple			decreased		
187	SALK_051913C	S	At5g05100	Single-stranded nucleic acid binding R3H protein			No								revolute							
188	SALK_019413C	NC	At5g19630	alpha/beta-Hydrolases superfamily protein			No	increased				increased			reclinate					increased		increased lamina length
189	SALK_047268C	HM	At4g39270	Leucine-rich repeat protein kinase family protein			No	decreased			decreased	decreased		elliptical								early flowering
190	SALK_017913C	HM	At3g18130	*RECEPTOR FOR ACTIVATED C KINASE 1C* (*RACK1C_AT*)			No															juvenile leaves are furrowed and stuck together
191	SALK_062900C	WT					N/A	decreased				decreased			concave			netted		decreased		early flowering (incomplete penetrance)
192	SALK_075362C	S	At4g39410	*WRKY DNA-BINDING PROTEIN 13* (*WRKY13*)			No								undulate							
193	SALK_042323C	WT					N/A	decreased		compact		decreased			reclinate					decreased		
194	SALK_040155C	HM	At5g48300	*ADP GLUCOSE PYROPHOSPHORYLASE 1* (*ADG1*)			Yes	increased				increased								increased		
195	SALK_041111C	HM	At3g09370	*MYB DOMAIN PROTEIN 3R-3* (*MYB3R-3*)			No	increased				increased								increased		
196	SALK_044616C	WT					N/A	decreased				decreased					pale green			decreased		
197	SALK_062875C	HM	At1g09430	*ATP-CITRATE LYASE A-3* (*ACLA-3*)			No													increased		early flowering
198	SALK_072896C	HM	At3g16857	*RESPONSE REGULATOR 1* (*RR1*)			Yes								reclinate				lobed			
199	SALK_047815C	HM	At1g22430	GroES-like zinc-binding dehydrogenase family protein			No								flat				toothed			
200	SALK_004741C	HM	At1g42980	Actin-binding FH2 (formin homology 2) family protein			No										pale green		toothed			
201	SALK_009736C	HM	At1g17130	Protein of unknown function			No							ovate								
202	SALK_009798C	HM	At2g23090	Uncharacterised protein family SERF	Two independent alleles found with similar phenotypes	SALK_072218C	No							spatulate	concave		dark green				increased	
203	SALK_010286C	HM	At1g24180	*IAA-CONJUGATE-RESISTANT 4* (*IAR4*)	Same phenotype as in The Chloroplast 2010 project (Lu et al. 2011)	SALK_010286, SALK_011308, SALK_042087, SALK_091909	Yes	decreased				decreased		elliptical			dark green		toothed	decreased		
204	SALK_014727C	HM	At3g58960	F-box/RNI-like/FBD-like domains-containing protein			No	increased				increased										
205	SALK_015252C	HM	At1g24310	Protein of unknown function			No	decreased				decreased		elliptical	reclinate							
206	SALK_017692C	S	At2g29670	Tetratricopeptide repeat (TPR)-like superfamily protein			No	decreased				decreased								decreased		
207	SALK_022035C	HM	At2g18790	*PHYTOCHROME B* (*PHYB*)	Same phenotype as in The Chloroplast 2010 project (Lu et al. 2011)	SALK_022035	Yes	increased		loose		increased					pale green			increased		
208	SALK_024270C	HM	At5g17510	Protein of unknown function			No	increased			decreased	increased								increased		early flowering
209	SALK_024760C	HM	At5g01310	*APRATAXIN-LIKE* (*APTX*)			No										pale green					
210	SALK_024963C	HM	At1g49210	RING/U-box superfamily protein			No	decreased		compact		decreased		ovate			pale green			decreased		
211	SALK_025730C	HM	At2g22470	*ARABINOGALACTAN PROTEIN 2* (*AGP2*)			No	decreased	abnormal			decreased		elliptical						decreased		
212	SALK_027847C	HM	At3g12490	*CYSTATIN B* (*CYSB*)			Yes	increased				increased						netted	serrated	increased		
213	SALK_034362C	HM	At4g13120	Transposable element gene			No	decreased		compact	decreased	decreased					yellow green			decreased		
214	SALK_034684C	HM	At2g22420	Peroxidase superfamily protein			No	decreased				decreased		ovate	reclinate		dark green					
215	SALK_036463C	HM	At3g03520	*NON-SPECIFIC PHOSPHOLIPASE C3* (*NPC3*)			No	decreased		compact		decreased		roundish			pale green			decreased		
216	SALK_039359C	HM	At2g04550	*INDOLE-3-BUTYRIC ACID RESPONSE 5* (*IBR5*)			Yes	increased				increased							crenated	increased		
217	SALK_040660C	HM	At1g79090	Protein of unknown function			No	decreased				decreased		elliptical	reclinate					decreased		
218	SALK_041291C	HM	At2g22680	Zinc finger (C3HC4-type RING finger) family protein			No											netted				
219	SALK_043116C	HM	At1g54580	*ACYL CARRIER PROTEIN 2* (*ACP2*)			No	increased				increased			reclinate			netted				
220	SALK_045034C	HM	At5g17660	tRNA (guanine-N-7) methyltransferase			No											variegated				
221	SALK_046141C	HM	At2g03190	*SKP1-LIKE 16* (*SK16*)			No							ovate	reclinate							
222	SALK_056529C	HM	At1g20860	*PHOSPHATE TRANSPORTER 1.8* (*PHT1.8*)			No	decreased			increased	decreased			revolute		dark green			decreased		
223	SALK_057785C	HM	At1g22090	*EMBRYO DEFECTIVE 2204* (*emb2204*)			Yes	decreased		compact		decreased		roundish				variegated		decreased		
224	SALK_079285C	HM	At3g17040	*HIGH CHLOROPHYLL FLUORESCENT 107* (*HCF107*)			No	decreased		compact		decreased		roundish			yellow green			decreased		
225	SALK_087484C	HM	At1g77600	ARM repeat superfamily protein	Four independent alleles found with similar phenotypes. No complementation in allelism tests	SALK_087484, SALK_092843C, SAIL_1213_C02, SAIL_562_D01	No			compact										decreased		

Table S2a. Description of confirmed non-segregating mutants

UMH identifier	Salk line (isolated from)	Annotated locus genotype[1]	Gene mutated (AGI code)[2]	Gene description[2]	Evidence in favor of or against a gene-phenotype causality	Alleles associated with evidence of a gene-phenotype causality	Previously described alleles[3]	Rosette relative size	Rosette phyllotaxy	Rosette compactness	Rosette relative organ number	Leaf relative size	Leaf symmetry	Leaf 2D shape	Leaf 3D shape	Leaf surface deformation	Leaf color filling	Leaf color pattern	Margin 2D shape	Petiole relative length	Petiole relative width	Other traits[4]
226	SALK_087804C	HM	At3g45410	Receptor-like kinase			No	decreased				decreased						netted		decreased		
227	SALK_088750C	HM	At5g02510	Protein of unknown function			No	decreased				decreased					pale green			decreased		
228	SALK_095148C	HM	At1g70640	Octicosapeptide/Phox/Bem1p (PB1) domain-containing protein			No	decreased				decreased			reclinate			variegated	toothed	decreased		
229	SALK_100396C	HM	At1g49900	C2H2 type zinc finger transcription factor family			No										pale green					
230	SALK_101697C	HM	At2g17180	*DUO1-ACTIVATED ZINC FINGER 1* (*DAZ1*)	T-DNA insertion does not co-segregate with mutant phenotype		No	increased				increased										
231	SALK_101771C	HM	At1g18500	*METHYLTHIOALKYLMALATE SYNTHASE-LIKE 4* (*MAML-4*)			Yes	decreased				decreased		elliptical	undulate					decreased		protruding midvein
232	SALK_103127C	HM	At5g64080	*XYLOGEN PROTEIN 1* (*XYP1*)			No	decreased				decreased					pale green			decreased		
233	SALK_116141C	HM	At4g12990	Protein of unknown function			No	decreased				decreased		roundish			pale green			decreased		
234	SALK_117972C	HM	At2g44100	*GUANOSINE NUCLEOTIDE DIPHOSPHATE DISSOCIATION INHIBITOR 1* (*GDI1*)			No								reclinate, revolute							
235	SALK_122867C	HM	At1g18900	Pentatricopeptide repeat (PPR) superfamily protein			No		abnormal				asymmetrical		undulate							
236	SALK_092843C	HM	At1g77600	ARM repeat superfamily protein	Four independent alleles found with similar phenotypes, No complementation in allelism tests	SALK_087484, SALK_092843C, SAIL_1213_C02, SAIL_562_D01	No			compact				ovate						decreased		
237	SALK_057752C	S	At4g24805	S-adenosyl-L-methionine-dependent methyltransferases superfamily protein			No	decreased				decreased					yellow green	variegated	toothed	decreased		
238	SALK_026611C	S	At4g38560	Arabidopsis phospholipase-like protein (PEARLI 4) family			No	increased				increased			reclinate					increased		
239	SALK_026489C	NC	At1g01510	*ANGUSTIFOLIA* (*AN*)			Yes	decreased				decreased		elliptical	flat		dark green			increased		the lamina is darker than the midvein
240	SALK_027931C	HM	At4g02780	*GA REQUIRING 1* (*GA1*)			Yes	decreased		compact		decreased			circinate		dark green			decreased		
241	SALK_012816C	WT					N/A	decreased		compact		decreased		roundish			yellow green			decreased		
242	SALK_024210C	WT					N/A			compact										decreased		
243	SALK_037512C	WT					N/A	decreased				decreased						variegated	toothed	decreased		
244	SALK_045926C	WT					N/A	decreased		compact		decreased			reclinate		pale green		toothed	decreased		
245	SALK_102662C	WT					N/A											variegated, netted	lobed			
246	SALK_110691C	WT					N/A												toothed			
247	SALK_118239C	WT					N/A															glabrous
248	SALK_000739C	WT					N/A	decreased				decreased		elliptical					lobed	decreased		hirsute
249	SALK_003223C	HM	At1g79440	*ALDEHYDE DEHYDROGENASE 5F1* (*ALDH5F1*)			Yes	decreased				decreased	asymmetrical		undulate	rugose				decreased		impaired development
250	SALK_003249C	ND	At4g10630	Glutaredoxin family protein			No											netted				
251	SALK_011806C	ND	At1g16410	*CYTOCHROME P450 79F1* (*CYP79F1*)			Yes								concave, undulate							
252	SALK_013297C	HM	At3g50950	*HOPZ-ACTIVATED RESISTANCE 1* (*ZAR1*)			No	decreased				decreased						variegated		decreased		
253	SALK_013567C	HM	At1g13900	Purple acid phosphatases superfamily protein			No				increased				reclinate							
254	SALK_017444C	HM	At5g05730	*ANTHRANILATE SYNTHASE ALPHA SUBUNIT 1* (*ASA1*)	No complementation in allelism test, Same phenotype as in The Chloroplast Function Database (Myouga et al., 2010)	*wei2-1*, RIKEN-52-1097-1, RIKEN-54-3983-1	Yes								concave			netted				
255	SALK_018475C	ND	At5g67270	*END BINDING PROTEIN 1C* (*EB1C*)			Yes	decreased				decreased			reclinate		dark green			decreased		the abaxial surface petioles and veins is darker
256	SALK_018851C	HM	At4g32670	RING/FYVE/PHD zinc finger superfamily protein			No	decreased				decreased			reclinate		pale green			decreased		
257	SALK_023849C	ND	At2g01260	Protein of unknown function			No															
258	SALK_023910C	HM	At5g40020	Pathogenesis-related thaumatin superfamily protein			No	decreased				decreased					yellow green	variegated		decreased		
259	SALK_024285C	HM	At2g13540	*ABA HYPERSENSITIVE 1* (*ABH1*)	T-DNA insertion co-segregates with mutant phenotype		Yes	decreased				decreased					pale green		lobed	decreased		floppy lamina
260	SALK_026551C	HM	At2g22540	*SHORT VEGETATIVE PHASE* (*SVP*)	Two independent alleles found with similar phenotypes	SALK_072930C	Yes				decreased											early flowering
261	SALK_027288C	HM	At5g28470	Major facilitator superfamily protein			No											netted	crenated			
262	SALK_027485C	ND	At3g47300	*SELT-LIKE PROTEIN PRECURSOR* (*SELT*)			No	decreased				decreased		roundish				variegated, netted		decreased		
263	SALK_027524C	WT					N/A	decreased		compact		decreased								decreased		
264	SALK_027691C	HM	At4g36730	*G-BOX BINDING FACTOR 1* (*GBF1*)			No	decreased				decreased			reclinate			variegated	toothed	decreased	increased	
265	SALK_029389C	ND	At2g33050	*RECEPTOR LIKE PROTEIN 26* (*RLP26*)			No	decreased		compact		decreased			reclinate					decreased	increased	
266	SALK_029940C	ND	At5g17420	*IRREGULAR XYLEM 3* (*IRX3*)			Yes	decreased		compact		decreased		orbicular	reclinate		dark green			decreased		
267	SALK_030202C	HM	At1g71691	GDSL-like Lipase/Acylhydrolase superfamily protein			No	decreased		compact		decreased		elliptical	reclinate				toothed	decreased		
268	SALK_036569C	WT					N/A								reclinate, revolute							
269	SALK_039478C	HM	At3g27920	*MYB DOMAIN PROTEIN 0* (*MYB0*)			Yes															glabrous
270	SALK_046439C	HM	At3g29560	Protein of unknown function			No								undulate, concave,							
271	SALK_057480C	HM	At1g60800	Pseudogene, similar to 40S ribosomal protein S12 (RPS12B)			No	decreased				decreased					pale green			decreased		
272	SALK_057782C	HM	At2g35720	*ORIENTATION UNDER VERY LOW FLUENCES OF LIGHT 1* (*OWL1*)			Yes	decreased		compact		decreased					yellow green			decreased		
273	SALK_063843C	WT					No	increased		loose		increased		elliptical						increased		
274	SALK_067800C	HM	At4g16720	Ribosomal protein L23/L15e family protein			No	decreased				decreased		elliptical					toothed	decreased		
275	SALK_070088C	ND	At4g31990	*ASPARTATE AMINOTRANSFERASE 5* (*ASP5*)			No	decreased				decreased					yellow green			decreased		
276	SALK_072218C	ND	At2g23090	Uncharacterised protein family SERF			No													increased		
277	SALK_077062C	HM	At1g59790	Cullin family protein			No	decreased				decreased		elliptical	reclinate					decreased		variable expressivity
278	SALK_080604C	HM	At1g08135	*CATION/H+ EXCHANGER 6B* (*CHX6B*)			No															glabrous
279	SALK_082289C	HM	At2g33030	*RECEPTOR LIKE PROTEIN 25* (*RLP25*)			No								reclinate							
280	SALK_085503C	HM	At2g33420	Protein of unknown function, contains domain Munc13 homology 1			No	increased		loose		increased								increased		early flowering
281	SALK_085920C	HM	At5g25754	RNA polymerase I-associated factor PAF67			No	decreased				decreased					pale green			decreased		

Table S2a. Description of confirmed non-segregating mutants

UMH identifier	Salk line (isolated from)	Annotated locus genotype[1]	Gene mutated (AGI code)[2]	Gene description[2]	Evidence in favor of or against a gene-phenotype causality	Alleles associated with evidence of a gene-phenotype causality	Previously described allele[3]	Rosette relative size	Rosette phyllotaxy	Rosette compactness	Rosette relative organ number	Leaf relative size	Leaf symmetry	Leaf 2D shape	Leaf 3D shape	Leaf surface deformation	Leaf color filling	Leaf color pattern	Margin 2D shape	Petiole relative length	Petiole relative width	Other traits[4]
282	SALK_086452C	ND	At1g18560	BED zinc finger			No				increased								serrated			
283	SALK_086776C	HM	At4g00180	*YABBY3* (*YAB3*)	T-DNA insertion co-segregates with mutant phenotype		No								concave				serrated			
284	SALK_086834C	HM	At3g21640	*TWISTED DWARF 1* (*TWD1*)			Yes	decreased		compact		decreased			reclinate					decreased		
285	SALK_087642C	HM	At2g27530	*PIGGYBACK1* (*PGY1*)			No								reclinate							
286	SALK_087720C	HM	At4g28220	*NAD(P)H DEHYDROGENASE B1* (*NDB1*)			No	decreased				decreased			reclinate		abaxial: purple			decreased		
287	SALK_088140C	ND	At3g50080	*VIER F-BOX PROTEINE 2* (*VFB2*)			No	decreased		compact		decreased			undulate					decreased		
288	SALK_089912C	S	At1g72510	Protein of unknown function			No	decreased				decreased		elliptical	reclinate, revolute			netted		decreased		
289	SALK_090264C	HM	At5g53770	Nucleotidyltransferase family protein			No	decreased		compact		decreased		roundish				variegated		decreased		
290	SALK_094653C	HM	At3g49040	F-box/RNI-like superfamily protein			No	increased				increased					pale green					
291	SALK_094856C	HM	At1g63280	Serine protease inhibitor (SERPIN) family protein			No	decreased				decreased								decreased		
292	SALK_094948C	WT					N/A							elliptical					toothed			
293	SALK_097064C	HM	At5g26717	Plant thionin family protein			No	decreased		compact		decreased					yellow green		angular	decreased		
294	SALK_099684C	HM	At5g06410	DNAJ heat shock N-terminal domain-containing protein			Yes	increased		loose		increased					pale green			increased		early flowering
295	SALK_103728C	HM	At5g52930	Protein of unknown function			No							rhomboid	undulate			netted	toothed			
296	SALK_105495C	HM	At3g02260	*BIG* (*BIG*)			Yes	decreased		compact		decreased		ovate	reclinate					decreased		
297	SALK_105998C	ND	At2g07550	Transposable element gene			No								concave, undulat							
298	SALK_114293C	HM	At2g41680	*NADPH-DEPENDENT THIOREDOXIN REDUCTASE C* (*NTRC*)	Same phenotype as in The Chloroplast 2010 project (Lu et al. 2011)	SALK_114293	Yes									rugose	pale green					
299	SALK_116625C	HM	At1g76730	NagB/RpiA/CoA transferase-like superfamily protein			No	decreased		compact	increased	decreased		roundish	concave					decreased		hirsute
300	SALK_122911C	ND	At3g08920	Rhodanese/Cell cycle control phosphatase superfamily protein			No											netted				
301	SALK_132789C	WT					N/A										pale green					
302	SALK_142534C	HM	At1g70600	Ribosomal protein L18e/L15 superfamily protein			No							elliptical								
303	SALK_019830C	HM	At2g06260	Transposable element gene			No										pale green					
304	SALK_131854C	WT					No	decreased				decreased								decreased		
305	SALK_130695C	HM	At1g59750	*AUXIN RESPONSE FACTOR 1* (*ARF1*)			No				decreased											early flowering
306	SALK_131169C	HM	At4g34000	*ABSCISIC ACID RESPONSIVE ELEMENTS-BINDING FACTOR 3* (*ABF3*)			No	increased		loose		increased								increased		
307	SALK_130589C	HM	At1g76870	Protein of unknown function			No	decreased				decreased		elliptical	involute		pale green		toothed	decreased		early flowering
308	SALK_130719C	HM	At1g65270	Protein of unknown function			No										pale green					
309	SALK_116798C	HM	At4g32040	*KNOTTED1-LIKE HOMEOBOX GENE 5* (*KNAT5*)	Same phenotype as in The Chloroplast 2010 project (Lu et al. 2011)	SALK_116798, SALK_000339	No	decreased				decreased		elliptical					toothed	decreased		irregularly-shaped laminae
310	SALK_129969C	HM	At5g44160	*NUTCRACKER* (*NUC*)			Yes	decreased				decreased			reclinate					decreased		heterogeneous growth
311	SALK_150440C	S	At5g13120	*PHOTOSYNTHETIC NDH SUBCOMPLEX L 5* (*PNSL5*)			No	increased		loose				elliptical						increased		
312	SALK_115745C	HM	At4g26630	Protein of unknown function			No	decreased		compact	increased	decreased		elliptical						decreased		some plants are vitrified, early flowering, some having multiple shoot apical meristems
313	SALK_106273C	HM	At1g78280	Protein of unknown function			No	decreased			decreased	decreased		elliptical					toothed	decreased	decreased	
314	SALK_105449C	HM	At5g55050	Protein of unknown function			No	decreased			decreased	decreased		elliptical	concave	rugose		netted	toothed			
315	SALK_083098C	HM	At5g44925	Protein of unknown function			No								wavy							variable expressivity
316	SALK_106255C	HM	At5g02790	*GLUTATHIONE TRANSFERASE L3* (*GSTL3*)			No								reclinate		pale green		toothed			
317	SALK_059855C	HM	At5g44580	Protein of unknown function			No	decreased			decreased	decreased		lanceolate			pale green	netted	toothed	decreased	decreased	light colored teeth
318	SALK_099949C	WT					No	decreased		compact		decreased	asymmetrical	roundish	wavy							some leaves show an irregular shape
319	SALK_107389C	HM	At1g02670	Protein of unknown function			No				decreased		asymmetrical		reclinate							
320	SALK_082227C	HM	At4g22860	Protein of unknown function			No	decreased				decreased								decreased		glabrous
321	SALK_081001C	HM	At5g66330	Protein of unknown function			No	decreased			decreased	decreased					pale green			decreased	decreased	
322	SALK_042082C	HM	At3g59580	Plant regulator RWP-RK family protein			No	decreased			decreased	decreased		roundish	wavy		pale green	variegated		decreased	decreased	
323	SALK_046669C	HM	At1g06320	Protein of unknown function			No	decreased			decreased	decreased		roundish	concave, undulate		pale green	netted	toothed	decreased	decreased	
324	SALK_046469C	S	At3g23660	Sec23/Sec24 protein transport family protein			No	increased				decreased		ovate						increased		
325	SALK_033583C	HM	At2g33250	Protein of unknown function			No											variegated				only the youngest leaves are variegated
326	SALK_044811C	WT					No	decreased			decreased	decreased		elliptical					toothed	decreased	decreased	
327	SALK_044584C	HM	At4g25090	Riboflavin synthase-like superfamily protein			No	decreased				decreased		elliptical					serrated	decreased	decreased	
328	SALK_046686C	HM	At4g32930	Protein of unknown function			No				decreased			elliptical	concave, undulate		pale green		toothed			
329	SALK_043451C	HM	At5g23710	DNA-directed RNA polymerase			No	increased		loose				elliptical						increased		
330	SALK_044803C	ND	At5g47050	SBP (S-ribonuclease binding protein) family protein			No	decreased		compact	decreased	decreased		lanceolate	concave		pale green	variegated	toothed	decreased	decreased	
331	SALK_056799C	HM	At5g09580	Protein of unknown function			No	decreased	abnormal		decreased	decreased		roundish		rugose			crenated	decreased	decreased	
332	SALK_047566C	HM	At1g43690	Ubiquitin interaction motif-containing protein			No	decreased	abnormal		decreased	decreased	asymmetrical			rugose				decreased	decreased	amorphous
333	SALK_039252C	HM	At1g33270	Acyltransferase/acyl hydrolase/lysophospholipase superfamily protein			No	decreased			decreased	decreased		roundish			pale green			decreased	decreased	
334	SALK_016573C	HM	At4g20040	Pectin lyase-like superfamily protein			No	decreased				decreased								decreased	decreased	
335	SALK_046391C	HM	At5g41500	F-box and associated interaction domains-containing protein			No	decreased			decreased	decreased	asymmetrical	elliptical					toothed	decreased	decreased	some laminae are split in two
336	SALK_108955C	HM	At1g72810	Pyridoxal-5'-phosphate-dependent enzyme family protein			No	decreased		compact		decreased			undulate					decreased	decreased	
337	SALK_110931C	HM	At1g06340	Plant Tudor-like protein			No	decreased		loose		decreased			circinate					decreased	decreased	

Table S2a. Description of confirmed non-segregating mutants

UMH identifier	Salk line (isolated from)	Annotated locus genotype[1]	Gene mutated (AGI code)[2]	Gene description[2]	Evidence in favor of or against a gene-phenotype causality	Alleles associated with evidence of a gene-phenotype causality	Previously described allele[3]	Rosette relative size	Rosette phyllotaxy	Rosette compactness	Rosette relative organ number	Leaf relative size	Leaf symmetry	Leaf 2D shape	Leaf 3D shape	Leaf surface deformation	Leaf color filling	Leaf color pattern	Margin 2D shape	Petiole relative length	Petiole relative width	Other traits[4]
338	SALK_071402C	HM	At1g31140	*GORDITA (GOA)*			Yes	decreased				decreased		roundish				variegated		decreased	decreased	
339	SALK_073451C	HM	At1g72460	Leucine-rich repeat protein kinase family protein			No	decreased				decreased					dark green			decreased	decreased	
340	SALK_116898C	HM	At1g28130	*GH3.17*			Yes	increased		loose										increased		
341	SALK_073405C	HM	At4g08110	CACTA-like transposase family			No	decreased			decreased	decreased					white			decreased	decreased	
342	SALK_072581C	HM	At4g33520	*P-TYPE ATP-ASE 1 (PAA1)*			Yes	decreased		compact		decreased			reclinate					decreased	decreased	
343	SALK_071811C	HM	At3g52250	Encodes a protein with a putative role in mRNA splicing			No	decreased			increased	decreased			reclinate					decreased		
344	SALK_071501C	ND	At1g72620	Alpha/beta-Hydrolases superfamily protein			No	decreased			decreased	decreased					white			decreased	decreased	
345	SALK_015131C	HM	At3g25740	*METHIONINE AMINOPEPTIDASE 1C (MAP1B)*			No	decreased		loose		decreased		elliptical			white		toothed	increased		
346	SALK_016837C	WT					No	decreased		compact		decreased		roundish			pale green			decreased	decreased	
347	SALK_013071C	HM	At2g11851	Protein of unknown function			No	decreased				decreased					pale green			decreased	decreased	
348	SALK_011512C	HM	At3g25585	*AMINOALCOHOLPHOSPHOTRANSFERASE (AAPT2)*			No							ovate								
349	SALK_069199C	HM	At3g11397	*PRENYLATED RAB ACCEPTOR 1.A3 (PRA1.A3)*			No	decreased				decreased		roundish	undulate		pale green	variegated		decreased	decreased	
350	SALK_099638C	HM	At4g37130	Hydroxyproline-rich glycoprotein family protein			No	increased												increased	decreased	early flowering
400	SALK_038859C	WT					N/A	decreased	abnormal		decreased	decreased				rugose			toothed	decreased		
401	SALK_011586C	HM	At3g27620	*ALTERNATIVE OXIDASE 1C (AOX1C)*			No							elliptical	concave		pale green					
402	SALK_013253C	WT					N/A	decreased				decreased				rugose				decreased		
403	SALK_011867C	HM	At5g51750	*SUBTILASE 1.3 (SBT1.3)*			No								reclinate							
404	SALK_012683C	HM	At1g21326	VQ motif-containing protein			No	decreased				decreased						variegated		decreased		sensitive to environmental conditions
405	SALK_013461C	HM	At1g73490	RNA-binding (RRM/RBD/RNP motifs) family protein			No			compact							dark green			decreased		
406	SALK_020615C	HM	At1g76470	NAD(P)-binding Rossmann-fold superfamily protein			No	increased		loose		increased								increased		
407	SALK_021618C	HM	At2g47490	*NAD+ TRANSPORTER 1 (NDT1)*			No	decreased				decreased			concave					decreased		
408	SALK_021759C	HM	At4g32200	*ASYNAPTIC 2 (ASY2)*			No	decreased				decreased					dark green		toothed			
409	SALK_070464C	HM	At1g74420	*FUCOSYLTRANSFERASE 3 (FUT3)*			No	decreased				decreased					pale green	netted		decreased		
410	SALK_010588C	HM	At1g09330	Protein of unknown function			No	decreased				decreased						spotted		decreased		
411	SALK_044119C	HM	At2g35040	AICARFT/IMPCHase bienzyme family protein			No								reclinate, undulate							
412	SALK_005153C	HM	At5g13680	*ABA-OVERLY SENSITIVE 1 (ABO1)*			Yes	decreased				decreased		rhomboid						decreased		
413	SALK_064104C	NC	At4g20370	*TWIN SISTER OF FT (TSF)*			Yes				decreased											early flowering
414	SALK_045025C	HM	At3g20550	*DAWDLE (DDL)*	Annotated T-DNA was PCR-confirmed	*ddl-1, ddl-2*	Yes							ovate								yellow green petioles
415	SALK_057052C	HM	At5g54770	*THIAZOLE REQUIRING (TZ)*	Annotated T-DNA was PCR-confirmed	*tz-1*	Yes	decreased		compact		decreased					pale green	variegated		decreased		
416	SALK_005786C	HM	At3g27590	Protein of unknown function			No	decreased				decreased		ovate	concave			netted	toothed			
417	SALK_066708C	HM	At4g24175	Protein of unknown function			No								reclinate							
418	SALK_003711C	HM	At1g71760	Protein of unknown function			No								reclinate				serrated			
419	SALK_055996C	HM	At1g32500	*ATP-BINDING CASSETTE I7 (ABCI7)*			No										pale green					yellow green petioles
420	SALK_034227C	HM	At4g30114	RNA-binding (RRM/RBD/RNP motifs) family protein			No								undulate							
421	SALK_057083C	S	At5g61240	Leucine-rich repeat (LRR) family protein			No												crenated			
422	SALK_035241C	WT					N/A	decreased			decreased	decreased		elliptical					toothed	decreased		
423	SALK_043616C	WT					N/A	decreased			decreased	decreased		elliptical					toothed	decreased		
424	SALK_044034C	HM	At5g66490	Protein of unknown function			No	decreased			decreased	decreased		elliptical			pale green			decreased		
425	SALK_044091C	WT					N/A	decreased			decreased	decreased							toothed	decreased		
426	SALK_014587C	HM	At1g66250	O-Glycosyl hydrolases family 17 protein			No								reclinate				angular			
427	SALK_011376C	NC	At5g49940	*NIFU-LIKE PROTEIN 2 (NFU2)*			No	decreased		compact		decreased					pale green			decreased		
428	SALK_015522C	HM	At5g36880	*ACETYL-COA SYNTHETASE (ACS)*			No	decreased				decreased			reclinate			variegated	toothed	decreased		
429	SALK_015088C	HM	At5g61960	*MEI2-LIKE PROTEIN 1 (MLI1)*			No									rugose		blotched				
430	SALK_067582C	HM	At2g32540	*CELLULOSE SYNTHASE-LIKE B4 (CSLB04)*			No				decreased			elliptical								
431	SALK_047274C	WT					N/A	decreased				decreased			concave					decreased		
432	SALK_009623C	NC	At3g59730	Concanavalin A-like lectin protein kinase family protein			No	decreased				decreased					pale green	netted		decreased		
433	SALK_033455C	HM	At3g28860	*ATP-BINDING CASSETTE B19 (ABCB19)*	No complementation in allelism test	*mdr1-1, mdr1-3*	Yes	decreased		compact	decreased	decreased			reclinate					decreased		petioles grow upright
434	SALK_049200C	HM	At2g04043	Transposable element gene			No	decreased			decreased	decreased		elliptical			pale green	netted		decreased		
435	SALK_064915C	HM	At5g23980	*FERRIC REDUCTION OXIDASE 4 (FRO4)*			No	decreased				decreased					pale green	variegated		decreased		necrotic spots
436	SALK_045441C	WT					N/A		abnormal		decreased			elliptical								
437	SALK_008546C	WT					N/A	decreased				decreased						variegated		decreased		
438	SALK_070853C	HM	At3g60965	Transposable element gene			No		abnormal													
439	SALK_067058C	HM	At2g44970	Alpha/beta-Hydrolases superfamily protein			No	decreased				decreased				rugose		blotched		decreased		necrosis in margins
440	SALK_008561C	HM	At4g20290	Protein of unknown function			No	decreased				decreased						netted		decreased		
441	SALK_064507C	HM	At3g17750	Protein kinase superfamily protein			No								reclinate					increased		
442	SALK_009903C	WT					No	decreased				decreased		linear			pale green			decreased	increased	

Table S2a. Description of confirmed non-segregating mutants

UMH identifier	Salk line (isolated from)	Annotated locus genotype[1]	Gene mutated (AGI code)[2]	Gene description[2]	Evidence in favor of or against a gene-phenotype causality	Alleles associated with evidence of a gene-phenotype causality	Previously described allele[3]	Rosette relative size	Rosette phyllotaxy	Rosette compactness	Rosette relative organ number	Leaf relative size	Leaf symmetry	Leaf 2D shape	Leaf 3D shape	Leaf surface deformation	Leaf color filling	Leaf color pattern	Margin 2D shape	Petiole relative length	Petiole relative width	Other traits[4]
443	SALK_043549C	HM	At3g30737	Transposable element gene	T-DNA insertion does not co-segregate with mutant phenotype		No	increased		loose		increased							serrated	increased		
444	SALK_047105C	ND	At1g29900	*CARBAMOYL PHOSPHATE SYNTHETASE B* (*CARB*)			Yes	decreased				decreased					pale green			decreased		
445	SALK_066103C	HM	At1g03070	Bax inhibitor-1 family protein			No	increased		loose		increased			reclinate, revolute					increased		
446	SALK_066891C	ND	At1g52530	Protein of unknown function, contains domain: Hus1-like protein			No		abnormal						reclinate							
447	SALK_044371C	HM	At1g09320	Agenet domain-containing protein			No											netted	toothed			
448	SALK_006582C	HM	At3g62540	Pentatricopeptide repeat (PPR) superfamily protein			No							ovate					toothed		increased	bigger first two leaves
449	SALK_022083C	HM	At3g59460	Similar to F-box family protein			No									rugose		blotched				necrotic spots
450	SALK_022743C	HM	At1g70560	*TRYPTOPHAN AMINOTRANSFERASE OF ARABIDOPSIS 1* (*TAA1*)	No complementation in allelism test	*weß-1*	Yes	decreased		compact		decreased			reclinate					decreased		
451	SALK_008459C	HM	At2g47400	*CP12 DOMAIN-CONTAINING PROTEIN 1* (*CP12-1*)			No	decreased		compact		decreased								decreased		
452	SALK_026171C	WT					N/A	decreased				decreased				rugose		blotched	toothed	decreased		necrotic spots, disorganized leaf morphology
453	SALK_026036C	WT					N/A						asymmetrical			rugose		blotched				necrotic spots
454	SALK_006881C	HM	At2g37290	Ypt/Rab-GAP domain of gyp1p superfamily protein			No										pale green					
455	SALK_025508C	HM	At1g80430	pre-tRNA, tRNA-Ser (anticodon: AGA)			No			compact					reclinate					decreased		petioles grow upright
456	SALK_007784C	WT					N/A	decreased				decreased						variegated		decreased		
457	SALK_006410C	HM	At1g20580	Small nuclear ribonucleoprotein family protein			No	decreased				decreased		elliptical					toothed	decreased		
458	SALK_022640C	WT					N/A								reclinate							
459	SALK_023099C	WT					N/A										pale green					sensitive to environmental conditions
460	SALK_048891C	HM	At5g01730	*SCAR FAMILY PROTEIN 4* (*SCAR4*)			No								reclinate				toothed			
461	SALK_032659C	WT					N/A											netted				
462	SALK_025213C	HM	At5g01150	Protein of unknown function			No											netted				
463	SALK_031983C	HM	At1g15040	Class I glutamine amidotransferase-like superfamily protein			No	increased			increased	increased								increased		
464	SALK_063404C	HM	At4g18730	*RIBOSOMAL PROTEIN L16B* (*RPL16B*)	T-DNA insertion co-segregates with mutant phenotype		No											netted	toothed			
465	SALK_030932C	HM	At4g12640	RNA recognition motif (RRM)-containing protein			No								reclinate							
466	SALK_050231C	HM	At5g62290	Nucleotide-sensitive chloride conductance regulator (ICln) family protein			No								flat, concave							
467	SALK_060836C	HM	At5g01350	Protein of unknown function			No	decreased				decreased		elliptical						decreased		
468	SALK_016521C	WT					N/A							oblong								bigger first two leaves
469	SALK_009026C	NC	At1g32120	Protein of unknown function			No	decreased				decreased		elliptical		rugose		variegated	toothed	decreased		
470	SALK_022878C	HM	At5g13610	Protein of unknown function			No	decreased				decreased					pale green	variegated		decreased		split leaves (incomplete penetrance)
471	SALK_006042C	HM	At3g07610	*INCREASE IN BONSAI METHYLATION 1* (*IBM1*)	No complementation in allelism test	*ibm1-4*	Yes				increased		asymmetrical	elliptical								disorganized leaf morphology
472	SALK_062797C	HM	At3g29280	Protein of unknown function			No								reclinate							disorganized leaf morphology, two inflorescence primary shoots (incomplete penetrance)
473	SALK_025769C	NC	At5g58670	*PHOSPHOLIPASE C1* (*PLC1*)			No								reclinate							
474	SALK_025969C	WT					N/A											netted	toothed			
475	SALK_062509C	HM	At1g31970	*STRESS RESPONSE SUPPRESSOR 1* (*STRS1*)			No											netted				
476	SALK_025062C	HM	At2g47060	*PTO-INTERACTING 1-4* (*PTI1-4*)			No															disorganized leaf morphology and leaf emergence from the shoot apical meristem
477	SALK_119409C	HM	At2g23840	HNH endonuclease			No										pale green					
478	SALK_051228C	HM	At1g64840	Contains domain F-box, cyclin-like			No															adult leaves show abnormal morphology, some are stuck to each other
479	SALK_030155C	HM	At5g51880	2-oxoglutarate (2OG) and Fe(II)-dependent oxygenase superfamily protein			No	decreased				decreased						spotted	toothed	decreased		white spots (incomplete penetrance)
480	SALK_053063C	WT					N/A											variegated				
481	SALK_063054C	HM	At2g34260	*HUMAN WDR55* (*WD40 REPEAT*) *HOMOLOG* (*WDR55*)			No	decreased				decreased								decreased		
482	SALK_060686C	HM	At5g62190	DEAD/DEAH box RNA helicase PRH75	Two independent alleles found with similar phenotypes	SALK_062900C	No	decreased				decreased		elliptical	concave					decreased		
483	SALK_030106C	HM	At5g18390	Pentatricopeptide repeat (PPR) superfamily protein			No								involute					increased		
484	SALK_049146C	ND	At3g02730	*THIOREDOXIN F-TYPE 1* (*TRXF1*)			No	decreased				decreased			concave	rugose				decreased		
485	SALK_026306C	NC	At4g26380	Cysteine/Histidine-rich C1 domain family protein			No	decreased		compact		decreased					pale green			decreased		
486	SALK_059601C	HM	At1g09520	Similar to PHD finger family protein			No	increased		loose		increased								increased		
488	SALK_051857C	HM	At5g02270	*ATP-BINDING CASSETTE I20* (*ABCI20*)			No	decreased		compact		decreased			reclinate					decreased		vitrified leaves (incomplete penetrance)
489	SALK_146126C	HM	At1g19230	Riboflavin synthase-like superfamily protein			No	increased		loose		increased								increased		
490	SALK_138096C	HM	At3g11930	Adenine nucleotide alpha hydrolases-like superfamily protein			No								undulate							undulate adult leaves
491	SALK_012678C	WT					N/A	decreased		compact		decreased			reclinate					decreased		
492	SALK_021882C	HM	At3g52070	Protein of unknown function			No													decreased		adult leaves petioles are short, rosette has an oval shape
493	SALK_051894C	NC	At1g07660	Histone superfamily protein			No										pale green	netted	toothed			
494	SALK_050259C	S	At1g14770	RING/FYVE/PHD zinc finger superfamily protein			No	decreased				decreased								decreased		slow development
495	SALK_046384C	WT					No											netted	toothed			
496	SALK_051358C	ND	At4g23050	PAS domain-containing protein tyrosine kinase family protein			No											variegated				variegated adult leaves
497	SALK_088435C	HM	At1g31335	Protein of unknown function			No	decreased				decreased					pale green			decreased		
498	SALK_121366C	ND	At3g25470	Bacterial hemolysin-related			No	decreased				decreased			undulate				toothed	decreased		
499	SALK_141443C	NC	At1g20910	ARID/BRIGHT DNA-binding domain-containing protein			No								reclinate							

Table S2a. Description of confirmed non-segregating mutants

UMH identifier	Salk line (isolated from)	Annotated locus genotype[1]	Gene mutated (AGI code)[2]	Gene description[2]	Evidence in favor of or against a gene-phenotype causality	Alleles associated with evidence of a gene-phenotype causality	Previously described allele[3]	Rosette relative size	Rosette phyllotaxy	Rosette compactness	Rosette relative organ number	Leaf relative size	Leaf symmetry	Leaf 2D shape	Leaf 3D shape	Leaf surface deformation	Leaf color filling	Leaf color pattern	Margin 2D shape	Petiole relative length	Petiole relative width	Other traits[4]
500	SALK_011936C	HM	At3g57940	Putative ATPase			No											netted	toothed			
501	SALK_086913C	HM	At3g62870	Ribosomal protein L7Ae/L30e/S12e/Gadd45 family protein	Four independent alleles found with similar phenotypes. No complementation in allelism tests	SALK_016597C, SALK_086913, SAIL_515_C04, SAIL_393_D12	No											netted	toothed			
502	SALK_061595C	WT					N/A												serrated			
503	SALK_091886C	HM	At1g35612	Pseudogene of Ulp1 protease family protein			No							rhomboid				netted	toothed			
504	SALK_066806C	WT					N/A	decreased		compact		decreased					pale green			decreased		
505	SALK_110851C	WT					No								reclinate							
506	SALK_016130C	ND	At5g49000	Galactose oxidase/kelch repeat superfamily protein			No	decreased				decreased		elliptical				variegated	toothed	decreased		variable expressivity
507	SALK_004748C	ND	At1g67520	Lectin protein kinase family protein	Same phenotype as in The Chloroplast 2010 project (Lu et al. 2011)	SALK_004748	No	decreased				decreased						variegated		decreased		
508	SALK_130010C	HM	At4g37890	*EMBRYO SAC DEVELOPMENT ARREST 40* (*EDA40*)			No								undulate			netted				
509	SALK_122235C	HM	At3g08040	*FERRIC REDUCTASE DEFECTIVE 3* (*FRD3*)			Yes										pale green					
510	SALK_121288C	WT					N/A												lobed			
511	SALK_127920C	HM	At2g30170	Protein phosphatase 2C family protein			No								reclinate							
512	SALK_126725C	HM	At1g52240	*RHO GUANYL-NUCLEOTIDE EXCHANGE FACTOR 11* (*ROPGEF11*)			Yes	decreased				decreased					pale green		toothed	decreased		
513	SALK_128177C	NC	At5g54440	*CLUB* (*CLUB*)			Yes												serrated			
514	SALK_125621C	WT					N/A	decreased				decreased						netted	toothed	decreased		
515	SALK_119833C	WT					N/A												lobed, toothed			
516	SALK_126447C	WT					N/A								reclinate, revolute							
517	SALK_131604C	S	At4g04500	*CYSTEINE-RICH RLK* (*RECEPTOR-LIKE PROTEIN KINASE*) *37* (*CRK37*)			No															adult leaves are furrowed and stuck together
518	SALK_129213C	HM	At3g15480	Protein of unknown function			No	decreased				decreased					pale green	variegated		decreased		
519	SALK_138693C	HM	At1g16290	Contains domain Lytic transglycosylase-like, catalytic			No	decreased	abnormal			decreased			undulate			netted		decreased		
520	SALK_131610C	HM	At5g09810	*ACTIN 7* (*ACT7*)			Yes	increased		loose		increased			reclinate					increased		
521	SALK_132447C	HM	At5g48710	Ubiquitin-like superfamily protein			No	decreased				decreased						variegated, netted	angular	decreased		
522	SALK_150281C	WT					N/A								reclinate							
523	SALK_148815C	HM	At3g58360	TRAF-like family protein			No	increased		loose		increased					pale green			increased		
524	SALK_033728C	HM	At1g72560	*PAUSED* (*PSD*)			Yes												toothed			
525	SALK_135329C	HM	At5g06330	Late embryogenesis abundant (LEA) hydroxyproline-rich glycoprotein family			No												serrated			
526	SALK_024589C	HM	At3g49460	Protein of unknown function			No								undulate, involute	rugose						pale green petiole
527	SALK_045565C	ND	At3g16440	*MYROSINASE-BINDING PROTEIN-LIKE PROTEIN-300B* (*MLP-300B*)			No								reclinate, revolute							
528	SALK_113067C	HM	At3g01250	Protein of unknown function			No	decreased				decreased						netted, spotted	toothed	decreased		
529	SALK_114091C	HM	At1g47813	Protein of unknown function			No						asymmetrical		reclinate, undulate							heterogeneous phenotype, morphology abnormalities (incomplete penetrance)
530	SALK_118536C	HM	At5g51440	HSP20-like chaperones superfamily protein			No	decreased				decreased					pale green			decreased		
531	SALK_113246C	HM	At1g70940	*PIN-FORMED 3* (*PIN3*)			Yes												serrated			
532	SALK_113154C	HM	At2g25870	Haloacid dehalogenase-like hydrolase family protein			No	decreased				decreased			undulate		pale green			decreased		
533	SALK_119148C	HM	At4g09540	Transposable element gene			No	decreased		compact		decreased		roundish			pale green			decreased		
534	SALK_114696C	HM	At2g47360	Protein of unknown function			No															necrotic spots
600	SALK_004298C	HM	At5g47770	*FARNESYL DIPHOSPHATE SYNTHASE 1* (*FPS1*)			No				increased				reclinate							
601	SALK_027396C	HM	At1g69523	S-adenosyl-L-methionine-dependent methyltransferases superfamily protein			No	increased				increased								increased		
602	SALK_008887C	HM	At3g09720	P-loop containing nucleoside triphosphate hydrolases superfamily protein			No											netted	toothed			
603	SALK_119016C	ND	At2g31650	*HOMOLOGUE OF TRITHORAX* (*ATX1*)	T-DNA insertion does not co-segregate with mutant phenotype		Yes												serrated			
604	SALK_139246C	HM	At1g78030	Protein of unknown function	T-DNA insertion does not co-segregate with mutant phenotype		No	decreased				decreased								decreased		pale green petioles, hirsute
605	SALK_138001C	HM	At4g16460	Protein of unknown function			No	decreased				decreased						netted	toothed	decreased		
606	SALK_007214C	HM	At5g33320	*CAB UNDEREXPRESSED 1* (*CUE1*)	Complementation in allelism test	*cue1-2*	Yes								reclinate							
607	SALK_023198C	HM	At1g18530	EF hand calcium-binding protein family			No							elliptical				netted				
608	SALK_017975C	HM	At4g31490	Contains domain Coatomer, beta subunit			No	decreased				decreased			concave			netted		decreased		
609	SALK_102160C	HM	At2g36620	*RIBOSOMAL PROTEIN L24* (*RPL24A*)	Same phenotype as in The Chloroplast 2010 project (Lu et al. 2011)	SALK_102160, SALK_108755	No	decreased				decreased								decreased		disorganized leaf morphology (incomplete penetrance)
610	SALK_016447C	HM	At3g21610	Acid phosphatase/vanadium-dependent haloperoxidase-related protein			No															adult leaves are concave and some are stuck toghethe
611	SALK_057987C	HM	At4g08900	Encodes an arginase, likely to be involved in polyamine biosynthesis in pollen			Yes	increased				increased			reclinate		pale green		serrated	increased		
612	SALK_094291C	HM	At4g27060	*TORTIFOLIA 1* (*TOR1*)			Yes															clockwise twisted petioles
613	SALK_018552C	ND	At1g32330	*HEAT SHOCK TRANSCRIPTION FACTOR A1D* (*HSFA1D*)			No															seeds are pale yellow
614	SALK_073728C	HM	At1g80380	Glycerate kinase			Yes											blotched				variable expressivity
615	SALK_098071C	ND	At1g25430	Transposable element gene			No			compact					reclinate					decreased		
616	SALK_152677C	HM	At1g60190	*PLANT U-BOX 19* (*PUB19*)			No												serrated			
617	SALK_114083C	HM	At1g08410	P-loop containing nucleoside triphosphate hydrolases superfamily protein			No	decreased				decreased			concave					decreased		
618	SALK_102161C	WT					N/A															disorganized lamina
619	SALK_094849C	HM	At5g64710	Putative endonuclease or glycosyl hydrolase			No	decreased				decreased			reclinate		dark green			decreased		
620	SALK_150081C	HM	At3g46230	*HEAT SHOCK PROTEIN 17.4* (*HSP17.4*)			No	decreased				decreased					yellow green		toothed	decreased		

Table S2a. Description of confirmed non-segregating mutants

UMH identifier	Salk line (isolated from)	Annotated locus genotype[1]	Gene mutated (AGI code)[2]	Gene description[2]	Evidence in favor of or against a gene-phenotype causality	Alleles associated with evidence of a gene-phenotype causality	Previously described allele[3]	Rosette relative size	Rosette phyllotaxy	Rosette compactness	Rosette relative organ number	Leaf relative size	Leaf symmetry	Leaf 2D shape	Leaf 3D shape	Leaf surface deformation	Leaf color filling	Leaf color pattern	Margin 2D shape	Petiole relative length	Petiole relative width	Other traits[4]
621	SALK_116537C	HM	At2g42720	FBD, F-box, Skp2-like and Leucine Rich Repeat domains containing protein			No			compact				roundish			pale green			decreased		
622	SALK_022843C	HM	At5g53500	TransducinWD40 repeat-like superfamily protein			No	decreased		compact		decreased			reclinate					decreased		
623	SALK_078760C	WT					N/A								reclinate			blotched				necrotic patches
624	SALK_070975C	WT					N/A								concave							
625	SALK_075882C	HM	At1g70470	Protein of unknown function			No								reclinate, undulate							
626	SALK_127261C	HM	At1g17920	*HOMEODOMAIN GLABROUS 12* (*HDG12*)			No	decreased				decreased			concave, undulate					decreased		
627	SALK_116974C	HM	At5g11510	*MYB DOMAIN PROTEIN 3R-4* (*MYB3R-4*)	T-DNA insertion does not co-segregate with mutant phenotype		No	decreased		compact		decreased		roundish			pale green			decreased		
628	SALK_132810C	HM	At3g50910	Protein of unknown function			No									rugose						
629	SALK_104376C	HM	At1g11655	Protein of unknown function			No								undulate							
630	SALK_138605C	HM	At1g28210	DnaJ homolog AtJ1			No								reclinate							
631	SALK_011035C	HM	At5g04140	*GLUTAMATE SYNTHASE 1* (*GLU1*)	No complementation in allelism test, Same phenotype as in The Chloroplast 2010 project (Lu et al. 2011)	*gls1-30*, *gls1-103*, SALK_011035C	Yes											netted	toothed			
632	SALK_037636C	HM	At4g38600	*KAKTUS* (*KAK*)			Yes	increased				increased			reclinate			netted				
633	SALK_011049C	WT					N/A												toothed			
634	SALK_024556C	HM	At3g24060	Plant self-incompatibility protein S1 family	T-DNA insertion does not co-segregate with mutant phenotype		No												serrated			
635	SALK_013909C	HM	At4g14147	Actin-related protein 2/3 complex 34kDa subunit family			No							roundish								purple petioles
636	SALK_014614C	WT					N/A	decreased				decreased					dark green			decreased		
637	SALK_012011C	HM	At5g04885	Glycosyl hydrolase family protein			No	decreased		compact		decreased		oblong						decreased		
638	SALK_008178C	HM	At4g34730	Ribosome-binding factor A family protein	Same phenotype as in The Chloroplast 2010 project (Lu et al. 2011)	SALK_008178	No											variegated				pale green lamina base
639	SALK_032904C	HM	At5g45750	*RAB GTPASE HOMOLOG A1C* (*RABA1c*)			No								reclinate							
640	SALK_022780C	HM	At3g61460	*BRASSINOSTEROID-RESPONSIVE RING-H2* (*BRH1*)			No							elliptical	reclinate							pale green petioles
641	SALK_045401C	HM	At3g53020	*SHORT VALVE1* (*STV1*)			Yes								reclinate			netted	lobed			
642	SALK_026595C	HM	At3g15380	Plasma-membrane choline transporter family protein			No								reclinate, revolute							
643	SALK_039200C	HM	At5g63820	Protein of unknown function			No								reclinate					increased		
644	SALK_026226C	HM	At1g02480	pre-tRNA, tRNA-Phe (anticodon: GAA)			No	increased		loose		increased							serrated	increased		
645	SALK_026655C	WT					N/A	decreased				decreased								decreased		
646	SALK_016004C	HM	At1g26340	*CYTOCHROME B5 ISOFORM A* (*CB5-A*)			No			compact										decreased		
647	SALK_028581C	HM	At4g01960	Protein of unknown function			No										pale green	netted	angular			
648	SALK_035012C	ND	At2g05790	O-Glycosyl hydrolases family 17 protein			No							roundish	undulate							
649	SALK_020814C	HM	At1g47630	*CYTOCHROME P450, FAMILY 96, SUBFAMILY A, POLYPEPTIDE 7* (*CYP96A7*)			No								concave, undulat				lobed			
650	SALK_024627C	WT					N/A				increased			elliptical								heterogeneous size, early flowering
651	SALK_027461C	WT					N/A								reclinate			netted				
653	SALK_019081C	HM	At4g02715	Protein of unknown function			No	decreased				decreased			reclinate, undulate			netted		decreased		
654	SALK_012988C	HM	At4g23820	Pectin lyase-like superfamily protein			No	decreased			decreased	decreased						variegated		decreased		
655	SALK_045880C	HM	At1g24130	TransducinWD40 repeat-like superfamily protein			No	decreased			decreased	decreased			concave, undulate					decreased		
656	SALK_006616C	HM	At4g24600	Protein of unknown function			No								reclinate				serrated			
657	SALK_046378C	HM	At1g12400	Nucleotide excision repair, TFIIH, subunit TTDA			No	decreased			decreased	decreased		elliptical						decreased		
658	SALK_044478C	HM	At1g01320	Tetratricopeptide repeat (TPR)-like superfamily protein			No										pale green	netted				
659	SALK_021778C	NC	At2g40650	PRP38 family protein			No								reclinate					decreased		
660	SALK_057184C	HM	At5g58170	*SHV3-LIKE 5* (*SVL5*)			No	increased		loose		increased			reclinate					increased		
661	SALK_059367C	HM	At3g46610	Pentatricopeptide repeat (PPR-like) superfamily protein			No	decreased		compact		decreased		roundish			pale green			decreased		
662	SALK_046728C	HM	At2g40940	*ETHYLENE RESPONSE SENSOR 1* (*ERS1*)			No	decreased				decreased								decreased		dark petioles, hirsute
663	SALK_064329C	HM	At4g26480	RNA-binding KH domain-containing protein			No								reclinate, revolute		pale green					
664	SALK_073011C	HM	At2g29300	NAD(P)-binding Rossmann-fold superfamily protein			No	decreased				decreased			reclinate, undulate					decreased		petioles grow upright
665	SALK_050260C	NC	At5g46280	*MINICHROMOSOME MAINTENANCE 3* (*MCM3*)			No								concave				serrated			
666	SALK_049907C	NC	At5g24910	*CYTOCHROME P450, FAMILY 714, SUBFAMILY A, POLYPEPTIDE 1* (*CYP714A1*)			No	increased				increased			undulate, reclinate,					increased		twisted petioles
667	SALK_064524C	HM	At2g45310	*UDP-D-GLUCURONATE 4-EPIMERASE 4* (*GAE4*)			No			compact				roundish						decreased		
668	SALK_059412C	ND	At1g55530	RING/U-box superfamily protein			No	decreased				decreased						netted	toothed	decreased		
669	SALK_112720C	HM	At1g17840	*ATP-BINDING CASSETTE G11* (*ABCG11*)	Same phenotype as in The RIKEN Arabidopsis Phenome Information Database (Kuromori et al. 2006)	RIKEN:11-4276-1	Yes															folded young leaves
670	SALK_110873C	HM	At1g60140	*TREHALOSE PHOSPHATE SYNTHASE* (*TPS10*)			No	decreased		compact	decreased	decreased		elliptical			yellow green		toothed	decreased		
671	SALK_122701C	WT					N/A								revolute, reclinate							
672	SALK_112882C	HM	At3g60240	*EUKARYOTIC TRANSLATION INITIATION FACTOR 4G* (*EIF4G*)			No								concave							
673	SALK_016158C	ND	At5g09280	Pectin lyase-like superfamily protein			No	decreased				decreased			undulate, reclinate		pale green			decreased		
674	SALK_116744C	WT					N/A	decreased		compact		decreased					yellow green			decreased		
675	SALK_119125C	ND	At2g04740	Ankyrin repeat family protein			No	decreased				decreased		roundish			pale green			decreased		yellow young leaves
676	SALK_113585C	HM	At5g61170	Ribosomal protein S19e family protein			No	decreased				decreased							toothed	decreased		
677	SALK_078275C	HM	At3g55990	*ESKIMO 1* (*ESK1*)			Yes	decreased				decreased								decreased		

Table S2a. Description of confirmed non-segregating mutants

UMH identifier	Salk line (isolated form)	Annotated locus genotype[1]	Gene mutated (AGI code)[2]	Gene description[2]	Evidence in favor of or against a gene-phenotype causality	Alleles associated with evidence of a gene-phenotype causality	Previously described alleles[3]	Rosette relative size	Rosette phyllotaxy	Rosette compactness	Rosette relative organ number	Leaf relative size	Leaf symmetry	Leaf 2D shape	Leaf 3D shape	Leaf surface deformation	Leaf color filling	Leaf color pattern	Margin 2D shape	Petiole relative length	Petiole relative width	Other traits[4]
678	SALK_123405C	HM	At4g13770	*CYTOCHROME P450, FAMILY 83, SUBFAMILY A, POLYPEPTIDE 1 (CYP83A1)*			Yes								undulate							
679	SALK_113285C	HM	At1g79950	RAD3-like DNA-binding helicase protein			No												toothed			
680	SALK_124505C	ND	At2g21660	*COLD, CIRCADIAN RHYTHM, AND RNA BINDING 2 (CCR2)*			Yes	decreased				decreased					pale green			decreased		
681	SALK_074630C	HM	At1g10150	Carbohydrate-binding protein			No							roundish	concave							
682	SALK_080381C	HM	At1g62090	Pseudogene, similar to light repressible receptor protein kinase (LRRPK)			No								concave, revolute				toothed	increased		
683	SALK_082749C	HM	At5g39590	TLD-domain containing nucleolar protein			No							ovate								
684	SALK_085820C	HM	At4g02480	AAA-type ATPase family protein	Same phenotype as in The Chloroplast 2010 project (Lu et al. 2011)	SALK_085820	No			compact					concave				toothed			
685	SALK_074780C	HM	At3g63020	Protein of unknown function			No			compact				roundish	concave							
687	SALK_080831C	HM	At1g47890	*RECEPTOR LIKE PROTEIN 7 (RLP7)*			No				increased											
688	SALK_113110C	HM	At1g50140	P-loop containing nucleoside triphosphate hydrolases superfamily protein			No								concave							
689	SALK_118901C	HM	At4g32810	*CAROTENOID CLEAVAGE DIOXYGENASE 8 (CCD8)*			Yes				increased		asymmetrical						lobed			
690	SALK_102847C	HM	At5g55560	Protein of unknown function			No						asymmetrical									
691	SALK_067536C	HM	At4g15080	Protein of unknown function			No								revolute							
692	SALK_085468C	HM	At2g16970	*MATERNAL EFFECT EMBRYO ARREST 15 (MEE15)*			No	decreased				decreased			undulate			variegated		decreased		heterogeneous growth
693	SALK_093067C	HM	At5g05590	*PHOSPHORIBOSYLANTHRANILATE ISOMERASE 2 (PAI2)*			No	decreased				decreased					brown			decreased		leaves show premature death and calli
694	SALK_088542C	HM	At2g23380	*CURLY LEAF (CLF)*			Yes	decreased				decreased		elliptical	involute		pale green		toothed	decreased		early flowering
695	SALK_073682C	HM	At5g11240	Protein of unknown function			No	decreased				decreased			undulate, concave					decreased		
696	SALK_109175C	HM	At5g64790	Protein of unknown function			No			compact							pale green					
697	SALK_017154C	HM	At3g13730	*CYTOCHROME P450, FAMILY 90, SUBFAMILY D, POLYPEPTIDE 1 (CYP90D1)*			No	decreased		compact		decreased					pale green			decreased		
698	SALK_111280C	HM	At5g60410	*SIZ1*			Yes	decreased		compact		decreased			undulate				toothed	decreased		
699	SALK_086036C	WT					No	decreased			decreased	decreased	asymmetrical				pale green	netted	toothed	decreased		
700	SALK_014802C	HM	At3g28153	Protein of unknown function			No	decreased			decreased	decreased					brown	netted	elliptical	decreased		
701	SALK_020435C	HM	At1g09480	Protein of unknown function			No	decreased				decreased					yellow		toothed	decreased		early flowering
702	SALK_093159C	HM	At3g04490	Protein of unknown function			No	decreased		loose		decreased										
703	SALK_110522C	HM	At4g31110	Protein of unknown function			No	decreased			decreased	decreased								decreased		
704	SALK_079466C	HM	At1g02100	*SUPPRESSOR OF BRI1 (SBI1)*			No	increased		loose		increased		elliptical								
705	SALK_104832C	HM	At1g16470	*PROTEASOME SUBUNIT PAB1 (PAB1)*			No	increased				increased		elliptical						increased		
706	SALK_087793C	HM	At1g60995	Protein of unknown function			No	decreased			decreased	decreased			undulate		pale green		toothed	decreased		
707	SALK_096651C	HM	At5g11260	*ELONGATED HYPOCOTYL 5 (HY5)*			Yes	increased		loose		increased								increased		
708	SALK_016087C	HM	At5g45710	*ROOT HANDEDNESS 1 (RHA1)*			Yes	increased		loose		increased								increased		
709	SALK_098967C	S	At5g60790	*ATP-BINDING CASSETTE F1 (ABCF1)*			No	increased		loose			asymmetrical	elliptical					angular, toothed	increased		
712	SALK_096130C	HM	At4g18240	*STARCH SYNTHASE 4 (SS4)*			Yes										pale green	netted				
714	SALK_094540C	HM	At2g32760	Protein of unknown function			No	decreased		compact		decreased								decreased		
715	SALK_087859C	HM	At4g17380	*MUTS-LIKE PROTEIN 4 (MSH4)*			Yes	increased		compact		increased								decreased		
716	SALK_014615C	HM	At1g15750	*TOPLESS (TPL)*			Yes												toothed			
717	SALK_104023C	HM	At4g30540	Protein of unknown function			No	decreased				decreased					pale green			decreased		
718	SALK_098786C	HM	At4g39952	Protein of unknown function			No	decreased				decreased								decreased		
800	SALK_035363C	WT					N/A								undulate							heterogenous size
801	SALK_039718C	HM	At3g14950	*TETRATRICOPEPTIDE-REPEAT THIOREDOXIN-LIKE 2 (TTL2)*			No			loose										increased		
802	SALK_013940C	ND	At3g61170	Tetratricopeptide repeat (TPR)-like superfamily protein			No	decreased		compact		decreased					pale green	netted		decreased		sensitive to environmetal conditions
803	SALK_027747C	HM	At3g06270	Protein phosphatase 2C family protein			No	decreased		compact		decreased		ovate	undulate					decreased		
804	SALK_030862C	ND	At2g37650	GRAS family transcription factor	Same phenotype as in The Chloroplast 2010 project (Lu et al. 2011)	SALK_136555, SALK_030862	No	decreased		compact		decreased		roundish						decreased		
805	SALK_039706C	HM	At4g31530	NAD(P)-binding Rossmann-fold superfamily protein	Same phenotype as in The Chloroplast 2010 project (Lu et al. 2011)	SALK_061421, SALK_039706	No			compact	increased			ovate	convex							
806	SALK_069400C	HM	At1g26190	Phosphoribulokinase / Uridine kinase family			No	decreased		compact		decreased			reclinate					decreased		
807	SALK_060037C	ND	At1g72210	Basic helix-loop-helix (bHLH) DNA-binding superfamily protein			No	decreased				decreased			undulate, involute					decreased		
808	SALK_027928C	WT					N/A								reclinate							
810	SALK_054699C	ND	At5g43660	2-oxoglutarate (2OG) and Fe(II)-dependent oxygenase superfamily protein			No	decreased				decreased					pale green			decreased		
811	SALK_065777C	HM	At5g09570	Cox19-like CHCH family protein			No	increased				increased								increased		

Table S3. Ontological terms and their definitions

Entity	Attribute	Value	PATO ID	Common name	Definition
Phyllome - Rosette	Relative size	Increased size	PATO:0000586	Big	A size quality which is relatively high
		Decreased size	PATO:0000587	Small	A size quality which is relatively low
	Organ arrangement - Phyllotaxis	Abnormal	PATO:0000460	Altered	A quality inhering in a bearer by virtue of the bearer's deviation from normal or average.
	Compactness	Loose	PATO:0001802	Loose	A pattern quality inhering in a bearer by virtue of the bearer's not being compact or dense in arrangement.
		Compact	PATO:0001485	Compact	A structural quality inhering in a bearer by virtue of the bearer's being thicker or more closely packed together; pressed tightly together.
	Relative organ number	Increased number	PATO:0000470	More leaves	An amount which is relatively high.
		Decreased number	PATO:0001997	Fewer leaves	An amount which is relatively low.
Leaf lamina	Relative size	Increased size	PATO:0000586	Big	A size quality which is relatively high
		Decreased size	PATO:0000587	Small	A size quality which is relatively low
	Relative length	Increased length	PATO:0000573	Lon	A length quality which is relatively large.
		Decreased length	PATO:0000574	Short	A length quality which is relatively small.
	Relative width	Increased width	PATO:0000600	Wide	A width which is relatively large.
		Decreased width	PATO:0000599	Narrow	A width which is relatively small.
	Symmetry	Symmetrical	PATO:0000632	Symmetrical	A symmetry quality inhering in a bearer by virtue of the bearer's being capable of division by a longitudinal plane into similar halves
		Asymmetrical	PATO:0000616	Asymmetrical	A symmetry quality inhering in a bearer by virtue of the bearer's lacking symmetry.
	Geometric shape - 2D	Roundish	PATO:0001935	Roundish	A shape quality inhering in a bearer by virtue of the bearer's being roundish, a little inclining to be oblong.
		Ovate	PATO:0001891	Oval	A spheroid quality inhering in a bearer by virtue of the bearer's exhibiting a continuous convex surface with an axis of symmetry and one axis longer than the other; egg-shaped.
		Orbicular	PATO:0001934	Roundish	A shape quality inhering in a bearer by virtue of the bearer's being perfectly circular.
		Oblong	PATO:0000946	Blunt ended	A shape quality inhering in a bearer by virtue of the bearer's having a somewhat elongated form with approximately parallel sides.
		Elliptical	PATO:0000947	Elliptical (or) Pointed	A spheroid quality inhering in a bearer by virtue of the bearer's being oval with two axes of symmetry, as produced by a conical section.
		Lanceolate	PATO:0001877	Pointed	A shape quality inhering in a bearer by virtue of the bearer's being shaped like a lance-head, considerably longer than wide, tapering towards the tip from below the middle; attached at the broad end.
		Linear	PATO:0001199	Linear	A shape quality inhering in a bearer by virtue of the bearer's being narrow, with the two opposite margins parallel.
		Spatulate	PATO:0001937	Spatulate	A shape quality inhering in a bearer by virtue of the bearer's being oblong, with the lower end very much attenuated.
		Cuneate	PATO:0001955	Cuneate	A shape quality inhering in a bearer by virtue of the bearer's being narrowly triangular, wider at the apex and tapering toward the base.
		Subulate	PATO:0001954	Narrow and pointed	A shape quality inhering in a bearer by virtue of the bearer's being linear, very narrow, tapering to a very fine point from a narrow base.
		Rhomboid	PATO:0001938	Rhomboid	A spheroid quality inhering in a bearer by virtue of the bearer's being oval and a little angular in the middle.
		Triangular	PATO:0001875	Triangular	A shape quality inhering in a bearer by virtue of the bearer's having three angles.
		Heart-shaped	PATO:0000948	Heart shaped	A concave 3-D shape quality inhering in a bearer by virtue of the bearer's having a sinus or rounded lobe at the base.
		Reniform	PATO:0001871	Kidney shaped	A concave 3-D shape quality inhering in a bearer by virtue of the bearer's having the shape of a kidney.
		Arrow-shaped	PATO:0001881	Arrow shaped	A shape quality inhering in a bearer by virtue of the bearer's forming two equal obtuse triangles with a short side in common.
	Geometric shape - 3D	Convex	PATO:0001355	Convex	A shape quality that obtains by virtue of the bearer having inward facing edges; having a surface or boundary that curves or bulges outward, as the exterior of a sphere.
		Concave	PATO:0001857	Concave	A shape quality in a bearer by virtue of the bearer's curving inward
		Flat	PATO:0000407	Flat	A curvature quality inhering in a bearer by virtue of the bearer's having a horizontal surface without a slope, tilt, or curvature.
		Undulate	PATO:0000967	Wavy	A shape quality inhering in a bearer by virtue of the bearer's having a sinuate margin and rippled surface.
		Involute	PATO:0001962	Upwards folded	A curled quality inhering in a bearer by virtue of the bearer's edges of its surface being rolled inwards spirally on each side.
		Revolute	PATO:0001963	Downwards folded	A curled quality inhering in a bearer by virtue of the bearer's edges of its surface being rolled backwards spirally on each side.
		Convolute	PATO:0001966	Rolled	A curled quality inhering in a bearer by virtue of the bearer's one edge of its surface being wholly rolled up in another.
		Circinate	PATO:0001964	Rolled	A curled quality inhering in a bearer by virtue of the bearer's edges of its surface being rolled spirally downwards.
		Reclinate	PATO:0001965	Bent down	A curled quality inhering in a bearer by virtue of the bearer's edges of its surface being bent down upon their stalk.
	Surface - deformation	Smooth	PATO:0000701	Smooth	A texture quality inhering in a bearer by virtue of the bearer's processing a surface free of roughness or irregularities.
		Rugose	PATO:0001359	Wrinkled	A surface feature shape quality inhering in a bearer by virtue of the bearer's having many wrinkles or creases on the surface.
	Color - filling	Green	PATO:0000320	Green	A color hue with medium-low wavelength of that portion of the visible spectrum lying between yellow and blue, evoked in the human observer by radiant energy with wavelengths of approximately 490 to 570 nanometers.
		Pale green	PATO:0001272	Pale green	A color consisting of green hue and low saturation.
		Yellow green	PATO:0001941	Yellow green	A color consisting of yellow and green hues.
		Dark green	PATO:0001249	Dark	A color consisting of green hue and low brightness.
		White	PATO:0000323	White	An achromatic color of maximum brightness; the color of objects that reflect nearly all light of all visible wavelengths.
		Yellow	PATO:0000324	Yellow	A color hue with medium wavelength of that portion of the visible spectrum lying between orange and green, evoked in the human observer by radiant energy with wavelengths of approximately 570 to 590 nanometers
		Purple	PATO:0000951	Purple	A color that falls about midway between red and blue in hue
	Color - pattern	Mono-colored	PATO:0001532	Plain	A color pattern inhering in a bearer by virtue of the bearer's having one hue
		Variegated	PATO:0001533	Variegated	A color pattern inhering in a bearer by virtue of bearer's having two or more hues or degrees of saturation.
		Spotted	PATO:0000333	Spotted	A color pattern inhering in a bearer by virtue of bearer's being marked with a round area of different hue or degree of saturation.
		Blotched	PATO:0000329	Blotched	A color pattern inhering in a bearer by virtue of bearer's being marked with irregularly shaped spots or blots of a different hue or degree of saturation.
		Netted	PATO:0001947	Netted	A color pattern inhering in a bearer by virtue of bearer's being covered with reticulated lines of a different hue or degree of saturation.
Leaf margin	Geometric shape - 2D	Continuous	PATO:0000689	Continuous	A quality of a single process inhering in a bearer by virtue of the bearer's being uninterrupted in time, sequence, substance, or extent.
		Crenated	PATO:0001889	Crenated	A surface feature shape quality inhering in a bearer by virtue of the bearer's having the border, edge, or outline cut into a series of segments of circles resembling a scallop-shell
		Serrated	PATO:0001206	Serrated	A shape quality inhering in a bearer by virtue of having sharp straight-edged teeth pointing to the apex.
		Toothed	PATO:0001205	Toothed	A surface feature shape quality inhering in a bearer by virtue of the bearer's having toothlike projections in the margin.
		Lobed	PATO:0001979	Lobed	A shape quality inhering in a bearer by virtue of the bearer's being partly divided into a determinate number of regions.
		Angular	PATO:0001977	Angular	A shape quality inhering in a bearer by virtue of the bearer's having several salient angles on the margin.
Leaf petiole	Relative length	Increased length	PATO:0000573	Long	A length quality which is relatively large.
		Decreased length	PATO:0000574	Short	A length quality which is relatively small.
	Relative width	Increased width	PATO:0000600	Thick	A width which is relatively large.
		Decreased width	PATO:0000599	Thin	A width which is relatively small.

Table S4. Rosette phenotypes of the mutants used in allelism tests and of the F_1 progeny of their crosses.

AGI code and gene name	T-DNA line	Rosette phenotype	Published allele(s) tested (reference)	Published allele phenotype	F_1 phenotype[1]	Parental phenotype comparison test / F_1 allelism test
At3g07610 *INCREASE IN BONSAI METHYLATION 1*	SALK_006042C		*ibm1-4* (Saze *et al.*, 2008)			Similar overall phenotypes / No complementation
At5g33320 *CAB UNDEREXPRESSED 1*	SALK_007214C		*cue1-2* (Streatfield *et al.*, 1999)			Different phenotypes / Complementation
At1g65310 *XYLOGLUCAN ENDOTRANSGLUCOSY-LASE/HYDROLASE 17*	SALK_008429C		*xth17-1* (Sasidharan *et al.*, 2010)			Different phenotypes / Complementation
At5g04140 *FERREDOXIN-DEPENDENT GLUTAMATE SYNTHASE 1*	SALK_011035C		*gls1-30*, *gls1-103* (Coschigano *et al.*, 1998)			Similar overall phenotypes / No complementation
At5g05730 *WEAK ETHYLENE INSENSITIVE 2*	SALK_017444C		*wei2-1* (Alonso *et al.*, 2003)			Similar overall phenotypes / No complementation

Table S4. Rosette phenotypes of the mutants used in allelism tests and of the F_1 progeny of their crosses.

AGI code and gene name	T-DNA line	Rosette phenotype	Published allele(s) tested (reference)	Published allele phenotype	F_1 phenotype[1]	Parental phenotype comparison test / F_1 allelism test
At1g70560 *WEAK ETHYLENE INSENSITIVE 8*	SALK_022743C		*wei8-1* (Stepanova *et al.*, 2008)			Similar overall phenotypes / No complementation
At3g28860 *MULTIDRUG RESISTANCE PROTEIN 11*	SALK_033455C		*mdr1-1*, *mdr1-3* (Noh *et al.*, 2001)			Similar overall phenotypes / No complementation
At2g15790 *SQUINT*	SALK_033511C		*sqn-1*, *sqn-2* (Berardini *et al.*, 2001)			Similar overall phenotypes / No complementation
At2g44950 *ANGUSTA 4*	SALK_044415C		*ang4-1* (Berná *et al.*, 1999)			Different phenotypes / Complementation
At3g20550 *DAWDLE*	SALK_045025C		*ddl-1*, *ddl-2* (Morris *et al.*, 2006)			Similar overall phenotypes / NV

Table S4. Rosette phenotypes of the mutants used in allelism tests and of the F_1 progeny of their crosses.

AGI code and gene name	T-DNA line	Rosette phenotype	Published allele(s) tested (reference)	Published allele phenotype	F_1 phenotype[1]	Parental phenotype comparison test / F_1 allelism test
At5g54770 *THIAZOLE REQUIRING*	SALK_057052C	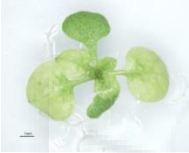	*tz-1* (Li and Redei, 1969)			Similar overall phenotypes / NV
At5g35220 *ETHYLENE-DEPENDENT GRAVITROPISM-DEFICIENT AND YELLOW-GREEN 1*	SALK_061494C		*egi1-1* (Chen *et al.*, 2005)			Similar overall phenotypes / No complementation
At3g22590 *PLANT HOMOLOGOUS TO PARAFIBROMIN, CDC73*	SALK_150644C		*cdc73-1*, *cdc73-2* (Yu *et al.*, 2010)			Similar overall phenotypes / No complementation
At3g62980 *TRANSPORT INHIBITOR RESPONSE 1*	SALK_151603C		*tir1-1* (Ruegger *et al.*, 1998)			Different phenotypes / Complementation
At3g44200 *NIMA-RELATED KINASE 6, IBO1*	SALK_152782C		*ibo1-4* (Motose *et al.*, 2008)			Similar overall phenotypes / No complementation

The table is sorted by the second column. [1]Pictures were taken 15 das. Scale bars: 1 mm. The picture(s) shown correspond to the underlined allele. NV: Sterile parental(s) or non-viable F_1 offspring.

Table S5. Primers used for the genotyping of annotated T-DNA insertions

Line	LP sequence (5'→3')	RP sequence (5'→3')
SALK_000028	CCGGTATGGAAGAAGGAGAAG	CGTTTCGGCAACACTCTTTAG
SALK_000739	TCGATTCCTCAAGAGGTGTTG	CTCCATTAGTTTCGTTGGTGG
SALK_000901	AACAGTTTCGATACTAATCTTCAC	GAAGCAGTCTATTGAACACAAAC
SALK_001004	AAGAGAATGTTGGTGGTGGTG	TACCTTATGGATTGCAGGTGC
SALK_001364	TTTTTGGTCATCGGTACTTGG	GATTTGTCTAGGGTTTTCGCC
SALK_001496	TGGTCTTTGGTGCGATAATTC	GCACCTTTTGGAGGATTTTTC
SALK_002057	GCCAGAGCTAAAACCAAAAGC	AAAACCCAACACGCATCATAC
SALK_003223	TTGAAGATCCCATAGTGCACC	AAATGGTATTGTAGGTCGGCC
SALK_003711	CTCTCTTCATCGCTCTCCAATG	GTACCTCGTCGTCTACTATCTG
SALK_004298	AAAACCATTGCATCAGGTCAG	TGTTGTTGTAGGAATCTGGGC
SALK_004741	AGTATCCTTCCAGGGTGAGTG	TCTAAGTGAACAAGGTCATTACC
SALK_005153	GAAAAACGTTTTGAGGATGCTG	GCTGACTGAAGCAGCAGAACC
SALK_005786	AATTGCACCAATGCAATCTTG	AATGCCAAAAGGCTAAAAAGG
SALK_006042	CTTAGCTGTTGCCTTGAGATCC	GCATCTACCAGAAAAGGCAAAAC
SALK_006410	AAACCCTAGAATGCGTGATCC	ATGACAGAACCAAGAAAGGCG
SALK_006582	CTCTTCGCTTTCGTCTACTGC	TCGCATCAAGCAGTTGTACAG
SALK_006616	AGGATATTGGGATCGTATGGG	GTTGTGGGATGGTGAAAACAC
SALK_006881	TGTTTTTCATTGCACTTGCAG	CGCTTGCTCACCAAAGATAAC
SALK_007214	CCTTCAAACTTGTTCATTTTTGC	GAGCTTTGCATCGTTGAGATC
SALK_007784	TCCAGTTGCTTGGATAATTGC	CTCTCATTCAAAAGCCTGCAC
SALK_007854	ACCCAAGAGAAAGAGAGACGG	CAGGCAGAAAGTACAGGCAAG
SALK_008088	CATGCAGACAGAAAGGGAAAG	CGAACGCCATTCTTGTAAGAG
SALK_008178	GATTTGTGTGCTGGACCTAGC	GTTCTCCATTCCGCCTTAGTC
SALK_008429	CGACATCGATTATTGCAATTG	TTTGTCGAGCGAGAGAGAAAG
SALK_008459	CAAGCTTTATGAAAGCGCATC	TCATCAACCAAACCAAAAACAC
SALK_008546	GAGGATTAAGGTTCACGAATTG	TTTGATAGCGTACTTCCTTATTG
SALK_008561	TTTGTTTTTGTTCAAAAGGCG	TGGATACAGACCCTGAAATGG
SALK_008887	GTGTTTGCCCTTAAGACCCTC	GCAGCATCCAATGGTAAATTG
SALK_009026	AGGTGACACAAACAAGCCAAC	AATCGAACAGGACACCATCTG
SALK_009120	CGCTCCGTCAATATACTTAGAG	GTGGTCCGAACGGCAGTGAA
SALK_009370	CGCAATGGGATTACCACATAC	ATCAAGCCAAGAACGATGATG
SALK_009623	TGTCTGAGGATCAAATCCCTG	GATCTGTTGCCTCTGCTTCTG
SALK_009736	TGCTTCCGAAATATCGTGTTC	TTCAATTACCTCGCCAATGAC
SALK_009798	TCTTGTTAGCTTCCAATTGGC	ATAGAAACCACTCATTCGCCG
SALK_010286	TTTAGCGGTGGGAATGGAAGCG	CAGTGCATCCATACCATCCAC
SALK_010406	ATGTTGAACCAGAGGTTGCTG	CAATACCCATGTTTGAGCAAG
SALK_010588	GGGAGAAAGTGTCTGGAAATTC	AGACAAGGGTGAAGGCAGATTG
SALK_011035	TGCAGACACTTATCGCAAATG	AATAACACCAGCAACACGACC
SALK_011049	AAACTGCTTCTTCTTCCGGAG	TCAATTCCGTCTTCAAGTTGC

Table S5. Primers used for the genotyping of annotated T-DNA insertions

Line	LP sequence (5'→3')	RP sequence (5'→3')
SALK_011376	AGGGGAGACAGCTTCATATCC	ATCACAACACCAAATTCGAGC
SALK_011586	TTTATCTTCGCCAAAACATCG	TTGGTGATTTTCATTGGCTTC
SALK_011867	AACCCTTACCCATCTCGACAC	TTTGATCAAATCAAGGCATCC
SALK_011936	AGAGATCACACTGACTTGGCG	TCAAGCTGTGATTTGAGTCCC
SALK_012011	TCAGGTTGATCTTTCCATTCG	GGAACAGAAGGCCAAGGTATC
SALK_012678	TGATCAAGAGCATTTTCCTGC	TTTTCGGTTCTTCAATCCAAG
SALK_012771	ACTTTGGTCAAACATCCAACG	TCTCCTTAGGTGAGAGGGAGG
SALK_012816	GCTATGTCATGTGTGAACCCC	CCAAACCTTTTGGACTCTTCC
SALK_012836	AGTGAAGCTGAGGTCTTGGATG	TAACTGCTAAAGCCATATCCTG
SALK_012970	GAGACTTTCCTTGCGTTAGGG	TTCGCTTCTTCTACTTGCTCG
SALK_012988	GCAGACGTTGTAGCTGGAATC	TGGGACTCTGGACAGTTATGG
SALK_013253	CGATTCACTCTTTTCGTCAGC	TCCATTCTTTGCAATTTACGG
SALK_013273	AGTTTTGGGTCCGATAAGACG	GGGAATTGAAGAGCAGAGTCC
SALK_013297	CAGAGCATTTTCAGGATGAGC	TACCTCAACATCGGAAGCTTG
SALK_013461	ACCTAAAAATCCGAAGCAACC	TTCTCATCCTCACACGGTTTC
SALK_013567	TTGAAGTTTAACATGCCTGGG	TCCAATGCTCGATTGATTAGC
SALK_013909	ACTTGAAAAGCTTCTGCCCTC	AAGTCTGGTGCAAGTCTCGAG
SALK_014243	GATGGTGACGCTAGAGAATGG	CTGGGCAAATTTGATTCAATC
SALK_014499	CATGAAGAGCTGGTGGAGAAG	CACTGTGACCAATTGACATCG
SALK_014587	ACCTGCATTGAAACAACCAAG	CGCAATGTCATTGCACATTAC
SALK_014614	TGCCATAATCCAATAAGCTGC	ACCAGTTTGTGAATTGGCTTG
SALK_014727	TTTGACGGATTTCTTGAATGG	CAGAGTTCGCCAACAGAATTC
SALK_015088	ACCGTATATTACGTGGGGAGG	TCTTCTCGGTTTTCAGAAACG
SALK_015251	GAAGCTAAGCATTGATGTGGC	CCATGGAGATCAGATGATTGC
SALK_015252	AGGTATGGATTCAACAGAAAGAG	TACGTTCCCAAGTCTTCCTATG
SALK_015522	GGCAAGTGCAATAAGCTGATC	TGCCGGATATTATTTCAGTGG
SALK_016004	TATCTGGCCATGGAGTAGCAG	AGCCATATCATTTTCTTGGGG
SALK_016311	TATCGCCAAAAGGACATTGAC	CCCTAAATCGCGTTTCTTCTC
SALK_016447	TGGAATGCCTTCTTCTCATTC	AGAGAGAATGTTGAGAAGGCG
SALK_016521	TGGGCCATATATTAGACACGG	GCTTGCAGGTGAAGGATACTG
SALK_017254	TTCTTGATTCTTTTGATCCCG	GCTGGTGTTGTTCTCTTGCTC
SALK_017444	ACTTGGTGGCCAAGTTACATG	GAAGGAGACTCCACCAAAACC
SALK_017692	TCCCGAGTGAGTTTCGCTTTC	AGCAACACGCAGATTCACCAG
SALK_017913	TTAGGACTGAAGCAAAGCGAG	ACTGTGTGCTGTGCACTTCAC
SALK_017975	ACTCAATGTTCCATCCGTTTG	AGATATGGTTGGAATCCTGCC
SALK_018321	AAGCATGAGGAACCACACAAC	CCGTAGAAGAAGTCGTTGGTG
SALK_018664	TATTTATTGGGCCTATTCGGG	GAAGTTCAACGCAAGACCAAG
SALK_019044	AGCCATCAACATCGACAATTC	GAAGCTGTTGCTAAAGGCAAG
SALK_019081	TGCAATAATTTCGGAATTTGG	AAGCGTCTCTGAAGCTCACAG

Table S5. Primers used for the genotyping of annotated T-DNA insertions

Line	LP sequence (5'→3')	RP sequence (5'→3')
SALK_019175	TGAAAATTTGCATTTGGGTTC	AAGAGTTAAGCGGCAGAGAGG
SALK_019359	ACCACCACGCTTATACGATTG	CGAATTCGAGAAAAAGCAATG
SALK_019413	GTCTCCCAAAGGAAATTCTCG	AGAGATGTCGCGTATGAATGC
SALK_019830	GACATAGTAGCACGGCACACC	ATAGTGAGTAGCACGGAACGC
SALK_019994	ACGACTCAATTGATGAATCGG	GTGTGGAGAAGCTCCACTTTG
SALK_020615	AAAAGTTGCATGCATTGATCC	TCCGTGAAACTGCCAATAAAC
SALK_020801	TGATCAACTCCGCTGGATATC	CTTTTGCAAGGACTACGTTGC
SALK_020814	ATTCTGTTTTGCACAGGTTGG	CCTCAAGAGAATACCGGGAAG
SALK_020957	CAGTCTGCTTTTTCATTCAAAGG	AGTTTCGTCAACAATCATGCC
SALK_021062	GGTTTAAAAGACGGTTCCTCG	CAGCCCACACATAAGGATTTC
SALK_021171	AACGATAATTTGAAGCATCGG	GTTTCTGAGCATTGTAAGGCG
SALK_021217	GTCTGATGAAGCAAATGCTACTG	GTTGTAGCAGATTGTTGAAAG
SALK_021618	GTCATGGCTCTTCTCTCCAATTG	AGTATAGAGCTTTGCTCAGAAG
SALK_021650	TAAAGGGGAACCAACGTAACC	CCAGAGAGGTTTGAATTTCCC
SALK_021759	AACATCACGTGTTAACTGTAAAG	ACTCAGAACTTCTGGTCTTAGG
SALK_021778	TGATATCACTTTCACCCGCTC	TCAATATGAGGCAAAGGAACG
SALK_021882	CTGAGATGTTGCCAGGAGAAG	AGGATGTGTGGTGAGAGGATG
SALK_022035	CATCATCAGCATCATGTCACC	TTCACGAAGGCAAAAGAGTTG
SALK_022083	CAACAAAAGCAATAAGCGGTC	TGGATGTAAAGGCTCAACCAC
SALK_022117	CAACAAAGGCAATGAAGAAGC	TTTTTCCGACAATCCTGATTG
SALK_022640	GGGGATTCGAATATGGTTTTC	GTTTGTGATGGAACACAACCC
SALK_022743	TCTTTTCCATTACAACGTGGG	CGTCAAGACCATGACATCATG
SALK_022780	TGGAGCCAACCACTACATAGC	GACTTGCCACGCTTTTATGTG
SALK_022843	AAGAGTGGGTAAATCGCCAAG	AGCAACATGGTGTGGATTCTC
SALK_022878	TTTCGTCACCTTCGAGTACATC	AATCTGGACACATGGATGGAG
SALK_023099	AGAAAACTGGGACGCAATTTC	GAGTCTGGAAAACCCGTTTTC
SALK_023198	TTTGGAAAGGTTGCTGAGAAG	GCAACCATTAACAAACCAACG
SALK_023910	TTGCAGACATGATCCATCTTG	TTCAAAGTCCGATCAAAATGC
SALK_024210	CAGAGCGAATTTTAGCACTCG	CGAAACGAATTTGAATCATCC
SALK_024270	TCTTCTCTCGAAGATGCTTGC	TCTGACTGTTGTTTCCCCATC
SALK_024285	AATACTTGGCCATATCGCTCC	TAATTTAGGCTCTTCCGGGTG
SALK_024556	TCCATTGTCTCCATTCTACGC	AAAGAGGAAACAGTTCGAGGC
SALK_024589	CATTTTTGACGAATGAATGCC	AGCTAGCTTGCACTTACGCAG
SALK_024627	GACCTTGGATTCCCTGACTTC	CGCGTTTGAAATTCGTAAGAG
SALK_024759	ACCCTTCAACATCAACCTTCAAG	AAGATCCTCCGTTCAGCTTTCG
SALK_024760	GAAGACATGGATTGGGACAAG	CCCAAATTTACATTAAAACGCC
SALK_024963	ATTCGCTCTGTCGACACTTTG	AGCATCTTGTGGTTAGAGGGG
SALK_025062	TGAGCAAATTAACAACGACAAC	TCTCTCCTCAGGGAGAAAAGG
SALK_025213	GCTCAAAGCAGAGGATGTCAC	TGCGGAAAATTTATGAACGAG

Table S5. Primers used for the genotyping of annotated T-DNA insertions

Line	LP sequence (5'→3')	RP sequence (5'→3')
SALK_025508	GTTGGTCCTTCATCCTTAGGC	TGCAAGCTTTAGCTTCTCCAG
SALK_025598	TTCATGCGAGAACAAGAAAGC	GTCTGAGAAACACACGAAGGC
SALK_025730	GAAATGAAGCATTTCACACCG	CTGGAGTTGGCTCGTTAACTG
SALK_025769	AAACGCGTTCTCCTTAACCAC	TACTTTGGGTCAACGGTTCTG
SALK_025969	CCTTCTCGCAGAGTCATGATC	AATTCACAGCAAACGAACCAC
SALK_026036	CTGGTCTTCGCTCTATGATGG	AGAGTTCTTACAGCAATGCGC
SALK_026171	TTCAAGTGCATATGCATGGTC	TTTGATAAAAGCTAAACAACCAGG
SALK_026226	TCTCACAGTTGCAACCTGATG	GGGGTTTTACAGGTTTTGGAC
SALK_026289	TCCGACCAATCTATCATCTGC	ACAAGAATAGCCAGTGAACCG
SALK_026306	TTCGATACCAATCTTTGCAGTG	AGGGAGAGCCTGAAGAAGTTG
SALK_026489	CGACCTAGGTCTCCGACTTG	AAGGGCGCAGCCAGCTATAG
SALK_026551	TCCAATAACCACCACACACAG	TGCATATCCAGATTTACATCTTTTTG
SALK_026595	TTGGACAAAAAGCTCGAGAAG	TCTCTATGCACAGGCATGTTG
SALK_026611	GAGGGGACAAAAGAATATCGG	CTCACTTTCTTCGTGTGGAGG
SALK_026655	TTTGATTTCATCTTTGGGCAG	GAAACAAAGACTCCAGATTCTGG
SALK_026667	TTGGTGTTGAACCAACTCCTC	TTGGAACCAAGCACATCTACC
SALK_027152	CTGGAATTTTTCTTGCGTCAG	TTCTGATTGAGGGATTGCATC
SALK_027288	TGGCCTCAATGAGCTTAATTG	TAGATTAGGCCACCGGTTAGG
SALK_027396	CAAGGAGGGGTTTTCATCTTC	CTTGAAGTTGGGACCTGTTCC
SALK_027461	AAATCCATCCAATCCTCATCC	TGTTTTTATCACCGAATTCGC
SALK_027524	GACGAGAAATCGAAGCATACG	AACCTGAGTTTGGCCTTTAGC
SALK_027691	GGCATGCTAGGATGAGCATAG	TTGTCTGATCTGTCGGAGAGG
SALK_027747	GAAACGGGGAGAAAATAAACG	CGATTCCTGTCTTTAACAGCG
SALK_027847	AACCAAAGATTGCATGCACTC	ATTATTCGGTGATGAAATGCG
SALK_027928	TCGTTCTACTGTCGTGGAAGC	TCCAGTGGATATTTGGTCTCG
SALK_027931	ACGACGTTTGGATTGGCAAGAC	CCGCTAAGTAGTAACACTCGAG
SALK_030106	CAAACCAGCTTTGTTTAACGG	CATATTCCATGGAGGTTGGTG
SALK_030155	ATCGTTCACTGAGATCCGATG	TTTCCCCAAAATCACAGTCAG
SALK_030202	AACTTACCAATCCCATCGACC	CCTCGTCTTCGACATAACTGG
SALK_030624	ATGCTTTTATCATTCCCTCGG	ATGGAAATGTTGTCTGCTTGG
SALK_030786	ATCCCATCAGCTTGTTCATTG	CTAGAACACAGGGGACTGCAG
SALK_030930	CAGTGGAACGAGAGCAAGTTC	AATGCTCTTTTCGCTTCTTCC
SALK_030932	TCATCCGAGTAACAACTTATCCAG	GGGATTTGAAGGTTTTTGCTC
SALK_031983	CCAAGATTCTCCCCAGAGTTC	ACACATGAGTTCCTCACCGTC
SALK_032511	CAAGGATGTTGAAGAAGGCTG	ACTTTCATCATCCGAATCGTG
SALK_032659	CGTGCTAGAGTCGGATTTGAG	GCAGAACTACAGAAGATGCCG
SALK_032904	TTTTTGGATTTTGGATTGTGG	TGACCAGCAGTATCCCAAATC
SALK_032963	GCAATGAACCTCTGGTGGAAG	TAGAAGATGGATTTGGTGAGCTT
SALK_033307	TCGAATCCAAGACGAATCAAC	AGAACAAGCGTAAGGCCCTAG

Table S5. Primers used for the genotyping of annotated T-DNA insertions

Line	LP sequence (5'→3')	RP sequence (5'→3')
SALK_033455	TAGTTGGATTTGTATCAGCATGG	TGTGTCGTAGCCTTTAGGAAGT
SALK_033511	ACGAGTACTGCCTTGCGTAAG	TTTGCGGTACTGCTTTTTCTC
SALK_033728	AATGTCATACCATGCTCTGGC	ACCCTACAGCTCCGTCTTCTC
SALK_034362	CGGACTCATGAGCAAAAGAAG	ATGGTGATTTCTTGCGTATGC
SALK_034684	CTTGACGACACACCAAACATGC	TCACCAGGTCTCCCAGATTGC
SALK_035241	GCAATGTGAGCAAGAGACAGC	ACACTCCTGACGTAATTTGCG
SALK_035363	TCTGATCTTTGACAGTGCGC	TCAGGCAGATCAACATAACCC
SALK_035676	CAACAGCGAAGATCTGGAGAC	CTGGAACCTGTTTTGCTTCTG
SALK_036097	ACACCCGCACTTGACATAAAG	TAACCACCCCCTCTCTCTCTC
SALK_036463	CCAACCCACTTTCTACATCTGA	CACGTACTTCAGTTTCCTCATG
SALK_036569	GGAGGAATCCGATGTAATTCC	CCACTCTGATTCCTTCAGCTG
SALK_037023	TTGGTTCTACTCGACCCAATG	TGGCCTATTACTACCATCCCC
SALK_037483	ATGGGTAGGCAAACCAAAATC	GCTTTTTGATTGTTGCTCGAC
SALK_037512	TCCCTTGTCATCGTGAAAGTC	AGAGAGCTGCCTTGGGAATAG
SALK_037549	ATTATGTCAACAGCCAGCTGC	AATGAAAAGGAAGAAGGCGAG
SALK_037675	GGGTTCCAATTCTCCAGATTC	AAGCTTCATCTACCTCCCTGC
SALK_038138	AGCCTCAAAGCTTTTCCAAAG	TTTGATTTGTTGGTGCCTCTC
SALK_038240	TCAACCGAAATTCCACAAAAC	AGGGACATCGATCATTCATTG
SALK_038804	GACCACGAGTCTCTCAAGCAC	TTGGGACAAAACTTGACAAGG
SALK_038835	TATGCAGAACCAAGAAAACCG	CTCCCAGTGTTTCAAAAGCTG
SALK_038859	CAAGCACTAACTGGGATCAGG	AGGAGAAGAGACTTATCGCCG
SALK_038907	GGTTTAGCCGTTTAGGTTTCG	TTTAATTTCGACACAAACGCC
SALK_039030	GAAGAACCAGCTTCACAGTCG	ATAAACTTCTCGCTCGTCACG
SALK_039212	TTTGTCGTGGTTGATTAACCG	AGTTCAGGTTTTGACACGTGG
SALK_039359	TATGTGGAGTCTGTGGTCACTG	TTCGTTTCATCAAGTACGCTAC
SALK_039478	TGAAACTCAACCGATGTGTTG	AGATGAACGTCGATAAGCGTG
SALK_039706	TTGACCAATAACAACTGCACG	TTTATCTTCGTCAATCACGCC
SALK_039718	TGGTTTTTCTTGAGTCATGCC	CATTTGACTAAGCAAAATCTCGTG
SALK_040155	AACATTTCTCTAATGTGTGTTATTCATG	ACACACAGCCGCGTTATTTAC
SALK_040244	CGAAAGATCTCTTGCCATGTC	CCCCATAAGCTCTTCAATTCC
SALK_040660	CTAGAGTGTACATTGAGGATGG	CTCTGTACAGAGACCAAACTTC
SALK_040739	CGCCAAAATCTTGAGTAAACG	TCATTTCTGTTTCAATTCTCCG
SALK_041111	CAGCTCTTGCCTTTAAACGTG	AAGTAACGGTGTGACGTCAGC
SALK_041291	AAAAGAACAAGGGATCTCTTCTTG	CTCTGCTTGAATCGGAGTTTG
SALK_041437	TCGAAACCCTAATCCGATTTC	TATGGGCATGACCGTTTAGAG
SALK_042323	TTTCTGGAAACTTGTTTTCCG	ACAAGAGGAATGCACCAATTG
SALK_043116	TTATTCCGGTGATTAGCAACG	TAGTCGTGGCTGGGTTTAATG
SALK_043149	TTATTTCTTGCTAGTTCTGGCC	TAGCGGAGATACTCGCAGAAG
SALK_043549	TCAGCTAGCATTGTCCCTTTC	ATGTGGCGTACTTTTGCATTC

Table S5. Primers used for the genotyping of annotated T-DNA insertions

Line	LP sequence (5'→3')	RP sequence (5'→3')
SALK_043616	AACAGCATCAACAATTGCCTC	GCCGAACAGAAATCTCAAGTG
SALK_044018	ACGCGGTTTTACTAAACCGAC	TTTACCGGTGTATCGTCCTTG
SALK_044034	TGGATTTGTCCACAAAGAAGC	GGTAGCGGTACTCAGTGCTTG
SALK_044091	TTCCAATACGGTAGATCGGTG	CAATCATCGGAGTCCATTTTG
SALK_044119	ATCAAGCCATCAAAACCACTG	AGAGAAGCCAAGTCCCTCTTG
SALK_044145	AAGTCATTGGTTCAATGTTTGC	CAGTCGATCGATTACACATGG
SALK_044371	CCTCTAATGGAGGCTTCCAAG	TGCATCTTCTGTTCATGTTGC
SALK_044415	TTTTCTGTTTCAGGGATGTCG	TTGGCTATTTCCATTTCCTCC
SALK_044478	GCCCTTAAACCCTGTGTTCTC	ACTGCACCCAATTCAAACATC
SALK_044496	AGCTAATAAGCTCCTCCGCAC	AATAAAGGTGACAAGGTCCCG
SALK_044616	GATCCTTACAAGGCACCTTCC	TTCCGAGGTAGCTTGTCTGTG
SALK_045025	GGTTGAGACTCTTGAGCATGG	TCATCTTACTTGATAATGATTTCATGTC
SALK_045034	TAGTGGCAGATTTCTCCTATGG	TTCTTGCACCTTCGAACTCTGC
SALK_045441	TTTGGGGATCGTATCAATACG	AGATGACCATGACCAAGTTGC
SALK_045619	CGTCCATTCTATTACCAGAAAAC	TTTCCAAGTTCTTGTTCCTCATC
SALK_045623	CAATTCTTTCGCATGAGCTTC	ACAGCTCGAGACTGCTCTGTC
SALK_045880	AAAATGATTGGAACTGGTCCC	TGTGTTTAGCAGTTGCGTCTG
SALK_046141	GAGTCTGCCACTACATAACTGCC	GCGTCTTCTTCTTCAGGTGTG
SALK_046378	TGATACCCACTTGCCAAAAAG	ATGCAATCAAAGGAGTGTTCG
SALK_046439	GATTTTATGGGGAAAACTCCG	TGACAAGATCACCACCTCCTC
SALK_046728	CGCAAATCATTAAGAGCCAAG	GACACAGGGTGTGGAATTCAC
SALK_047268	CTATGTGTCTCATAAGCGGCC	TCCCTCAAGAGGAGGAGTCTC
SALK_047274	CGCAGAGGTTTACCTCAACAG	TCAGAAACCATCCGATGTAGC
SALK_048174	TAGAACGATTGGAGACGAACG	TGTCGTTTATGTTGCATGTGG
SALK_048175	CAGCTTGGATTCCTTCTGATG	ATTGAAGGACATTTCAGCCG
SALK_048627	CTTAGGAGCAACAGTTGGTCG	GCTGTTCGAGACTATTGCCAG
SALK_048891	GAAGTCTGCTTCGAGGTGTTG	TGGATGTAACGATCAAAAGCAG
SALK_049200	CATTGAAATCATGCTTTTACCG	TGCAGAAAATCCTCAATGGTC
SALK_049907	TCCTTTGTTGGTCGTTTTGAG	GTTCCCATGCTTCTTAGTCCC
SALK_050137	CGAAGATCTTCGAATTCAACG	TAGTCCTCTTGCAGAGCAAGC
SALK_050231	TGGCTAAAGGATACGCAGTTG	TGAACCATCTCTTCAGCATCC
SALK_050259	ACATATTAATGGACCAGGCCC	TGGCAAACACAAGTTCTTGTG
SALK_050260	CAAGTTTCTCTTGCTCATGGC	CTCTGCAGCAAGGATTGAAAC
SALK_051228	GGACAACTTTTTGGGTTTAGGC	AAGGTTGAGTAGCTCTTCCGG
SALK_051857	TACACGTCTTCTTTGGCCATC	ACTTCACCAAAAATGGTGTCG
SALK_051913	AGCTAGAGAGGGGCAACAAAC	AACACGGTGAGCAATAAGACG
SALK_053063	GCAGAGTTGGTTCTGATGAGG	TGTTGACAGTTGCTGCAAGTC
SALK_053198	GAATCTCGGATAGAGCTTGATC	GAAACGTAATCCAAATGTATGTAG
SALK_054336	CGGCGTAGTCTTGAGAGTCTG	TTCGGGCATACAAACATCTTC

Table S5. Primers used for the genotyping of annotated T-DNA insertions

Line	LP sequence (5'→3')	RP sequence (5'→3')
SALK_054681	CGGTTACAAAACATAACTGAATTCC	AACAAGTTGGTCTGGGTTGTG
SALK_055458	AAAATTGGCTCCACAACTGTC	TCGTTCATGATATGTTTTGACG
SALK_055996	CGGCTTACGCTAGATTGACAC	ATCGTCAAATTCGACACGAAC
SALK_056529	CCTCCTTTCATTTCTCGTTCC	TCGAGATCATCATCGTGTCTG
SALK_057033	GTGACACCAAGAGGACTAGTG	CTTGTGCCGGAAGTCCCTTC
SALK_057052	TCTCGTCATCTCACGTGACAC	ACCAACCGGAAGTTTATACGG
SALK_057083	CGAGGATGAAGCAAAGTTTTG	TTGTTACTGCAATGGGGAAAG
SALK_057184	GATAGAGAGGTGTTACCGGGG	AAGATGCTAGGCCGAGAGAAG
SALK_057480	GGTCAAAACTCTCAAACGCAG	TGGTTACAGTCTTCAGCCACC
SALK_057752	CCTCTTGCAAATGATGCTCTC	CACTTTCTTCCGACGTCTCAG
SALK_057782	ATATCCGTTGGAAATTCTCCG	TTACGGATCCAACCAAGTGTC
SALK_057785	TAGCTCCTCCGCAGAGGAATG	GGAGTCTCAAGAGTCCCGTAG
SALK_057986	AACCCATTCGGGTAATTCTTG	TAAGTGAAGAAAGGGCCTTCC
SALK_057987	AACTATTTGCGTATTTGATCCG	AGCTTCTCGAATACGAGGAGG
SALK_059367	TGGACTACTTTGCACACGATG	ACTACCGAAGCAAGCCTGTTC
SALK_059601	GCCCTTCCACAATTTAAAAGG	ATGTGAGTCAAGGAGTGGCAC
SALK_060403	CGCGATGGAAAAACAAAGTAG	GACCAAAAAGGGAATTTCTGC
SALK_060686	TTTTCGTAAGACAAACCGCAG	CTTGTAATAAGGCAGCCATGG
SALK_060822	TCTGGTGGTAGTGCACAGAAAC	ACCCTTTATTGTCGTTTTGGG
SALK_060836	CTGCAGCGTAGGAAGTTTGAG	ATTGGACTATTGGGCCGATAC
SALK_060871	ACATGTACCAAAACGCTCCAG	AAATCCCAATACATAAGCGGC
SALK_061494	TATTACCTGTGTGATTGCCCC	ACTAGCAGCAGCAACGAGTTC
SALK_061595	AACACAAGGCAAAGGATGATG	ATGATGACATAACTCGCACCC
SALK_062509	TGTCCTCCCGATTCTGTGTAC	ATATGGGTTTCGAGGAACCTG
SALK_062797	TTGCAGTGAAATCAAGCAATG	CGCAGCAATCTCTAACACCTC
SALK_062875	GGCTTTGACAAAGTCTGCAAC	ATTCAGAGGGCATGTAACACG
SALK_062900	TTGGGTTTTGCTTATTATGCG	AGAAGCAAGCGAAAAGGTCTC
SALK_063054	AGACGGGACTTTGTCTGTCTG	TTGGAAGGATCATTGTCAAGG
SALK_063404	ACACGAGCCACAAGGTCATAG	GTCTGACCACTGAGCTGTTCC
SALK_063595	GATCTCATGAAGCTCGAAACG	CTCTAGCCAATGTTGCTCCAG
SALK_063956	ACGCATCAGTGACTCGAACTC	TAGTAAGCACAACGATTGGGG
SALK_064104	AGTTAGAGGAAACGCAGCAGG	TTGGCCAATTGTTCACTTTTC
SALK_064329	CGTGGTTACACGCAAAATTTC	CTTTCTACTTCTGATGCCCCC
SALK_064507	TTAGGCAACCAATTGAGGATG	GGCCCATGACTAGTTTCTTCC
SALK_064524	CGTCAATCTCCTCGAGATCTG	AAAACGTTTAATGCTCGAGGC
SALK_064915	GATACCAGTAACTGACCAACCG	GCACAAGATTCGTGCCTAGAC
SALK_065118	TGTCCAAGTTTGATAATCGCC	GCAAGCAGAATGTTTGCTACC
SALK_065777	GTTTATGATTCTGGCGACGAG	AGTTGATTAAGCAGCCACCAC
SALK_066103	TTGCTTCTAGGGATTTTCACG	GCGTTTCAATTTTCAAAGCAG

Table S5. Primers used for the genotyping of annotated T-DNA insertions

Line	LP sequence (5'→3')	RP sequence (5'→3')
SALK_066708	GCAACTAATACGACCAATAAG	TCATCTTCTGACTCTGTTTCTG
SALK_066806	TTGCAGTTCAGTTCAGTTTGTG	ACCATTACGTTGCGATTGATC
SALK_067017	GACCTCCTCTCAAGTTTTGAGC	AACCTGGGTTTGAAGATTTCG
SALK_067058	GAGCTGTTTTTCTGACTATTCAG	CCTTCACGGAGGATATCTGTAG
SALK_067582	AGGTGGTATGGGAAAACAAGG	ACGAGAACCGTGAATGATTTG
SALK_067800	TGTTACTGGGATTTGGATTGC	GCTGGGAGTACAGACAGCAAC
SALK_069400	AGTTGCCGATCTTTACCTTGC	TTTGAGTGAAAAACTGCGACC
SALK_069422	ATGAATGCAAATGCGATTTTC	TTTACCTTTGGCTGCATCAAG
SALK_070464	TTCATCCAAAAATGTCGAAGC	TTACCTTGGTGCAATCTGCTC
SALK_070853	TCCCGAATAAGTGACGTATGG	TACTTCTCGAGAAATCGTCGG
SALK_070975	TACAGCAAGCTGATATTGGGG	CATGCATATTTGAATGCGATG
SALK_072705	GTCACTTTATGCGTCGCCATC	GAATGGAATTTGTGATAGCGTTC
SALK_072771	AGCATTGCAAAGACCAAACTG	ATGCCTTGGTTTGACAGATTG
SALK_072930	TCATCCATATCTTGCAATGCC	TCAGCGAACTTCAGAAAAAGG
SALK_073011	AATTTCCTTAGAACAACGGCG	TGAACCACTCACTTGAAACCC
SALK_073728	ATCTCAAAGCATCTGTCCACG	CCAAACCAACACAATGGAAAC
SALK_074630	TCGAATGAGTTTACGGATTCG	TGGAAAACAGGCTTGTTGATC
SALK_074780	TTTTAGCGATTGCCATTTGTC	TCAAAAATGGTGGCAGATCTC
SALK_075362	TTCAAATATGATCCTCCTGCC	CAAAAGCTTGACGAAGGTGAG
SALK_075661	GGGACCGACAAAGAGTCTCTC	TCATGTCCACAAGGTAAAGCC
SALK_075797	TTCTCCGCTTCTTCTTCTTCC	ACCTCACCATGAAACAACCAC
SALK_075882	CATTCTCTCTTGTGGAACCCC	TCCACAGGTCTAATCTCACGG
SALK_075970	TCGATACAAGCGAATAAACCC	CAGGTTCAACGTCTCTGAAGC
SALK_076935	AGGTTAACCACGAGCAAGAGC	TAACCCCTCAAGCCCATCTTC
SALK_077062	GCTGCTGTGAATAATCGGATC	TATACCAATTGAGCTCCCCAC
SALK_077069	ATTTCCACGGGTAATTCAACC	AAAATGATAAAGCCGGGACTG
SALK_077422	GTGTAATGATCCAAACGGTGG	GATGGTCAATAACGGTCCATG
SALK_077716	AATGAACCCTCCCTATTGCTG	ATGAAAGCTCTATAATGCGCG
SALK_078275	GACACCAATGGATACAATCGG	CGAGTATGAGGAGATCGAACG
SALK_078760	TGGTGGCATAATTGACTCCTC	TCTGCCACTGGCTAACAAAAC
SALK_079285	CGGTCCAGATTGATACGTACG	TATCGGAATTCTCCAACAACG
SALK_080188	ATTTACAATAGCATTCCGGGC	TCGATCAATCACTGTCACTGG
SALK_080381	TTTCCACTTTCTGATGTTGGG	CTCCGGTCAAATTGTTATTCG
SALK_080604	CAAAAGCAAATGCGCCTATAG	GTGCCTGCTCTATGATAACGC
SALK_080831	TGGTTTGGATTTCCTCAGTTG	CCCAGAGAAAGCCTCTAGAGG
SALK_082289	ATGTACCCCAAAAACGAGAGG	ACTAGGTGATGTTCAATGCGG
SALK_082482	AAGGTTTATTGGTCTTTCGGG	CATTGATCATGATCGCAAATG
SALK_082749	GGACAACATTAATTGCCCATG	GCTCAAACCAAAACTTTGCTG
SALK_083333	GCAGTGCTGAGTCTTTGGAAC	GATTTGACTACAATCGCTTTGTC

Table S5. Primers used for the genotyping of annotated T-DNA insertions

Line	LP sequence (5'→3')	RP sequence (5'→3')
SALK_085503	ATGATTCGTAACGCTGGTCTG	CTTGAGAAGGTCTTGGTGCAG
SALK_085820	GATGCTGACAAATCTAAGGCG	AGTACCAGGGGTAGAAGCAGC
SALK_085920	AAAGATTTGATCCCACGAACC	CAACAGACCTGAAAGAGGCTG
SALK_086240	TGGTGGAATGTATTCCTTAAATTTG	GAACGAGGGAAAAGGTTTTTG
SALK_086630	CTGTTATGGCTTAAGCCCAAC	CGGCTCAAGCAAGACTAACAC
SALK_086690	TTGGATTTCATTGGATTGAGC	TTCAAAGGTCAATTCTGGTGG
SALK_086834	GAGTGTTGTTCCGTTCTCGAG	TCGGCTTTTGATTAGTCATGG
SALK_087484	ACCACGGCGAAGCAATCATTG	GTAACCTTTGCAAGCGTATGAC
SALK_087642	TGAAACTGTGTTGTCGTGGAG	AACATGGATGTTGAGGCTTTG
SALK_087720	TCAACAGTTCCACAAGTGACG	TTTCCAGATTTGGCATTTGTC
SALK_087804	TGCCATCTTACTTTTCCAACG	ATAAGCAAGCCTCTTTCCAGC
SALK_088435	AAGTTGCGGTTCATTGACTTG	ATTTGTACGGATCTCACGACG
SALK_088750	TTCAATGGGGATTCTGATAGAAC	TAGATGTCTGGAGGCAAATTCC
SALK_089798	TGATCTAGTTCATCTTGTAGCAATG	AGTCACACAATGAATCAGGCC
SALK_089912	TCCCTTCTTAAAACCCTTCCTC	CCCTACCTTCCATGGTTTTTG
SALK_091886	TTGCAATAAGAAACATGCTTTTG	TTCAAGTCACACCCGCTATTC
SALK_092843	CAGGTCGATGTGCGAATAAAAG	TTGGACCCAGTGCCGCATCC
SALK_094291	ATCCATAGTCGAACATGCGTC	TAAGGCTGGTGTTGTAAACGG
SALK_094653	CAGAAAATCACAATGGCTTTTG	GTTGCAAATCCTCAAGCTCAC
SALK_094849	GGTAGAGCATCCGAAGGATTC	GGTGGTATCCTAAGGGAGCAG
SALK_094856	CGTGACCCATTTATCATTTGG	AATCCAGACGATGGTACAACG
SALK_094948	TCTTTGCCTTGTGATTGGATC	AATGACCAGATGGCTGAAATG
SALK_095148	CAAATGTTCATGGTCGTTGTG	ACAGATAACCGGTGAGTGTGC
SALK_097064	TTCGATCAATTCGAAGGATTG	AAAACAATGATGTTTTTGCGG
SALK_098395	TCCCGGTAAGTGATACCAGTG	TTCGTCTCTGGAATTTTGGTG
SALK_099684	TTGCCAATCTTTGTACTTGCC	CATCACCGTATCGTTACCACC
SALK_100396	GAACAGAGTTGCTAACACGGG	AGGCTAGCCACAGGACTAAGC
SALK_101697	ACCATCACACTCAAACCGTTC	TGCAAGAAATGGGATTCTACG
SALK_101771	CTGGGATGCAGACACAACCTC	TAAAGCTATTATGTCCGCATCAG
SALK_102160	AAAACATTTCTTTCATGGGCC	GAAAGAAACAAACCGTAGGGC
SALK_102161	CTCCAACTCATTCCACTCAGC	GACACAGAGAGAACAGGACCG
SALK_102662	AGCGCCTCCTCAAAGCTATAC	CACGCAATCCTTTTTAATCCC
SALK_103127	TGCCACGAAACATTTTGTTTC	TGTTGCTCCAAGTACTGCTCC
SALK_103278	CAGTGCGGTCAAAGAATTAGC	GCGCTCATTAAACGTATCAGC
SALK_103728	TTTGGGATCTGAATCAGATGC	CAATGTCACTCATTCCCCAAG
SALK_104376	TTGGAACATCTTCTTCAACGC	AAAAATTGTTGGCTCCGAAAC
SALK_106689	TGGATTGCCCCAACGTCTCC	GCTGAACCGAAGGTTGTTAATG
SALK_106720	AATGGCTCTCTCACTCTGCAC	TTTAGCTGTGCCTATGTTGGC
SALK_107544	CCGGTCCGAACAGTATAGATG	GGAGTTGGTGGACCCTTAAAG

Table S5. Primers used for the genotyping of annotated T-DNA insertions

Line	LP sequence (5'→3')	RP sequence (5'→3')
SALK_108010	TTCATGCTGGTGAAAATTTTG	TTCGTGTTTCCTCTTCTTCCC
SALK_108337	AATTTCCCAAAATCGGCTATG	TGTTACTTGTCGTCGTTGTCG
SALK_110242	ACGCCACATCAATTTCAACTC	TGTGAATGCAATTCCAACATG
SALK_110691	GAGAAGACTTTGGGATCGAGAG	TGGTCTCGGGCTTTTTCATCAG
SALK_110749	TCTGGTACATCTTTGCTTGCC	TGAACACATCTCCCAAGATCC
SALK_110873	TTGCTCTCTTGCTCGATCTTC	TGTCATGCTGCTGTAGAATGC
SALK_111394	GTTCTGGAACAAGTTTCTGCG	AAAAGGTGAGGAACAGAACCAC
SALK_112720	CTACGAAGAATGCCATCAAGG	ACTCCGTTGGAGCTTTCTCTC
SALK_112882	GAACGCACCAGAGTGCTTATC	AGGTTCATGTTGATCAATGCC
SALK_113067	ATTGAAAATGGTGATGCAAGC	ACAGAGCATGGAAGGAGAATG
SALK_113154	TGGTCAAACAATGTCAAGCAG	TGGGTTGCTACATCTACTGGG
SALK_113246	TGCCACCTTCAATTCAAAAAC	TGATTTTCTTGAGACCGATGC
SALK_113285	CCTTTTTGTGCTATGTCCAGC	CAAGAGAGCTTCACAAGGACG
SALK_113585	TGACGATGTCTGTCCACAGAG	TTCAAATCCTATTTTTGCCCC
SALK_113836	GGAATCGAGGAAATCCTCAAC	TCAAACAATCGAATGGAATGC
SALK_114083	CTCGAGAACTACTGCGACAGG	TGGAGACAACCCGATAACTTG
SALK_114091	GCGGAAATTTAACGACATGTC	ACCCAAAGGTACCGAAGCTAG
SALK_114679	AGACGGGTAGAGGATACACGC	GCATGATAAAGCTTAGTGGAGAAAG
SALK_114696	TATAGACATGGCACCCACTCC	AAGCAGTAGGAATTCCACGTG
SALK_116141	TAAGCAAGGGAGAGCATCTCC	TCAAATCCTCACCAAGTCCAG
SALK_116537	TTCTTGTTCTTCCACCCAATG	AATTGGGGACTGAATTTGGAG
SALK_116625	AAACACATGTCATCGTGATCTG	TGATTCCACACCCGTTGTTAC
SALK_116744	GAGATCAAAGCGCTGAATGAC	TCAACAAGAGGTATCCGCAAC
SALK_116974	AGGTGAACCAGTGATCTGGTG	AAAAGTCGGTCGCTAATCAGG
SALK_117972	CCTGAACTTCTTCCACAGCTG	AGAGGAGATGGGAAGATGAGC
SALK_118239	CGTTTGCTTCGATGTTAGGTC	AAAGCAAAGGTGTGATGATGG
SALK_118536	CTTCGCATCGAACTTCTCATC	CCTACTCGTAAACCTCCGTCC
SALK_119148	CAATGGGTTCTCCATGATTTG	AAGTGGATGTGGAGCATGTTC
SALK_119409	TTGAATACTTTTTGGGATCTATCAAAC	ATCCTGCGTTTTTGTTGATTG
SALK_119457	AAAACCACCATCACGTAGCAG	AATTCACGAATTCGTGAGGTG
SALK_119833	CAGAAAAGGTCCTTAATCCGG	ACTCAATTACCCCATCCTTGG
SALK_119925	AAAGAGACCCTGATGAGGAGG	CAAGACTTGTTGCCTTTCCAG
SALK_120077	TGGTCCAGAAACAGATCCAAG	CCTCTGAGTAATGCTTCGTGG
SALK_121288	TGTAAACAAGGACAGGATGGC	GTACTAGCGGTGACAATTCGG
SALK_121961	AAACATCGATCCAGATTCGTG	GCTGAAACATTAGGGCACTTG
SALK_122235	TGCATACCATGGAGTATGCAG	ATTTGCAGTTTGGAAGGTTCC
SALK_122701	TTACTATGGATGTCACGCGTG	AATCAGCTCCAACTGTGTTGG
SALK_122867	CAGGGACATCAATAATCATAACC	CCCAGTTCTTTCAGCTTCCTTG
SALK_123405	TAGGAAGCAGAACAATGGTGG	GGCCTAAACTCATCAGGGTTC

Table S5. Primers used for the genotyping of annotated T-DNA insertions

Line	LP sequence (5'→3')	RP sequence (5'→3')
SALK_124393	CACTCCTGCGACTTTCTTCTC	ACCATGTCCAACACATCCTTC
SALK_125189	ATGTTCAACAAAAGCGGAAAG	TACCCGTGCAAACTTGCTAAC
SALK_125416	CCTCTCTAATGGCGTACTAGGG	TAGGACAGTTTCATGGTTGGG
SALK_125621	AGGGAAGAAGCCTGCATAAAG	ATCAAGAGGCCTTCTTTGAGC
SALK_126071	GCATATTCTTTCTCCCCCAAC	ATCTCTTTTTGCAGTTGCTCG
SALK_126447	TCGACGATAAAAACATCGGAG	GGCCAACTTCTCCTGGTTATC
SALK_126725	TCAGAGAGAGGTCAAAATTGAGG	TACCTGCGAGATTGGTAATGG
SALK_126818	TGTCCGTAACGAATTCCTCAG	ACCCTTAGGCATCACATCCTC
SALK_127261	CTATTCCCCGAGATCTTTTGG	TGGCTGAGATGGTAAACTTGG
SALK_127430	GTAAATTGTGGCATTAAGAACG	TCAAGATGCTCGCCACACTGA
SALK_127920	CACACACAAAGTACGCACCAC	AGCAGACCCCTCAGAGCTTAG
SALK_128177	AGAAGCAGTTGCTTCGATCAG	ATGTGCCCCTTTTGTTTCTTC
SALK_129037	CCCATTGAACCTAAAAGGACC	ATCAGATGCTGGTGTTGGATC
SALK_129213	TCATTCATTGTTCCCAAATCAG	TGCATAGTTTCGATTCATGACC
SALK_129352	CCATGGGTTAAAGATCATTGG	TTGTTGTGGGAACTCTATCGG
SALK_130010	TCATACCACTTTGTTAGACGTGC	AAGGAATGGTAGGAGAGCAGG
SALK_130499	TCCGTTCTATTACCTTGCACG	GGGAAAGGACTTGCAGATTTC
SALK_130961	TGCAGATGCAGATTTTGACTG	CTCTTTGGCCTTTGTGATGTC
SALK_131604	TAGTCAAAGGGTGTGACCTGC	AATTCATCAGTGACCCACGAG
SALK_131610	GGAAGAGCATACCCCTCGTAG	AAATCTTTGTTTTGGGGGTTG
SALK_132447	GTTGCTTCCCTTTCCTCAAAG	TTGTCCCCTTCGTACTGTCAC
SALK_132789	TGCATGGAAAAGGTTCATACC	TGACAGGTCTTTTGGAACAGC
SALK_132810	TTTTCGTGCGAGAATTGAATC	ATGACAAGGCGCTACTACTGC
SALK_133751	TTCTTCTCCTTAGGTCCCGTC	GTGGCAAAGGAGTCTCAACAG
SALK_133963	AATGTGCGATAATTGGTTTGC	GATCTTTCTCCACTCTTGGCC
SALK_135329	ACACCGTACAAATGGTTACCG	CTCTCTACCACCAAACCTCCC
SALK_136507	GTTGCTTGGAAAGAGACAACG	AAACCTCGCCCACATAAATTC
SALK_138001	GGCCCTTAAATCTCACCAGTC	AATTTTCACACGCATAATCGC
SALK_138229	CCAAAGCAATCAGCTTTTCAG	TCCCTACCCATAACCAAAACC
SALK_138474	TACCTTCATGAGGTTGCAACC	TCATCCGCCAACTGAAGTAAG
SALK_138605	AGCTTCTTGATGTTCTGGTGG	TAAAACTCAACGAAGCATGGC
SALK_138650	ACTTGAAGATGGGAGCCGTAC	TTACTGATGTCCCAGAGACCG
SALK_138693	TTTGATTCCATCTTGGATTCG	AGCTAAAGCATTGCCACACTG
SALK_139246	GCAAACGAGAGTGGAATCATC	GAATAACACTGGCATGGATCG
SALK_139777	AAACAGAGCCACCATCATTTG	AAGGAGCAAAATCAAAATGAAGAC
SALK_139862	TCCGCTGATTCATTTTCATTC	TTCGAGACCACTTCTCAGGTC
SALK_141603	TATCCGCCTCACAACTTATGC	ACTGTTATCACACTCGGCTGC
SALK_142112	TGTTGGACCCCTAACACTCTG	CCACATTTCAAGTATAGATGAATTGG
SALK_142184	TTTTTCCACCAGAACCATGAC	CGATGCTCCAGAGGTAAGTTG

Table S5. Primers used for the genotyping of annotated T-DNA insertions

Line	LP sequence (5'→3')	RP sequence (5'→3')
SALK_142534	TACATTGCCGGATTTTCTCAG	AGTCACATCGATCAACGGAAC
SALK_143087	CAATCTGCTACTGAAGTCGGC	GAAGGTCGGAGGATATATCGC
SALK_143422	GCATTACTGCTTCGGTGACTC	ACCACACAAGGACAGGACAAC
SALK_144022	CTCTGTGACGCCGAGGTTGC	TATCCTGGATCTCTCAATCTGG
SALK_144264	GAATGTTGAAAGGCTGGATTAC	TTTATCGACCAACGCCTATGCT
SALK_145086	ACGACACGTTTCTTGAAGCAG	GATTTTCGGGCTTCTTTCATC
SALK_145158	ACGTGTGAAGTGTGATTTCCC	ATTTTCCCAAAACCACGAATC
SALK_145203	GACTCTTCGACCTTAAATCACC	GTTCAACTCTAGTTTTCTCAAGC
SALK_145983	CATAATTTGGATACCAGTACTAAG	TATATAAGCCCATCTTCACCATG
SALK_146126	ATTTTGGCGGCTTAAACTTTG	ATTGACTTACCAACGCACTCG
SALK_146865	TTAGCTATGCATGCAATGCAG	TCAGTTAAAGTGTCGTGGTCAC
SALK_147068	AGCTTCTTCTCGAACTTTCCG	TTCCCTAGAATGCAATTGCAC
SALK_147685	AATGAATCCAGCATCAAGCAG	CTAGCACTAATCCCGGATTCC
SALK_147805	TTGACAAAAAGGCAATGGATC	ATACCCTGGATGCTCTATCCG
SALK_148403	ATGCAGAGCTTGAGCTAAACG	AGACGGCTCTGGAGTTTTCTC
SALK_148633	TGCGGTTATACAATCCTCTGC	TTAAAATGGGGGACAAGATCC
SALK_148815	TTATATCCCTTGGGATAGGCC	CTCAGGAGCTCAACAAGGTTG
SALK_150081	CGACGACCTTACTGGATGAAC	CGTTTCGCTTACTCTGTTTGC
SALK_150281	ATTCAATTGTGGTTGCGAGAG	TTTAAATCTCCCAAACCCCAC
SALK_150306	CTAGCGTAAACCGGGAAAATC	AACACCAGGAACAACCTCATG
SALK_150644	ATCGAAAGCCAAGATGTAGCC	CAACCTCCATATCTGCAATCG
SALK_151239	GAGCAGAATCAGCAGGAAATG	CTTTACGAAGAATGCAATCGC
SALK_151478	CGAAATTGATTCCAAGAGCTG	ATAGTGTTGGTCATCCGCTTG
SALK_151603	TTTATGAATCCAAGTGGTGGG	ATACACGTAACCTCCCCATCC
SALK_152677	CTTTCTAGAACCGGTTCACCC	TGATCTTCGTTGTCCGATTTC
SALK_152782	CTTTGAAAGCAGGTCGATACG	TTTGGTTACAGGGCTGAGTTG

Table S6. Oligonucleotides used for adapter ligation-mediated PCR

Name	Sequence (5'→3')	Description (O'Malley *et al.*, 2007)
LS1	GTAATACGACTCACTATAGGGCACGCGTGGTCGACGGCCCGGGCTGC	Long strand of adapters 1.1 and 1.2
SS1.1	P-AATTGCAGCCCG-aminoC7	Short strand of adapter 1.1
SS1.2	P-AGCTGCAGCCCG-aminoC7	Short strand of adapter 1.2
LS2	GTAATACGACTCACTATAGGGCACGCGTGGTCGACGGCCCGGGCTGTGC	Long strand of adapter 2
SS2	P-TAGCACAGCCCG-aminoC7	Short strand of adapter 2
AP1	GTAATACGACTCACTATAGGGC	Primer for adapters 1.1, 1.2 and 2 in first PCR
AP2	TGGTCGACGGCCCGGGCTGC	Primer for adapters 1.1 and 1.2 in nested PCR
AP3	TGGTCGACGGCCCGGGCTGT	Primer for adapter 2 in nested PCR
LBa1	TGGTTCACGTAGTGGGCCATCG	Primer for T-DNA LB in first PCR
LBb1	GCGTGGACCGCTTGCTGCAACT	Primer for T-DNA LB in nested PCR
RBa1	AGCTGATAGTGACCTTAGGCGAC	Primer for T-DNA RB in first PCR
RBb1	CGGCTGAGTGGCTCCTTCAACG	Primer for T-DNA RB in nested PCR

Table S7. Primers used for the genotyping of non-annotated T-DNA insertions

Primer name	Forward primer sequence (5'→3')	Reverse primer sequence (5'→3')	Target
2.3.2	TTGATGGCTACTGGCATGTGC	AAAGTAATACACTCAATGGTCAAG	SALK_021618 non-annotated insertion #2
1.4.2	TACGAATCAATAGATATGCCCAG	TTAGAGCGCATGGAGCTCATG	SALK_077716 non-annotated insertion #1
1.4.3	GCAAAAAAAGGTGAATGGAACC	GAGAATCTGAACGAATCGTCTC	SALK_077716 non-annotated insertion #2
2.1.1	TTTCCAAACACATTCAAAAAACGC	ACGTACGGAGAGTTTAATGAGG	SALK_113067 non-annotated insertion #1
2.2.1	ATCAGCATGTGTGATATGTTAAAG	TTGGTACACTTTCGCTACCTTG	SALK_113067 non-annotated insertion #2
2.2.3	GGATCAAGTGGTGAAAATGCTG	GACAACGTTGAGCCCACTCG	SALK_113067 non-annotated insertion #3
2.3.3	CTAACGGAACGCTTCATCATAG	CACAGGAACTTCTCGCATTATC	SALK_121288 non-annotated insertion #1
1.5.1	TCAGCTGAGTGAGCCAGGAG	CTTTATTAGGTCAAAGTCGTCC	SALK_025062 non-annotated insertion #2
1.2.1	ATTTAGCATTATTTAGATGTTTTCG	AGGGATTATGTCGGTCAAAGG	SALK_026171 non-annotated insertion #1
1.3.2	GCTAACTTAGTTTCTCTTATTGTT	TTGGCCTGTCTGCAATTTTCC	SALK_026171 non-annotated insertion #2
1.3.3	TGTTAGCGTAAATGTAGGAGAG	CGTTTGAAACTGTAAAGTCTAAG	SALK_026171 non-annotated insertion #3
1.4.1	CAAAGAAACTTAGACCATGCAC	TCGGTTTAAGATTAATGTGAATAG	SALK_026171 non-annotated insertion #4
1.5.2	GTCGTGACTGAATAAAGTCATG	TTGACCAACTTTGCTTGTGTGG	SALK_101771 non-annotated insertion #2
1.1.a	TTACTTGCCCGGTGGTAGCC	AACTGGAAAATTATGGCTCTTCG	Artifact #1 (see Figure 6e)
2.3.a	TTCTTTGCTGTGGCCTTGGAG	GACTAACACATCATCGGCAAAG	Artifact #2 (see Figure 6e)
LBb1.3	ATTTTGCCGATTTCGGAAC	Locus specific	T-DNA left border
RB1	CGTGACTCCCTTAATTCTCCGC	Locus specific	T-DNA right border
pbinprok2-1F	GCGCGATAATTTATCCTAGTTTG	Locus specific	pBIN-pROK2
pbinprok2-1R	GCGCAAACTAGGATAAATTATCG	Locus specific	pBIN-pROK2
pbinprok2-2	AATGGTACAGGTCGGGGACC	Locus specific	pBIN-pROK2
pbinprok2-3F	GTGCCGTAAAGCACTAAATCG	Locus specific	pBIN-pROK2
pbinprok2-3R	GTGCTTTACGGCACCTCGAC	Locus specific	pBIN-pROK2
pbinprok2-4F	GGAAACGTCACCAATGAAACC	Locus specific	pBIN-pROK2
pbinprok2-4R	CTGCTATCGATGGTTTCATTGG	Locus specific	pBIN-pROK2

Role of *DESIGUAL1* and auxin in bilateral symmetry of Arabidopsis leaves

David Wilson-Sánchez, Sebastián Martínez-López, Sara Jover-Gil, and José Luis Micol

Instituto de Bioingeniería, Universidad Miguel Hernández, Campus de Elche, 03202 Elche, Spain

Corresponding author: J.L. Micol (telephone: 34 96 665 85 04; fax: 34 96 665 85 11; E-mail: jlmicol@umh.es)

Running head: *DEAL1* participates in leaf margin patterning.

Keywords: Leaf, leaf margin, development, cell proliferation, auxin, *CUC2*

Word count (total): 9902.

Word count (Introduction, Results and Discussion): 5315.

Word count breakdown: Title page, 118; Summary, 184; Introduction, 617; Results, 3516; Discussion, 1182; Experimental procedures, 1347; Acknowledgements, 111; References, 1229; Figure legends, 1460; Supplementary tables, 186

Figures : 8 Tables : 0 Supplementary Figures : 9 Supplementary Tables : 2

SUMMARY

Bilateral symmetry, a striking property of many plants and animals, remains poorly understood. *Arabidopsis thaliana* has bilaterally symmetric leaves with interspersed marginal lobes and indentations along the margin. Several overlapping regulatory pathways establish these marginal features; these pathways involve feedback loops of auxin, the PIN-FORMED1 (PIN1) auxin efflux carrier, and the CUP-SHAPED COTYLEDON2 (CUC2) transcriptional regulator. Here, we identified a novel gene involved in leaf margin patterning, *DESIGUAL1* (*DEAL1*), which affects leaf bilateral symmetry. The *deal1* mutants have randomly asymmetric leaves that fail to acquire symmetry in the early stages of leaf primordium development, but instead form ectopic lobes and sinuses. Among other defects, *deal1* mutants show aberrant recruitment of marginal cells expressing properly polarized PIN1, resulting in misplaced auxin maxima. Normal PIN1 polarization requires *CUC2* expression and *CUC2* genetically interacts with *DEAL1*; *DEAL1* also affects *CUC2* expression in the leaf primordium margin. DEAL1, a protein of unknown molecular function, localizes to the endoplasmic reticulum membrane and functions in the leaf, acting partially redundantly with its two closest paralogs. *DEAL1* also participates in flower development, revealing that this gene has diverse functions in plant morphogenesis.

Leaf function critically depends on leaf form[1]. Therefore, genetically dissecting the acquisition of leaf shape during development, through the identification and characterization of the underlying genes, can improve our understanding of leaf function. Leaf development begins at the flanks of the shoot apical meristem (SAM) with the commitment of a group of cells, called a leaf primordium, to form a leaf. Class I *KNOTTED1*-like homeobox (KNOX) genes are expressed in the SAM to maintain a continuous source of pluripotent cells. In leaf primordia, *ASYMMETRIC LEAVES1* (*AS1*) and *ASYMMETRIC LEAVES1* (*AS2*) repress class I KNOX genes, thereby conferring determinate growth[2,3] with cell division occurring a finite number of times. After cell proliferation, cell differentiation and expansion complete the development of a leaf. The shift from cell proliferation to expansion and differentiation occurs basipetally[4]. In many plant species, including Arabidopsis, an exception to this global cell proliferation pattern occurs at the leaf margins[4]. There, class I KNOX genes are transiently derepressed to delay differentiation, allowing a secondary proliferative stage to build margins of varied shapes,[5] which include intercalated lobes and sinuses. The developmentally competent strip of marginal cells created by expression of class I KNOX genes requires positional information, which is provided by auxin, to determine the positions of these lobes and sinuses[6,7]. The auxin transport system appears to be the most important factor in creating a non-homogeneous distribution of this hormone. Abolishing polar auxin transport, either genetically, or chemically by adding exogenous auxin at the leaf primordia margins, results in the absence of auxin maxima in the margins and defects in lobe and sinus morphogenesis[7,8].

It has been proposed that the precise margin position towards which auxin is transported depends on self-organized feedback loops involving the PIN-FORMED1 (PIN1) auxin efflux carrier, the CUP-SHAPED COTYLEDON2 (CUC2) transcriptional regulator, and auxin itself[7,9]. These feedback loops create mutually exclusive spatial domains of auxin and CUC2 along the margin. In one loop, CUC2 influences auxin distribution in the marginal cells by polarizing PIN1 to the plasma membrane pole furthest from its own expression domain. Auxin, in turn, negatively affects *CUC2* transcription where the hormone is more

concentrated. This loop helps to establish juxtaposed CUC2 and auxin domains. In a second loop, auxin upregulates *PIN1* transcription and also induces PIN1 localization to the pole of the cell with the highest auxin concentration[10,11,12], thus self-perpetuating the maximum created by the first loop. Auxin- and CUC2-positive patches propagate from the primordium tip basipetally along the margin[7]. This propagation results in periodic, interspersed domains of auxin and CUC2 that mark the lobes and sinuses, respectively, of the developing leaf. The sizes of the auxin maxima and lobes directly depend on the dose of CUC2: the loss-of-function *cuc2-3* allele causes absence of auxin maxima[7] and smooth margins[13,14], whereas leaves expressing the *CUC2g-m4* gain-of-function allele display the opposite traits[15]. Recent work found that auxin influx carriers of the AUXIN1/LIKE AUX1 (AUX1/LAX) family influence the extent of leaf serration by regulating auxin dynamics in the leaf margin[9]. Leaf symmetry is very sensitive to auxin distribution: leaf primordia that develop with slightly unbalanced auxin supply at each flank, either artificially, or naturally in species with spiral phyllotaxis, produce asymmetric leaves[16,17].

Here we report the characterization of *DESIGUAL1* (*DEAL1*), which is expressed in leaf primordia and is necessary for the proper coordination of cell proliferation between different domains of the leaf lamina. This work investigates loss-of-function *deal1* alleles that cause stochastic alterations in the size, shape and spatial arrangement of the auxin and CUC2 leaf margin domains, and loss of bilateral symmetry of the leaf. We describe the participation of *DEAL1* in plant morphogenesis, where it functions to modulate margin configuration and bilateral symmetry by interactions with auxin- and CUC2-dependent pathways.

RESULTS

The *deal1* mutations perturb leaf bilateral symmetry

We previously screened the Salk collection of homozygous T-DNA lines[18] for mutants with altered leaf form[19]. Among the 706 leaf mutants that we identified, only one had leaves that clearly deviated from bilateral symmetry: the SALK_047972 line. Plants from this line had clear patterning defects at the rosette leaf margins, resulting in asymmetric leaf laminae (Fig. 1A, B). Based on the rarity of this phenotype, we considered this mutant of particular interest for studying plant organ ontogeny.

SALK_047972 is annotated to harbor a T-DNA insertion in the At2g32280 gene. We identified two independent insertional alleles in this gene from public collections, carried by the SAIL_237_C09 and SALK_023737 lines. Both of these lines also show leaf asymmetry and they fail to complement the allele carried by SALK_047972 (Fig. 1C, D). To confirm a gene-phenotype causal relationship, we transformed SALK_047972 plants with a *35S$_{pro}$:At2g32280:CFP* construct. All analyzed transformants (10 independent events) had wild-type leaf laminae (Fig. 1E) confirming that disruption of At2g32280 causes the observed mutant phenotype. We named the gene *DEAL1* (*DESIGUAL1*) and the three alleles *deal1-1* (SALK_047972), *deal1-2* (SALK_023737), and *deal1-3* (SAIL_237_C09) (Fig. 1F). We characterized the *DEAL1* mRNAs produced in these mutants. The *deal1-1* mutant contains a T-DNA insertion in exon 3, and produces a truncated protein (Fig. S1A, B). The *deal1-2* allele contains a T-DNA insertion in the first intron that is spliced out in 32% of the transcripts, which result in wild-type mRNAs (Fig. S1A, C, E). The *deal1-3* allele contains an insertion in the first intron and a deletion that spans part of intron 1 and exon 2, which results in the absence of wild-type protein (Fig. S1A, D). The *deal1-1* and *deal1-3* alleles were used in all subsequent experiments since they seem to represent a more complete loss of function. *DEAL1* has also been named *VASCULATURE COMPLEXITY AND CONNECTIVITY* (*VCC*) and a previous study showed that it is required for embryo provasculature development[20].

The *deal1* mutants show perturbed bilateral symmetry in adult vegetative leaves

The patterning defects in *deal1* mutants produce rosette leaves with abnormal lobes and sinuses that override the serrations of wild-type Col-0 leaves. We assessed whether this phenotype is a consequence of insufficient and/or excessive local growth by comparing *deal1* leaf silhouettes to a consensus Col-0 leaf outline. Localized sparse growth and overgrowth were both identified in these morphological characterizations (Fig. 2A-C). These patterning defects arise at random positions, with random sizes and shapes; similarities between leaf halves or between equivalent leaves from different *deal1* plants were not observed. The randomness of these shape defects ultimately causes loss of leaf bilateral symmetry and these defects exclusively affect tissue growth along the mediolateral axes of the leaf. Measurements to identify altered tissue growth along the proximodistal axis in mutant leaves, by measuring whole leaf and lamina lengths, did not find significant differences between Col-0 and *deal1* plants (Fig. S2A). We conclude that the mutant phenotype arises exclusively from uncoordinated expansion of the lamina along the mediolateral axis in each leaf half.

To quantify the severity of the leaf phenotype of *deal1* mutants, we devised a quantitative procedure to measure bilateral symmetry, the Leaf Symmetry Index (LSI). This index compares both sides of the lamina, as mirror images, to calculate the non-overlapping area. This area calculation is then compared to total leaf area (Fig. 2D). LSI values range from 0 for leaves having no symmetry, to 1 for leaves having perfect symmetry. We compared the LSI of individual rosette leaves from Col-0 and *deal1* plants. While rosette leaves 1 to 4 (from the first to the fourth nodes) are similar in both genetic backgrounds (LSI > 0.9), symmetry generally decreases from leaves 5 to 14 in *deal1* mutants (Fig. 2E). We did not observe any symmetry defects in cotyledons or in cauline leaves. Rosette leaf 10 was chosen as the model for all subsequent analyses. Based on LSI values of the basal and apical halves of leaf 10 laminae, the basal half is the main contributor to the leaf asymmetry shown by *deal1* mutants (Fig. 2F). The asymmetry was incompletely penetrant in our growth conditions (Fig. 2G). Therefore, in all subsequent experiments involving leaf

phenotype characterization, we measured both its penetrance and LSI. We did not find differences in LSI (Fig. S2B, C) or penetrance (Fig. S2D) among the three *deal1* alleles under study.

The *deal1* leaves show defects in cell proliferation but not in cell expansion

In plant organs, morphogenesis depends upon the interplay between cell proliferation and cell expansion. To ascertain which processes are defective in *deal1* leaves, we first examined leaf primordia before the onset of cell differentiation and expansion, analyzing patterning and symmetry in the absence of cell growth. Patterning defects and a loss of symmetry in *deal1* leaf primordia were detected at an early developmental stage (Fig. 3A-G) suggesting that proliferation is impaired and that this impairment accounts for the mutant phenotype. We also monitored cell division using the *CYCB1;1*$_{pro}$*:GUS* marker, a reporter for the G2/mitotic phase of the cell cycle (Ferreira et al. 1994). With this reporter, Col-0 showed uniform, symmetrical GUS staining on both sides of the lamina. In contrast, *deal1* mutants had visible heterogeneous patches (Fig. 3H, I), and spots with abnormally intense staining in basal tissue margins (Fig. 3J). These observations directly associate *DEAL1* with the regulation of cell proliferation.

Cell expansion was analyzed by measuring the size of palisade mesophyll cells and surveying for abnormal lobes and sinuses in fully expanded Col-0 and *deal1* leaf laminae. Cell size was similar in equivalent regions of Col-0 and *deal1* leaves with shape defects (Fig. 3K); specifically, cell sizes were homogeneous across the entire leaf with the exception of the marginal tissue, where cell size abruptly decreased in both wild-type and mutant plants. Abnormal lobes and sinuses were not accompanied by either an increase or decrease in cell size. These results indicate that cell size is uncoupled from the formation of the mutant ectopic lobes or sinuses and, therefore, is not a driving agent of the mutant phenotype. Taking these results together, we conclude that *DEAL1* participates in acquisition of bilateral symmetry in the lamina through cell proliferation. This role in leaf development is consistent with its expression pattern (see below).

DEAL1 is broadly expressed

DEAL1 has previously been reported to be expressed in the embryo[20]. Our results further suggest that *DEAL1* is required for leaf patterning in early stages of development. Since patterning genes often show constrained spatiotemporal expression domains, useful to infer their function, we characterized *DEAL1* expression *in vivo*. To do this, six independent transgenic plants that stably express a $DEAL1_{pro}$*:GUS* transgene were analysed by leaf staining at various stages of development.

High levels of expression were observed as dark blue staining in leaf primordia (Fig. 4A). During the transition to cell differentiation and expansion, GUS staining became localized to the margins and the base of the lamina (Fig. 4B, C). One day later, only the domain that eventually creates the petiole remained blue (Fig. 4D). Observation under higher magnification showed that blue staining coincided with tissue in a proliferative state that fades upon cell differentiation (Fig. 4E, F). The observed $DEAL1_{pro}$*:GUS* expression pattern and domain are reminiscent of that of the $CYCB1;1_{pro}$*:GUS* proliferation marker[4]; they are also consistent with a role for *DEAL1* in early leaf patterning and during the cell proliferation stage in plant leaves. GUS staining was also detected in flower primordia (Fig. 4G). After the differentiation of root and aerial tissues, GUS activity reappears in the vasculature (Fig. 4H, I), indicating that *DEAL1* is expressed in a broad range of tissues.

The leaf patterning defects in *deal1* mutants are independent of the class I KNOX-AS developmental module

The *DEAL1* expression pattern and the mutant phenotype of *deal1* leaves suggest that *DEAL1* acts at early stages of leaf development. Two other regulatory modules, KNOX-AS and auxin-CUC2, similarly operate at these stages and are involved in leaf margin patterning. We thus hypothesized that class I KNOX gene expression might be perturbed in *deal1* leaf primordia, causing unbalanced cell proliferation in the leaf margin[5]. To test this hypothesis, we assayed the expression of an STM_{pro}*:GUS* reporter in *deal1* leaf primordia and quantified the transcript abundance of *SHOOTMERISTEMLESS* (*STM*), *KNOTTED-*

LIKE FROM ARABIDOPSIS THALIANA2 (*KNAT2*), and *KNAT6* in young Col-0 and *deal1* aerial tissues using qRT-PCR. STM_{pro}*:GUS* expression was similarly observed in discrete margin domains in both backgrounds (Fig. S3A, B), and *STM* and *KNAT2* levels were also comparable (Fig. S3C). *KNAT6* transcripts, however, generally increased (approximately 1.5 fold) in *deal1* leaves as compared to Col-0 (Fig. S3C).

Class I KNOX genes are de-repressed in leaves of the *as1-1* and *as2-1* mutants. These mutants exhibit asymmetric basal lobe phenotypes[2,3,21] that are similar to those displayed by *deal1* mutants. We crossed *deal1* plants to both of these mutants and evaluated the double mutant phenotypes. All the *deal1 as1-1* and *deal1 as2-1* double mutants showed an additive phenotype (Fig. S3D-H) suggesting that the KNOX-AS regulatory module is not affected in *deal1* mutants.

Auxin is abnormally distributed in the *deal1* leaf margin

Auxin and *CUC2* are central to shaping the leaf margin, which is abnormally patterned in *deal1* mutants (Fig. 5A, B). Exogenous application of auxin to discrete spots in developing primordia is sufficient to trigger the development of vascularized lamina from the petiole domain and override bilateral symmetry[16,17], traits that spontaneously occur in *deal1* leaves (Fig. 5C, D). We hypothesized that the auxin-CUC2 regulatory module is spatially deregulated at the primordium margins, preventing cells from performing their appropriate roles during their proliferative period. To know whether *DEAL1* is related to auxin distribution in the leaf, we cultivated Col-0 and *deal1* plants in the presence of the polar auxin transport inhibitor 1-N-naphthylphthalamic acid (NPA). NPA has been shown to smooth leaf margin serration when applied at 1 to 5 μM concentrations[8,9] and to abolish serrations when applied at 10 μM[22]. Growth on medium supplemented with 0.6 μM NPA had no visible effect on Col-0 leaf margins, but was sufficient to increase penetrance of the *deal1* phenotype from 55 to 95% (Fig. 5E). This result suggests that the *deal1* defects are dependent on polar auxin transport. We also quantified phenotype severity by evaluating leaf symmetry, but we observed no significant differences between the mutants and the wild type (Fig. 5F).

Evaluations performed at higher NPA concentrations exhibited growth retardation in Col-0 making it difficult to characterize any specific *DEAL1*-associated effects in the margins. Crosses between *deal1-1* and *pin1-1* mutant plants were performed to better understand auxin function. The *deal1-1 pin1-1* double mutant plants showed heterogeneous morphological aberrations that ranged from symmetrical leaves with smooth margins to amorphous leaves with split petioles, the latter appearing at a higher frequency than in the *pin1-1* single mutant (Fig. 5G-J). In a complementary approach, we grew Col-0 and *deal1* plants in the presence of 0.1 µM of the synthetic auxin 1-naphthaleneacetic acid (NAA). This NAA concentration decreased the penetrance of the *deal1* phenotype from 55 to 14% (Fig. 5K) and also decreased the severity of the leaf asymmetry (Fig. 5L). In our culture conditions, 0.1 µM NAA does not have any visible effect on margin development in Col-0 leaves. These results further support a role for *DEAL1* in auxin function in leaf margin development.

To assess whether auxin transport, signal transduction, or perception are impaired in *deal1* leaves, we monitored the *in vivo* expression of $PIN1_{pro}$*:PIN1:GFP*[23] and the auxin-responsive marker $DR5rev_{pro}$*:GFP*[24]. The PIN1:GFP protein appears properly polarized in the membranes of the margin cells, and similar fluorescence intensities were observed in both backgrounds (Fig. 5M, N). The tissue domain whose cells are coordinated to pump auxin in the same direction, however, is randomly misplaced in the *deal1* leaf margin (Fig. 5O, P). The $DR5rev_{pro}$*:GFP* maxima in the primordial margins showed a similar intensity in the mutant and the wild type, ruling out an auxin transduction or perception problem in *deal1* cells (confirmed by auxin-induced root growth inhibition tests; Fig. S4). However, several defects in auxin maxima were observed: (1) Auxin maxima were often misplaced in the *deal1* mutant [Fig. 5R (m)] and lacked the regular spatial arrangement along the margin seen in Col-0 (Fig. 5Q); the unique defects on each side of the lamina cause asymmetric patterns. (2) The number of maxima differed between lamina sides causing asymmetry [Fig. 5R (n)]. (3) Auxin maxima of incorrect shape and/or size were present [Fig. 5R, S (sh, si)]. We conclude that the magnitude of the PIN1-mediated auxin transport is not altered in *deal1*

leaves, but occurs in a different bi-dimensional pattern, and this causes auxin to accumulate incorrectly.

Leaf vascular network in *deal1* leaves

Vein density and complexity (the number of branches and junction points per unit of area) are normally compromised when auxin function is altered[25,26,27]. We measured venation density, branches per leaf area, and branching points per leaf area in tenth-node rosette leaves and found a slight reduction, for all traits, in *deal1* leaves as compared to Col-0 leaves (Table S1). Connectivity appeared unaltered, as both genotypes have the same numbers of free-ending veins. Observation of cleared tissue showed that mutant lamina lobes have a proportionally extended vascular network with all the vein orders present (Fig. S5A, B). Sinuses showed a reduction or absence of secondary and higher order veins connected to the primary vein (Fig. S5A, C). These observations indicate that differentiation of the vasculature is not impaired in *deal1* mutants and that its layout during differentiation is coupled to the abnormal shape acquired earlier during proliferation; this is consistent with a role for *DEAL1* prior to cell differentiation.

***DEAL1* and *CUC2* influence one another**

The CUC2 transcription factor has been proposed to be critical for the proper positioning of the convergent PIN1 marginal domains that build auxin maxima at the tip of developing lobes[7]. Notably, we found a correlation between the severity of asymmetry at each rosette leaf and its degree of serration (Fig. S6), which depends on *CUC2* activity at the margin[13,15]. To explore a possible relationship between *DEAL1* and *CUC2*, we crossed *deal1* plants to plants carrying the strong *cuc2-3* allele[28]. Analysis of the double mutants obtained revealed that the absence of CUC2 causes a reduction in the penetrance of the random lobes and sinuses from 58 to 18% (Fig. 6A). Moreover, those plants that still retained leaf traits of the phenotype of *deal1-1* had high LSI values, more similar to Col-0 than to *deal1-1* (Fig. 6B, C). We also crossed *deal1-1* with the *CUC2*-overexpressor mutant *CUC2g-m4*[13]. Leaves

from *CUC2g-m4* generally possessed large lobes and deep sinuses. Many lobes were misplaced or failed to form in the *deal1-1 CUC2g-m4* double mutant (Fig. 6C). These complex epistatic relationships between *deal1-1* and the lack or excess of *CUC2* function suggest that *DEAL1* and *CUC2* are dependent on one another during margin morphogenesis.

We investigated whether expression of *DEAL1* and *CUC2* depend on each other by measuring mRNA levels in different backgrounds. We found that *DEAL1* transcription in leaf primordia was similar in Col-0 and *CUC2g-m4*, but significantly less (0.67 fold) in the *cuc2-3* background (Fig. S7A). *CUC2* expression levels remained the same in the absence of *DEAL1* (Fig. S7B). To determine whether there is a qualitative (spatial) influence, we studied the spatial pattern of $CUC2_{pro}$*:CUC2:RFP* fluorescence. In Col-0 primordium margins, RFP-positive domains appeared well-defined and evenly spaced proximodistally along both margins (Fig. 6D). These domains were present in developing sinuses of the serrated leaf margin and are spatially complementary to $DR5rev_{pro}$*:VENUS*-expressing cells. Equivalent domains were generally similar in size and shape among Col-0 primordia (Fig. 6D). In *deal1* leaf margins, however, the wild-type CUC2:RFP pattern was randomly lost; abnormally close or distant consecutive CUC2-positive patches were frequently observed [Fig. 6E (1, 2)]. In addition, the size and shape of these patches were heterogeneous and asymmetric (Fig. 6E). Overall, these observations show that the spatial pattern of *CUC2* expression is altered in *deal1* primordia.

The DEAL1 protein localizes at the endoplasmic reticulum

DEAL1 encodes a protein of 163 amino acids. Most sequence analysis programs from the Aramemnon database[29] predict an N-terminal targeting peptide for the secretory pathway (Fig. S8A). To investigate the localization of the DEAL1 protein, we used a $35S_{pro}$*:DEAL1:CFP* construct, which retains DEAL1 function, as verified by complementation of *deal1-1* plants (Fig. 1E). Ten independent transformants showed the same fluorescence pattern, which consists of round spots (Fig. 7A). We performed co-

localization experiments with propidium iodide and the endoplasmic reticulum (ER) and Golgi markers AtWAK2:YFP:HDEL and Man49:YFP[30]. The CFP blots sometimes appeared to be associated with the nucleus, but did not overlap (Fig. 7B). Golgi vesicles also appeared to be systematically associated with the CFP spots but the two fluorescent signals could be clearly differentiated (Fig. 7C, D). We also found that DEAL1:CFP is normally intimately associated with a sub-section of the ER; however, we did not observe a matching intensity pattern indicating strict co-localization of these two assayed proteins (Fig. 7E-J). The same observations were made in root and leaf cells. The data gathered suggest that the protein resides in a compartment that belongs to, or is functionally related to, the ER.

DEAL1 has four predicted transmembrane domains (Fig. S8B). To test whether DEAL1 localizes to the ER membrane, we performed a split-ubiquitin yeast two-hybrid membrane localization assay[31,32]. We detected strong ubiquitin re-association when co-expressing the fusion protein DEAL1-Cub (Cub is the C-terminal half of ubiquitin) with the fusion proteins Nub-Alg5 and Nub-Ost1 (Nub is the N-terminal half of ubiquitin; Alg5 and Ost1 are known to reside in the yeast ER membrane; Fig. 7K). Weak ubiquitin re-association could be detected with Nub-Fur4, targeted to the plasma membrane, and no interaction was detected with Nub-Tom20, in the mitochondria outer membrane (Fig. 7K). Cytosolic proteins interact with the mitochondria outer membrane while membrane-associated proteins do not. These results confirm that DEAL1 is not cytoplasmic. The co-localization of DEAL1 with Alg5 and Ost1 suggests that DEAL1 resides in an ER membrane, supporting the DEAL1:CFP subcellular localization results presented above. Both Nter-DEAL1-Cub-Cter and Nter-Cub-DEAL1-Cter showed interaction with Nub-Alg5 and Nub-Ost1, which have their ubiquitin fragment at the cytosolic side of the membrane. This reveals that both ends of the DEAL1 protein orient towards the cytoplasm, and implies an even number of transmembrane domains.

DEAL1 **genetically interacts with other members of the DUF1218 family**

The DEAL1 protein sequence contains the DUF1218 conserved domain, of unknown

function, which defines a gene family only present in multicellular plants[20]. In DEAL1, this domain spans 58% of the protein (Fig. 8A), including the 2nd, 3rd, and 4th transmembrane domains, and two soluble peptides (15 and 17 amino acids in length). In Arabidopsis, 15 proteins contain this domain, but to date only DEAL1 has been studied experimentally. Within the family, the DUF1218 amino acid sequence from DEAL1 shares high sequence similarity with three other proteins of the family, At4g21310, At1g11500, and At1g05291[20], which we named *DEAL2*, *DEAL3*, and *DEAL4*, respectively. To explore whether any of these genes is functionally related to *DEAL1*, we studied their spatial expression pattern by RT-PCR (Fig. 8B). Expression of *DEAL1* is relatively uniform across roots, developing leaves and flowers, and lower in mature leaves. The expression pattern of *DEAL3* is similar to that of *DEAL1*. Expression levels of *DEAL2* are lower in developing leaves than *DEAL1* and *DEAL2*, but comparable in flowers and roots. *DEAL4* is absent from leaves and roots and only expressed in flowers.

T-DNA alleles for *DEAL2* (SALK_099815) and *DEAL3* (SAIL_140_H09) were obtained from public collections and named *deal2-1* and *deal3-1*, respectively (Fig. S9). The *deal1-3 deal2-1 deal3-1* triple mutant showed an increase in leaf phenotype penetrance to 86% (Fig. 8C). This penetrance is 30% higher than that observed in the *deal1-3* single mutant, or in the *deal1-3 deal2-1* and *deal1-3 deal3-1* double mutants. This reveals some degree of functional redundancy and confirms that the *deal2-1* and *deal3-1* mutations alone do not modify the phenotype caused by *deal1* mutations.

We also tested the interaction between these genes and auxin homeostasis by growing the single, double, and triple mutants in media supplemented with 0.6 μM NPA or 0.1 μM NAA. Only leaves from *deal1* plants were sensitive to NPA, as seen by their phenotype penetrance (Fig. 8C). As in the single mutant, NPA does not increase the severity of the phenotype of the double and triple mutants (Fig. 8D). Addition of 0.1 μM NAA exerted a relative change in the penetrance and severity of the symmetry defects that was similar in all genotypes carrying the *deal1-3* mutation (Fig. 8C, D).

RT-PCR results revealed expression of *DEAL1* in roots and inflorescences (Fig. 8B)

and prompted us to evaluate the phenotype of these organs in the mutants. While we did not observe changes in root development, the pistils of *deal1-1* and *deal2-1* flowers showed developmental defects (Fig 8E, F): some were bent or coiled or twisted, and some pistils showed unfused carpels with exposed ovules. These defects were only observed at a very low frequency and addition of 0.6 μM NPA did not modify the phenotype (Fig. 8G). Addition of higher NPA concentrations compromised flower emergence and development in both Col-0 and the mutants.

DISCUSSION

Modular role of *DEAL1* in plant development

In this report, we present a role for the *DEAL1* gene in leaf morphogenesis, in addition to its previously characterized role in embryo provasculature development[20]. Both roles show *DEAL1* involvement in tissue patterning, consistent with this protein performing an evolutionarily important process in multicellular photosynthetic organisms[20]. An even broader role for this gene is expected, since we also observed *DEAL1* transcription in roots and floral organs. The plant-wide function predicted for *DEAL1* could be associated with multiple unrelated developmental roles of the protein, depending on the organ, as well as timing and location of expression. We propose this hypothesis based on the fact that *DEAL1* and *OCTOPUS*, a gene involved in embryo provasculature development in the embryo, genetically interact in the embryo[20], but not during leaf development. An example of a gene with many independent functions in different organs is *CUC2*, which participates in ovule development[33], meristem function[34], leaf margin patterning[13], and carpel fusion during gynoecium formation[35].

The study of leaf margins in *deal1* mutants has revealed that equivalent cells from both sides of the lamina do not divide equivalently. We also found evidence of unbalanced auxin supply to the margins. Since auxin maxima formation precedes proliferation foci that build the serrations in the margins[6], it is likely that aberrant coordination of cell proliferation is a consequence of the aberrant distribution of auxin. The *DEAL1* expression pattern in the earliest stages of leaf development is consistent with this hypothesis. We found that leaf primordia containing undifferentiated cells already show patterning defects and an altered expression pattern of a cell-cycle marker. Vascular pattern analyses revealed that these defects are not coupled to cell proliferation anomalies, since venation density was not altered in the *deal1* mutant lobes or sinuses. Even the ectopic laminae often found in *deal1* petioles present vascular tissue undistinguishable from that of a wild-type lamina. Taken together, these results indicate a role for *DEAL1* prior to cell differentiation and vasculature layout formation in the leaves. We think that the *deal1* mutants could also serve as a tool to

unravel how differentiation adapts to the pre-existing cellular matrix formed during cell proliferation.

DEAL1 could coordinate growth-promoting and growth-repressing signals to stabilize patterning

Areas of increased and reduced lamina expansion randomly coexist in different locations of a single *deal1* leaf, and therefore *DEAL1* cannot be considered a promoter or repressor of lamina expansion. One explanation for this observation is that *DEAL1* is necessary for communication between growth-promoting and growth-repressing signals that operate in a juxtaposed manner on the plane defined by the leaf proximodistal and mediolateral axes. These signals could be the lamina-promoting hormone auxin and the lamina-repressing transcription factor CUC2. We present evidence that the auxin-*CUC2* module, which establishes the position of the marginal lobes and sinuses in simple leaves, fails to do so when *DEAL1* is absent. Based on this observation, *DEAL1* could have an intermediary role in the crosstalk between auxin and *CUC2* that happens during leaf development[7]. Two observations support this idea: (1) margins indistinguishable to those cause by *CUC2* loss and excess of function can simultaneously be identified in a population of *deal1* leaves, and (2) *CUC2* loss of function partially suppresses the defects of *deal1* mutants whereas the *deal1* mutations partially suppress the margin phenotype caused by *CUC2* excess of function.

A proposed model of the Arabidopsis leaf margin[7] can successfully predict the position and magnitude of lobes and sinuses. Simulations based in this model in which the auxin supply rate was stochastic led to non-symmetrically positioned lobes and sinuses. From this model, *DEAL1* could have a role in buffering the auxin concentration to stabilize patterning. This hypothesis is supported by our NPA and NAA supplementation experiments, which respectively enhanced and suppressed the phenotypic effects caused by the lack of function of *DEAL1* in the leaf margin. It has been proposed that plant patterning progresses through mechanisms with inherent stochasticity, such as cell division

orientation, and that such stochasticity is compensated for by a series of control regulatory networks acting at the whole organ level[36]. In this context, auxin could be central for buffering stochasticity in the leaf and could perform this function via *DEAL1*.

Our results indicate that increasing auxin availability can partly replace the loss of *DEAL1* function. We found that the DEAL1 protein localizes at the membrane of the ER, an organelle known to be involved in auxin homeostasis[37]. Indeed, PIN5 is the major auxin transporter toward the ER lumen and regulates the level of active cytoplasmic auxin; high PIN5 levels can lead to leaves with severe developmental defects[38]. To ascertain if *DEAL1* could be involved in auxin homeostasis through hormone sequestering in the ER via PIN5, we generated *deal1 pin5* double mutants, which did not show any genetic interaction. Alternatively, *DEAL1* could be part of an independent developmental module superimposed on, and providing robustness to, the auxin-*CUC2* module. An example of such a dual system was recently described[39], in which a novel cytokinin-based signaling mechanism in the SAM that overlaps with the auxin inhibitory fields mechanism[40,41] and that is required to provide robustness to phyllotaxis. In the wild type, at a very low frequency, the auxin-inhibitory fields mechanism stochastically fails to produce lateral organs at the correct divergence angle. When the overlapping cytokinin mechanism is genetically broken by mutant alleles of the *ARABIDOPSIS HISTIDINE PHOSPHOTRANSFER PROTEIN6* (*AHP6*) gene, the frequency of incorrect angles increases. Random deviations from bilateral symmetry in the *CUC2* and auxin expression patterns, and in leaf shape, are also observed in the wild type, although at a very low frequency and severity. This is observed in all biological structures with bilateral symmetry and is called fluctuating asymmetry[42]. Reminiscent of the *ahp6* mutant, absence of *DEAL1* dramatically increases the frequency and severity of these deviant fluctuations.

The function of *DEAL1* paralogs

We found that *DEAL2* and *DEAL3* are functionally redundant with *DEAL1* in the leaf. The penetrance of the phenotype increased from 56% in the *deal1-1* single mutant to 86% in

the triple mutant. The *deal2-1* and *deal3-1* single mutants exhibit phenotypically wild-type leaves, suggesting that *DEAL2* and *DEAL3* contribute to margin development at a lower level than *DEAL1*. It is possible that these paralogs play a more prominent function in other organs. Supporting evidence for this role is based on the observation of developmental defects in *deal1* and *deal2* floral tissues and the detection of transcripts following RT-PCR assays on these organs. Among other defects, pistils exhibited open ovaries due to unfused carpels. Carpels are modified leaves that require CUC2 and auxin for their margins to fuse together[35], which supports the hypothesis that DEAL1 acts in concert with CUC2 and auxin in carpel morphogenesis. However, the frequency of flower organ morphological defects in *deal* single and multiple mutants is extremely low, making a comprehensive characterization of the phenotype impossible, and suggesting functional redundancy with other genes. We found that *DEAL4* is exclusively expressed in flowers, but we failed to isolate a loss-of-function allele from public collections. It is tempting to think that the function of this gene masks additional phenotypes in the flowers.

EXPERIMENTAL PROCEDURES

Plant material and culture conditions

Seeds of the *Arabidopsis thaliana* (L.) Heynh. wild-type accession Columbia-0 (Col-0) and SALK_047972C were obtained from the Arabidopsis Biological Resource Center (ABRC) and SALK_023737, SAIL_237_C09, SAK_099815, SAIL_140_H09 and *pin1-1* seeds, from the Nottingham Arabidopsis Stock Centre (NASC). T-DNA lines were backcrossed to Col-0 at least once before analyses. Other lines used in this work have been published previously: *CYCB1;1*$_{pro}$*:GUS*[43], *PIN1*$_{pro}$*:PIN1:GFP*[23], *DR5rev*$_{pro}$*:GFP*[24], *STM*$_{pro}$*:GUS*[44], *cuc2-3*[28], and *CUC2g-m4*[13]. The *CUC2*$_{pro}$*:CUC2:RFP* and *DR5rev*$_{pro}$*:VENUS* lines (unpublished) were kindly provided by Patrick Laufs. All analyses and crosses were done with the *deal1-1* and *deal1-3* alleles. Crosses involving the *CUC2g-m4* dominant allele and the transgenes encoding fluorescent markers were analyzed in F_3 *DEAL1*/*DEAL1* and *deal1*/*deal1* siblings. Three independent F_3 families of each genotype were analyzed to take into account transgene dose oscillations.

For standard leaf phenotype analyses, plants were cultured under sterile conditions on half-strength Murashige and Skoog (MS, Phytotechnology Laboratories) 0.65% agar medium with 1% sucrose at a density of 0.18 plants cm^{-2}. For flower organ morphological studies and plant propagation, plants were grown in a 1:2:2 moss:peat:vermiculite mixture. All cultures were maintained at 20°C, 60-70% relative humidity, under continuous fluorescent illumination of ≈ 80 µmol m^{-2} s^{-1}, as described previously[45]. NPA, IAA, and NAA (Sigma-Aldrich) were dissolved in dimethyl sulfoxide (DMSO). The final concentration of these compounds in MS medium is indicated in the results section. MS plates with the same DMSO concentration were used as controls. In the NPA and IAA treatments, seeds were sown in non-supplemented MS medium and then transferred to supplemented media 5 and 4 days after stratification (das), respectively.

Leaf, vasculature, and cell morphometry

Leaf morphometry was performed on fully expanded (35 das) tenth-node leaves, which were flattened between glass slides, photographed with a Nikon SMZ1500 stereomicroscope equipped with a Nikon DXM1200F digital camera, and converted to silhouettes. Leaf pictures were rotated until the imaginary line that cuts the leaf tip and the middle of the petiole (sagittal plane) was vertical. Consensus Col-0 leaf contours were obtained by overlapping 10 leaves and calculating the median of the stack image. Mutant leaf silhouettes were overlaid with the Col-0 contour for comparisons. To obtain the Leaf Symmetry Index (LSI), leaf silhouettes were horizontally folded along the sagittal plane, with left and right halves overlaid to obtain mirror images. Total leaf area (A_T) and non-overlapping area (A_{NO}) were measured using ImageJ 1.49v (National Institutes of Health, USA; http://imagej.nih.gov/ij/) and used to calculate LSI as $1 – (A_{NO} / A_T)$. The Leaf Dissection Index was calculated as described previously[7]. At least 10 leaves were analysed for each genotype studied. All image processing was done using Photoshop CS3 (Adobe).

Palisade mesophyll cells were used for all cell morphometric analyses. Leaves were collected and cleared with 70% ethanol for 24 h at 4°C and 16 M chloral hydrate for 7 days at room temperature. Microscopy of leaf tissues was performed using differential interference contrast optics on a Leica DMRB microscope equipped with a Nikon DXM1200F digital camera. Cells were extracted from photographs by drawing cell contours with Photoshop CS3 on a Cintiq 18SX Interactive Pen Display screen (Wacom). To reconstruct tissue areas larger than a single microscope field, digital images were joined together based on their XY microscope stage coordinates. Cell count, position, and area measurements were done with ImageJ 1.49v. Cell area heatmaps were created with Excel 2013 (Microsoft).

Leaf venation patterns were obtained as described previously[46]. Veins were manually drawn from micrographs using Photoshop CS3 on a Cintiq 18SX Interactive Pen Display screen. Skeletonization was done with ImageJ 1.49v and network parameter measurements were performed with the ImageJ plugin Analyze Skeleton

(https://github.com/fiji/AnalyzeSkeleton/)[47].

Leaf primordia GUS analyses

Leaf primordia were excised with a scalpel, perpendicularly to the shoot apical-basal axis, and placed in a drop of water on a microscope slide. All primordia were imaged using bright-field microscopy with a Nikon D-Eclipse C1 microscope equipped with a Nikon DS-Ri1 camera. GUS staining was performed as described previously[4]. X-Gluc buffer incubation times for *DEAL1$_{pro}$:GUS*, *CYCB1;1$_{pro}$:GUS*, and *STM$_{pro}$:GUS* were 4, 4, and 2 hours, respectively. Tissue was then processed as described above for cell morphometry analyses.

RNA isolation, cDNA synthesis, RT-PCR, and quantitative RT-PCR

Leaf primordia were collected 15 das, when they are just becoming visible. Roots, shoots, and leaves longer than 5 mm were excised to obtain plant material enriched in leaf primordia and immediately frozen in liquid nitrogen. Purification of total RNA was done using standard protocols as described previously[48]. Three different biological replicates were used in triplicate reactions. Relative quantification of gene expression data was performed using the $2^{-\Delta\Delta C_T}$ method[49,50]. The housekeeping gene *ACTIN2* (At3g18780) was used to normalize the expression levels in all RT- and qRT-PCR experiments. The PCR primers used in these experiments are listed in Table S2. A Mann-Whitney U test was used for mean ΔC_T statistical comparisons in qRT-PCR experiments.

Gene constructs and plant transformation

Gene constructs were engineered using Gateway Technology (Life Technologies), following the manufacturer's protocol, and mobilized into plants as described previously[51]. Transgene integrity in T_1 plants was verified by PCR. To generate the *DEAL1$_{pro}$:GUS* transgene, the intergenic region between Atg2g32275 and Atg2g32280 (TAIR10 chromosome 2, coordinates 13,710,358 to 13,713,209) was PCR amplified from Col-0

genomic DNA using At2g32280_attB primers (Table S2). The PCR product was cloned into the pMDC163 vector[52]. Col-0 and Col-5 *glabra-1* plants were transformed and T_1 transformants were selected on MS supplemented with 15 µg l^{-1} hygromycin B (Invitrogen). To construct the *35S$_{pro}$:DEAL1:CFP* transgene, a fragment of the At2g32280 cDNA that spanned the coding region (TAIR10 At2g32280 cDNA coordinates 170 to 664), was amplified using At2g32280_attB primers (Table S2) and cloned into the pEarleyGate102 vector[53]. The *deal1-1* plants were transformed and T_1 transformants were selected on sand watered with a 15 mg l^{-1} solution of BASTA (Finale; Bayer). The *AtWAK2$_{pro}$:YFP:HDEL* and *Man49$_{pro}$:YFP* constructs[30] were obtained from the ABRC (CD3-957 and CD3-965 stock numbers, respectively). *35S$_{pro}$:DEAL1:CFP* plants were transformed as previously described and transformant seeds were selected on MS supplemented with 50 mg l^{-1} kanamycin (Duchefa).

Confocal laser scanning microscopy

Confocal laser scanning microscopy images were obtained from a D-Eclipse C1 confocal microscope equipped with a DS-Ri1 camera and the EZ-C1 software (all components from Nikon). CFP was excited at 408 nm with a modulated diode laser and its emission collected with 450/35 and 515/30 nm wavelength/bandwidth filters. GFP and YFP were excited at 488 nm with an argon ion laser. Their emissions were detected at 515/30 and a combination of 515/30 and 605/75 nm filters, respectively. RFP and propidium iodide were excited with a 543 nm laser and detected with a 605/75 nm filter. To stain nuclei, we incubated *35S$_{pro}$:DEAL1:CFP* seedlings with a 10 mg ml^{-1} solution of propidium iodide (Sigma-Aldrich) for 30 min at room temperature. All images from a given GFP marker at a defined time point were taken using the same settings.

Split-ubiquitin yeast two-hybrid membrane-based protein localization assay

Split-ubiquitin Y2H membrane-based assay[31,32] was performed by Hybrigenics, S.A. (France) and used to test the co-localization of DEAL1 protein with several yeast proteins

with known subcellular localizations. In short, two membrane-associated proteins, used respectively as bait and prey, were fused to the N- and C-terminal halves of ubiquitin (Nub and Cub, respectively) and introduced in a *HIS3*$^-$ yeast strain. If the bait and the prey reside in the same cell membrane, Nub and Cub can re-associate and trigger an enzymatic cascade that activates *HIS3* transcription. The full-length coding sequence of At2g32280 was cloned into vector pB102, in-frame with Cub, coupled to the artificial transcription factor LexA. Preys were fused to Nub and expressed from the pPR3-N vector. Yeast strains NMY32-DeltaGal4 (mata) and YHGX13 (Y187 ade2-101::loxP-kanMX-loxP, mat$^-$) were used in these assays. Diploid cells were grown on DO-2 (-Trp -Leu) medium to check co-transformation with the prey and bait plasmids. The re-association of ubiquitin was assayed on DO-3 medium (-Trp -Leu -His). 20 mM of 3-aminotriazole (3-AT), a competitive inhibitor of the *HIS3* reporter gene product, was used to increase the stringency of the tests. Interaction assays were done in duplicate as two independent clones from each condition were picked for the growth assay.

ACKNOWLEDGEMENTS

The authors wish to thank their colleagues who provided seeds or plasmids: P. Laufs for *cuc2-3*, *CUC2g-m4* and *CUC2$_{pro}$:RFP DR5rev$_{pro}$:VENUS*; L. De Veylder for *CYCB1;1$_{pro}$:GUS*; W. Werr for *STM$_{pro}$:GUS*; and B. Scheres for the pGEM-T Easy221 vector. We also thank M.R. Ponce for useful discussions and the suggestion of the *DESIGUAL* gene name, and J.M. Serrano and J.M. Sánchez-Larrosa for their excellent technical assistance. This work was supported by grants from the Ministerio de Economía y Competitividad of Spain (BIO2011-22825 and BIO2014-53063-P) and the Generalitat Valenciana (PROMETEOII/2014/006) to JLM. SJG held the PIRG06-GA-2009-256579 (ARABIGANS) grant from the European Commission, and DWS the ACIF/2012/137 predoctoral fellowship from the Generalitat Valenciana (VALi+d program).

SUPPLEMENTARY INFORMATION

Figure S1. Molecular characterization of *deal1* mRNAs.

Figure S2. Length and asymmetry of *deal1* leaves.

Figure S3. Expression of class I KNOX genes in *deal1* leaves.

Figure S4. Effects of auxin on root growth in the *deal1-1* and *deal1-3* mutants.

Figure S5. Leaf venation pattern of the *deal1-1* mutant.

Figure S6. Correlation between the degree of dissection in Col-0 leaves and the severity of the asymmetry in *deal1-1* leaves across all rosette nodes.

Figure S7. Functional relationship between *DEAL1* and *CUC2*.

Figure S8. *In silico* prediction of the subcellular localization of the DEAL1 protein.

Figure S9. Expression analysis of *deal2-1* and *deal3-1*.

Table S1. Vascular parameters of *deal1-1* rosette leaves.

Table S2. PCR primers used in this work.

REFERENCES

1. Nicotra A. B.*, et al.* The evolution and functional significance of leaf shape in the angiosperms. *Funct. Plant Biol.* **38**, 535-552 (2011).
2. Byrne M. E.*, et al. Asymmetric leaves1* mediates leaf patterning and stem cell function in *Arabidopsis*. *Nature* **408**, 967-971 (2000).
3. Semiarti E.*, et al.* The *ASYMMETRIC LEAVES2* gene of *Arabidopsis thaliana* regulates formation of a symmetric lamina, establishment of venation and repression of meristem-related homeobox genes in leaves. *Development* **128**, 1771-1783 (2001).
4. Donnelly P. M., Bonetta D., Tsukaya H., Dengler R. E., Dengler N. G. Cell cycling and cell enlargement in developing leaves of *Arabidopsis*. *Dev. Biol.* **215**, 407-419 (1999).
5. Hay A., Tsiantis M. The genetic basis for differences in leaf form between *Arabidopsis thaliana* and its wild relative *Cardamine hirsuta*. *Nat. Genet.* **38**, 942-947 (2006).
6. Barkoulas M., Hay A., Kougioumoutzi E., Tsiantis M. A developmental framework for dissected leaf formation in the *Arabidopsis* relative *Cardamine hirsuta*. *Nat. Genet.* **40**, 1136-1141 (2008).
7. Bilsborough G. D.*, et al.* Model for the regulation of *Arabidopsis thaliana* leaf margin development. *Proc. Natl. Acad. Sci. USA* **108**, 3424-3429 (2011).
8. Hay A., Barkoulas M., Tsiantis M. *ASYMMETRIC LEAVES1* and auxin activities converge to repress *BREVIPEDICELLUS* expression and promote leaf development in *Arabidopsis*. *Development* **133**, 3955-3961 (2006).
9. Kasprzewska A.*, et al.* Auxin influx importers modulate serration along the leaf margin. *Plant J.* **83**, 705-718 (2015).
10. Heisler M. G.*, et al.* Patterns of auxin transport and gene expression during primordium development revealed by live imaging of the *Arabidopsis* inflorescence meristem. *Curr. Biol.* **15**, 1899-1911 (2005).

11. Scarpella E., Marcos D., Friml J., Berleth T. Control of leaf vascular patterning by polar auxin transport. *Genes Dev.* **20**, 1015-1027 (2006).

12. Paciorek T.*, et al.* Auxin inhibits endocytosis and promotes its own efflux from cells. *Nature* **435**, 1251-1256 (2005).

13. Nikovics K.*, et al.* The balance between the *MIR164A* and *CUC2* genes controls leaf margin serration in Arabidopsis. *Plant Cell* **18**, 2929-2945 (2006).

14. Kawamura E., Horiguchi G., Tsukaya H. Mechanisms of leaf tooth formation in *Arabidopsis*. *Plant J.* **62**, 429-441 (2010).

15. Larue C. T., Wen J., Walker J. C. A microRNA-transcription factor module regulates lateral organ size and patterning in *Arabidopsis*. *Plant J.* **58**, 450-463 (2009).

16. Chitwood D. H.*, et al.* Leaf asymmetry as a developmental constraint imposed by auxin-dependent phyllotactic patterning. *Plant Cell* **24**, 2318-2327 (2012).

17. Koenig D., Bayer E., Kang J., Kuhlemeier C., Sinha N. Auxin patterns *Solanum lycopersicum* leaf morphogenesis. *Development* **136**, 2997-3006 (2009).

18. Alonso J. M.*, et al.* Genome-wide insertional mutagenesis of *Arabidopsis thaliana*. *Science* **301**, 653-657 (2003).

19. Wilson-Sánchez D.*, et al.* Leaf phenomics: a systematic reverse genetic screen for Arabidopsis leaf mutants. *Plant J.* **79**, 878-891 (2014).

20. Roschzttardtz H.*, et al.* The *VASCULATURE COMPLEXITY AND CONNECTIVITY* gene encodes a plant-specific protein required for embryo provasculature development. *Plant Physiol.* **166**, 889-902 (2014).

21. Ha C. M.*, et al.* The *BLADE-ON-PETIOLE 1* gene controls leaf pattern formation through the modulation of meristematic activity in *Arabidopsis*. *Development* **130**, 161-172 (2003).

22. Mattsson J., Ckurshumova W., Berleth T. Auxin signaling in *Arabidopsis* leaf vascular development. *Plant Physiol.* **131**, 1327-1339 (2003).

23. Xu J.*, et al.* A molecular framework for plant regeneration. *Science* **311**, 385-388 (2006).

24. Friml J.*, et al.* Efflux-dependent auxin gradients establish the apical-basal axis of *Arabidopsis*. *Nature* **426**, 147-153 (2003).

25. Mattsson J., Sung Z. R., Berleth T. Responses of plant vascular systems to auxin transport inhibition. *Development* **126**, 2979-2991 (1999).

26. Sieburth L. E. Auxin is required for leaf vein pattern in *Arabidopsis*. *Plant Physiol.* **121**, 1179-1190 (1999).

27. Alonso-Peral M. M.*, et al.* The *HVE*/*CAND1* gene is required for the early patterning of leaf venation in *Arabidopsis*. *Development* **133**, 3755-3766 (2006).

28. Hibara K.*, et al. Arabidopsis CUP-SHAPED COTYLEDON3* regulates postembryonic shoot meristem and organ boundary formation. *Plant Cell* **18**, 2946-2957 (2006).

29. Schwacke R.*, et al.* ARAMEMNON, a novel database for *Arabidopsis* integral membrane proteins. *Plant Physiol.* **131**, 16-26 (2003).

30. Nelson B. K., Cai X., Nebenfuhr A. A multicolored set of in vivo organelle markers for co-localization studies in *Arabidopsis* and other plants. *Plant J.* **51**, 1126-1136 (2007).

31. Johnsson N., Varshavsky A. Split ubiquitin as a sensor of protein interactions in vivo. *Proc. Natl. Acad. Sci. USA* **91**, 10340-10344 (1994).

32. Stagljar I., Korostensky C., Johnsson N., te Heesen S. A genetic system based on split-ubiquitin for the analysis of interactions between membrane proteins in vivo. *Proc. Natl. Acad. Sci. USA* **95**, 5187-5192 (1998).

33. Gonçalves B.*, et al.* A conserved role for *CUP-SHAPED COTYLEDON* genes during ovule development. *Plant J.* **83**, 732-742 (2015).

34. Aida M., Ishida T., Fukaki H., Fujisawa H., Tasaka M. Genes involved in organ separation in Arabidopsis: an analysis of the *cup-shaped cotyledon* mutant. *Plant Cell* **9**, 841-857 (1997).

35. Kamiuchi Y., Yamamoto K., Furutani M., Tasaka M., Aida M. The *CUC1* and *CUC2* genes promote carpel margin meristem formation during *Arabidopsis* gynoecium development. *Front. Plant Sci.* **5**, 165 (2014).

36. Collaudin S., Mirabet V. Models to reconcile plant science and stochasticity. *Front. Plant Sci.* **5**, 643 (2014).

37. Friml J., Jones A. R. Endoplasmic reticulum: the rising compartment in auxin biology. *Plant Physiol.* **154**, 458-462 (2010).

38. Mravec J.*, et al.* Subcellular homeostasis of phytohormone auxin is mediated by the ER-localized PIN5 transporter. *Nature* **459**, 1136-1140 (2009).

39. Besnard F.*, et al.* Cytokinin signalling inhibitory fields provide robustness to phyllotaxis. *Nature* **505**, 417-421 (2014).

40. Reinhardt D.*, et al.* Regulation of phyllotaxis by polar auxin transport. *Nature* **426**, 255-260 (2003).

41. Sassi M., Vernoux T. Auxin and self-organization at the shoot apical meristem. *J. Exp. Bot.* **64**, 2579-2592 (2013).

42. Palmer A. R. Symmetry breaking and the evolution of development. *Science* **306**, 828-833 (2004).

43. Ferreira P. C.*, et al.* Developmental expression of the arabidopsis cyclin gene *cyc1At*. *Plant Cell* **6**, 1763-1774 (1994).

44. Kirch T., Simon R., Grunewald M., Werr W. The *DORNROSCHEN*/*ENHANCER OF SHOOT REGENERATION1* gene of *Arabidopsis* acts in the control of meristem cell fate and lateral organ development. *Plant Cell* **15**, 694-705 (2003).

45. Ponce M. R., Quesada V., Micol J. L. Rapid discrimination of sequences flanking and within T-DNA insertions in the *Arabidopsis* genome. *Plant J.* **14**, 497-501 (1998).

46. Candela H., Martínez-Laborda A., Micol J. L. Venation pattern formation in *Arabidopsis thaliana* vegetative leaves. *Dev. Biol.* **205**, 205-216 (1999).

47. Arganda-Carreras I., Fernández-González R., Muñoz-Barrutia A., Ortiz-De-Solorzano C. 3D reconstruction of histological sections: Application to mammary gland tissue. *Microsc. Res. Tech.* **73**, 1019-1029 (2010).

48. Sánchez-García A. B., Aguilera V., Micol-Ponce R., Jover-Gil S., Ponce M. R. Arabidopsis *MAS2*, an essential gene that encodes a homolog of animal NF-kappa B activating protein, is Iinvolved in 45S ribosomal DNA silencing. *Plant Cell* **27**, 1999-2015 (2015).

49. Livak K. J., Schmittgen T. D. Analysis of relative gene expression data using real-time quantitative PCR and the 2(-Delta Delta C(T)) method. *Methods* **25**, 402-408 (2001).

50. Schmittgen T. D., Livak K. J. Analyzing real-time PCR data by the comparative C(T) method. *Nat. Protoc.* **3**, 1101-1108 (2008).

51. Clough S. J., Bent A. F. Floral dip: a simplified method for *Agrobacterium*-mediated transformation of *Arabidopsis thaliana*. *Plant J.* **16**, 735-743 (1998).

52. Curtis M. D., Grossniklaus U. A gateway cloning vector set for high-throughput functional analysis of genes in planta. *Plant Physiol.* **133**, 462-469 (2003).

53. Earley K. W.*, et al.* Gateway-compatible vectors for plant functional genomics and proteomics. *Plant J.* **45**, 616-629 (2006).

FIGURE LEGENDS

Figure 1. Leaf phenotypes and molecular nature of the *deal1* mutations.

(A, B) Leaves of (A) the Col-0 wild type and (B) the *deal1-1* mutant.

(C, D) Leaves of F1 plants derived from (C) SALK_047972 × SALK_023737 and (D) SALK_047972 × SAIL_237_C09 crosses, showing that the *deal1-1*, *deal1-2*, and *deal1-3* mutations do not complement each other.

(E) Phenotypically wild-type *deal1-1* $35S_{pro}$*:DEAL1:CFP* leaf, showing rescue of the mutant phenotype of *deal1-1* by the wild-type allele of At2g32280.

(F) *DEAL1* gene structure with indication of the position of the mutations studied in this work. Exons are represented by boxes, introns by lines between boxes, and T-DNA insertions by triangles. Open boxes correspond to untranslated regions.

Pictures (A-E) show the abaxial side of tenth-node rosette leaves. Scale bars: (A-E) 2 mm. Pictures were taken 25 days after stratification (das).

Figure 2. Morphological characterization of *deal1-1* leaves.

(A) Consensus outline (in black; see Methods) of Col-0 tenth-node rosette leaves (n = 10) overlaid to the silhouette (in grey) of a *deal1-1* tenth-node leaf showing (lo) an ectopic lobe and (si) an ectopic sinus.

(B, C) Detail of extreme examples of (B) ectopic sinus and (C) ectopic lobe, both highlighted by an asterisk.

(D) From the top to the bottom, successive steps in leaf silhouette processing in order to obtain the areas used to calculate the Leaf Symmetry Index (LSI = 1 – [A_{NO} / A_T]). SP: sagittal plane. Lm-l: left mediolateral axis. Rm-l: right mediolateral axis. A_T: total area. A_{NO}: non-overlapping area.

(E) LSI values of rosette leaves from the first to the fourteenth node (leaves 1 to 14) from Col-0 and the *deal1-1* mutant (n = 10).

(F) LSI values of tenth-node rosette leaf apical and basal halves from Col-0 and *deal1-1* (n = 10).

(G) Penetrance of the leaf phenotype of *deal1-1*.

Scale bars: (A) 4 mm and (B, C) 1 mm. Pictures were taken after full leaf expansion (35 das). Error bars indicate standard deviations. Asterisks indicate values significantly different from the corresponding wild type in a Mann-Whitney U-test (*$p < 0.05$, **$p < 0.01$, n = 10).

Figure 3. Leaf cell proliferation and growth in the *deal1-1* mutant.

(A-G) Defective patterning in proliferating tissues of *deal1-1* leaf primordia. Similar results were obtained with *deal1-2* and *deal1-3*. (A, B, E, F) Excised leaf primordia from (A, E) Col-0 and (B, F) *deal1-1*. (C, D, G) Magnification of areas framed in B and F, showing proliferating undifferentiated protodermal cells.

(H-J) *CYCB1;1$_{pro}$:GUS* expression in (H) Col-0 and (I, J) *deal1-1* leaves. (J) Detail of strong GUS staining in a group of marginal cells of a *deal1-1 CYCB1;1$_{pro}$:GUS* leaf.

(K) Cell size heatmaps of Col-0 and an asymmetric *deal1-1* leaf. Numbers represent leaf regions with equivalent cell sizes. Each heatmap unit represents 1/16 mm^2.

Scale bars: (A, B, E, F, H, I) 100, (J) 40 and (C, D, G) 20 µm. Pictures and measurements were taken from tenth-node leaves collected (A-J) 14 das, and (K) after full expansion (35 das).

Figure 4. *DEAL1* expression analysis in *DEAL1$_{pro}$:GUS* transgenic plants in a Col-0 background.

(A-D) GUS staining in tenth-node developing leaves collected at the time shown.

(E, F) GUS staining fade-out coinciding with the transition from proliferative to differentiated tissue. a: apical. b: basal. m: differentiated margin cell.

(G) Emerging axillary shoots with developing flowers showing GUS staining.

(H, I) GUS-stained vascular tissues in (H) a fully-expanded third-node leaf and (I) a root.

Pictures were taken (E, F, I) 10, (G) 45 and (H) 25 das. Scale bars: (A, I) 50 µm, (B-D, G) 100 µm, (E, F) 10 µm, and (H) 1 mm.

Figure 5. Effects of pharmacological treatments, genetic interactions and auxin spatial distribution of the *deal1-1* mutant.

(A-D) Abnormal leaf margin in *deal1-1* plants. (A-C) Ectopic lamina emerging from (A) the base of the lamina and (B, C) the petiole of *deal1-1* leaves. (D) Normal vascular differentiation in a *deal1-1* ectopic lobe. In the drawing, veins are shown in red and the leaf margin in blue.

(E, F) Effects of NPA on the (E) penetrance and (F) severity of the phenotype of *deal1-1*.

(G-J) Leaf phenotypes of (G) Col-0, the (H) *deal1-1* and (I) *pin1-1* single mutants, and (J) the *deal1-1 pin1-1* double mutant.

(K, L) Effects of NAA on the (H) penetrance and (I) severity of the phenotype of *deal1-1*.

(M, N) PIN1:GFP membrane localization in marginal cells of Col-0 and *deal1-1* leaf primordia developing serrations.

(O, P) $PIN1_{pro}$*:PIN1:GFP* expression pattern in (O) Col-0 and (P) *deal1-1* leaf primordia.

(Q-S) $DR5rev_{pro}$*:GFP* expression pattern in (Q) Col-0 and (R, S) *deal1-1* leaf primordia. m: misplaced auxin maximum coinciding with a sinus. n: different number of maxima at each side of the leaf. si: maximum of abnormal size. sh: maximum of abnormal shape.

All rosette leaves studied (A-L) were excised from the tenth node. Primordia (M-S) correspond to any node from the eighth to the twelfth; these nodes are extremely difficult to distinguish to each other at their early stages of development. Pictures were taken (A-D, G-J) 30 and (M-S) 14 das. Scale bars: (A-D) 1 mm, (G-J) 2 mm, (M, N) 15 µm, (O, P) 50 µm, and (Q-S) 100 µm. Error bars indicate standard deviations. Asterisks indicate values significantly different from the corresponding control in a Mann-Whitney U-test (*$p < 0.05$, n = 10).

Figure 6. Genetic interactions between *DEAL1* and *CUC2*.

(A, B) Leaf phenotypes caused by the *deal1-1* and *cuc2-3* loss-of-function mutations, the *CUC2g-m4* excess-of-function mutation, and their genetic combinations. The (A) penetrance and (B) severity of the phenotypes of the single and double mutants is shown.

(C) Representative leaf silhouettes of the genotypes analyzed in (A) and (B).

(D, E) Expression patterns of the *CUC2$_{pro}$:CUC2:RFP* (red) and *DR5rev$_{pro}$:VENUS* (greenish yellow) markers in Col-0 and *deal1-3* leaf primordia. (E1) Consecutive CUC2:RFP-positive patches abnormally close. (E2) Consecutive CUC2:RFP-positive patches abnormally far apart.

All fully expanded rosette leaves studied (A-C) were excised from the tenth node. The primordia shown in (D, E) correspond to any node from the eighth to the twelfth. Leaves were collected (A-C) 35 and (D, E) 14 das. Scale bars: (C) 2 mm and (D, E) 50 µm. Error bars indicate standard deviations. Asterisks indicate values significantly different from that of the *deal1-1* single mutant in a Mann-Whitney U-test (*$p < 0.05$, n = 10).

Figure 7. Subcellular localization of the DEAL1 protein.

(A, B) Root cells expressing *35S$_{pro}$:DEAL1:CFP* (DEAL1, blue) stained with propidium iodide (PI, red) to mark the nuclei and plasma membranes.

(C, D) Cells expressing *35S$_{pro}$:DEAL1:CFP* (DEAL1, blue), and the Golgi marker *35S$_{pro}$:Man49:YFP* (Golgi, yellow).

(E-G) Cell expressing *35S$_{pro}$:DEAL1:CFP* [blue in (E) and cyan in (G)], and the ER marker *35S$_{pro}$:AtWAK2:YFP:HDEL* [red in (F) and green in (G)]. (G) Partial overlap between YFP and CFP signals in ER cisternae-like structures.

(H-J) Cell expressing the same markers as in (E-G) showing contiguous signals of YFP and CFP.

Pictures in (A-J) were taken 10 das. Scale bars: (A) 20 µm and (B-J) 2 µm.

(K) Split-ubiquitin Y2H membrane-based localization assay. Yeast growth indicates membrane colocalization of the prey and bait proteins (see Methods). Nub: N-terminal half of ubiquitin. Cub: C-terminal half of ubiquitin. Alg5, Ost1, Fur4 and Tom20 are the names of the yeast proteins used in the assay. ER: endoplasmic reticulum. PM: plasma membrane. M: mitochondria. DO-2: Selective medium for co-transformation with the bait and prey plasmids. DO-3: Selective medium for ubiquitin re-association. 3-AT: 3-Aminotriazole. Alg5

homodimerization was used as a positive control for ubiquitin re-association.

Figure 8. Functional analysis of *DEAL1* paralogs.

(A) Gene structure of members of the *DEAL* gene family with indication of the mutations (T-DNA insertions, shown as triangles) studied in this work. The conserved DUF1218 domain is shown in blue. Arrows indicate the position of the primers used in (B), which are not drawn to scale.

(B) Semiquantitative RT-PCR expression analysis of the *DEAL1*, *DEAL2* (At421310), *DEAL3* (At1g11500), and *DEAL4* (At1g05291) genes in different plant tissues. I: inflorescences. ML: mature tenth-node leaves. DL: developing eighth- to twelfth-node leaves. R: roots. Two biological replicates are shown for each gene and tissue combination. The house-keeping gene *ACTIN2* (*ACT2*) was used as control. The primers used are listed in Table S2.

(C, D) Effects of NPA and NAA on the (C) penetrance and (D) severity (LSI) of the *deal* mutants. Blue asterisks indicate values obtained from untreated plants that were significantly different from those of the *deal1-3* single mutant. Red and green asterisks indicate values obtained from treated plants that were significantly different from those of the corresponding controls (untreated plants of the same genotype). A Mann-Whitney U-test was applied (*$p < 0.05$, **$p < 0.01$, n = 10).

(E, F) Abnormal ovaries of *deal1-1* and *deal2-1* plants. Scale bars: 0.5 mm.

(G) Quantification of abnormal siliques in the *deal* single and triple mutants.

Wilson-Sánchez *et al*., Figure 1

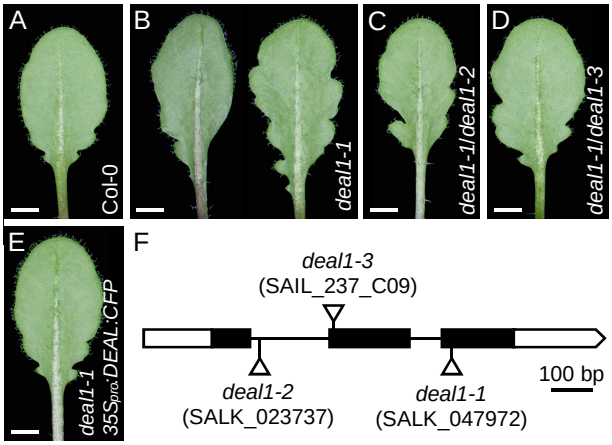

Figure 1. Leaf phenotypes and molecular nature of the *deal1* mutations.
(A, B) Leaves of (A) the Col-0 wild type and (B) the *deal1-1* mutant.
(C, D) Leaves of F1 plants derived from (C) SALK_047972 × SALK_023737 and (D) SALK_047972 × SAIL_237_C09 crosses, showing that the *deal1-1*, *deal1-2*, and *deal1-3* mutations do not complement each other.
(E) Phenotypically wild-type *deal1-1* $35S_{pro}$*:DEAL1:CFP* leaf, showing rescue of the mutant phenotype of *deal1-1* by the wild-type allele of At2g32280.
(F) *DEAL1* gene structure with indication of the position of the mutations studied in this work. Exons are represented by boxes, introns by lines between boxes, and T-DNA insertions by triangles. Open boxes correspond to untranslated regions.
Pictures (A-E) show the abaxial side of tenth-node rosette leaves. Scale bars: (A-E) 2 mm. Pictures were taken 25 days after stratification (das).

Wilson-Sánchez *et al*., Figure 2

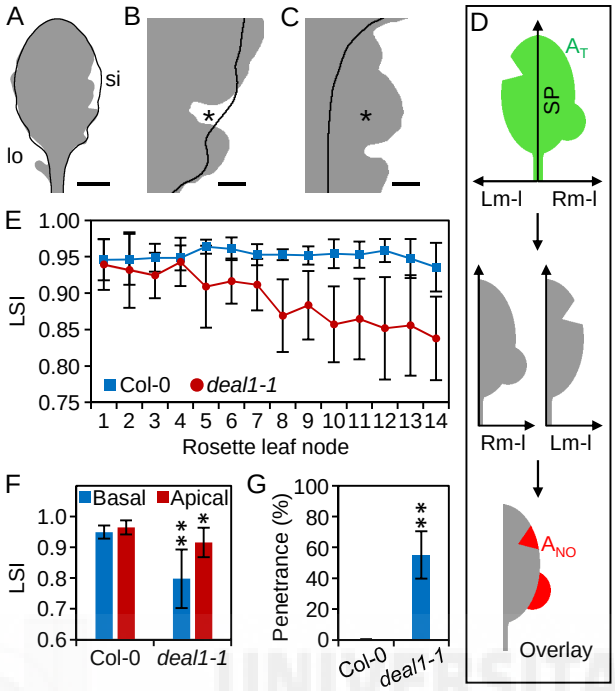

Figure 2. Morphological characterization of *deal1-1* leaves.
(A) Consensus outline (in black; see Methods) of Col-0 tenth-node rosette leaves (n = 10) overlaid to the silhouette (in grey) of a *deal1-1* tenth-node leaf showing (lo) an ectopic lobe and (si) an ectopic sinus.
(B, C) Detail of extreme examples of (B) ectopic sinus and (C) ectopic lobe, both highlighted by an asterisk.
(D) From the top to the bottom, successive steps in leaf silhouette processing in order to obtain the areas used to calculate the Leaf Symmetry Index (LSI = 1 – [A_{NO} / A_T]). SP: sagittal plane. Lm-l: left mediolateral axis. Rm-l: right mediolateral axis. A_T: total area. A_{NO}: non-overlapping area.
(E) LSI values of rosette leaves from the first to the fourteenth node (leaves 1 to 14) from Col-0 and the *deal1-1* mutant (n = 10).
(F) LSI values of tenth-node rosette leaf apical and basal halves from Col-0 and *deal1-1* (n = 10).
(G) Penetrance of the leaf phenotype of *deal1-1*.
Scale bars: (A) 4 mm and (B, C) 1 mm. Pictures were taken after full leaf expansion (35 das). Error bars indicate standard deviations. Asterisks indicate values significantly different from the corresponding wild type in a Mann-Whitney U-test (*$p < 0.05$, **$p < 0.01$, n = 10).

Wilson-Sánchez *et al.*, Figure 3

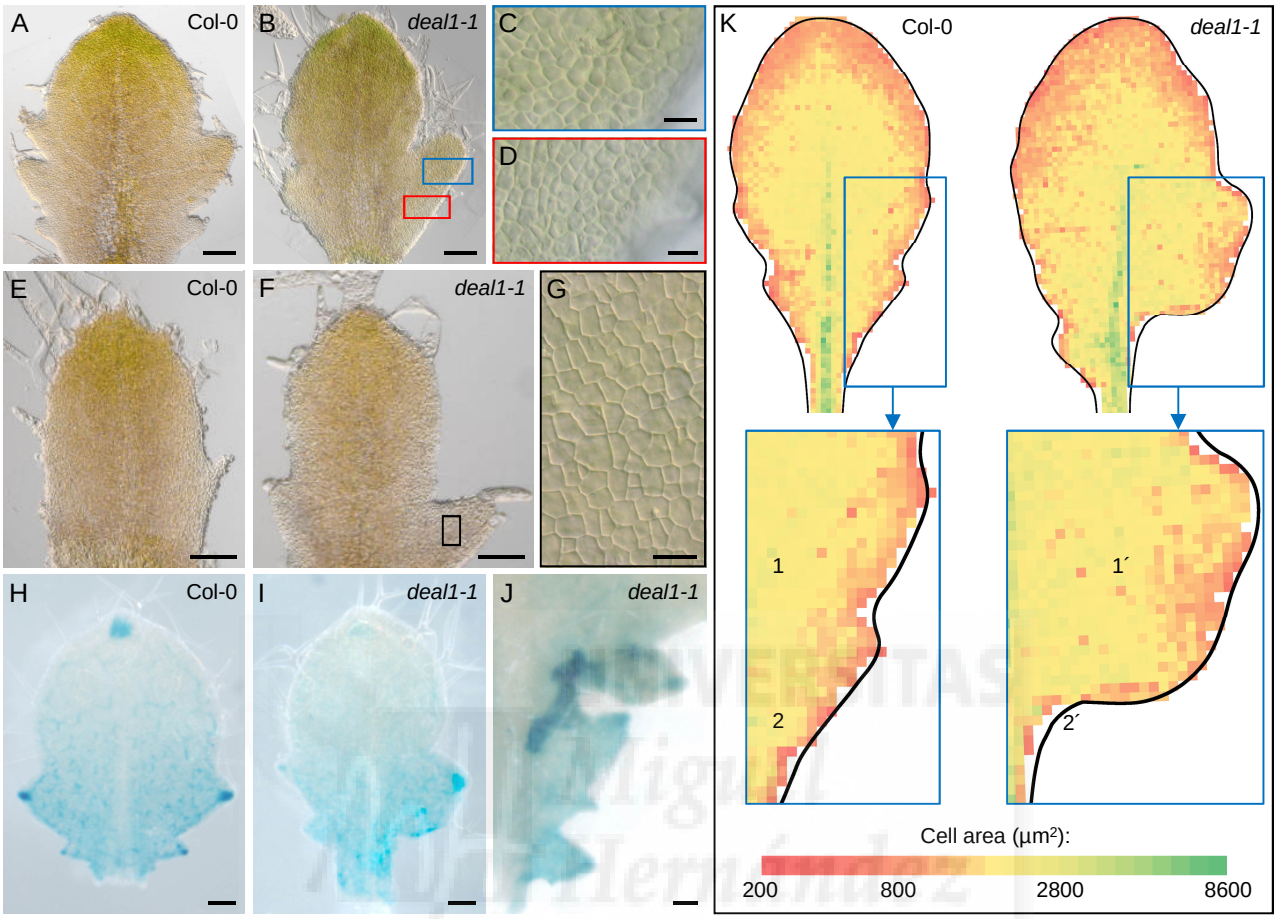

Figure 3. Leaf cell proliferation and growth in the *deal1-1* mutant.
(A-G) Defective patterning in proliferating tissues of *deal1-1* leaf primordia. Similar results were obtained with *deal1-2* and *deal1-3*. (A, B, E, F) Excised leaf primordia from (A, E) Col-0 and (B, F) *deal1-1*. (C, D, G) Magnification of areas framed in B and F, showing proliferating undifferentiated protodermal cells.
(H-J) *CYCB1;1*$_{pro}$*:GUS* expression in (H) Col-0 and (I, J) *deal1-1* leaves. (J) Detail of strong GUS staining in a group of marginal cells of a *deal1-1 CYCB1;1*$_{pro}$*:GUS* leaf.
(K) Cell size heatmaps of Col-0 and an asymmetric *deal1-1* leaf. Numbers represent leaf regions with equivalent cell sizes. Each heatmap unit represents 1/16 mm^2.
Scale bars: (A, B, E, F, H, I) 100, (J) 40 and (C, D, G) 20 µm. Pictures and measurements were taken from tenth-node leaves collected (A-J) 14 das, and (K) after full expansion (35 das).

Wilson-Sánchez *et al*., Figure 4

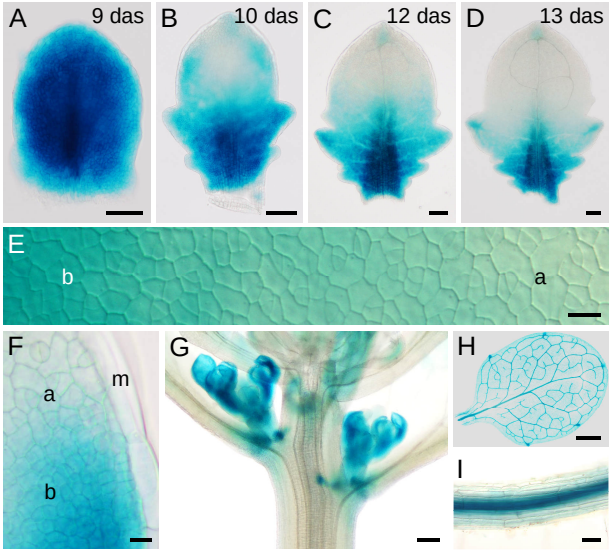

Figure 4. *DEAL1* expression analysis in *DEAL1*$_{pro}$*:GUS* transgenic plants in a Col-0 background.
(A-D) GUS staining in tenth-node developing leaves collected at the time shown.
(E, F) GUS staining fade-out coinciding with the transition from proliferative to differentiated tissue. a: apical. b: basal. m: differentiated margin cell.
(G) Emerging axillary shoots with developing flowers showing GUS staining.
(H, I) GUS-stained vascular tissues in (H) a fully-expanded third-node leaf and (I) a root.
Pictures were taken (E, F, I) 10, (G) 45 and (H) 25 das. Scale bars: (A, I) 50 µm, (B-D, G) 100 µm, (E, F) 10 µm, and (H) 1 mm.

Wilson-Sánchez *et al.*, Figure 5

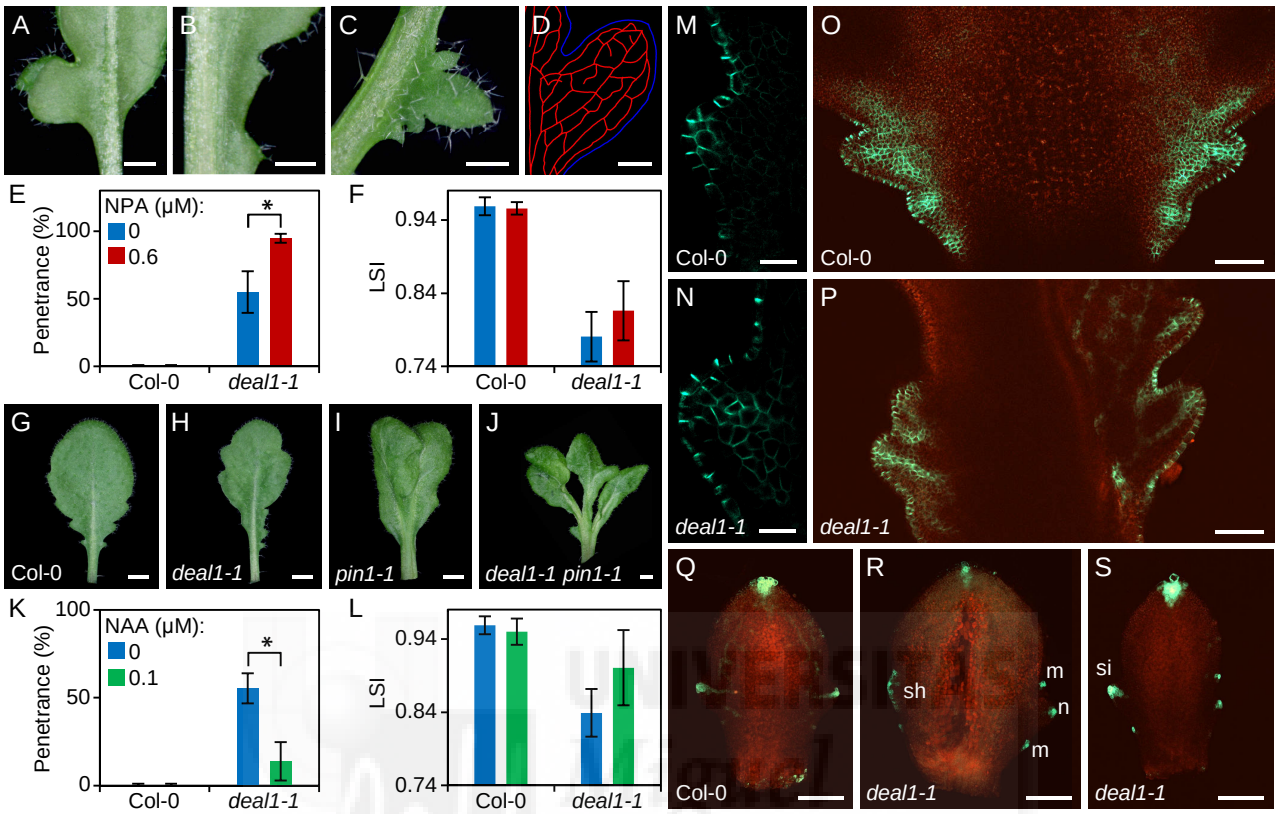

Figure 5. Effects of pharmacological treatments, genetic interactions and auxin spatial distribution of the *deal1-1* mutant.

(A-D) Abnormal leaf margin in *deal1-1* plants. (A-C) Ectopic lamina emerging from (A) the base of the lamina and (B, C) the petiole of *deal1-1* leaves. (D) Normal vascular differentiation in a *deal1-1* ectopic lobe. In the drawing, veins are shown in red and the leaf margin in blue.

(E, F) Effects of NPA on the (E) penetrance and (F) severity of the phenotype of *deal1-1*.

(G-J) Leaf phenotypes of (G) Col-0, the (H) *deal1-1* and (I) *pin1-1* single mutants, and (J) the *deal1-1 pin1-1* double mutant.

(K, L) Effects of NAA on the (H) penetrance and (I) severity of the phenotype of *deal1-1*.

(M, N) PIN1:GFP membrane localization in marginal cells of Col-0 and *deal1-1* leaf primordia developing serrations.

(O, P) $PIN1_{pro}$*:PIN1:GFP* expression pattern in (O) Col-0 and (P) *deal1-1* leaf primordia.

(Q-S) $DR5rev_{pro}$*:GFP* expression pattern in (Q) Col-0 and (R, S) *deal1-1* leaf primordia. m: misplaced auxin maximum coinciding with a sinus. n: different number of maxima at each side of the leaf. si: maximum of abnormal size. sh: maximum of abnormal shape.

All rosette leaves studied (A-L) were excised from the tenth node. Primordia (M-S) correspond to any node from the eighth to the twelfth; these nodes are extremely difficult to distinguish to each other at their early stages of development. Pictures were taken (A-D, G-J) 30 and (M-S) 14 das. Scale bars: (A-D) 1 mm, (G-J) 2 mm, (M, N) 15 µm, (O, P) 50 µm, and (Q-S) 100 µm. Error bars indicate standard deviations. Asterisks indicate values significantly different from the corresponding control in a Mann-Whitney U-test (*$p < 0.05$, n = 10).

Wilson-Sánchez *et al.*, Figure 6

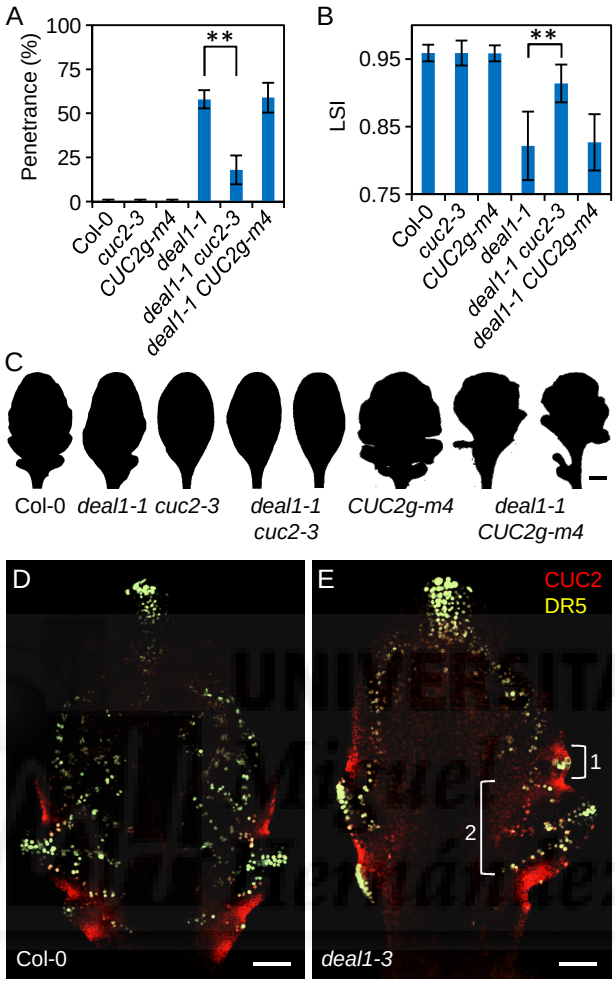

Figure 6. Genetic interactions between *DEAL1* and *CUC2*.
(A, B) Leaf phenotypes caused by the *deal1-1* and *cuc2-3* loss-of-function mutations, the *CUC2g-m4* excess-of-function mutation, and their genetic combinations. The (A) penetrance and (B) severity of the phenotypes of the single and double mutants is shown.
(C) Representative leaf silhouettes of the genotypes analyzed in (A) and (B).
(D, E) Expression patterns of the $CUC2_{pro}$*:CUC2:RFP* (red) and $DR5rev_{pro}$*:VENUS* (greenish yellow) markers in Col-0 and *deal1-3* leaf primordia. (E1) Consecutive CUC2:RFP-positive patches abnormally close. (E2) Consecutive CUC2:RFP-positive patches abnormally far apart.
All fully expanded rosette leaves studied (A-C) were excised from the tenth node. The primordia shown in (D, E) correspond to any node from the eighth to the twelfth. Leaves were collected (A-C) 35 and (D, E) 14 das. Scale bars: (C) 2 mm and (D, E) 50 µm. Error bars indicate standard deviations. Asterisks indicate values significantly different from that of the *deal1-1* single mutant in a Mann-Whitney U-test (*$p < 0.05$, n = 10).

Wilson-Sánchez *et al*., Figure 7

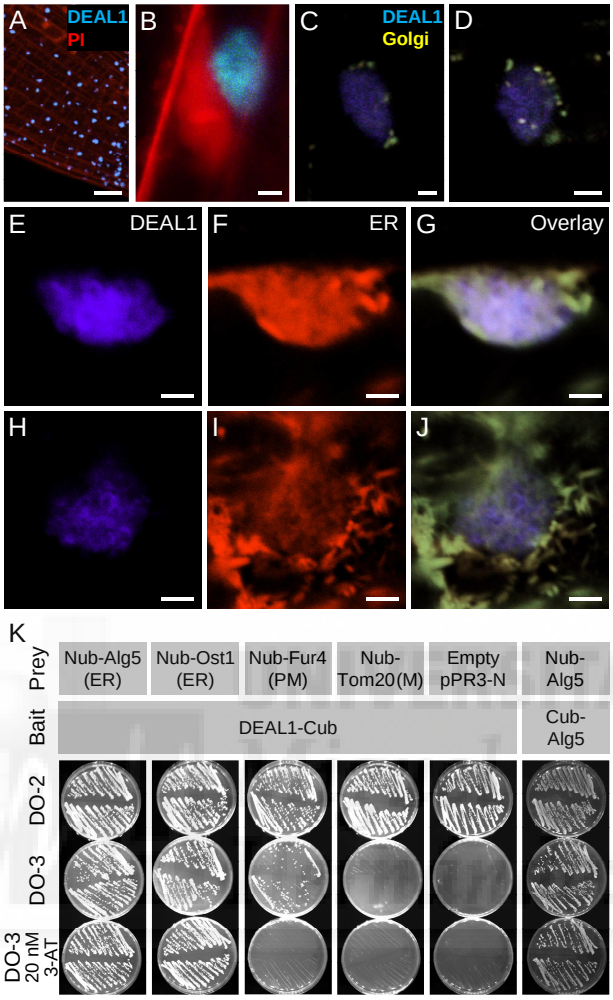

Figure 7. Subcellular localization of the DEAL1 protein.
(A, B) Root cells expressing *35S$_{pro}$:DEAL1:CFP* (DEAL1, blue) stained with propidium iodide (PI, red) to mark the nuclei and plasma membranes.
(C, D) Cells expressing *35S$_{pro}$:DEAL1:CFP* (DEAL1, blue), and the Golgi marker *35S$_{pro}$:Man49:YFP* (Golgi, yellow).
(E-G) Cell expressing *35S$_{pro}$:DEAL1:CFP* [blue in (E) and cyan in (G)], and the ER marker *35S$_{pro}$:AtWAK2:YFP:HDEL* [red in (F) and green in (G)]. (G) Partial overlap between YFP and CFP signals in ER cisternae-like structures.
(H-J) Cell expressing the same markers as in (E-G) showing contiguous signals of YFP and CFP. Pictures in (A-J) were taken 10 das. Scale bars: (A) 20 µm and (B-J) 2 µm.
(K) Split-ubiquitin Y2H membrane-based localization assay. Yeast growth indicates membrane colocalization of the prey and bait proteins (see Methods). Nub: N-terminal half of ubiquitin. Cub: C-terminal half of ubiquitin. Alg5, Ost1, Fur4 and Tom20 are the names of the yeast proteins used in the assay. ER: endoplasmic reticulum. PM: plasma membrane. M: mitochondria. DO-2: Selective medium for co-transformation with the bait and prey plasmids. DO-3: Selective medium for ubiquitin re-association. 3-AT: 3-Aminotriazole. Alg5 homodimerization was used as a positive control for ubiquitin re-association.

Wilson-Sánchez *et al.*, Figure 8

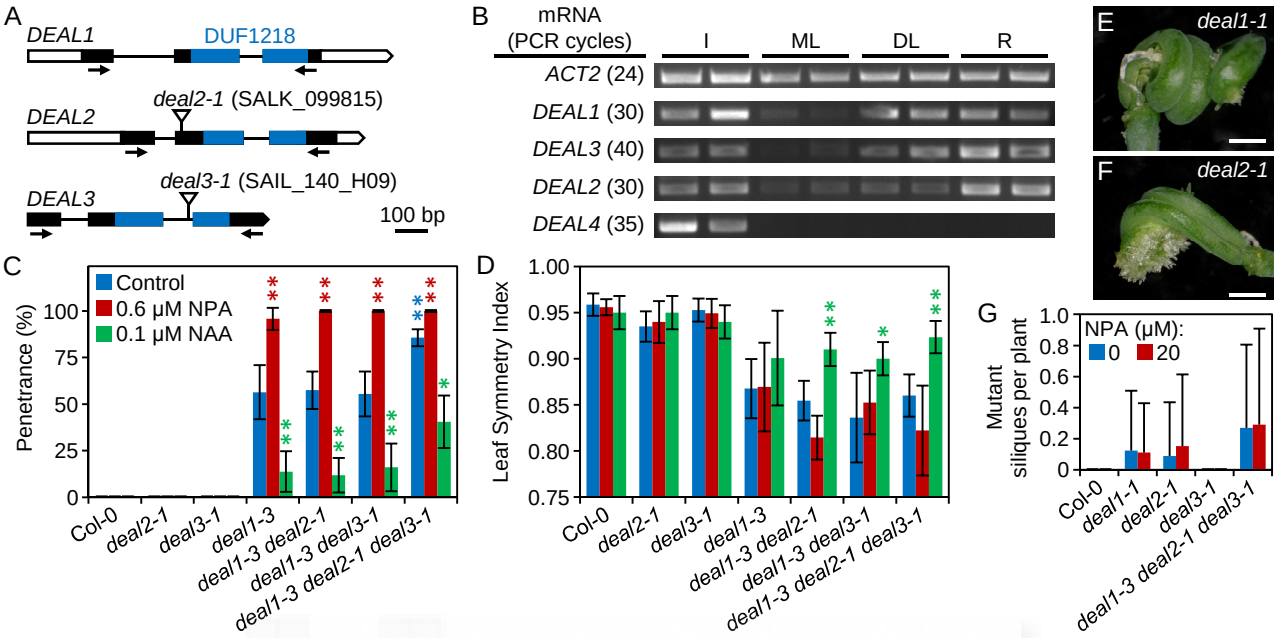

Figure 8. Functional analysis of *DEAL1* paralogs.
(A) Gene structure of members of the *DEAL* gene family with indication of the mutations (T-DNA insertions, shown as triangles) studied in this work. The conserved DUF1218 domain is shown in blue. Arrows indicate the position of the primers used in (B), which are not drawn to scale.
(B) Semiquantitative RT-PCR expression analysis of the *DEAL1*, *DEAL2* (At421310), *DEAL3* (At1g11500), and *DEAL4* (At1g05291) genes in different plant tissues. I: inflorescences. ML: mature tenth-node leaves. DL: developing eighth- to twelfth-node leaves. R: roots. Two biological replicates are shown for each gene and tissue combination. The house-keeping gene *ACTIN2* (*ACT2*) was used as control. The primers used are listed in Table S2.
(C, D) Effects of NPA and NAA on the (C) penetrance and (D) severity (LSI) of the *deal* mutants. Blue asterisks indicate values obtained from untreated plants that were significantly different from those of the *deal1-3* single mutant. Red and green asterisks indicate values obtained from treated plants that were significantly different from those of the corresponding controls (untreated plants of the same genotype). A Mann-Whitney U-test was applied (*$p < 0.05$, **$p < 0.01$, n = 10).
(E, F) Abnormal ovaries of *deal1-1* and *deal2-1* plants. Scale bars: 0.5 mm.
(G) Quantification of abnormal siliques in the *deal* single and triple mutants.

Role of *DESIGUAL1* and auxin in bilateral symmetry of Arabidopsis leaves

David Wilson-Sánchez, Sebastián Martínez-López, Sara Jover-Gil, and José Luis Micol

Supplementary material

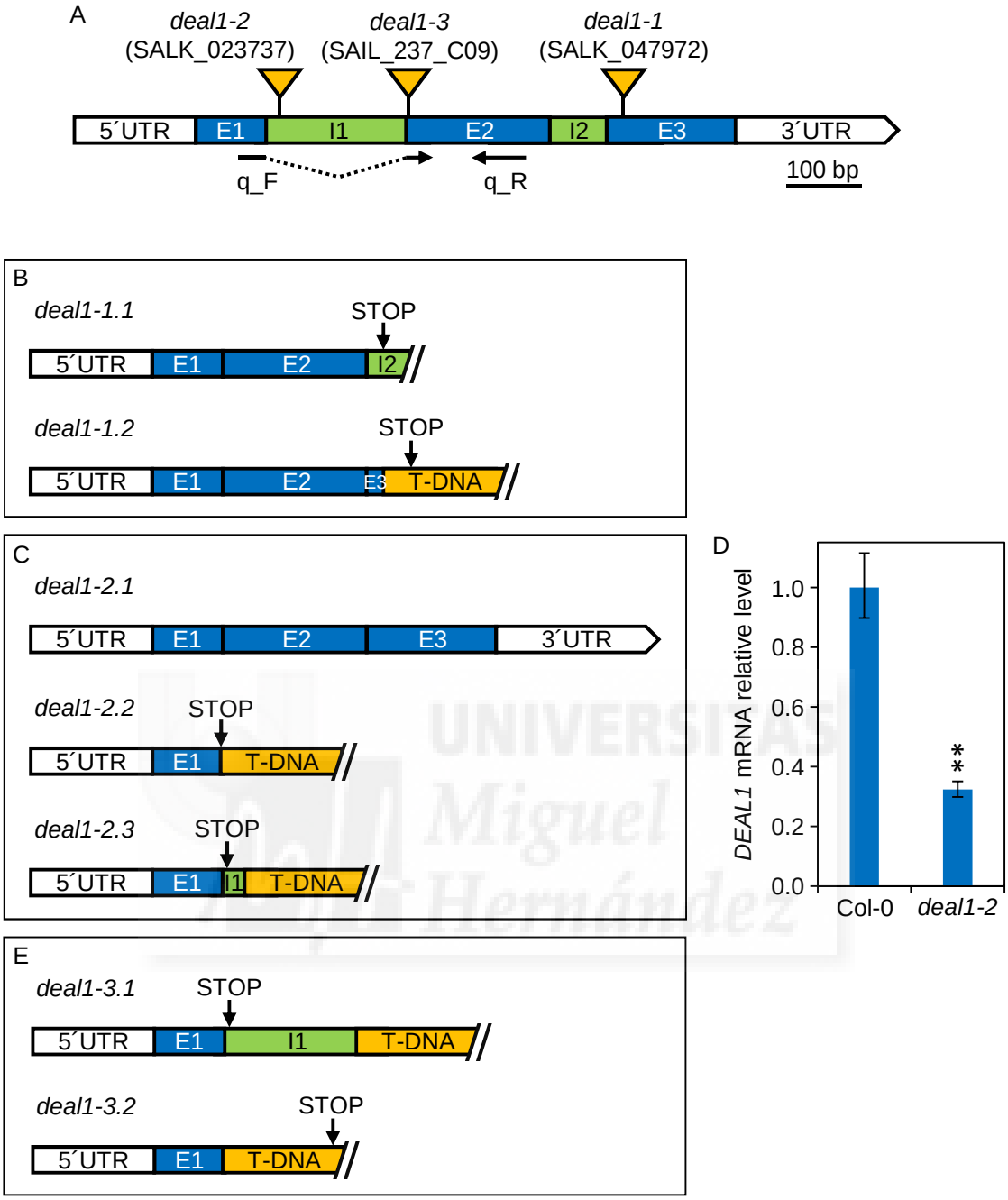

Figure S1. Molecular characterization of *deal1* mRNAs.
(A) *DEAL1* gene structure with indication of the position of the T-DNA insertions carried by the *deal1* alleles (triangles). Arrows represent the primers used to analyze the *deal1-2* transcripts shown in (C), which are not drawn to scale. E: exon. I: intron.
(B-D) Structure of the *DEAL1* mRNAs detected in the (B) *deal1-1*, (C) *deal1-2* and (D) *deal1-3* mutants. More than one transcript was found in the three mutants. The presence of intronic and T-DNA sequences in the aberrant mature mRNAs is due to missplicing. STOP: premature stop codon.
(E) Expression of the *deal1-2.1* wild-type mRNA variant detected in the *deal1-2* mutant. Error bars in this and all other Supplementary Figures indicate standard deviation. Asterisks indicate values significantly different from Col-0 in a Mann-Whitney U-test (**$p < 0.01$, n = 9).

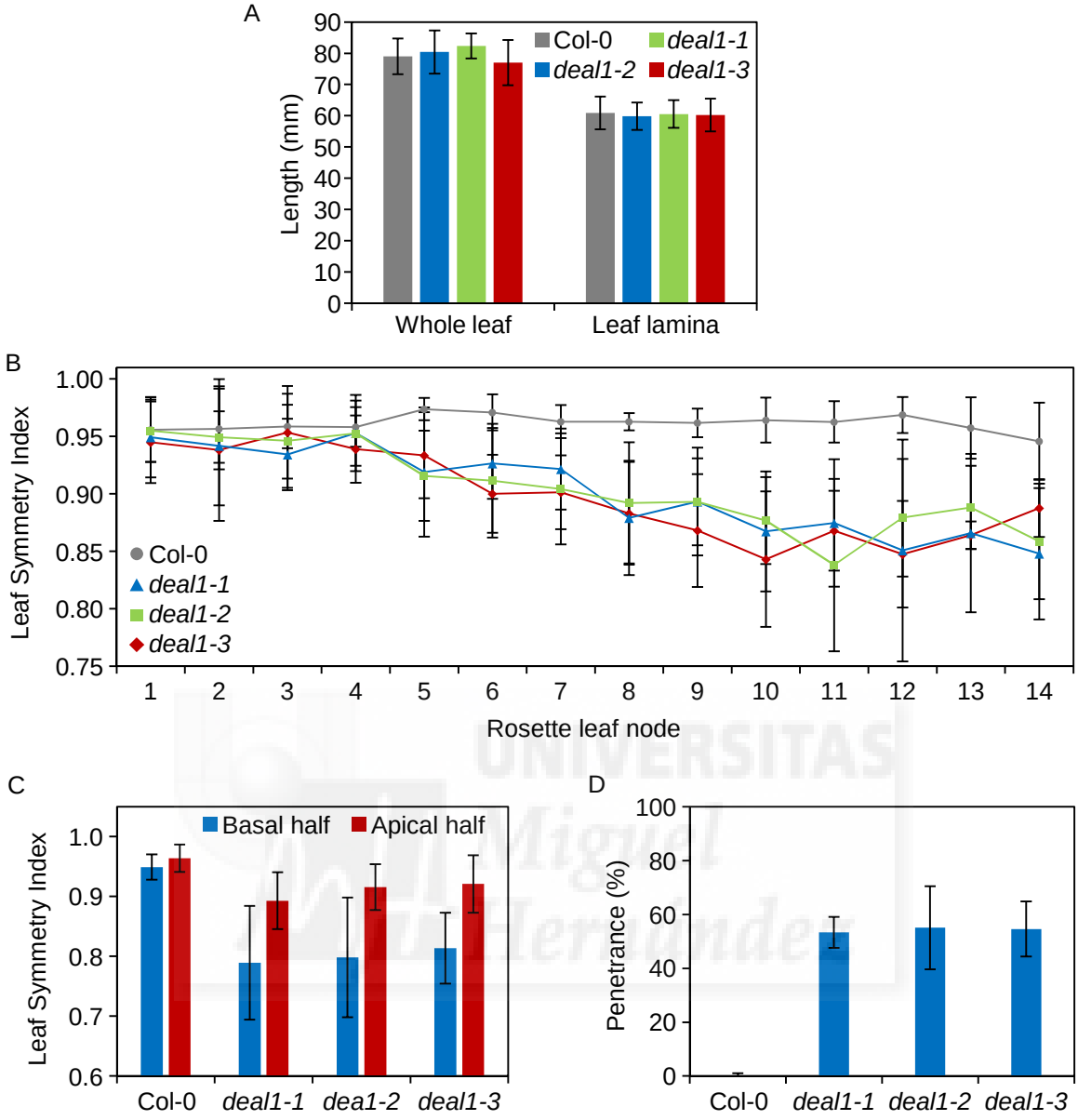

Figure S2. Length and asymmetry of *deal1* leaves.
(A) Whole leaf and lamina lengths in Col-0 and the *deal1* mutants (n = 10).
(B) LSI (Leaf Symmetry Index) of rosette leaves 1 to 14 from Col-0 and the *deal1* mutants (n = 10).
(C) LSI of tenth-node rosette leaf apical and basal halves from Col-0 and the *deal1* mutants (n = 10).
(D) Penetrance of the mutant phenotype of tenth-node leaves from the *deal1* mutants.
All leaves were collected after full leaf expansion (35 das).

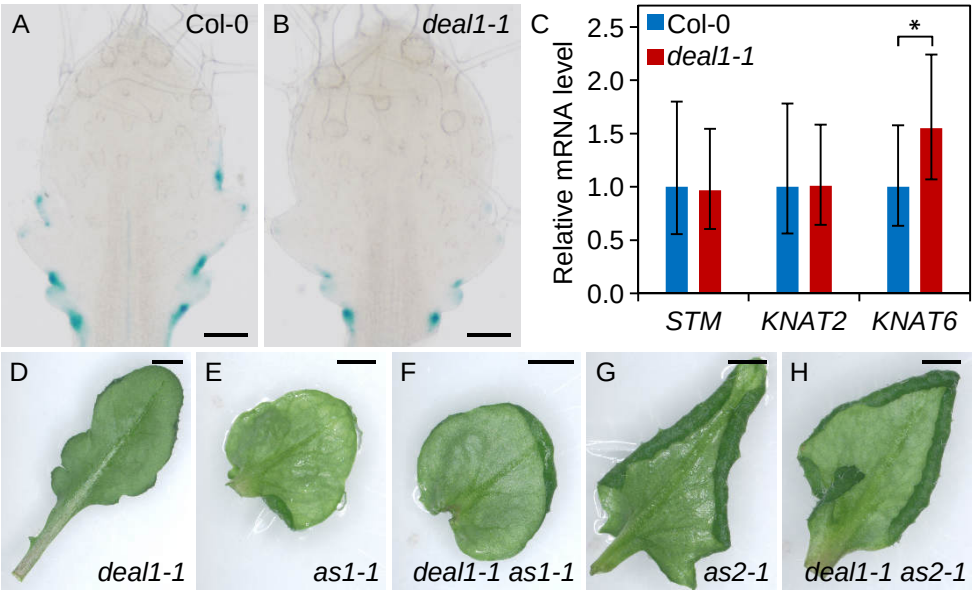

Figure S3. Expression of class I KNOX genes in *deal1* leaves.
(A, B) STM_{pro}:*GUS* expression pattern in Col-0 and *deal1-1* backgrounds. The leaves shown might correspond to any node from the ninth to eleventh and were collected 14 das.
(C) qRT-PCR expression analysis of the *STM*, *KNAT1* and *KNAT6* genes in Col-0 and *deal1-1* backgrounds. The asterisk indicates a statistically significant difference with the wild type in a Mann-Whitney U test ($p < 0.05$, n = 10).
(D-H) Abaxial side of (D) *deal1-1*, (E) *as1-1*, (F) *deal1-1 as1-1*, (G) *as2-1* and (H) *deal1-1 as2-1* tenth-node leaves, collected 25 das.
Scale bars: (A) 100 µm and (B-E) 2 mm.

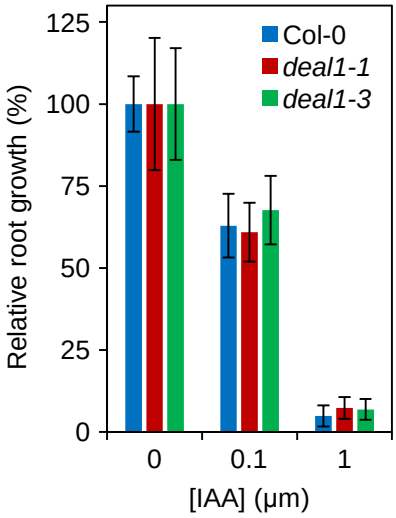

Figure S4. Effects of auxin on root growth in the *deal1-1* and *deal1-3* mutants. Root length was measured between 4 and 10 das (n = 15).

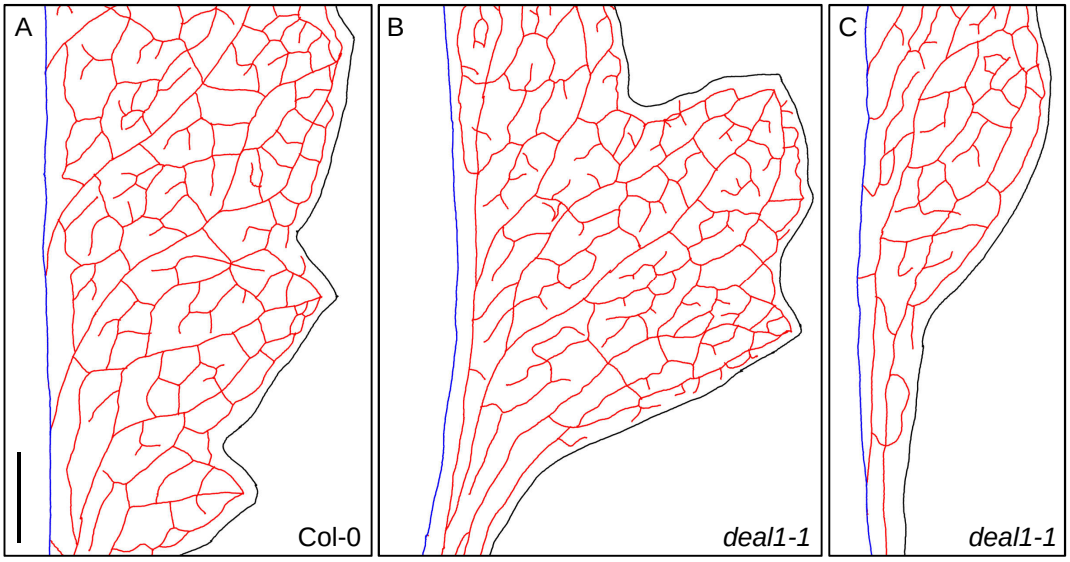

Figure S5. Leaf venation pattern of the *deal1-1* mutant.
Diagrams of half of a leaf from (A) Col-0 and (B, C) *deal1-1* strains. Blue, red and black lines represent the primary vein, all other veins, and the leaf margin, respectively. Tenth-node leaves were collected after full leaf expansion (35 das). Scale bar: 1 mm.

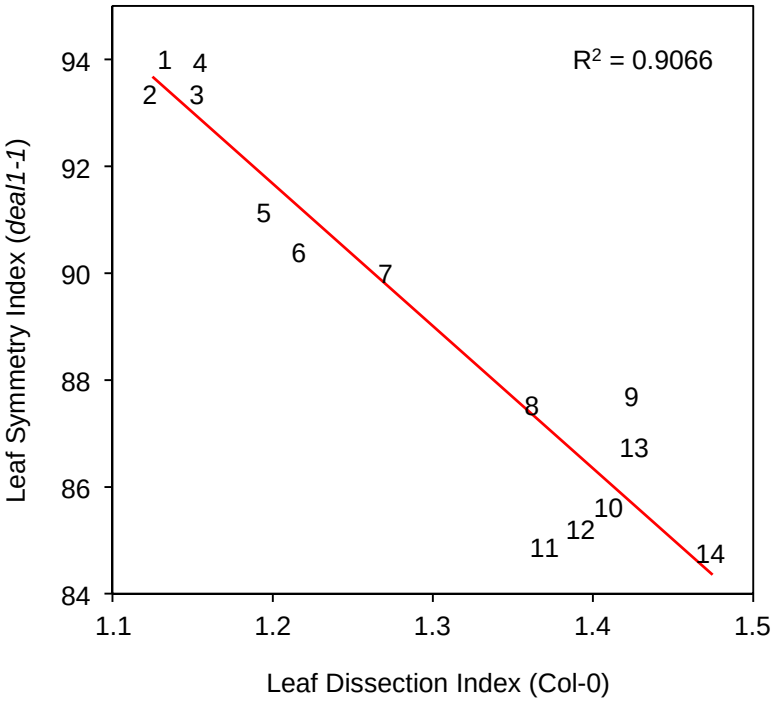

Figure S6. Correlation between the degree of dissection in Col-0 leaves and the severity of the asymmetry in *deal1-1* leaves across all rosette nodes.
The scatter plot shows each node as an ordinal number. Each X and Y value was calculated as the mean of 10 samples. The Leaf Dissection Index was calculated as [perimeter^2 / (4 × π × area)]. A trend line is shown in red, which was calculated by linear regression. R^2: coefficient of determination. Measurements were performed in leaves collected after full leaf expansion (35 das).

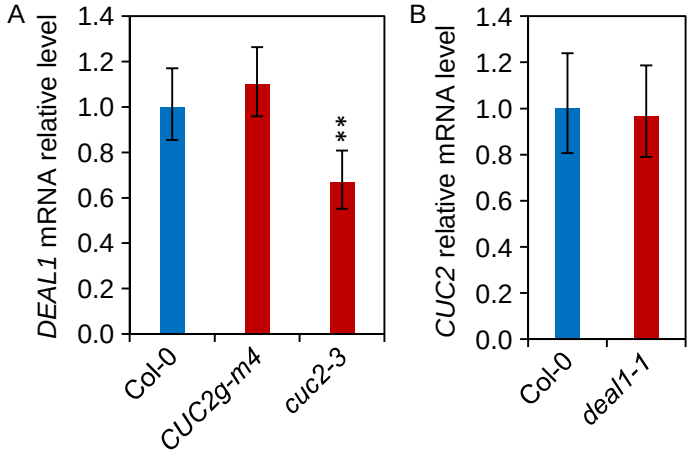

Figure S7. Functional relationship between *DEAL1* and *CUC2*.
Relative levels of the (A) *DEAL1* and (B) *CUC2* mRNAs in Col-0 and mutant backgrounds. Asterisks indicate values significantly different from the wild type in a Mann-Whitney U-test (**$p < 0.01$, n = 9).

Figure S8. *In silico* prediction of the subcellular localization of the DEAL1 protein.
(A) Predicted subcellular localization of DEAL1. Data were obtained with the sequence analysis programs indicated, as shown in the Aramemnon database (Schwacke *et al.*, 2003).
(B) Predicted transmembrane domains in DEAL1. Data was obtained with the topology prediction programs indicated, as shown in the Aramemnon database.

Figure S9. Expression analysis of *deal2-1* and *deal3-1*.
Semiquantitative RT-PCR expression analysis of *DEAL2* (At4g21310) and *DEAL3* (At1g11500) in Col-0, *deal2-1* (SALK_099815) and *deal3-1* (SAIL_140_H09) plants. The *ACTIN2* (*ACT2*) gene was used as a control. The primers used are listed in Table S2.

Supplemental table S1. Vascular parameters of *deal1-1* rosette leaves

	Col-0	*deal1-1*
Leaf area (mm^2)	94.17 ± 22.89	87.71 ± 16.49
Venation density ($mm \cdot mm^{-2}$)	4.69 ± 0.25	4.34 ± 0.14**
Branches per leaf area (mm^2)	16.50 ± 1.64	14.10 ± 1.17**
Branching points per leaf area (mm^2)	9.88 ± 0.91	8.34 ± 0.72**
Free-ending veins per venation length (mm)	0.52 ± 0.06	0.52 ± 0.06

Measurements were made on tenth-node rosette leaves collected after full leaf expansion (35 das). Asterisks indicate values significantly different from Col-0 in a Mann-Whitney U-test (**$p < 0.01$, n = 10).

Supplemental table S2. PCR primers used in this work

Purpose	Name	Oligonucleotide sequence (5´ → 3´)	
		Forward primer (F)	Reverse primer (R)
Cloning	At2g32280_attB_1_F/R	GGGGACAAGTTTGTACAAAAAAGCAGGCTCT GACCTTCACTCATGTTTAATC	GGGGACCACTTTGTACAAGAAAGCTGGGTTT TCAAATCTCTTAACTTAGTAGGA
	At2g32280_attB_2_F/R	GGGGACAAGTTTGTACAAAAAAGCAGGCTTG AAAATGACAAAGATAGGAGGTA	GGGGACCACTTTGTACAAGAAAGCTGGGTAC TTAGCTTCATCTTTGGCCG
	At2g32280_Y2H_F/R	GGGGACAAGTTTGTACAAAAAAGCAGGCTTG AAAATGACAAAGATAGGAGGTA	GGGGACCACTTTGTACAAGAAAGCTGGGTCG TGACACTTTGTCACTTAGC
Genotyping	SALK_023737_LP/RP	CCTGTTCCATCATTAACCGTG	TTTCTTCCACACCCTCACAAC
	SALK_047972_LP/RP	GATGTAGCTGCTGCAATCCTC	TTTCAAGTTTCCCGTGACAAG
	SAIL_237_C09_LP/RP	GGGGTTATAATTGATCTGATTCG	TCCAATGGAGAGAAAATGGTG
	SALK_0999815_LP/RP	ATTTGTTTGTTTCTGGCGATG	ATCTTTTCGAGGACATTGCAC
	SAIL_140_H09_LP/RP	TTTTGTCTTGCAGTGAGAGGC	GTTCTTTTTGCAGAAGCATGG
	LBb1.3	ATTTTGCCGATTTCGGAAC	
	LB1	GCCTTTTCAGAAATGGATAAATAGCCTTGCT TCC	
qRT-PCR	At2g32280_q_F/R	TCGCCCAAAATCAGGTGAAGCA	TAGGACATGAGCCATTACCAAT
	STM_q_F/R	TGGTGCTCCAACCTTCTGACA	GTCAAGGCCAAGATCATGGCT
	KNAT2_q_F/R	CTCTTTCAGATGATGGTGCGGTT	GCGTAGTAGCTGGTCCTTCAGATC
	KNAT6_q_F/R	GGGAGTTTCTGAGGATGGTGTAA	TTTGAGGTCCCGGTCTTCACA
	CUC2_q_F/R	CTCAAGAAGCTCCAAGGATGA	TTACGCTCACAGTTGCTCCT
	ACTIN2_q_F/R	GCACCCTGTTCTTCTTACCG	AACCCTCGTAGATTGGCACA
RT-PCR	At2g32280_RT_F/R	GAAGCTTCTCCTGTTCTTTATTC	GCAGTGGCAGAAACGTAATAAG
	At1g11500_RT_F/R	GGAAAGTGAACTTGGGTTCTTG	TTATGCGCGGCTTCTATTTG
	At4g21310_RT_F/R	CTGCGCTTGTCTGTTCTCG	GCGAGGAATGTAGGGTTCTTC
	At1g05291_RT_F/R	CGAGCCCTTGCTACAATAGAC	CTGGTTTCGTCGGATTACAAG
	ACTIN2_RT_F/R	CTCCGGCGACTTGACAGAG	CAAGGTCAAGACGGAGGATG

VI.- ANEXO: COMUNICACIONES A CONGRESOS

A reverse genetics approach to the analysis of leaf development

Muñoz-Viana, R., Rubio-Díaz, S., Pérez-Pérez, J.M., Wilson-Sánchez, D., Ponce, M.R., and Micol, J.L.

Instituto de Bioingeniería, Universidad Miguel Hernández, Campus de Elche, Alicante, Spain.

Because of their photosynthetic activity, leaves are the ultimate source of most of the oxygen that we breathe and of the food that we eat. Yet the processes by which these organs grow are poorly understood. Previous forward genetics studies yielded a large number of mutations affecting Arabidopsis leaf development, shape or size. However, none of these earlier attempts reached genome saturation. The group of Prof. J.R. Ecker at the Salk Institute is obtaining a large collection of gene-indexed homozygous T-DNA insertion mutants that will cover 25,000 genes of the Arabidopsis genome. To identify novel genes required for leaf growth regulation, we have begun a reverse genetics screening using the 14,000 T-DNA insertion lines available in batches from the ABRC, which correspond to 10,800 different Arabidopsis genes. These lines are grown in vitro and those exhibiting aberrant leaf phenotypes are documented and kept for further studies. In order to saturate the Arabidopsis genome with viable and fertile leaf mutations, we plan to screen the entire Salk homozygous T-DNA insertion collection for visible leaf phenotypes.

XVIII Congress of the Federation of European Societies of Plant Biology
Valencia, 2010
Póster

A reverse genetics approach to the analysis of leaf development

R. Muñoz-Viana, S. Rubio-Díaz, J.M. Pérez-Pérez, D. Wilson-Sánchez, M.R. Ponce, and J.L. Micol

Instituto de Bioingeniería, Universidad Miguel Hernández, Campus de Elche, 03202 Elche, Alicante. Spain

rmunoz@umh.es jlmicol@umh.es www.agron-omics.eu genetica.umh.es

Because of their photosynthetic activity, leaves are the ultimate source of most of the oxygen that we breathe and of the food that we eat. Yet the processes by which these organs grow are poorly understood. Previous forward genetics studies yielded a large number of mutants affecting leaf growth, shape or size. However, none of these previous attempts reached genome saturation[1]. The group of Prof. Ecker at the Salk Institute is obtaining a large collection of sequence-indexed homozygous T-DNA insertion mutants that will cover 25,000 genes of the Arabidopsis genome[2,3].

To identify novel genes required for leaf growth regulation, we have begun a reverse genetics screen using homozygous T-DNA Salk lines provided by ABRC. Plants were grown *in vitro*, and the vegetative phenotype of those displaying abnormal leaves was documented both at the T4 and T5 generations, in order to avoid false positives (Fig. 1).

We have grown 9,760 T4 lines, 2,034 of which exhibited abnormally sized or shaped leaves. 1,301 T5 progenies have been studied so far, only 173 of which displayed the same leaf morphological aberrations than their T4 parentals (Table 1 and Fig. 2). We genotyped 10 lines randomly chosen among the above mentioned 173, and found that all of them were homozygous for a T-DNA insertion in the gene annotated by Ecker´s lab (Fig. 3B).

We expect to identify about 600 gene-indexed leaf mutants. A database of the genes causing leaf phenotypes will be made publicly available in the context of the Agron-Omics project.

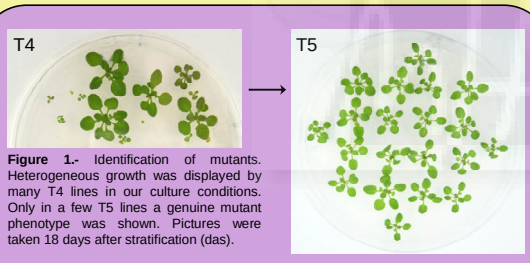

Figure 1.- Identification of mutants. Heterogeneous growth was displayed by many T4 lines in our culture conditions. Only in a few T5 lines a genuine mutant phenotype was shown. Pictures were taken 18 days after stratification (das).

Figure 2.- Rosettes of (A) the wild type Col-0 and (B-X) 23 of the mutants identified in our screening. Pictures were taken 21 das. Scale bars: 1 mm.

Table 1.- Progress of our screening for leaf mutants

	T4 lines		
	studied	exhibiting abnormal leaves	T5 genuine mutants confirmed
Completed	6,866	1,301	173
In progress	2,894	733	72*
Total	9,760	2,034	245*

*Expected values.

Table 2.- Functional clasification of the leaf mutans identified

		Number	%
Gene function already described			
	in leaf development	21	12
	in other processes	37	22
Unknown gene function			
	belongs to a gene family	68	39
	encodes a known domain	12	7
	completely unknown	29	17
Transposons		6	3
Total		173	100

Table 2.- Classification of the loci affecting leaf morphogenesis identified in our screening. 58 genes out of the 173 found (34%) had been already studied at some level. 109 (63%) had no previously described mutant alleles, 80 of which either belong to known gene families or contain a known protein domain, 29 are completely unknown, and 6 are transposons.

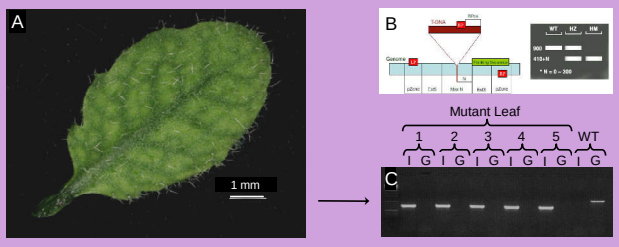

Figure 3.- Genotyping of a phenotypically mutant T5 line. (A) Leaves were collected from 5 plants of a T5 line displaying an unambiguous leaf mutant phenotype. (B) Genotyping for the presence of the T-DNA insertion in the annotated gene was performed as recommended by the Ecker group (http://signal.salk.edu/isects.html). (C) Amplification products obtained in the genotyping of the line shown in A. Numbers indicate different plants. The I and G lanes correspond to PCR amplification products obtained using the BP+RP and LP+RP primer pairs, respectively [see (B)].

ACKNOWLEDGEMENTS

Research in the laboratory of J.L.M. is supported by grants from the Ministerio de Ciencia e Innovación of Spain [BIO2008-04075 and CSD2007-00057 (TRANSPLANTA)], the Generalitat Valenciana (PROMETEO/2009/112) and the European Commission [LSHG-CT-2006-037704 (AGRON-OMICS)].

REFERENCES

1.- Berná, G., Robles, P., and Micol, J.L. (1999). *Genetics* **152,** 729-742.
2.- Alonso, J.M., *et al* . (2003). *Science* **301,** 653-657.
3.- O´Malley, R.C., and Ecker, J.R. (2010). *Plant Journal* **61,** 928-940.

Genética inversa del desarrollo foliar

Muñoz-Viana, R., Rubio-Díaz, S., Pérez-Pérez, J.M., Wilson-Sánchez, D., Ponce, M.R., y Micol, J.L.

Instituto de Bioingeniería, Universidad Miguel Hernández, Campus de Elche, 03202 Elche, Alicante.

Las hojas de las plantas producen el oxígeno que respiramos y constituyen la fuente directa o indirecta de casi todos los alimentos que consumimos. El interés del estudio y la eventual manipulación del desarrollo de las hojas radica en que son el órgano fotosintético básico, en torno al cual gravita la vida en nuestro planeta. Mediante abordajes genéticos clásicos se han obtenido muchos mutantes que manifiestan perturbaciones en el desarrollo foliar, pero no se ha alcanzado la saturación del genoma de Arabidopsis.

El grupo del Prof. J.R. Ecker, del Salk Institute, está generando una colección indexada de líneas homocigóticas para inserciones de ADN-T en unos 25.000 genes de Arabidopsis. Con el objetivo de identificar nuevos genes implicados en la regulación de la forma o el tamaño de la hoja, estamos sometiendo a escrutinio a 14.000 de estas líneas de ADN-T, las que por ahora pueden obtenerse por lotes en el ABRC, que corresponden a mutaciones en 10.800 genes. Cultivamos estas líneas in vitro y conservamos y analizamos morfométricamente las que muestran hojas anormales. Nuestros resultados se reflejarán en una base de datos pública.

X Reunión de Biología Molecular de Plantas
Valencia, 2010
Póster

Genética inversa del desarrollo foliar

R. Muñoz Viana, S. Rubio Díaz, J.M. Pérez Pérez, D. Wilson Sánchez, M.R. Ponce, y J.L. Micol

Instituto de Bioingeniería, Universidad Miguel Hernández, Campus de Elche, 03202 Elche, Alicante.
rmunoz@umh.es jlmicol@umh.es www.agron-omics.eu genetica.umh.es

El interés del estudio y la eventual manipulación del desarrollo de las hojas radica en que son el órgano fotosintético básico, en torno al cual gravita la vida en nuestro planeta. Mediante abordajes genéticos clásicos se han obtenido muchos mutantes que manifiestan perturbaciones en el desarrollo foliar, pero no se ha alcanzado la saturación del genoma de Arabidopsis[1]. El grupo del Prof. J.R. Ecker, del Salk Institute, está generando una colección indexada de líneas homocigóticas para inserciones de ADN-T en unos 25.000 genes de Arabidopsis[2,3].

Con el objetivo de identificar nuevos genes implicados en la regulación de la forma o el tamaño de la hoja, estamos sometiendo a escrutinio a 14.000 de estas líneas de ADN-T, que corresponden a mutaciones en 10.800 genes. Cultivamos estas líneas *in vitro* y documentamos las que muestran fenotipos foliares anormales tanto en la generación T4 como en su progenie T5 (Fig. 1).

Hemos cultivado 9.760 líneas T4, 2.034 de las cuales presentaron fenotipos foliares aberrantes. Hemos estudiado hasta ahora 1.301 de sus descendientes T5, confirmando su fenotipo mutante en 173 casos (Tabla 1 y Fig. 2). Hemos genotipado 10 de estas 173 líneas elegidas al azar, comprobando que todas ellas eran homocigóticas para la inserción de ADN-T en el gen anotado por el grupo de Ecker (Fig. 3B).

Esperamos identificar unos 600 mutantes foliares que se reflejarán en una base de datos pública.

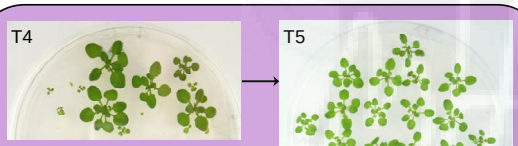

Figura 1.- Identificación de mutantes. Crecimiento heterogéneo observado en numerosas líneas T4 en nuestras condiciones de cultivo. Sólo algunas líneas T5 exhibieron un fenotipo mutante genuino. Las fotos se tomaron 18 días después de la estratificación (dde).

Figura 2.- Rosetas de (A) el tipo silvestre Col-0 y (B-X) 23 de los mutantes identificados en nuestro escrutinio. Las fotos se tomaron 21 dde. Barras de escala: 1 mm.

Tabla 1.- Progreso de nuestro escrutinio de mutantes foliares

	Líneas T4		
	estudiadas	con hojas anormales	mutantes genuinos confirmados en T5
Completados	6.866	1.301	173
En proceso	2.894	733	72*
Total	9.760	2.034	245*

*Valores esperados.

Tabla 2.- Clasificación funcional de los mutantes foliares encontrados

	Número	Porcentaje
Genes de función descrita previamente		
en el desarrollo foliar	21	12
en otros procesos	37	22
Genes de función desconocida		
pertenecientes a una familia génica	68	39
que codifican un dominio conocido	12	7
totalmente desconocidos	29	17
Transposones	6	3
Total	173	100

Tabla 2.- Clasificación de los genes que perturban la morfología foliar identificados en nuestro estudio. 58 de los 173 genes encontrados (34%) han sido caracterizados previamente a algún nivel. Para 109 de los mutantes encontrados (63%) no hay alelos mutantes previamente descritos, y los 6 mutantes restantes corresponden a inserciones anotadas en transposones.

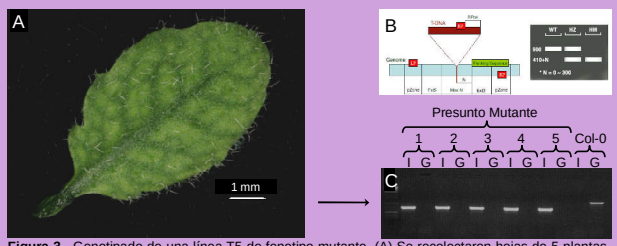

Figura 3.- Genotipado de una línea T5 de fenotipo mutante. (A) Se recolectaron hojas de 5 plantas de una línea T5 que mostró un fenotipo mutante foliar inequívoco. (B) El genotipado para confirmar la presencia de la inserción de ADN-T en el gen anotado se hizo según la recomendaciones del laboratorio de J. Ecker (http://signal.salk.edu/isects.html). (C) Productos de amplificación obtenidos genotipando la línea mostrada en A. Los números indican diferentes plantas. Las calles I y G corresponden a amplificaciones de PCR realizadas usando las parejas de cebadores BP+RP y LP+RP, respectivamente (vease el apartado B).

AGRADECIMIENTOS

El laboratorio de José Luis Micol está financiado por la Comisión Europea (Agron-Omics, LSHG-CT-2006-037704), la Generalitat Valenciana (PROMETEO/2009/112) y el Ministerio de Ciencia e Innovación [BIO2008-04075 y CSD2007-00057 (TRANSPLANTA)].

BIBLIOGRAFÍA

1.- Berná, G., Robles, P., y Micol, J.L. (1999). *Genetics* **152,** 729-742.
2.- Alonso, J.M., *et al.* (2003). *Science* **301,** 653-657.
3.- O´Malley, R.C., y Ecker, J.R. (2010). *Plant Journal* **61,** 928-940.

A reverse genetics approach to the analysis of leaf development

Muñoz-Viana, R., Rubio-Díaz, S., Pérez-Pérez, J.M., Wilson-Sánchez, D., Ponce, M.R., and Micol, J.L.

Instituto de Bioingeniería, Universidad Miguel Hernández, Campus de Elche, Alicante, Spain.

Because of their photosynthetic activity, leaves are the ultimate source of most of the oxygen that we breathe and of the food that we eat. Yet the processes by which these organs grow are poorly understood. Previous forward genetics studies yielded a large number of mutations affecting Arabidopsis leaf development, shape or size. However, none of these earlier attempts reached genome saturation. The group of Prof. J.R. Ecker at the Salk Institute is obtaining a large collection of gene-indexed homozygous T-DNA insertion mutants that will cover 25,000 genes of the Arabidopsis genome. To identify novel genes required for leaf growth regulation, we have begun a reverse genetics screening using the 14,000 T-DNA insertion lines available in batches from the ABRC, which correspond to 10,800 different Arabidopsis genes. These lines are grown in vitro and those exhibiting aberrant leaf phenotypes are documented and kept for further studies. In order to saturate the Arabidopsis genome with viable and fertile leaf mutations, we plan to screen the entire Salk homozygous T-DNA insertion collection for visible leaf phenotypes.

Plant Biology (Joint Annual Meetings of the American Society
of Plant Biologists and the Canadian Society of Plant Physiologists)
Montreal (Canadá), 2010
Póster

A reverse genetics approach to the analysis of leaf development

R. Muñoz-Viana, S. Rubio-Díaz, J.M. Pérez-Pérez, D. Wilson-Sánchez, M.R. Ponce, and J.L. Micol

Instituto de Bioingeniería, Universidad Miguel Hernández, Campus de Elche, 03202 Elche, Alicante. Spain

rmunoz@umh.es jlmicol@umh.es www.agron-omics.eu genetica.umh.es

Because of their photosynthetic activity, leaves are the ultimate source of most of the oxygen that we breathe and of the food that we eat. Yet the processes by which these organs grow are poorly understood. Previous forward genetics studies yielded a large number of mutants affecting leaf growth, shape or size. However, none of these previous attempts reached genome saturation[1]. The group of Prof. Ecker at the Salk Institute is obtaining a large collection of sequence-indexed homozygous T-DNA insertion mutants that will cover 25,000 genes of the Arabidopsis genome[2,3].

To identify novel genes required for leaf growth regulation, we have begun a reverse genetics screen using homozygous T-DNA Salk lines provided by ABRC. Plants were grown *in vitro*, and the vegetative phenotype of those displaying abnormal leaves was documented both at the T4 and T5 generations, in order to avoid false positives (Fig. 1).

We have grown 10,442 T4 lines, 2,189 of which exhibited abnormally sized or shaped leaves. 1,301 T5 progenies have been studied so far, only 173 of which displayed the same leaf morphological aberrations than their T4 parentals (Table 1 and Fig. 2). We genotyped 10 lines randomly chosen among the above mentioned 173, and found that all of them were homozygous for a T-DNA insertion in the gene annotated by Ecker´s lab (Fig. 3B).

We expect to identify about 600 gene-indexed leaf mutants. A database of the genes causing leaf phenotypes will be made publicly available in the context of the Agron-Omics project.

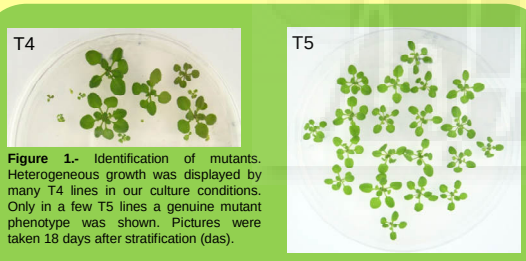

Figure 1.- Identification of mutants. Heterogeneous growth was displayed by many T4 lines in our culture conditions. Only in a few T5 lines a genuine mutant phenotype was shown. Pictures were taken 18 days after stratification (das).

Figure 2.- Rosettes of (A) the wild type Col-0 and (B-X) 23 of the mutants identified in our screening. Pictures were taken 21 das. Scale bars: 1 mm.

Table 1.- Progress of our screening for leaf mutants

	T4 lines		T5 genuine
	studied	exhibiting abnormal leaves	mutants confirmed
Completed	6,866	1,301	173
In progress	3,576	888	90*
Total	10,442	2,189	263*

*Expected values.

Table 2.- Functional clasification of the leaf mutans identified

		Number	%
Gene function already described			
	in leaf development	21	12
	in other processes	37	22
Unknown gene function			
	belongs to a gene family	68	39
	encodes a known domain	12	7
	completely unknown	29	17
Transposons		6	3
Total		173	100

Table 2.- Classification of the loci affecting leaf morphogenesis identified in our screening. 58 genes out of the 173 found (34%) had been already studied at some level. 109 (63%) had no previously described mutant alleles, 80 of which either belong to known gene families or contain a known protein domain, 29 are completely unknown, and 6 are transposons.

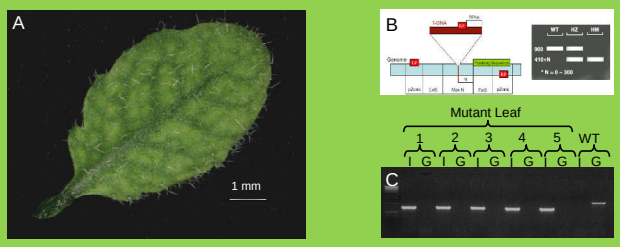

Figure 3.- Genotyping of a phenotypically mutant T5 line. (A) Leaves were collected from 5 plants of a T5 line displaying an unambiguous leaf mutant phenotype. (B) Genotyping for the presence of the T-DNA insertion in the annotated gene was performed as recommended by the Ecker group (http://signal.salk.edu/isects.html). (C) Amplification products obtained in the genotyping of the line shown in A. Numbers indicate different plants. The I and G lanes correspond to PCR amplification products obtained using the BP+RP and LP+RP primer pairs, respectively [see (B)].

ACKNOWLEDGEMENTS

Research in the laboratory of J.L.M. is supported by grants from the Ministerio de Ciencia e Innovación of Spain [BIO2008-04075 and CSD2007-00057 (TRANSPLANTA)], the Generalitat Valenciana (PROMETEO/2009/112) and the European Commission [LSHG-CT-2006-037704 (AGRON-OMICS)].

REFERENCES

1.- Berná, G., Robles, P., and Micol, J.L. (1999). *Genetics* **152,** 729-742.
2.- Alonso, J.M., *et al* . (2003). *Science* **301,** 653-657.
3.- O´Malley, R.C., and Ecker, J.R. (2010). *Plant Journal* **61,** 928-940.

Reverse genetics of leaf development

Wilson-Sánchez, D., Muñoz-Viana, R., Rubio-Díaz, S., Pérez-Pérez, J.M., Jover-Gil, S., Ruiz-Pino, A., Díaz-Cruz, M.A., Sánchez-Herrero, J.F., Ponce, M.R., and Micol, J.L.

Instituto de Bioingeniería, Universidad Miguel Hernández, Campus de Elche, 03202 Elche, Alicante, Spain.

The interest of the study, and eventual manipulation, of leaf development lays on the fact that leaves are the fundamental photosynthetic organ, of vital importance for life in our planet. Although hundreds of mutants that show altered leaf development have been isolated using forward genetics, Arabidopsis genome saturation has not yet been reached. The group of Prof. J.R. Ecker, at The Salk Institute, is obtaining a large collection of gene-indexed homozygous T-DNA insertion mutants that will cover the 27,000 genes of the Arabidopsis genome. Aiming to identify novel genes involved in leaf shape and size regulation, we are screening 20,718 of these lines, which correspond to 14,585 genes. So far, we have analyzed the leaf phenotype of 13,367 lines, and identified 382 that show a mutant phenotype with full penetrance and quite constant expressivity. We have genotyped 199 of these genuine leaf mutants, assessing that a T-DNA insertion is homozygous at the annotated locus in 75% of them. A public database will collect the results of our screen and the preliminary characterization of their mutant phenotypes.

Plant Growth Biology and Modeling Workshop
Elche, 2011
Póster

Reverse genetics of leaf development

Wilson-Sánchez, D., Muñoz-Viana, R., Rubio-Díaz, S., Pérez-Pérez, J.M., Ruiz-Pino, A., Díaz-Cruz, M.A., Sánchez-Herrero, J.F., Jover-Gil, S., Ponce, M.R., and Micol, J.L.

Instituto de Bioingeniería, Universidad Miguel Hernández, Campus de Elche, 03202 Elche, Alicante. Spain
dwilson@umh.es jlmicol@umh.es www.agron-omics.eu genetica.umh.es

Because of their photosynthetic activity, leaves are the ultimate source of most of the oxygen that we breathe and of the food that we eat. The identification of the genes that control leaf development is a necessary step towards its understanding and eventual engineering. In Arabidopsis, forward genetics approaches have identified hundreds of mutants that show altered leaf development, but did not reach genome saturation[1].

The lab of J.R. Ecker, at The Salk institute, is obtaining an indexed collection of homozygous T-DNA insertion mutants intended to cover all Arabidopsis genes[2,3]. In order to identify novel genes with a role in leaf morphogenesis, we are performing a reverse genetics screen on this collection. T_4 generation lines received from ABRC were grown in vitro and analyzed 18 days after stratification (das) and those displaying abnormal leaf traits were grown to the next generation to confirm or discard their phenotypes.

So far, we have analyzed the leaf phenotype of 16,060 T_4 lines, 2,883 of which displayed abnormally shaped or sized leaves. The analysis of the T_5 offspring of 2,518 of them revealed that only 410 lines (2.9% of total T_4 lines studied) show the same mutant phenotype as their parental with full penetrance and almost constant expressivity (Fig. 1, Table 1 and Fig. 2). 199 of these genuine leaf mutants were genotyped, assessing that a T-DNA insertion is homozygous at the annotated locus in 76.7% of them (Fig. 3 and Table 2). Known-genotype seeds were preserved.

We expect to identify over 600 leaf mutants at the end of this project. A comprehensive database will collect the results of our screen and the preliminary characterization of the mutant phenotypes, which will comprise an ontological description and several pictures.

Figure 1.- Identification of mutants. Heterogeneous growth was displayed by many T_4 lines in our culture conditions. Only in a few T_5 lines a genuine mutant phenotype was shown. Pictures were taken 18 das.

Table 1.- Progress of our screening for leaf mutants

	T_4 lines		T_5 genuine mutants confirmed
	studied	exhibiting abnormal leaves	
Completed	14,084	2,518	410
In progress	1,976	365	57*
Total	16,060	2,883	467*

*Expected values.

Table 2.- Genotyping of mutant T_5 families

Genotype	Number of lines	Percentage
Homozygote	135	76.7
Segregant	5	2.8
Wild type	36	20.4
Total	176	100
Non conclusive*	23	-

*These lines will require the genotyping of a higher number of individuals.

Figure 2.- Rosettes of (A) the wild type Col-0 and (B-X) 23 of the mutants identified in our screening. Pictures were taken 21 das. Scale bars: 1 mm.

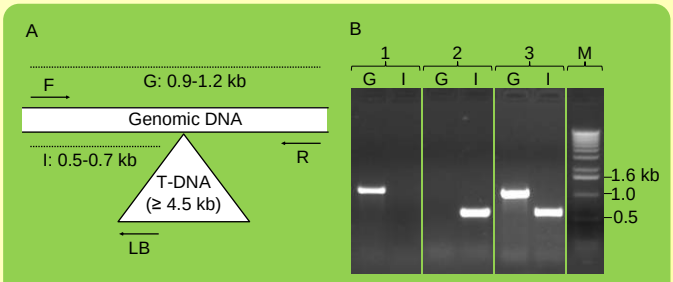

Figure 3.- Genotyping procedure of T_5 mutants. Leaves were collected from 7 plants of a T_5 line displaying an unambiguous leaf mutant phenotype. (A) Genotyping of the T-DNA insertions in the annotated genes was performed as recommended by the Ecker group (http://signal.salk.edu/isects.html). (B) Amplification products of a (1) wild-type, (2) homozygous and (3) heterozygous plant for a given insertion. Numbers indicate different plants. The G and I gel lanes correspond to PCR amplification products obtained using the F+R and F+LB primer pairs, respectively [see (A)].

ACKNOWLEDGEMENTS

Research in the laboratory of J.L.M. is supported by grants from the Ministerio de Ciencia e Innovación of Spain [BIO2008-04075 and CSD2007-00057 (TRANSPLANTA)], the Generalitat Valenciana (PROMETEO/2009/112) and the European Commission [LSHG-CT-2006-037704 (AGRON-OMICS)].

REFERENCES

1.- Berná, G., Robles, P., and Micol, J.L. (1999). *Genetics* **152,** 729-742.
2.- Alonso, J.M., *et al* . (2003). *Science* **301,** 653-657.
3.- O´Malley, R.C., and Ecker, J.R. (2010). *Plant Journal* **61,** 928-940.

Forward and reverse approaches to the genetic dissection of leaf development

Mollá-Morales, A., Sarmiento-Mañús, R., Ferrández-Ayela, A., Rubio-Díaz, S, Muñoz-Viana, R., Esteve-Bruna, D., Casanova-Sáez, R., Muñoz-Nortes, T., Wilson-Sánchez, D., González-Bayón, R., Jover-Gil, S., Candela, H., Pérez-Pérez, J.M., Ponce, M.R., and Micol, J.L.

Instituto de Bioingeniería, Universidad Miguel Hernández, 03202 Elche, Alicante, Spain.

Plant leaves are the best solar panels ever built, and they also perform well as air purifiers and food factories. Leaves efficiently trap sunlight, remove carbon dioxide from the air, and are the ultimate source of most of the oxygen that we breathe and of the food that we eat. Understanding how a leaf is made is important for several reasons, which include gaining knowledge of the biology and evolution of a multicellular organ with no equivalents in the animal kingdom, as well as identifying —and eventually manipulating, to increase crop yield— the genetic, environmental, and hormonal cues that determine its final architecture and function.

To shed light on the making of plant leaves, we took a forward genetics approach to the saturation of the Arabidopsis genome with viable mutations causing abnormal leaf morphology. The identified mutations fell into 147 complementation groups. Using a high throughput gene mapping method that we developed, we have already cloned 47 of these genes identified by mutation. The products of these genes participate in various developmental processes, such as polar cell expansion, transduction of hormonal signals, gene regulation, plastid biogenesis, and chromatin remodeling, among others. The broad spectrum of leaf morphological alterations that we identified is helping to dissect specific leaf developmental processes.

We are now combining traditional linkage analysis and next-generation sequencing techniques in order to positionally clone 40 non-allelic mutations already isolated in our laboratory, which affect leaf morphology. In addition, we have started to use clonal analysis to study essential, embryonic-lethal genes that are expressed in wild-type leaves.

We also aim at identifying genes involved in the development of an organ —the leaf— at a scale with no precedent in plants, and perhaps animals. The Ecker laboratory is producing 50,000 sequence-indexed homozygous T-DNA lines representing all the protein coding genes in the Arabidopsis genome. We are searching this collection for leaf morphological aberrations, and have already identified 340 genes required for normal leaf

development. These leaf mutants provide an opportunity to propose models and test hypotheses about how genes control plant development at the organ level.

Plant Growth Biology and Modeling Workshop

Elche, 2011

Conferencia pronunciada por J.L. Micol, por invitación.

Genética inversa del desarrollo foliar

Wilson-Sánchez, D., Muñoz-Viana, R., Rubio-Díaz, S., Pérez-Pérez, J.M., Jover-Gil, S., Ruiz-Pino, A., Sánchez-Herrero, J.F., Ponce, M.R., y Micol, J.L.

Instituto de Bioingeniería, Universidad Miguel Hernández, Campus de Elche, 03202 Elche, Alicante.

Las hojas de las plantas producen el oxígeno que respiramos y constituyen la fuente directa o indirecta de casi todos los alimentos que consumimos. El interés del estudio y la eventual manipulación del desarrollo de las hojas radica en que son el órgano fotosintético básico, en torno al cual gravita la vida en nuestro planeta. Mediante abordajes genéticos clásicos se han obtenido centenares de mutantes que manifiestan perturbaciones en el desarrollo foliar, pero no se ha alcanzado la saturación del genoma de Arabidopsis.

El grupo del Prof. J.R. Ecker, en el Salk Institute, está generando una colección indexada de líneas homocigóticas para inserciones de ADN-T en los 27.000 genes de Arabidopsis. Con el objetivo de identificar nuevos genes implicados en la regulación de la forma o el tamaño de la hoja, estamos sometiendo a escrutinio 20.718 de estas líneas, que corresponden a 14.585 genes. Por ahora hemos analizado el fenotipo foliar de 13.367 líneas, identificando 382 que muestran un fenotipo foliar mutante con penetrancia completa y expresividad relativamente constante. Hemos genotipado 199 de ellas, comprobando en el 75% de los casos que la inserción de ADN-T está presente en homocigosis en el locus anotado. Los resultados de la caracterización de estos mutantes se reflejarán en una base de datos pública.

XXXVIII Congreso de la Sociedad Española de Genética

Murcia, 2011

Póster

Genética inversa del desarrollo foliar

Wilson-Sánchez, D., Muñoz-Viana, R., Rubio-Díaz, S., Pérez-Pérez, J.M., Ruiz-Pino, A., Sánchez-Herrero, J.F., Jover-Gil, S., Ponce, M.R., y Micol, J.L.

Instituto de Bioingeniería, Universidad Miguel Hernández, Campus de Elche, 03202 Elche, Alicante
dwilson@umh.es jlmicol@umh.es www.agron-omics.eu genetica.umh.es

Las hojas de las plantas producen el oxígeno que respiramos y constituyen la fuente directa o indirecta de casi todos los alimentos que consumimos. El interés del estudio y la eventual manipulación del desarrollo de las hojas radica en que son el órgano fotosintético básico, en torno al cual gravita la vida en nuestro planeta. Mediante abordajes genéticos clásicos se han obtenido centenares de mutantes que manifiestan perturbaciones en el desarrollo foliar, pero no se ha alcanzado la saturación del genoma de Arabidopsis[1].

El grupo del Prof. J.R. Ecker, en el Salk Institute, está generando una colección indexada de líneas homocigóticas para inserciones de ADN-T en los 27.000 genes de Arabidopsis[2,3]. Con el objetivo de identificar nuevos genes implicados en la regulación de la forma o el tamaño de la hoja, estamos sometiendo a escrutinio 20.718 de estas líneas, que corresponden a 14.585 genes. Las semillas T_4 que recibimos del ABRC son cultivadas *in vitro* y analizadas 18 días después de su estratificación (dde). Aquéllas que presentan un fenotipo foliar anormal son seleccionadas para confirmar o descartar su fenotipo tras el estudio de su descendencia.

Por ahora hemos analizado el fenotipo foliar de 16.060 líneas, identificando 410 que muestran un fenotipo foliar mutante con penetrancia completa y expresividad relativamente constante (Fig. 1 y 2, Tabla 1). Hemos genotipado 199 de ellas, comprobando en el 76,7% de los casos que la inserción de ADN-T está presente en homocigosis en el locus anotado (Fig. 3 y Tabla 2). Las semillas de los individuos genotipados se etiquetan y conservan para su futuro estudio.

Esperamos identificar cerca de 600 mutantes una vez finalizado el proyecto. Los resultados de la caracterización de estos mutantes se reflejarán en una base de datos pública.

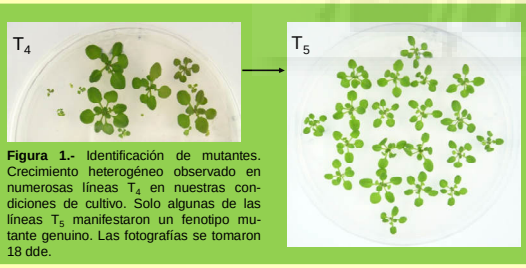

Figura 1.- Identificación de mutantes. Crecimiento heterogéneo observado en numerosas líneas T_4 en nuestras condiciones de cultivo. Solo algunas de las líneas T_5 manifestaron un fenotipo mutante genuino. Las fotografías se tomaron 18 dde.

Tabla 1.- Progreso de nuestro escrutinio de mutantes foliares

	Líneas T_4 estudiadas	Líneas T_4 con hojas anormales	mutantes genuinos confirmados en T_5
Completadas	14.084	2.518	410
En estudio	1.976	365	57*
Totales	16.060	2.883	467*

*Valores esperados

Tabla 2.- Genotipado de familias T_5 mutantes

Genotipo	Numero de lineas	Porcentaje
Homocigótico	135	76,7
Segregante	5	2,8
Silvestre	36	20,4
Total	176	100,0
No concluyente*	23	-

*Será necesario genotipar más individuos de estas líneas

Figura 2.- Rosetas de (A) el tipo silvestre Col-0 y (B-X) 23 de los mutantes identificados en nuestro escrutinio. Las fotografías se tomaron 21 dde. Barras de escala: 1 mm.

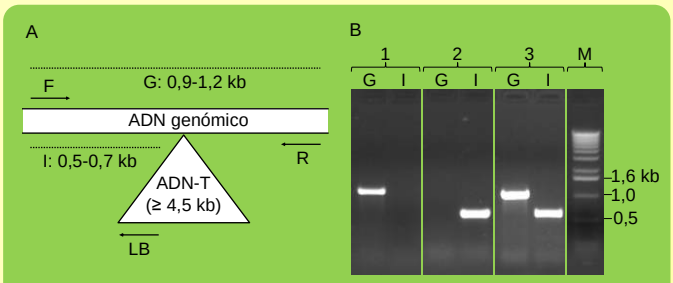

Figura 3.- Genotipado de líneas T_5 con fenotipo mutante. Se recolectaron hojas de 7 plantas T_5 que mostraban inequívocamente el fenotipo mutante. (A) El genotipado de las inserciones de ADN-T en los genes anotados se realizó siguiendo las recomendaciones del laboratorio de J.R. Ecker (http://signal.salk.edu/isects.html). (B) Productos de la amplificación del ADN de una planta (1) silvestre, (2) homocigótica y (3) heterocigótica para la inserción a estudio. Las calles G e I corresponden a los productos de amplificación obtenidos empleando las parejas de cebadores F+R y F+LB, respectivamente [ver (A)].

AGRADECIMIENTOS

El laboratorio de José Luis Micol está financiado por el Ministerio de Ciencia e Innovación [BIO2008-04075 y CSD2007-00057 (TRANSPLANTA)], la Generalitat Valenciana (PROMETEO/2009/112) y la Comisión Europea [LSHG-CT-2006-037704 (AGRON-OMICS)].

REFERENCIAS

1.- Berná, G., Robles, P., y Micol, J.L. (1999). *Genetics* **152,** 729-742.
2.- Alonso, J.M., *et al*. (2003). *Science* **301,** 653-657.
3.- O´Malley, R.C., y Ecker, J.R. (2010). *Plant Journal* **61,** 928-940.

Reverse genetics of leaf development

Micol, J.L.[1], Wilson-Sánchez, D.[1], Jover-Gil, S.[1], Lièvre, M.[2], Granier, C.[2], Pérez-Pérez, J.M.[1], and Ponce, M.R.[1]

[1]Instituto de Bioingeniería, Universidad Miguel Hernández de Elche, Spain.
[2]Laboratoire d'Ecophysiologie de Plantes sous Stress Environnementaux UMR759, France.

The interest of the study and eventual manipulation of leaf development lays on the fact that leaves are the fundamental photosynthetic organ, of vital importance for life in our planet. Although hundreds of mutants with altered leaf development have been isolated using forward genetics, saturation has not yet been reached for the Arabidopsis genome. The group of Prof. J.R. Ecker, at The Salk Institute, is obtaining a large collection of gene-indexed homozygous T-DNA insertion mutants. Aiming to identify novel genes required for leaf growth, we are screening 20,718 of these lines, which correspond to 14,585 genes. So far, we have analyzed the leaf phenotype of 16,400 lines, and identified 518 that show a mutant phenotype with full penetrance and almost constant expressivity. We have genotyped 300 of these genuine leaf mutants, finding that a T-DNA insertion is homozygous at the annotated locus in 74% of them. According to TAIR functional annotation, 56% of the loci for which we identified a mutant allele have no previously described mutant alleles. We have designed and implemented a public database and a web-based query application that collects the results of our screen and the preliminary characterization of the mutant phenotypes. 120 genuine leaf mutants with a confirmed homozygous T-DNA insertion have been subjected to detailed time-lapse qualitative and quantitative phenotypic analyses (see poster by Maryline Lièvre et al.).

23rd International Conference on Arabidopsis Research
Viena, 2012
Póster

Reverse genetics of leaf development

José Luis Micol, David Wilson-Sánchez, Sara Jover-Gil,
Maryline Lièvre, Christine Granier,
José Manuel Pérez-Pérez, and María Rosa Ponce.

Instituto de Bioingeniería, Universidad Miguel Hernández, Campus de Elche, 03202 Elche, Alicante, Spain.
jlmicol@umh.es dwilson@umh.es www.agron-omics.eu genetica.umh.es

The interest of the study and eventual manipulation of leaf development lays on the fact that they are the fundamental photosynthetic organ, of vital importance for life in our planet. Although hundreds of mutants with altered leaf development have been isolated using forward genetics, saturation has not yet been reached for the Arabidopsis genome[1].

The group of Prof. J.R. Ecker, at The Salk Institute, is obtaining a large collection of gene-indexed homozygous T-DNA insertion mutants[2,3]. Aiming to identify novel genes required for leaf growth, we are screening 20,718 of these lines, which correspond to 14,585 genes. So far, we have analyzed the leaf phenotype of 16,400 lines, and identified 518 that show a mutant phenotype with full penetrance and almost constant expressivity (Figure 1 and Table 1). We have genotyped 340 of these genuine leaf mutants, finding that a T-DNA insertion is homozygous at the annotated locus in 252 of them (Figures 2 and 3). Among these 252 genes interrupted, only 40 have previously characterized alleles[4] and, according to TAIR functional annotation, there is no information available on the function of 135 of them. These figures highlight the value of our collection.

We have implemented a public database and a web-based query application that collects the results of our screen and the preliminary characterization of the mutant phenotypes (Figure 4). It will be soon available at http://agron-omics.umh.es.

120 genuine leaf mutants with a confirmed homozygous T-DNA insertion have been subjected to detailed time-lapse qualitative and quantitative phenotypic analyses (see poster by Maryline Lièvre *et al.*).

Table 1.- Progress of our screening

	T_4 lines		T_5 genuine mutants confirmed
	studied	exhibiting anormal leaves	
Completed	16,400	2,567	518
In progress	2,500	450	79*
Total	18,900	3,017	597*

*Expected values

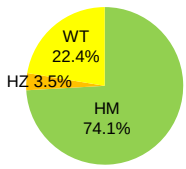

Figure 2.- Genotyping of genuine leaf mutants. Almost three quarters of all lines genotyped are homozygous for the annotated insertion, 3.5% harbour a segregating insertion, and in the remaining 22.4% the insertion is absent from the annotated locus.

Figure 1.- Rosettes of (A) the wild type Col-0 and (B-X) 23 of the leaf mutants identified in our screening. Pictures were taken 21 days after stratification (das). Scale bars: 1 mm.

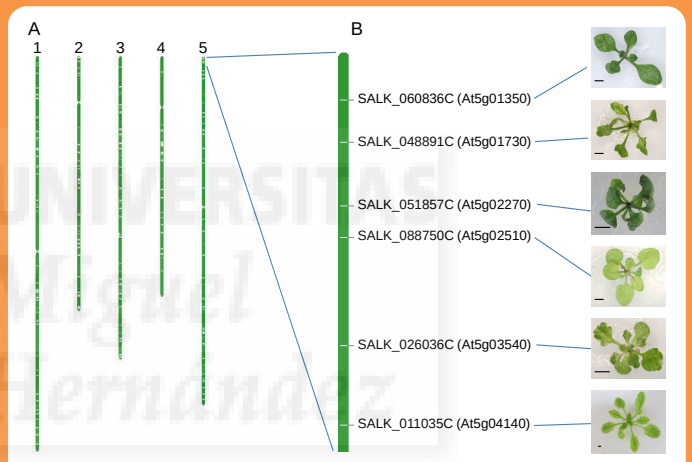

Figure 3.- We performed a phenotype-driven screen on a gene-indexed mutant collection. (A) Position of the 252 homozygous T-DNA insertions confirmed in our laboratory so far, laid out using the TAIR map visualization tool (http://www.arabidopsis.org/servlets/ViewChromosomes). Numbers on the top of each bar identify the 5 Arabidopsis chromosomes. (B) Enlargement of a randomly chosen interval showing 6 loci disrupted by T-DNA insertions, with their corresponding Salk codes and rosette phenotypes observed. Scale bars: 2 mm.

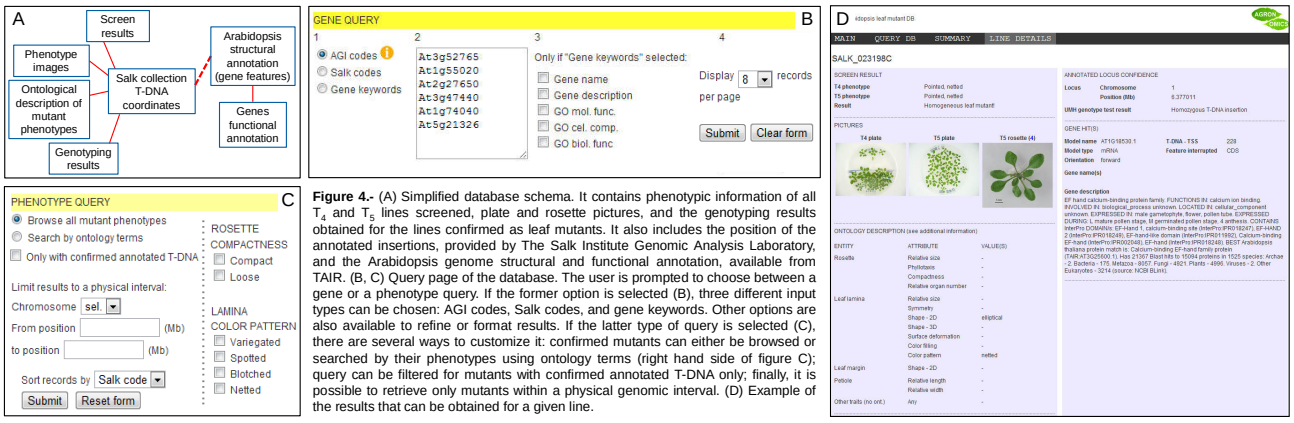

Figure 4.- (A) Simplified database schema. It contains phenotypic information of all T_4 and T_5 lines screened, plate and rosette pictures, and the genotyping results obtained for the lines confirmed as leaf mutants. It also includes the position of the annotated insertions, provided by The Salk Institute Genomic Analysis Laboratory, and the Arabidopsis genome structural and functional annotation, available from TAIR. (B, C) Query page of the database. The user is prompted to choose between a gene or a phenotype query. If the former option is selected (B), three different input types can be chosen: AGI codes, Salk codes, and gene keywords. Other options are also available to refine or format results. If the latter type of query is selected (C), there are several ways to customize it: confirmed mutants can either be browsed or searched by their phenotypes using ontology terms (right hand side of figure C); query can be filtered for mutants with confirmed annotated T-DNA only; finally, it is possible to retrieve only mutants within a physical genomic interval. (D) Example of the results that can be obtained for a given line.

ACKNOWLEDGEMENTS

Research in the laboratory of J.L.M. is supported by grants from the Ministerio de Ciencia e Innovación of Spain [BFU2011-22825 and CSD2007-00057 (TRANSPLANTA)], the Generalitat Valenciana (PROMETEO/2009/112) and the European Commission [LSHG-CT-2006-037704 (AGRON-OMICS)]. D.W.-S. is a predoctoral fellow of the Generalitat Valenciana VALI+d programme.

REFERENCES

1.- Berná, G., Robles, P., and Micol, J.L. (1999). *Genetics* **152,** 729-742.
2.- Alonso, J.M., *et al.* (2003). *Science* **301,** 653-657.
3.- O´Malley, R.C., and Ecker, J.R. (2010). *Plant J.* **61,** 928-940.
4.- Lloyd, J. and Meinke, D. (2012). *Plant Physiol.* **158**, 1115-1129

Genética inversa del desarrollo foliar

Wilson-Sánchez, D., Jover-Gil, S., Pérez-Pérez, J.M., Ponce, M.R., y Micol, J.L.

Instituto de Bioingeniería, Universidad Miguel Hernández, Campus de Elche, 03202 Elche, Alicante.

Las hojas de las plantas producen el oxígeno que respiramos y constituyen la fuente directa o indirecta de casi todos los alimentos que consumimos. El interés del estudio y la eventual manipulación del desarrollo de las hojas radica en que son el órgano fotosintético básico, en torno al cual gravita la vida en nuestro planeta. Mediante abordajes genéticos clásicos se han obtenido centenares de mutantes que manifiestan perturbaciones en el desarrollo foliar, pero no se ha alcanzado la saturación del genoma de Arabidopsis.

El grupo del Prof. J.R. Ecker, en el Salk Institute, está generando una colección indexada de líneas homocigóticas para inserciones de ADN-T en casi todos los genes de Arabidopsis. Con el objetivo de identificar nuevos genes implicados en la regulación de la forma o el tamaño de la hoja, estamos sometiendo a escrutinio 20.718 de estas líneas, que corresponden a 14.585 genes. Hemos analizado la morfología foliar de 16.400 líneas, identificando 518 que muestran un fenotipo mutante con penetrancia completa y expresividad relativamente constante. Hemos genotipado 300 de ellas, comprobando en el 74% de los casos que la inserción de ADN-T está presente en homocigosis en el locus anotado. Esta colección resultará especialmente útil para el estudio del crecimiento de las plantas: No existen alelos previamente descritos de los genes mutados en el 56% de estas líneas; entre los restantes, solo un 15% han sido relacionados con el desarrollo foliar.

Con el objetivo de compartir la información obtenida, que incluye imágenes y descripciones ontológicas de los fenotipos encontrados, hemos implementado una base de datos y una aplicación web para su consulta.

XI Reunión de Biología Molecular de Plantas
Segovia, 2012
Póster

Genética inversa del desarrollo foliar

Wilson-Sánchez, D., Jover-Gil, S., Pérez-Pérez, J.M., Ponce, M.R., y Micol, J.L.

Instituto de Bioingeniería, Universidad Miguel Hernández, Campus de Elche, 03202 Elche, Alicante.
dwilson@umh.es jlmicol@umh.es www.agron-omics.eu genetica.umh.es

Las hojas de las plantas producen el oxígeno que respiramos y constituyen la fuente directa o indirecta de casi todos los alimentos que consumimos. El interés del estudio y la eventual manipulación del desarrollo de las hojas radica en que son el órgano fotosintético básico, en torno al cual gravita la vida en nuestro planeta. Mediante abordajes genéticos clásicos se han obtenido centenares de mutantes que manifiestan perturbaciones en el desarrollo foliar, pero no se ha alcanzado la saturación del genoma de Arabidopsis[1].

El grupo del Prof. J.R. Ecker, en el Salk Institute, está generando una colección indexada de líneas homocigóticas para inserciones de ADN-T en casi todos los genes de Arabidopsis[2,3]. Con el objetivo de identificar nuevos genes implicados en la regulación de la forma o el tamaño de la hoja, estamos sometiendo a escrutinio 20.718 de estas líneas, que corresponden a 14.585 genes. Hemos analizado la morfología foliar de 16.400 líneas, identificando 518 que muestran un fenotipo mutante con penetrancia completa y expresividad relativamente constante (Fig. 1 y 2, y Tabla 1). Hemos genotipado 300 de ellas, comprobando en el 74% de los casos que la inserción de ADN-T está presente en homocigosis en el locus anotado (Fig. 3 y Tabla 2). Esta colección resultará especialmente útil para el estudio del crecimiento de las plantas: No existen alelos previamente descritos[4] de los genes mutados en el 56% de estas líneas; entre los restantes, solo un 15% han sido relacionados con el desarrollo foliar.

Con el objetivo de compartir la información obtenida, que incluye imágenes y descripciones ontológicas de los fenotipos encontrados, hemos implementado una base de datos pública y una aplicación web para su consulta (Fig. 4). Las semillas de las líneas con fenotipo mutante serán depositadas en los centros de distribución.

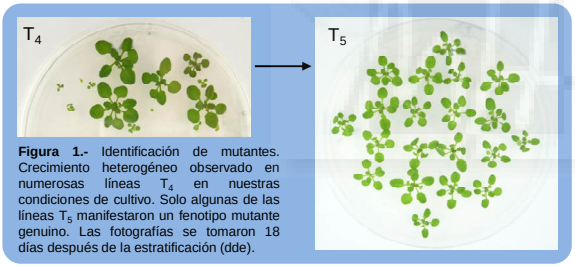

Figura 1.- Identificación de mutantes. Crecimiento heterogéneo observado en numerosas líneas T_4 en nuestras condiciones de cultivo. Solo algunas de las líneas T_5 manifestaron un fenotipo mutante genuino. Las fotografías se tomaron 18 días después de la estratificación (dde).

Tabla 1.- Progreso de nuestro escrutinio de mutantes foliares

	Líneas T_4		Mutantes genuinos confirmados en la generación T_5
	estudiadas	con hojas anormales	
Completadas	16.400	2.567	518
En estudio	2.500	450	79*
Total	18.900	3.017	597*

*Valores esperados

Tabla 2.- Genotipado de familias T_5 mutantes

Genotipo respecto a la inserción anotada	Número de líneas	Porcentaje
Homocigóticas	252	74,1
Segregantes	12	3,5
Silvestres	76	22,4
Total	340	100,0

AGRADECIMIENTOS

Esta investigación ha sido financiada por la Generalitat Valenciana (PROMETEO/2009/112) y la Comisión Europea [LSHG-CT-2006-037704 (AGRON-OMICS)]. D.W.-S. es contratado del programa VALi+d de la Generalitat Valenciana.

REFERENCIAS

1.- Berná, G., Robles, P., y Micol, J.L. (1999). *Genetics* **152,** 729-742.
2.- Alonso, J.M., *et al.* (2003). *Science* **301,** 653-657.
3.- O´Malley, R.C., y Ecker, J.R. (2010). *Plant J.* **61,** 928-940.
4.- Lloyd, J. y Meinke, D. (2012). *Plant Physiol.* **158,** 1115-1129

Figura 2.- Rosetas de (A) el tipo silvestre Col-0 y (B-T) 23 de los mutantes foliares identificados en nuestro escrutinio. Las fotografías se tomaron 21 dde. Barras de escala: 1 mm.

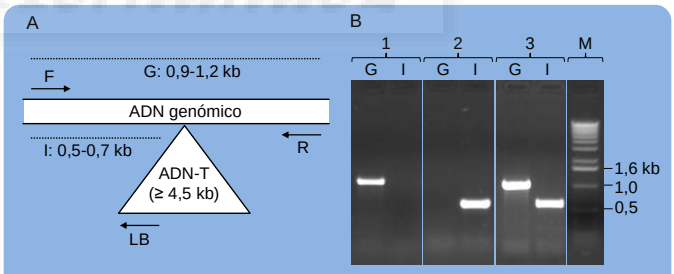

Figura 3.- Genotipado de líneas T_5 con fenotipo mutante. Se recolectaron hojas de 7 plantas T_5 que mostraban inequívocamente el fenotipo mutante. (A) El genotipado de las inserciones de ADN-T en los genes anotados se realizó siguiendo las recomendaciones del laboratorio de J.R. Ecker (http://signal.salk.edu/isects.html). (B) Productos de la amplificación del ADN de una planta (1) silvestre, (2) homocigótica y (3) heterocigótica para la inserción a estudio. Las calles G e I corresponden a los productos de amplificación obtenidos empleando las parejas de cebadores F+R y F+LB, respectivamente.

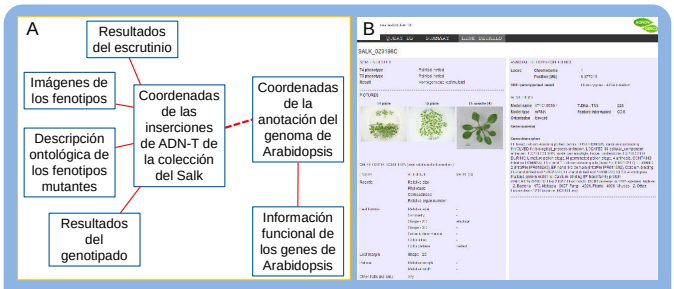

Figura 4.- (A) Estructura de la base de datos relacional que hemos implementado. Contiene información fenotípica de todas las líneas analizadas en nuestro escrutinio, fotografías de placa con grupos de plantas de las generaciones T_4 y T_5, fotografías de rosetas individuales, y los resultados del genotipado de las que mostraron fenotipo foliar. La comparación entre las coordenadas de las inserciones de ADN-T y las de la anotación del genoma de Arabidopsis permite detectar los genes interrumpidos en cada caso. En nuestra base de datos pueden emplearse como criterios de búsqueda rasgos fenotípicos y códigos AGI de genes de Arabidopsis. (B) Volcado de pantalla de la aplicación web de consulta, en el que se muestra información sobre el fenotipo de una línea insercional y el gen que presuntamente lo causa. La aplicación estará disponible en http://agron-omics.umh.es.

A collection of Arabidopsis gene-indexed leaf mutants

Wilson-Sanchez, D., Jover-Gil, S., Pérez-Pérez, J.M., Sáez-Chica, D., Ponce, M.R., and Micol, J.L.

Instituto de Bioingeniería, Universidad Miguel Hernández, 03202 Elche, Alicante, Spain.

The interest of the study and eventual manipulation of plant leaf development lays on the fact that they are the fundamental photosynthetic organ, of vital importance for life in our planet. Although hundreds of Arabidopsis mutants with altered leaf development have been isolated using forward genetics, saturation has not yet been reached. The group of Prof. J.R. Ecker, at The Salk Institute, is producing a large collection of gene-indexed homozygous T-DNA insertion mutants. Aiming to identify novel genes required for leaf development, we are screening 24,000 of these lines, which correspond to 17,850 genes. So far, we have identified 585 lines that exhibit a leaf phenotype with full penetrance and almost constant expressivity. We genotyped the annotated locus in 450 mutants and found that the indexed mutation is present in 76% of them. Together with cosegregation and allelism tests, these results indicate that at least 50% of our mutants owe their phenotypes to the annotated T-DNA insertion. Adapter ligation-mediated PCR and deep-sequencing allowed us to determine that the average number of T-DNA insertions in our leaf mutants is 2.1. We implemented a public database and a web-based query application that collects the results of our screen and the characterization of the mutants.

Society for Experimental Biology Annual Meeting
Valencia, 2013
Conferencia pronunciada por J.L. Micol, por invitación.

A collection of Arabidopsis gene-indexed leaf mutants

David Wilson-Sánchez, Sara Jover-Gil, José Manuel Pérez-Pérez, Diana Sáez-Chica, María Rosa Ponce, and José Luis Micol.

Instituto de Bioingeniería, Universidad Miguel Hernández, Campus de Elche, 03202 Elche, Alicante, Spain.
jlmicol@umh.es dwilson@umh.es www.agron-omics.eu genetica.umh.es

The interest of the study and eventual manipulation of leaf development lays on the fact that they are the fundamental photosynthetic organ, of vital importance for life in our planet. Although hundreds of mutants with altered leaf development have been isolated using forward genetics, saturation has not yet been reached for the Arabidopsis genome[1].

The group of Prof. J.R. Ecker, at The Salk Institute, is obtaining a large collection of gene-indexed homozygous T-DNA insertion mutants[2,3]. Aiming to identify novel genes required for leaf growth, we are screening 20,718 of these lines, which correspond to 14,585 genes. So far, we have analyzed the leaf phenotype of 16,400 lines, and identified 518 that show a mutant phenotype with full penetrance and almost constant expressivity (Figure 1 and Table 1). We have genotyped 450 of these genuine leaf mutants, finding that a T-DNA insertion is homozygous at the annotated locus in 342 of them (Figures 2 and 3). Among these 342 genes interrupted, only 50 have previously characterized alleles[4] and, according to TAIR functional annotation, there is no information available on the function of 195 of them. These figures highlight the value of our collection.

We have implemented a public database and a web-based query application that collects the results of our screen and the preliminary characterization of the mutant phenotypes (Figure 4). It will be soon available at http://agron-omics.umh.es.

120 genuine leaf mutants with a confirmed homozygous T-DNA insertion have been subjected to detailed time-lapse qualitative and quantitative phenotypic analyses.

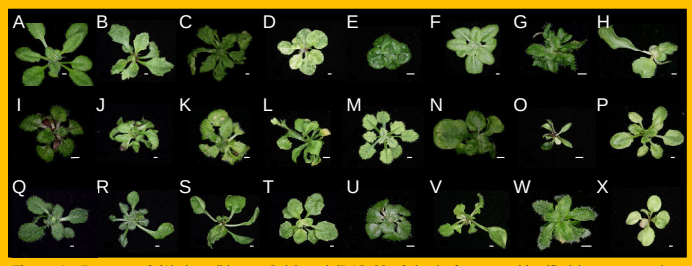

Figure 1.- Rosettes of (A) the wild type Col-0 and (B-X) 23 of the leaf mutants identified in our screening. Pictures were taken 21 days after stratification (das). Scale bars: 1 mm.

Table 1.- Progress of our screening

	T_4 lines		T_5 genuine mutants confirmed
	studied	exhibiting anormal leaves	
Completed	18,400	3,170	585
In progress	1,600	250	46*
Total	20,000	3,420	631*

*Expected values

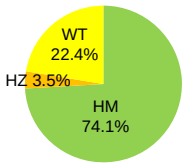

Figure 2.- Genotyping of genuine leaf mutants. Almost three quarters of all lines genotyped are homozygous for the annotated insertion, 3.5% harbour a segregating insertion, and in the remaining 22.4% the insertion is absent from the annotated locus.

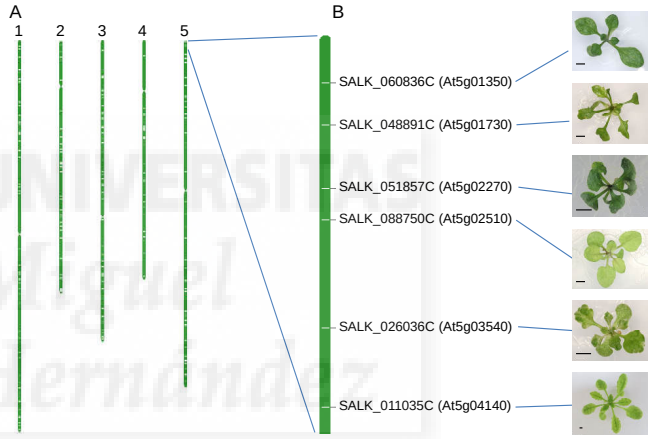

Figure 3.- We performed a phenotype-driven screen on a gene-indexed mutant collection. (A) Position of the 252 homozygous T-DNA insertions confirmed in our laboratory so far, laid out using the TAIR map visualization tool (http://www.arabidopsis.org/servlets/ViewChromosomes). Numbers on the top of each bar identify the 5 Arabidopsis chromosomes. (B) Enlargement of a randomly chosen interval showing 6 loci disrupted by T-DNA insertions, with their corresponding Salk codes and rosette phenotypes observed. Scale bars: 2 mm.

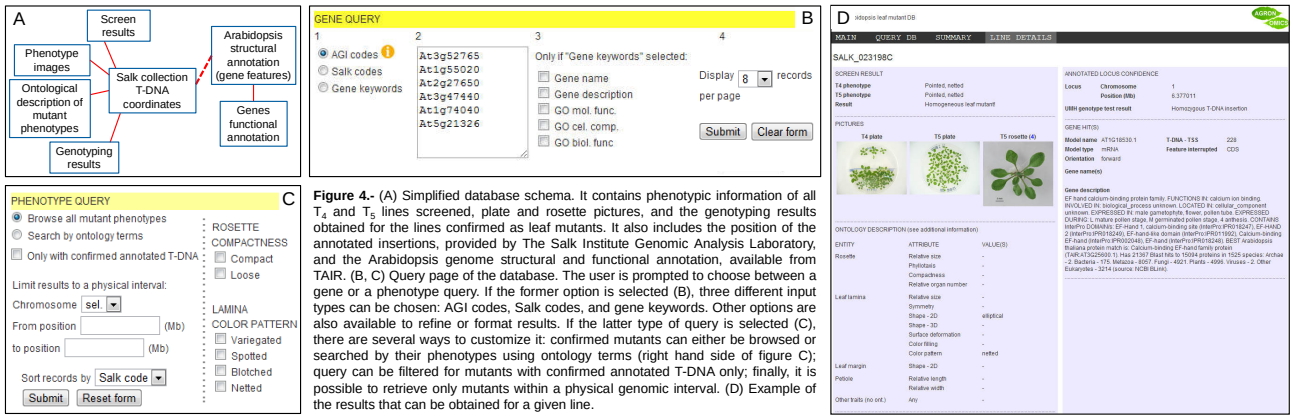

Figure 4.- (A) Simplified database schema. It contains phenotypic information of all T_4 and T_5 lines screened, plate and rosette pictures, and the genotyping results obtained for the lines confirmed as leaf mutants. It also includes the position of the annotated insertions, provided by The Salk Institute Genomic Analysis Laboratory, and the Arabidopsis genome structural and functional annotation, available from TAIR. (B, C) Query page of the database. The user is prompted to choose between a gene or a phenotype query. If the former option is selected (B), three different input types can be chosen: AGI codes, Salk codes, and gene keywords. Other options are also available to refine or format results. If the latter type of query is selected (C), there are several ways to customize it: confirmed mutants can either be browsed or searched by their phenotypes using ontology terms (right hand side of figure C); query can be filtered for mutants with confirmed annotated T-DNA only; finally, it is possible to retrieve only mutants within a physical genomic interval. (D) Example of the results that can be obtained for a given line.

ACKNOWLEDGEMENTS

Research in the laboratory of J.L.M. is supported by grants from the Ministerio de Ciencia e Innovación of Spain [BFU2011-22825 and CSD2007-00057 (TRANSPLANTA)], the Generalitat Valenciana (PROMETEO/2009/112) and the European Commission [LSHG-CT-2006-037704 (AGRON-OMICS)]. D.W.-S. is a predoctoral fellow of the Generalitat Valenciana VALI+d programme.

REFERENCES

1.- Berná, G., Robles, P., and Micol, J.L. (1999). *Genetics* **152,** 729-742.
2.- Alonso, J.M., *et al*. (2003). *Science* **301,** 653-657.
3.- O´Malley, R.C., and Ecker, J.R. (2010). *Plant J.* **61,** 928-940.
4.- Lloyd, J. and Meinke, D. (2012). *Plant Physiol.* **158**, 1115-1129

A genetic and molecular study of leaf lamina symmetry

Wilson-Sanchez, D., Jover-Gil, S., Sáez-Chica, D., and Micol, J.L.

Instituto de Bioingeniería, Universidad Miguel Hernández, 03202 Elche, Alicante, Spain.

We screened for perturbations in leaf bilateral symmetry among 17,000 Arabidopsis lines from the Salk homozygous T-DNA collection. One of the mutants that we isolated exhibited asymmetric leaf laminae and impaired reproductive organ development. In this mutant, lamina asymmetry arises because of outgrowths and/or growth defects, pointing to a role of the mutated gene in the coordination of lamina growth. The mutant phenotype is more extreme in adult rosette leaves, suggesting that the gene mutated is regulated over time and that could be related to the molecular machinery that controls leaf heteroblasty. Symmetry deviations are mostly limited to the basal region of the leaf lamina. The flowers and siliques of this mutant also show morphological aberrations. About 5% of the flowers are misshappen, the ovary being the most affected organ. Some, but not all these flowers also present organ identity defects, such as ectopic ovules and stigma hairs. An equal percentage of siliques are bent or twisted. To determine the contribution of cell division and cell expansion to the observed asymmetries, we analyzed young 8th-node leaf primordia in which the cells of the basal portion of the lamina had not yet started to expand. These primordia were already asymmetric, confirming that cell division regulation is altered and that this contributes to the observed asymmetry. A *CYCB1;1pro:GUS* transgene was transferred into our mutant in order to monitor cell division. Mutations in previously described genes also cause leaf asymmetry and impaired flower and silique development: *ASYMMETRIC LEAVES2*, *BARELY ANY MERISTEM*, *JAGGED LATERAL ORGANS*, *STRUBBELIG*, *TORNADO* and *BLADE-ON-PETIOLE* genes. A genetic analysis of their potential functional relationships with the gene under study is underway. We confirmed that At2g32280 is the gene responsible for the phenotype of SALK_047972 by analyzing several independent alleles and complementation analyses. We are studying its expression pattern and the subcellular localization of its protein product. We are also studying its closest paralogs and their genetic interactions.

Society for Experimental Biology Annual Meeting
Valencia, 2013
Póster

A genetic and molecular study of leaf lamina symmetry

Wilson-Sánchez, D., Jover-Gil, S., Sáez-Chica, D., and Micol, J.L.

Instituto de Bioingeniería, Universidad Miguel Hernández, Campus de Elche, 03202 Elche, Alicante, Spain
dwilson@umh.es jlmicol@umh.es genetica.umh.es

We screened for perturbations in leaf bilateral symmetry among 17,000 Arabidopsis lines from the Salk homozygous T-DNA collection[1] (oral communication C1.17). One of the mutants that we isolated exhibited asymmetric leaf laminae and impaired reproductive organ development (Figs. 1A and 3). In this mutant, lamina asymmetry arises because of outgrowths and/or growth defects (Fig. 1B, C), pointing to a role of the mutated gene in the coordination of lamina growth. The mutant phenotype is more extreme in adult rosette leaves (Fig. 1D, E), suggesting that the gene mutated is regulated over time and that could be related to the molecular machinery that controls leaf heteroblasty. Symmetry deviations are mostly limited to the basal region of the leaf lamina.

The flowers and siliques of this mutant also show morphological aberrations. About 5% of the flowers are misshappen, the ovary being the most affected organ. Some, but not all these flowers also present organ identity defects, such as ectopic ovules and stigma hairs (Fig. 2A-C). An equal percentage of siliques are bent or twisted (Fig. 2D-F).

To determine the contribution of cell division and cell expansion to the observed asymmetries, we analyzed young 8th-node leaf primordia (Fig. 3A-D) in which the cells of the basal portion of the lamina had not yet started to expand (Fig. 3E-G). These primordia were already asymmetric (Fig. 3D), confirming that cell division regulation is altered and that this contributes to the observed asymmetry. A *CYCB1;1$_{pro}$:GUS* transgene was transferred into our mutant in order to monitor cell division.

Mutations in previously described genes also cause leaf asymmetry and impaired flower and silique development: *ASYMMETRIC LEAVES2*, *BARELY ANY MERISTEM*, *JAGGED LATERAL ORGANS*, *STRUBBELIG*, *TORNADO* and *BLADE-ON-PETIOLE* genes. A genetic analysis of their potential functional relationships with the gene under study is underway.

We confirmed that At2g32280 is the gene responsible for the phenotype of SALK_047972 by analyzing several independent alleles (Fig. 4) and complementation analyses. We are studying its expression pattern and the subcellular localization of its protein product. We are also studying its closest paralogs and their genetic interactions.

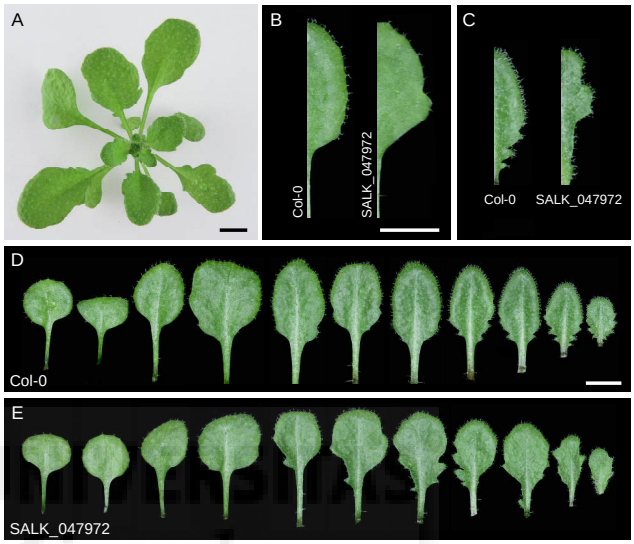

Figure 1.- Leaf phenotype of SALK_047972. (A) Mutant rosette showing some asymmetric leaves. (B) Comparison of Col-0 (left) and mutant (right) laminae, showing an outgrowth in the basal region. (C) Comparison of Col-0 (left) and mutant (right) laminae, showing an invagination in the basal region. (D, E) Cotyledons and leaves of (D) Col-0 and (E) SALK_047972, showing increased asymmetry in adult leaves. (B, C) Pictures correspond to (B) 6th- and (C) 10th-node leaves. Pictures were taken 21 days after stratification (das). Scale bars: 5 mm.

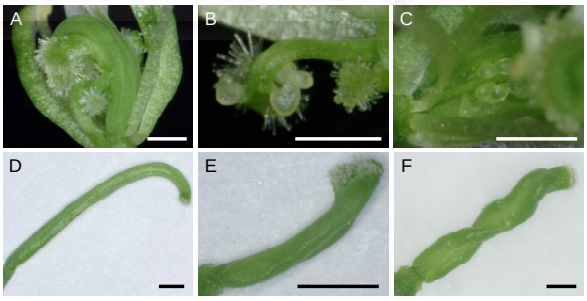

Figure 2.- Flower and silique phenotypes of SALK_047972. (A) Flower showing a bent ovary and an staminoid structure with stigma hairs. Some petals and sepals have been removed. (B) Aberrant organ comprising an anther filament-like structure with ectopic stigma hairs and ovule-like structures attached to the tip. (C) Unfused gynoecium with ovules exposed. (D-F) Siliques exhibiting different degrees of bending, twisting and helical rotation. Scale bars: (A-C) 0.5 and (D-F) 1 mm.

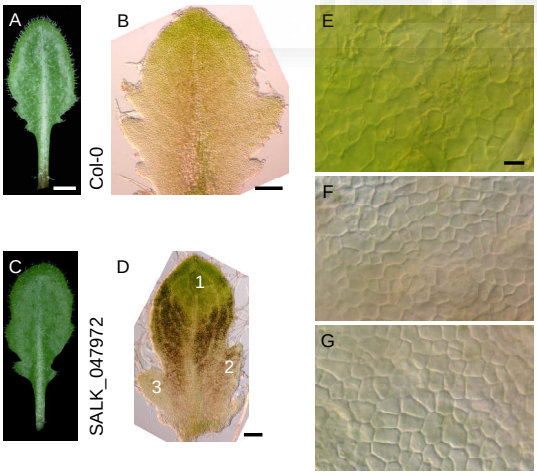

Figure 3.- Histology of SALK_047972. (A, D) 8th-node (A, C) leaves and (B, D) primordia from (A-B) Col-0 and a (C-D) mutant plant. The primordium in (D) is already asymmetric. (E-G) Magnifications of the abaxial epidermis of the primordium shown in (D), showing the epidermal cells from regions marked as (E) '1', (F) '2', and (G) '3'. In regions 2 and 3, where asymmetry occurs, cells display a square-like shape and still do not form a jigsaw puzzle pattern, indicating that they are not differentiated, and that expansion has not started yet[2,3]. In region 1 both processes have only just started. Pictures were taken (A, C) 21 and (B, D, E-F) 14 das. Scale bars: (A, C) 2 mm, (B, D) 100 and (E-G) 10 µm.

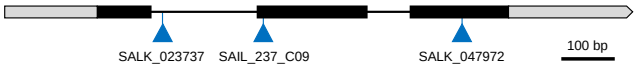

Figure 4.- Structure of At2g32280 and position of the T-DNA insertions studied. Exons are depicted as boxes, and their translared regions shaded black. Introns are represented as lines.

REFERENCES

1.- Alonso, J.M., *et al*. (2003). *Science* **301**, 653-657.
2.- González, N., Vanhaeren, H., and Inzé, D. (2012). *Trends Plant Sci.* **17-6**, 332-340.
3.- Adriankaja, M., *et al.* (2012). *Dev. Cell* **22**, 64-78.

ACKNOWLEDGEMENTS

Research in the laboratory of J.L.M. is supported by grants from the Ministerio de Economía y Competitividad of Spain [BFU2011-22825 and CSD2007-00057 (TRANSPLANTA)], the Generalitat Valenciana (PROMETEO/2009/112) and the European Commission [LSHG-CT-2006-037704 (AGRON-OMICS)]. D.W.-S. is a predoctoral fellow of the Generalitat Valenciana VALI+d programme.

Genética inversa del desarrollo foliar

Wilson-Sánchez, D., Jover-Gil, S., Pérez-Pérez, J.M., Ponce, M.R., y Micol, J.L.

Instituto de Bioingeniería, Universidad Miguel Hernández, Campus de Elche, 03202 Elche, Alicante.

Las hojas de las plantas producen el oxígeno que respiramos y constituyen la fuente directa o indirecta de casi todos los alimentos que consumimos. El interés del estudio y la eventual manipulación del desarrollo de las hojas radica en que son el órgano fotosintético básico, en torno al cual gravita la vida en nuestro planeta. Mediante abordajes genéticos clásicos se han obtenido centenares de mutantes que manifiestan perturbaciones en el desarrollo foliar, pero no se ha alcanzado la saturación del genoma de Arabidopsis. El grupo del Prof. J.R. Ecker, en el Salk Institute, está generando una colección indexada de líneas homocigóticas para inserciones de ADN-T en casi todos los genes de Arabidopsis. Con el objetivo de identificar nuevos genes implicados en la regulación de la forma o el tamaño de la hoja, estamos sometiendo a escrutinio 20.718 de estas líneas, que corresponden a 14.585 genes. Hemos analizado la morfología foliar de 16.400 líneas, identificando 518 que muestran un fenotipo mutante con penetrancia completa y expresividad relativamente constante. Hemos genotipado 300 de ellas, comprobando en el 74% de los casos que la inserción de ADN-T está presente en homocigosis en el locus anotado. Esta colección resultará especialmente útil para el estudio del crecimiento de las plantas: No existen alelos previamente descritos de los genes mutados en el 56% de estas líneas; entre los restantes, solo un 15% han sido relacionados con el desarrollo foliar. Con el objetivo de compartir la información obtenida, que incluye imágenes y descripciones ontológicas de los fenotipos encontrados, hemos implementado una base de datos y una aplicación web para su consulta.

XXXIX Congreso de la Sociedad Española de Genética

Girona, 2013

Póster

Genética inversa del desarrollo foliar

Wilson-Sánchez, D., Jover-Gil, S., Pérez-Pérez, J.M., Ponce, M.R., y Micol, J.L.

Instituto de Bioingeniería, Universidad Miguel Hernández, Campus de Elche, 03202 Elche, Alicante.
dwilson@umh.es jlmicol@umh.es www.agron-omics.eu genetica.umh.es

Las hojas de las plantas producen el oxígeno que respiramos y constituyen la fuente directa o indirecta de casi todos los alimentos que consumimos. El interés del estudio y la eventual manipulación del desarrollo de las hojas radica en que son el órgano fotosintético básico, en torno al cual gravita la vida en nuestro planeta. Mediante abordajes genéticos clásicos se han obtenido centenares de mutantes que manifiestan perturbaciones en el desarrollo foliar, pero no se ha alcanzado la saturación del genoma de Arabidopsis[1].

El grupo del Prof. J.R. Ecker, en el Salk Institute, está generando una colección indexada de líneas homocigóticas para inserciones de ADN-T en casi todos los genes de Arabidopsis[2,3]. Con el objetivo de identificar nuevos genes implicados en la regulación de la forma o el tamaño de la hoja, estamos sometiendo a escrutinio 20.718 de estas líneas, que corresponden a 14.585 genes. Hemos analizado la morfología foliar de 16.400 líneas, identificando 518 que muestran un fenotipo mutante con penetrancia completa y expresividad relativamente constante (Fig. 1 y 2, y Tabla 1). Hemos genotipado 300 de ellas, comprobando en el 74% de los casos que la inserción de ADN-T está presente en homocigosis en el locus anotado (Fig. 3 y Tabla 2). Esta colección resultará especialmente útil para el estudio del crecimiento de las plantas: No existen alelos previamente descritos[4] de los genes mutados en el 56% de estas líneas; entre los restantes, solo un 15% han sido relacionados con el desarrollo foliar.

Con el objetivo de compartir la información obtenida, que incluye imágenes y descripciones ontológicas de los fenotipos encontrados, hemos implementado una base de datos pública y una aplicación web para su consulta (Fig. 4). Las semillas de las líneas con fenotipo mutante serán depositadas en los centros de distribución.

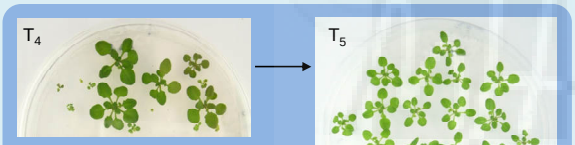

Figura 1.- Identificación de mutantes. Crecimiento heterogéneo observado en numerosas líneas T_4 en nuestras condiciones de cultivo. Solo algunas de las líneas T_5 manifestaron un fenotipo mutante genuino. Las fotografías se tomaron 18 días después de la estratificación (dde).

Tabla 1.- Progreso de nuestro escrutinio de mutantes foliares

	Líneas T_4		Mutantes genuinos confirmados en la generación T_5
	estudiadas	con hojas anormales	
Completadas	16.400	2.567	518
En estudio	2.500	450	79*
Total	18.900	3.017	597*

*Valores esperados

Tabla 2.- Genotipado de familias T_5 mutantes

Genotipo respecto a la inserción anotada	Número de líneas	Porcentaje
Homocigóticas	252	74,1
Segregantes	12	3,5
Silvestres	76	22,4
Total	340	100,0

AGRADECIMIENTOS

Esta investigación ha sido financiada por la Generalitat Valenciana (PROMETEO/2009/112) y la Comisión Europea [LSHG-CT-2006-037704 (AGRON-OMICS)]. D.W.-S. es contratado del programa VALi+d de la Generalitat Valenciana.

REFERENCIAS

1.- Bernà, G., Robles, P., y Micol, J.L. (1999). *Genetics* **152,** 729-742.
2.- Alonso, J.M., *et al.* (2003). *Science* **301,** 653-657.
3.- O´Malley, R.C., y Ecker, J.R. (2010). *Plant J.* **61,** 928-940.
4.- Lloyd, J. y Meinke, D. (2012). *Plant Physiol.* **158,** 1115-1129

Figura 2.- Rosetas de (A) el tipo silvestre Col-0 y (B-T) 23 de los mutantes foliares identificados en nuestro escrutinio. Las fotografías se tomaron 21 dde. Barras de escala: 1 mm.

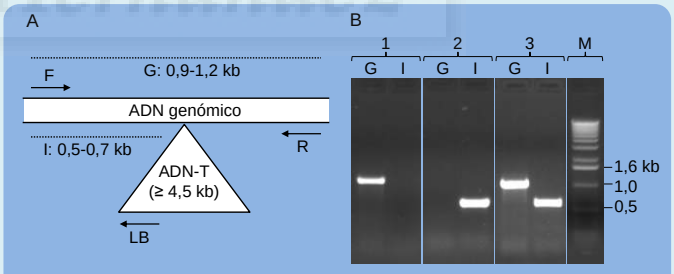

Figura 3.- Genotipado de líneas T_5 con fenotipo mutante. Se recolectaron hojas de 7 plantas T_5 que mostraban inequívocamente el fenotipo mutante. (A) El genotipado de las inserciones de ADN-T en los genes anotados se realizó siguiendo las recomendaciones del laboratorio de J.R. Ecker (http://signal.salk.edu/isects.html). (B) Productos de la amplificación del ADN de una planta (1) silvestre, (2) homocigótica y (3) heterocigótica para la inserción a estudio. Las calles G e I corresponden a los productos de amplificación obtenidos empleando las parejas de cebadores F+R y F+LB, respectivamente.

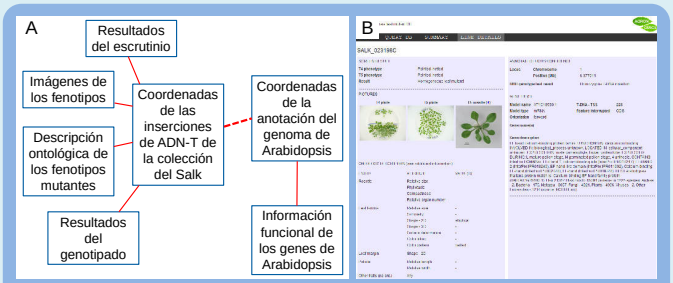

Figura 4.- (A) Estructura de la base de datos relacional que hemos implementado. Contiene información fenotípica de todas las líneas analizadas en nuestro escrutinio, fotografías de placa con grupos de plantas de las generaciones T_4 y T_5, fotografías de rosetas individuales, y los resultados del genotipado de las que mostraron fenotipo foliar. La comparación entre las coordenadas de las inserciones de ADN-T y las de la anotación del genoma de Arabidopsis permite detectar los genes interrumpidos en cada caso. En nuestra base de datos pueden emplearse como criterios de búsqueda rasgos fenotípicos y códigos AGI de genes de Arabidopsis. (B) Volcado de pantalla de la aplicación web de consulta, en el que se muestra información sobre el fenotipo de una línea insercional y el gen que presuntamente lo causa. La aplicación estará disponible en http://agron-omics.umh.es.

Leaf phenomics: a systematic reverse genetic screen for Arabidopsis leaf mutants

Wilson-Sánchez, D., Jover-Gil, S., Torres-Martínez, S., Ponce, M.R., and Micol, J.L.

Instituto de Bioingeniería, Universidad Miguel Hernández, 03202 Elche, Alicante, Spain.

The study and eventual manipulation of plant leaf development requires a thorough understanding of the genetic regulation of leaf organogenesis. Forward genetic screens have identified hundreds of Arabidopsis mutants with altered leaf development, but the genome has not yet been saturated. To identify novel genes required for leaf development, we are screening the Arabidopsis Salk Unimutant collection. So far, we have identified 608 lines that exhibit a leaf phenotype with full penetrance and almost constant expressivity, and 98 additional lines with segregating mutant phenotypes. To allow indexing and integration with other mutants, the mutant phenotypes were described using a custom leaf phenotype ontology. We found that the indexed mutation is present in the annotated locus for 78% of the 553 mutants genotyped, and that in half of these the annotated T-DNA is responsible for the phenotype. To quickly map non-annotated T-DNA insertions, we developed a cost-effective and easy method based on whole-genome sequencing, and proved its reliability. To enable comprehensive access to our data, we implemented a public web application named PhenoLeaf (http://genetics.umh.es/phenoleaf) that allows researchers to query the results of our screen, including text and visual phenotype information. We demonstrated how this new resource can facilitate gene function discovery by identifying and characterizing At1g77600, which we found to be required for proximal-distal cell cycle-driven leaf growth, and At3g62870, which encodes a ribosomal protein needed for cell proliferation and chloroplast function. This collection provides a valuable tool for the study of leaf development, characterization of biomass feedstocks, and examination of other traits in this fundamental photosynthetic organ.

XII Reunión de Biología Molecular de Plantas

Cartagena, 2014

Póster

Reverse genetics of leaf development

David Wilson-Sánchez, Sara Jover-Gil, José Manuel Pérez-Pérez, María Rosa Ponce and José Luis Micol

Instituto de Bioingeniería, Universidad Miguel Hernández, Campus de Elche, 03202 Elche, Alicante, Spain.
jlmicol@umh.es dwilson@umh.es www.agron-omics.ethz.ch genetics.umh.es

The study and eventual manipulation of plant leaf development requires a thorough understanding of the genetic regulation of leaf organogenesis. Forward genetic screens have identified hundreds of Arabidopsis mutants with altered leaf development, but the genome has not yet been saturated[1]. To identify novel genes required for leaf development, we are screening the Arabidopsis Salk Unimutant collection[2,3].

So far, we have identified 608 lines that exhibit a leaf phenotype with full penetrance and almost constant expressivity, and 98 additional lines with segregating mutant phenotypes (Figure 1 and Table 1). To allow indexing and integration with other mutant collections, the mutant phenotypes were described using a custom leaf phenotype ontology. We found that the indexed mutation is present in the annotated locus for 78% of the 553 mutants genotyped, and that in half of these the annotated T-DNA is responsible for the phenotype (Figures 2 and 3). To quickly map non-annotated T-DNA insertions, we developed a cost-effective and easy method based on whole-genome sequencing, and proved its reliability[4].

To enable comprehensive access to our data, we implemented a public web application named PhenoLeaf (http://genetics.umh.es/phenoleaf) that allows researchers to query the results of our screen, including text and visual phenotype information (Figure 4). We demonstrated how this new resource can facilitate gene function discovery by identifying and characterizing At1g77600, which we found to be required for proximal-distal cell cycle-driven leaf growth, and At3g62870, which encodes a ribosomal protein needed for cell proliferation and chloroplast function. This collection provides a valuable tool for the study of leaf development, characterization of biomass feedstocks, and examination of other traits in this fundamental photosynthetic organ[4].

Table 1.- Status of our screen

T_4 lines		T_5 genuine mutants confirmed
studied	exhibiting anormal leaves	
19,500	3,890	706

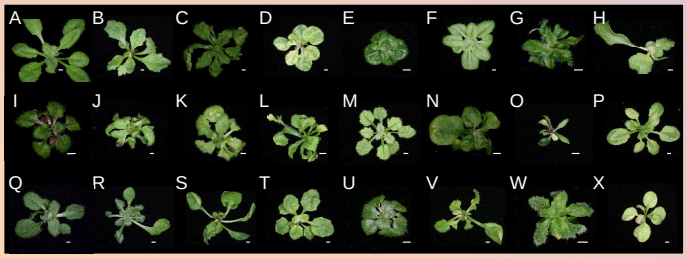

Figure 1.- Rosettes of (A) the wild type Col-0 and (B-X) 23 of the leaf mutants identified in our screening. Pictures were taken 21 days after stratification (das). Scale bars: 1 mm.

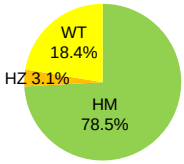

Figure 2.- Genotyping of genuine leaf mutants. More than three quarters of all lines genotyped are homozygous for the annotated insertion, 3.1% harbour a segregating insertion, and in the remaining 18.4% the insertion is absent from the annotated locus.

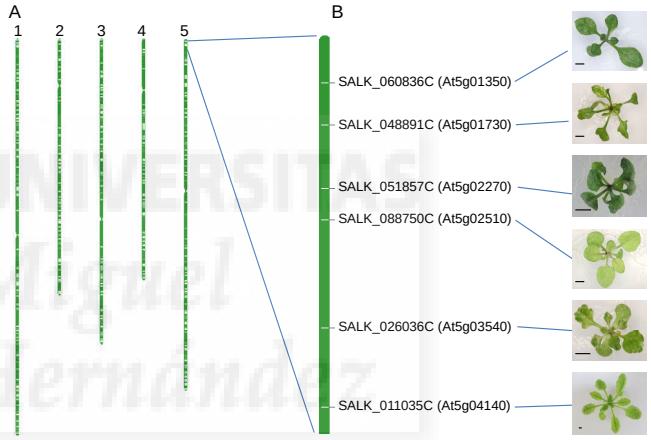

Figure 3.- We performed a phenotype-driven screen on a gene-indexed mutant collection. (A) Position of the 431 homozygous T-DNA insertions confirmed in our laboratory so far, laid out using the TAIR map visualization tool (http://www.arabidopsis.org/servlets/ViewChromosomes). Numbers on the top of each bar identify the 5 Arabidopsis chromosomes. (B) Enlargement of a randomly chosen interval showing 6 loci disrupted by T-DNA insertions, with their corresponding Salk codes and rosette phenotypes observed. Scale bars: 2 mm.

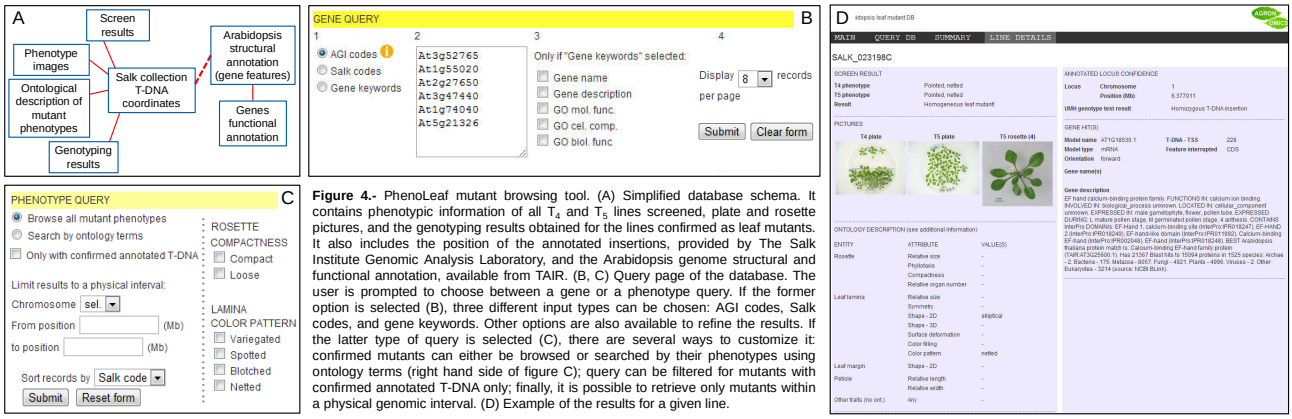

Figure 4.- PhenoLeaf mutant browsing tool. (A) Simplified database schema. It contains phenotypic information of all T_4 and T_5 lines screened, plate and rosette pictures, and the genotyping results obtained for the lines confirmed as leaf mutants. It also includes the position of the annotated insertions, provided by The Salk Institute Genomic Analysis Laboratory, and the Arabidopsis genome structural and functional annotation, available from TAIR. (B, C) Query page of the database. The user is prompted to choose between a gene or a phenotype query. If the former option is selected (B), three different input types can be chosen: AGI codes, Salk codes, and gene keywords. Other options are also available to refine the results. If the latter type of query is selected (C), there are several ways to customize it: confirmed mutants can either be browsed or searched by their phenotypes using ontology terms (right hand side of figure C); query can be filtered for mutants with confirmed annotated T-DNA only; finally, it is possible to retrieve only mutants within a physical genomic interval. (D) Example of the results for a given line.

ACKNOWLEDGEMENTS

Research in the laboratory of J.L.M. is supported by grants from the Ministerio de Ciencia e Innovación of Spain [BFU2011-22825 and CSD2007-00057 (TRANSPLANTA)], the Generalitat Valenciana (PROMETEO/2009/112) and the European Commission [LSHG-CT-2006-037704 (AGRON-OMICS)]. D.W.-S. is a predoctoral fellow of the Generalitat Valenciana VALI+d programme.

REFERENCES

1.- Berná, G., Robles, P., and Micol, J.L. (1999). *Genetics* **152,** 729-742.
2.- Alonso, J.M., *et al*. (2003). *Science* **301,** 653-657.
3.- O´Malley, R.C., and Ecker, J.R. (2010). *Plant J.* **61,** 928-940.
4.- Wilson-Sánchez, D., *et al.* (2014). *Plant J.*, in press.

DESIGUAL (*DEAL*) contributes to leaf bilateral symmetry maintenance through cell division

Wilson-Sánchez, D., Jover-Gil, S., García-Pérez, A., and Micol, J.L.

Instituto de Bioingeniería, Universidad Miguel Hernández, 03202 Elche, Alicante, Spain.

Plant leaves are a suitable model for developmental genetics due to its simplicity. Bilateral symmetry is an interesting but largely unknown leaf developmental trait. To identify novel genes required for the acquisition of leaf bilateral symmetry, we screened 15,000 Salk T-DNA mutants and found one that shows asymmetric leaves, which we named *desigual* (*deal*). Bilateral asymmetry appears only in deal adult leaves and arises from a combination of outgrowths and growth defects, pointing to a role of the mutated gene in the coordination of lamina expansion.

To assess the contribution of cell division and cell expansion to the observed asymmetry, we analyzed young leaf primordia in which the cells had not yet started to expand. Bilateral asymmetry was visible in these primordia, confirming that cell division regulation is altered at very early stages of deal leaf development. We tracked cell division using the *CYCB1;1pro:GUS* marker, showing that proliferation is unbalanced between both lamina halves. Cell morphometry across medial-lateral sections encompassing lamina lobes and sinuses revealed that cell expansion is not affected in the mutant. *deal* secondary vein terminations are also asymmetric, suggesting that auxin maxima formation is mislocalized. Furthermore, secondary vein connections to the midvein is altered, resembling weak *pin-formed 1* mutants. Thus, we started a set of experiments to ascertain whether there is a link between *DEAL* and auxin-driven patterning during leaf morphogenesis.

We identified *DEAL* as a gene of unknown function exclusive of multicellular plants, which has four predicted transmembrane spanning domains. GUS reporter analysis showed expression in the shoot apical meristem, leaf primordia and during early leaf development.

DESIGUAL contributes to leaf bilateral symmetry through cell division

Wilson-Sánchez, D., Jover-Gil, S., García-Pérez, A., and Micol, J.L.

Instituto de Bioingeniería,
Universidad Miguel Hernández,
Campus de Elche, 03202 Elche,
Alicante, Spain
dwilson@umh.es jlmicol@umh.es
genetics.umh.es

Plant leaves are a suitable model for developmental genetics due to its simplicity. Bilateral symmetry is an interesting but largely unknown leaf developmental trait. To identify novel genes required for the acquisition of leaf bilateral symmetry, we screened 15,000 Salk T-DNA mutants[1,2] and found one that shows asymmetric leaves, which we named *desigual* (*deal*). Bilateral asymmetry appears in *deal* adult leaves (Fig. 1A-C) and arises from a combination of outgrowths and growth defects (Fig. 1D,E), pointing to a role of the mutated gene in the coordination of lamina growth.

To assess the contribution of cell division and cell expansion to the observed asymmetry, we analyzed young leaf primordia in which cells had not yet started to expand. Bilateral asymmetry was visible in these primordia (Fig. 2A-G), confirming that cell division regulation is altered at very early stages of *deal* leaf development. We tracked cell proliferation using the *CYCB1;1pro:GUS* marker[4], showing that proliferation is unbalanced between both lamina halves (Fig. 2H-K). Cell morphometry across medial-lateral sections encompassing lamina lobes and sinuses revealed that cell expansion is not affected in the mutant (Fig. 3). *deal* secondary vein terminations and loops are also asymmetric, suggesting that auxin maxima formation is mislocalized. Furthermore, secondary vein connections to the midvein is altered, resembling weak *pin-formed 1* mutants. Thus, we started a set of experiments to ascertain whether there is a link between *DEAL* and auxin-driven patterning during leaf morphogenesis.

We identified *DEAL* as a gene of unknown function exclusive of multicellular plants, and predicted to be localized in the plasma membrane (Fig. 4AB). GUS reporter analysis showed expression in the shoot apical meristem, leaf primordia and during early leaf development (Fig. 4C-F).

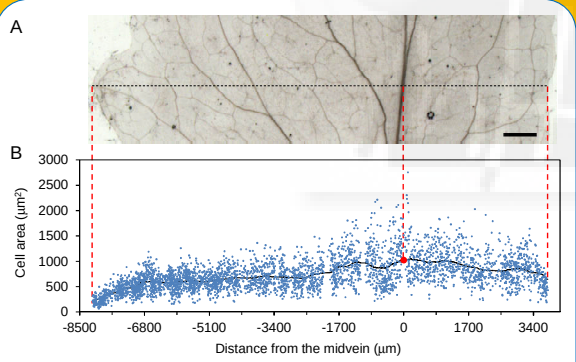

Figure 3.- Cell morphometry across a medial-lateral section of a *deal* leaf. (A) Portion of a fully-expanded 9th-node leaf showing more tissue growth to the left side of the midvein (8,164 versus 3,782 µm). Scale bar: 500 µm. (B) Cell area plotted against the distance from the midvein along the axis shown in (A) (dashed line). Note that cell proliferation accounts for the higher tissue growth at the left side of the midvein, and cell expansión does not. The red dot points the midvein position.

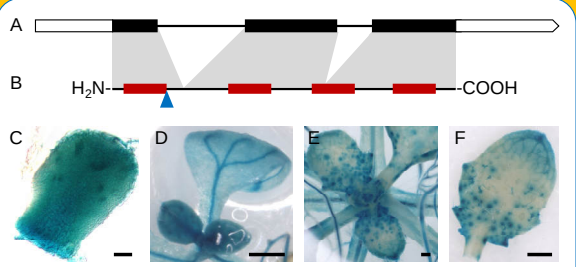

Figure 4.- *DEAL* expression and localization pattern. (A) *DEAL* transcript model, where the black boxes indicate exons. (B) DEAL protein model. The red boxes indicate predicted transmembrane domains and the blue arrow points the position of a predicted cleavage site of a target signal to the plasma membrane. (C-F) *DEALpro:GUS* staining in (C, D) 1st-node leaf primordia and (E, F) developing adult leaves. Scale bars: (C) 50 µm and (D-F) 500 µm.

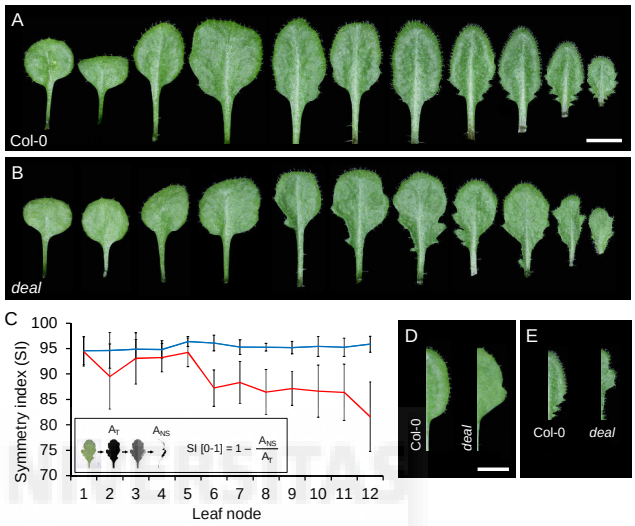

Figure 1.- Leaf macroscopic phenotype of *deal* mutants. (A, B) Dissected rosettes of Col-0 and *deal*, showing asymmetry in *deal* adult leaves. (C) Symmetry measurement by a quantitative method that we named Symmetry Index (SI). (D, E) Comparison of Col-0 and *deal* representative laminae, showing (D) an outgrowth and (E) an invagination in the basal region. Pictures correspond to (D) 6th- and (E) 10th-node leaves. Pictures were taken 21 days after stratification (das). Symmetry Index measurements were performed on fully expanded leaves. Scale bars: 5 mm.

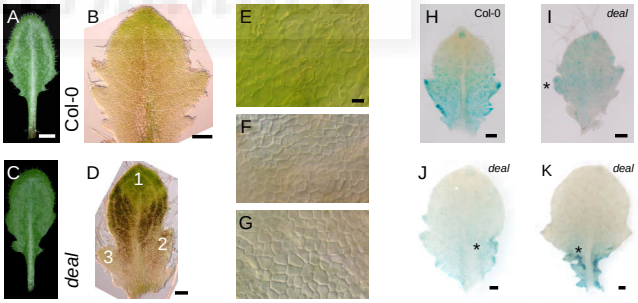

Figure 2.- Cell division-mediated lamina development in the *deal* mutant. (A-D) 8th-node (A, C) leaves and (B, D) primordia from (A-B) Col-0 and (C-D) *deal* plants. Note that the primordium in (D) is already asymmetric. (E-G) Magnifications of the abaxial protodermis of the primordium shown in (D), showing the protodermal cells from regions marked as (E) '1', (F) '2', and (G) '3'. In regions 2 and 3, where asymmetry occurs, cells display a square-like shape and still do not form a jigsaw puzzle pattern, indicating that they are not differentiated, and that expansion has not started yet[3]. In region 1 both processes have only just started. (H-K) *CYCB1;1pro:GUS* staining in *deal* leaves. Cell division arrest is not symmetric with respect to the midvein and the margin presents spots of abnormally high cyclin expression (asterisks). Scale bars: (A, C) 2 mm, (B, D) 100 µm, (E-G) 10 µm, (H-J) 100 µm, and (K) 200 µm.

ACKNOWLEDGEMENTS

Research in the laboratory of J.L.M. is supported by grants from the Ministerio de Economía y Competitividad of Spain [BFU2011-22825 and CSD2007-00057 (TRANSPLANTA)], the Generalitat Valenciana (PROMETEO/2009/112) and the European Commission [LSHG-CT-2006-037704 (AGRONOMICS)]. S.J-.G. holds the PIRG06-GA-2009-256579 (ARABIGANS) reintegrationgrant from the European Commission and D.W.-S. is a predoctoral fellow of the Generalitat Valenciana VALI+d programme.

REFERENCES

1.- Alonso, J.M., *et al.* (2003). *Science* **301**, 653-657.
2.- Wilson-Sánchez, D., *et al.* (2014). *Plant J.*, in press.
3.- Adriankaja, M., *et al.* (2012). *Dev. Cell* **22**, 64-78.
4.- Donnelly, P.M., et al. (1999). *Dev. Biol.* **215**, 407-419.

The *DESIGUAL* (*DEAL*) genes contribute to leaf bilateral symmetry

Wilson-Sánchez, D., Martínez-López, S., Jover-Gil, S., and Micol, J.L.

Instituto de Bioingeniería, Universidad Miguel Hernández, Campus de Elche, 03202 Elche, Alicante, Spain.

The body architectures of most multicellular organisms consistently display both symmetry and asymmetry, which raise fundamental biological questions on their underlying molecular mechanisms. Answers to these questions are lacking for plant leaves. We performed a large-scale search for leaf mutants among 21,000 Arabidopsis lines from the Salk homozygous T-DNA collection, and found only one exhibiting leaf bilateral symmetry breaking in a strict sense, with incomplete penetrance. We dubbed *desigual1-1* (*deal1-1*) this mutant, which also shows defects in flower and silique organogenesis. Bilateral symmetry is altered in all these organs of *deal1-1* in a random fashion, as a consequence of the presence of both outgrowths and invaginations, phenotypes that are more severe in adult rosette leaves. Asymmetry is apparent in *deal1-1* leaf primordia, where cell expansion has not yet started, suggesting impaired cell proliferation. There are three *DEAL* redundant paralogs in the Arabidopsis genome: the *deal1 deal2 deal3* triple mutant exhibits leaf bilateral symmetry breaking with complete penetrance. We are examining the action of the redundant DEAL genes and in particular their interactions with auxin-related genes, including *CUC2*.

26th International Conference on Arabidopsis Research

París, 2015

Póster

The *DESIGUAL* (*DEAL*) genes contribute to leaf bilateral symmetry

David Wilson-Sánchez, Sebastián Martínez-López, Sara Jover-Gil and José Luis Micol

Instituto de Bioingeniería, Universidad Miguel Hernández, Campus de Elche, 03202 Elche, Alicante, Spain
dwilson@umh.es jlmicol@umh.es http://genetics.umh.es

Symmetry is an important but poorly understood property of many biological systems[1]. In Arabidopsis, the leaf margin presents interspersed lobes and indentations; the positional information for such marginal configuration is provided by two feedback loops involving auxin, the PIN-FORMED1 (PIN1) auxin efflux carrier, and the CUP-SHAPED COTYLEDON2 (CUC2) transcriptional activator[2]. This system is deployed in both sides of the lamina, resulting in symmetric leaves.

We performed a large-scale screen for leaf mutants[3] among 15,000 Arabidopsis lines from the Salk homozygous T-DNA collection. More than 700 genuine leaf mutants were isolated, only one of which exhibited leaf bilateral symmetry breaking in a strict sense (Fig. 1A, B), with incomplete penetrance (Fig. 1C). We dubbed *desigual1-1* (*deal1-1*) this mutant, which also shows defects in flower and silique organogenesis.

Asymmetry is apparent in *deal1* leaf primordia before the onset of leaf expansion (Fig. 1D), suggesting impaired cell proliferation. We confirmed that cell proliferation is deregulated in *deal1* leaves using the cell division marker CYCB1;1:GUS: mutant leaves showed asymmetric cell division arrest and marginal spots of abnormally high expression (Fig. 1E). Two-dimensional monitoring of cell size and number (Fig. 1F) reconfirmed that lamina invaginations and outgrowths are due to altered proliferation and ruled out a role for cell expansion.

Treatment with NPA made asymmetry fully penetrant in the *deal1* mutants, suggesting a role for *DEAL1* in auxin function in leaves (Fig. 2A, B). PIN1:GFP was properly polarized in *deal1* leaf marginal cells, and DR5:GFP maxima were formed; both occurred at wrong margin positions (Fig. 2C, D), suggesting a role for the mutated gene in conferring positional information to cells. The wild-type CUC2:RFP leaf expression pattern was randomly lost in *deal1* primordium margins (Fig. 2E). *CUC2* loss of function suppresses asymmetry in *deal1* leaves (Fig. 3A-C), suggesting that *CUC2* and *DEAL1* are functionally related. *pin1 deal1* double mutant leaves exhibit an array of morphological aberrations including split petioles (Fig. 3D).

DEAL1 is expressed in leaf primordia (Fig. 4A). The DEAL1:CFP fusion protein localizes to the membrane of a sub-compartment of the endoplasmic reticulum (Fig. 4B). *DEAL1* belongs to a gene family: the *deal1 deal2 deal3* triple mutants show increased asymmetry penetrance (Fig. 4C, D), revealing functional redundancy. Our results uncover a new player on the leaf bilateral symmetry scene.

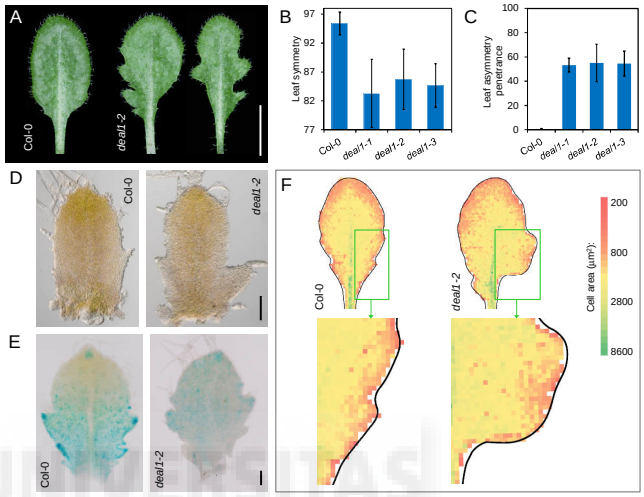

Figure 1.- Leaf phenotype in the *deal1* mutants. (A) Representative wild-type Col-0 and asymmetric *deal1-2* expanding leaves. (B, C) Leaf asymmetry phenotype in the *deal1* mutants: (B) expressivity (severity), calculated as the degree of leaf bilateral symmetry, and (C) penetrance. (D) Representative wild-type Col-0 and asymmetric *deal1-2* leaf primordia. (E) *CYCB1;1$_{pro}$:GUS* expression in Col-0 and *deal1-2* leaves. (F) Cell size heatmap in wild-type Col-0 and asymmetric *deal1-2* leaves. Each heatmap unit represents 0.0625 µm². Scale bars: (A) 5 mm, and (D, E) 100 µm. Pictures and measurements were taken from 10th-node leaves at (A) 21, (D) 12 and (E) 14 days after stratification (das), and (F) after full expansion (40 das).

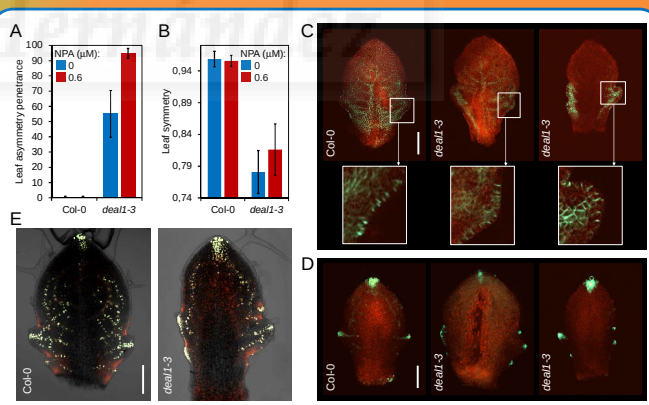

Figure 2.- Interplay between *CUC2* and auxin transport in *deal1* leaves. (A, B) Effects of the auxin polar transport inhibitor 1-N-Naphthylphthalamic acid (NPA) on the (A) penetrance and (B) severity of the leaf asymmetry phenotype of the *deal1-3* mutant. (C-E) Expression pattern in Col-0 and *deal1-3* leaf primordia of (C) PIN1:GFP, (D) DR5:GFP, and (E) DR5:VENUS (yellow) and CUC2:RFP (red). Magnification insets in C show PIN1:GFP polarization in the membranes of leaf margin cells. Scale bars: 100 µm. Pictures and measurements were taken from 10th-node leaves (A, B) after full expansion (40 das), and (C-E) at 12 to 14 das.

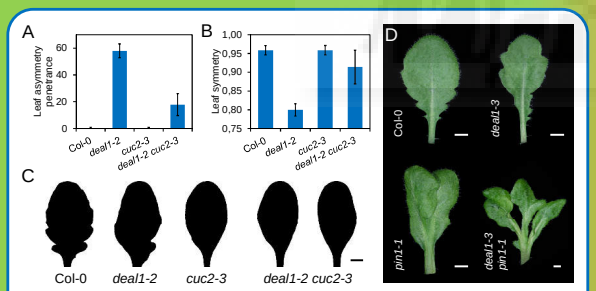

Figure 3.- Genetic interactions of *DEAL1* with *CUC2* and *PIN1*. (A-C) Leaf asymmetry in the *deal1-2* and *cuc2-3* single mutants and the *deal1-2 cuc2-3* double mutant: (A) penetrance and (B) severity, and (C) representative leaf silhouettes. (D) Leaf phenotypes of the *deal1-3* and *pin1-1* single mutants and the *deal1-3 pin1-1* double mutant. Scale bars: 2 mm. All pictures and measurements were taken from fully expanded 10th-node leaves (40 das).

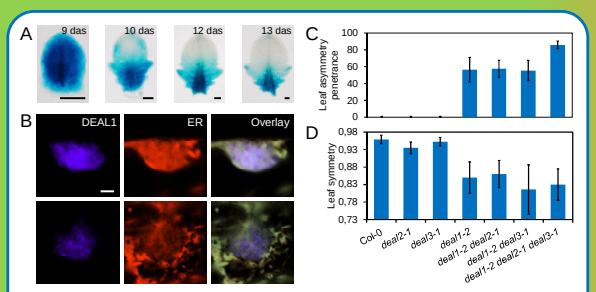

Figure 4.- Expression in leaf primordia, subcellular localization and redundancy of DEAL family members. (A) *DEAL1$_{pro}$-GUS* histochemical staining in leaf primordia. (B) Co-localization of DEAL1:CFP and the AtWAK2:YFP:HDEL[4] endoplasmic reticulum (ER) marker. (C, D) Leaf asymmetry in *deal* multiple mutant combinations: (C) penetrance and (D) severity. Scale bars: (A) 100 µm, and (B) 2 µm. Pictures and measurements were taken from 10th-node leaves (A) at 12 to 15 das, and (C, D) after full expansion (40 das).

ACKNOWLEDGEMENTS

This research was supported by grants to J.L.M. from the Ministerio de Economía y Competitividad of Spain (BIO2014-53063-P), the Generalitat Valenciana (PROMETEOII/2014/006), and the European Commission [LSHG-CT-2006-037704 (AGRON-OMICS)]. S.J.-G. held the PIRG06-GA-2009-256579 (ARABIGANS) reintegration grant from the European Commission. D.W.-S. is a predoctoral fellow of the Generalitat Valenciana VALI+d programme. The *DR5:VENUS* and *CUC2:RFP* transgenic lines were kindly provided by Prof. Patrick Laufs.

REFERENCES

1.- Muñoz-Nortes *et al.* (2014). *J. Exp. Bot.* **65,** 2645-2655.
2.- Bilsborough *et al.* (2011). *Proc. Natl. Acad. Sci. USA* **108,** 3424-3429.
3.- Wilson-Sánchez *et al.* (2014). *Plant J.* **79,** 878-891.
4.- Nelson *et al.* (2007). *Plant J.* **51,** 1126-1136.

Arabidopsis *DESIGUAL* (*DEAL*) genes are required for leaf bilateral symmetry

Wilson-Sánchez, D., Martínez-López, S., Gual-Barroso, F., Jover-Gil, S., and Micol, J.L.

Instituto de Bioingeniería, Universidad Miguel Hernández, 03202 Elche, Alicante, Spain.

Symmetry is an important but poorly understood property of many biological systems. We performed a large-scale search for leaf mutants among 15,000 Arabidopsis lines from the Salk homozygous T-DNA collection, and found only one exhibiting leaf bilateral symmetry breaking with incomplete penetrance. We dubbed *desigual1-1* (*deal1-1*) this mutant, which also shows defects in flower and silique organogenesis. Bilateral symmetry is altered in all these organs of *deal1-1* in a random fashion, as a consequence of the presence of both outgrowths and invaginations, phenotypes that are more severe in adult rosette leaves. Asymmetry is apparent in leaf primordia, where cell expansion has not yet started, suggesting impaired cell proliferation. There are three *DEAL* redundant paralogs in the Arabidopsis genome: the *deal1 deal2 deal3* triple mutants exhibit leaf bilateral symmetry breaking with complete penetrance. We are examining the action of the *DEAL* genes and in particular their interactions with auxin-related genes.

XIV Congreso Hispano-Luso de Fisiología Vegetal / XXI Reunión de la Sociedad Española de Fisiología Vegetal

Toledo, 2015

Póster

Arabidopsis *DESIGUAL* (*DEAL*) genes are required for leaf bilateral symmetry

David Wilson-Sánchez, Sebastián Martínez-López, Fernando Gual-Barroso, Sara Jover-Gil and José Luis Micol

Instituto de Bioingeniería, Universidad Miguel Hernández, Campus de Elche, 03202 Elche, Alicante.
dwilson@umh.es jlmicol@umh.es http://genetics.umh.es

Symmetry is an important but poorly understood property of many biological systems[1]. In Arabidopsis, the leaf margin presents interspersed lobes and indentations; the positional information for such marginal configuration is provided by two feedback loops involving auxin, the PIN-FORMED1 (PIN1) auxin efflux carrier, and the CUP-SHAPED COTYLEDON2 (CUC2) transcriptional activator[2]. This system is deployed in both sides of the lamina, resulting in symmetric leaves.

We performed a large-scale screen for leaf mutants[3] among 15,000 Arabidopsis lines from the Salk homozygous T-DNA collection. More than 700 genuine leaf mutants were isolated, only one of which exhibited leaf bilateral symmetry breaking in a strict sense (Fig. 1A, B), with incomplete penetrance (Fig. 1C). We dubbed *desigual1-1* (*deal1-1*) this mutant, which also shows defects in flower and silique organogenesis.

Asymmetry is apparent in *deal1* leaf primordia before the onset of leaf expansion (Fig. 1D), suggesting impaired cell proliferation. We confirmed that cell proliferation is deregulated in *deal1* leaves using the cell division marker CYCB1;1:GUS: mutant leaves showed asymmetric cell division arrest and marginal spots of abnormally high expression (Fig. 1E). Two-dimensional monitoring of cell size and number (Fig. 1F) reconfirmed that lamina invaginations and outgrowths are due to altered proliferation and ruled out a role for cell expansion.

Treatment with NPA made asymmetry fully penetrant in the *deal1* mutants, suggesting a role for *DEAL1* in auxin function in leaves (Fig. 2A, B). PIN1:GFP was properly polarized in *deal1* leaf marginal cells, and DR5:GFP maxima were formed; both occurred at wrong margin positions (Fig. 2C, D), suggesting a role for the mutated gene in conferring positional information to cells. The wild-type CUC2:RFP leaf expression pattern was randomly lost in *deal1* primordium margins (Fig. 2E). *CUC2* loss of function suppresses asymmetry in *deal1* leaves (Fig. 3A-C), suggesting that *CUC2* and *DEAL1* are functionally related. *pin1 deal1* double mutant leaves exhibit an array of morphological aberrations including split petioles (Fig. 3D).

DEAL1 is expressed in leaf primordia (Fig. 4A). The DEAL1:CFP fusion protein localizes to the membrane of a sub-compartment of the endoplasmic reticulum (Fig. 4B). *DEAL1* belongs to a gene family: the *deal1 deal2 deal3* triple mutants show increased asymmetry penetrance (Fig. 4C, D), revealing functional redundancy. Our results uncover a new player on the leaf bilateral symmetry scene.

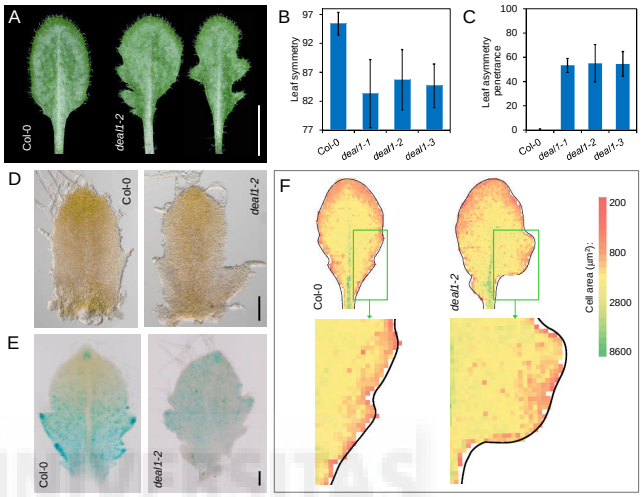

Figure 1.- Leaf phenotype in the *deal1* mutants. (A) Representative wild-type Col-0 and asymmetric *deal1-2* expanding leaves. (B, C) Leaf asymmetry phenotype in the *deal1* mutants: (B) expressivity (severity), calculated as the degree of leaf bilateral symmetry, and (C) penetrance. (D) Representative wild-type Col-0 and asymmetric *deal1-2* leaf primordia. (E) *CYCB1;1$_{pro}$:GUS* expression in Col-0 and *deal1-2* leaves. (F) Cell size heatmap in wild-type Col-0 and asymmetric *deal1-2* leaves. Each heatmap unit represents 0.0625 µm^2. Scale bars: (A) 5 mm, and (D, E) 100 µm. Pictures and measurements were taken from 10th-node leaves at (A) 21, (D) 12 and (E) 14 days after stratification (das), and (F) after full expansion (40 das).

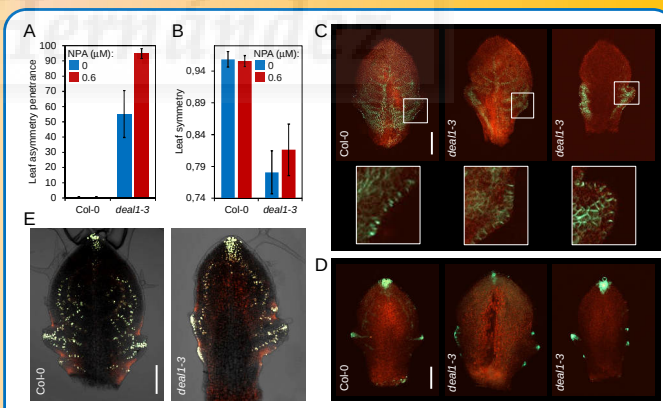

Figure 2.- Interplay between *CUC2* and auxin transport in *deal1* leaves. (A, B) Effects of the auxin polar transport inhibitor 1-N-Naphthylphthalamic acid (NPA) on the (A) penetrance and (B) severity of the leaf asymmetry phenotype of the *deal1-3* mutant. (C-E) Expression pattern in Col-0 and *deal1-3* leaf primordia of (C) PIN1:GFP, (D) DR5:GFP, and (E) DR5:VENUS (yellow) and CUC2:RFP (red). Magnification insets in C show PIN1:GFP polarization in the membranes of leaf margin cells. Scale bars: 100 µm. Pictures and measurements were taken from 10th-node leaves (A, B) after full expansion (40 das), and (C-E) at 12 to 14 das.

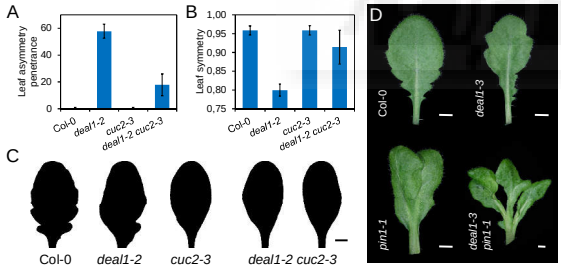

Figure 3.- Genetic interactions of *DEAL1* with *CUC2* and *PIN1*. (A-C) Leaf asymmetry in the *deal1-2* and *cuc2-3* single mutants and the *deal1-2 cuc2-3* double mutant: (A) penetrance and (B) severity, and (C) representative leaf silhouettes. (D) Leaf phenotypes of the *deal1-3* and *pin1-1* single mutants and the *deal1-3 pin1-1* double mutant. Scale bars: 2 mm. All pictures and measurements were taken from fully expanded 10th-node leaves (40 das).

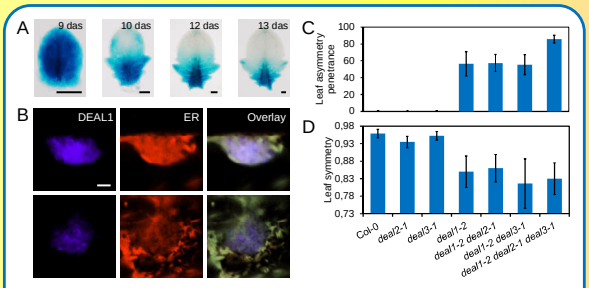

Figure 4.- Expression in leaf primordia, subcellular localization and redundancy of DEAL family members. (A) *DEAL1$_{pro}$:GUS* histochemical staining in leaf primordia. (B) Co-localization of DEAL1:CFP and the AtWAK2:YFP:HDEL[4] endoplasmic reticulum (ER) marker. (C, D) Leaf asymmetry in *deal* multiple mutant combinations: (C) penetrance and (D) severity. Scale bars: (A) 100 µm, and (B) 2 µm. Pictures and measurements were taken from 10th-node leaves (A) at 12 to 15 das, and (C, D) after full expansion (40 das).

ACKNOWLEDGEMENTS

This research was supported by grants to J.L.M. from the Ministerio de Economía y Competitividad of Spain [BFU2011-22825 and BIO2014-53063-P], the Generalitat Valenciana (PROMETEO/2009/112 and PROMETEOII/2014/006), and the European Commission [LSHG-CT-2006-037704 (AGRON-OMICS)]. S.J.-G. held the PIRG06-GA-2009-256579 (ARABIGANS) reintegration grant from the European Commission. D.W.-S. is a predoctoral fellow of the Generalitat Valenciana VALI+d programme. The *DR5:VENUS* and *CUC2:RFP* transgenic lines were kindly provided by Prof. Patrick Laufs.

REFERENCES

1.- Muñoz-Nortes *et al.* (2014). *J. Exp. Bot.* **65,** 2645-2655.
2.- Bilsborough *et al.* (2011). *Proc. Natl. Acad. Sci. USA* **108,** 3424-3429.
3.- Wilson-Sánchez *et al.* (2014). *Plant J.* **79,** 878-891.
4.- Nelson *et al.* (2007). *Plant J.* **51,** 1126-1136.

Mapping-by-sequencing in model systems and beyond

Wilson-Sánchez, D., Ponce, M.R., and Micol, J.L.

Instituto de Bioingeniería, Universidad Miguel Hernández, 03202 Elche, Spain.

Forward genetic screens in model systems have identified many genes and continue to be powerful tools for the dissection of gene action and interactions. Moreover, next-generation sequencing (NGS) has revitalized the classical, time-consuming genetic approach to the identification of the mutations causing a phenotype of interest. Mapping-by-sequencing combines NGS with classical mapping strategies and allows the rapid identification of point mutations. As in conventional linkage analyses, mapping-by-sequencing requires a phenotyped mapping population, but only a single round of crosses is required to define a very narrow candidate region and the causal mutation itself. In addition, the mapping populations are pooled for NGS; mapping-by-sequencing does not require individual genotypes. The single-nucleotide polymorphisms caused by the mutagenesis can be used as markers, enabling the use of a single backcross to obtain a mapping population and making polymorphic strains dispensable. Mapping-by-sequencing also does not require previous knowledge of the wild-type sequence, making this approach useful for non-model species. Mapping-by-sequencing has been used successfully for the rapid identification of chemically induced mutations in Arabidopsis and other plants, as well as in other model species such as *S. cerevisiae*, *D. melanogaster*, and *C. elegans*. Several simulations and case studies will be discussed.

Plant Genes and *Omics*: Technology Development
Viena, 2016
Conferencia pronunciada por J.L. Micol, por invitación.

***DESIGUAL1* is required for leaf bilateral symmetry in Arabidopsis**

Wilson-Sánchez, D., Navarro-Cartagena, S., Muñoz-Díaz, E., Martínez-López, S., Jover-Gil, S., and Micol, J.L.

Instituto de Bioingeniería, Universidad Miguel Hernández, Campus de Elche, 03202 Elche, Spain.

In bilateral organs such as plant leaves, acquisition of symmetry requires properly regulated development at both sides of the midplane. However, how this occurs remains unclear at the molecular level. To examine the regulation of symmetry in leaf development, we screened 19,850 *Arabidopsis thaliana* lines from the Salk homozygous T-DNA collection, and found 706 leaf mutants (Wilson-Sánchez et al., 2014). Only one of these mutants exhibited defects in bilateral symmetry; we named this mutant *desigual1-1* (*deal1-1*). The *deal1* mutants also show defects in flower and silique organogenesis. In the leaves of *deal1* mutants, improper regulation of cell proliferation (simultaneous over- and under-proliferation) along the organ margins alters bilateral symmetry during the primordium stage. Auxin maxima are mislocalized at the margins of expanding *deal1* leaves (Figure 1) and this asymmetry can be enhanced by treatment with the polar auxin transport inhibitor 1-N-naphthylphthalamic acid or alleviated by treatment with the synthetic auxin 1-naphthaleneacetic acid.

DEAL1 genetically interacts with *PIN1* and *CUC2*, which encode the PIN-FORMED1 auxin efflux carrier and the CUP-SHAPED COTYLEDON2 transcriptional regulator, respectively. PIN1, CUC2, and auxin interact in self-organized feedback loops that create mutually exclusive, interspersed auxin and CUC2 spatial domains along the leaf margin (Bilsborough et al., 2011; Kasprzewska et al., 2015). We identified the *DEAL1* gene, which is expressed during early leaf development and encodes a protein that resides at the membrane of a sub-compartment of the endoplasmic reticulum. A split-ubiquitin membrane-based yeast two-hybrid screen for DEAL1 interactors identified, among other proteins, several components of the Very-Long-Chain Fatty Acid (VLCFA) elongation complex; VLCFA lipids are known to negatively regulate leaf cell proliferation through cytokinins. To examine DEAL1 function further, we are using yeast one-hybrid screens and other approaches to identify components of the auxin- and cytokinin-mediated leaf developmental networks that provide positional information to leaf cells.

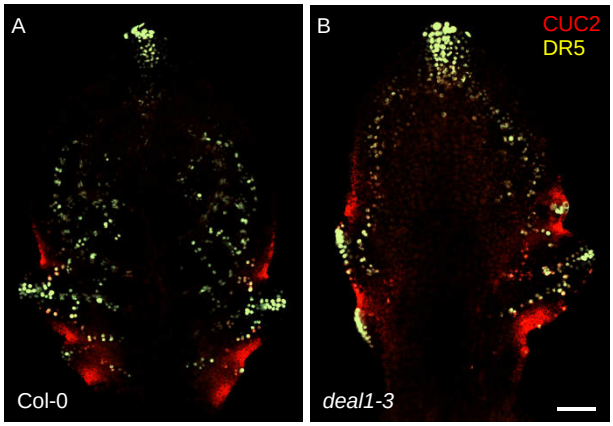

Figure 1. The patterns of auxin maxima and *CUC2* expression show defects in bilateral symmetry in expanding *deal1* leaves. Visualization of $CUC2_{pro}$:CUC2: RFP (red) and $DR5_{pro}$:VENUS (yellow) markers in (A) Col-0 and (B) *deal1-3* developing leaves. Confocal micrographs were taken from tenth-node leaves collected 14 days after stratification. Scale bar: 50 µm.

This research was supported by grants from the Ministerio de Economía y Competitividad of Spain (BFU2011-22825 and BIO2014-53063-P) and the Generalitat Valenciana (PROMETEOII/2014/006) to José Luis Micol. David Wilson-Sánchez held a predoctoral fellowship from the Generalitat Valenciana (ACIF/2012/137).

Bilsborough GD, Runions A, Barkoulas M, Jenkins HW, Hasson A, Galinha C, Laufs P, Hay A, Prusinkiewicz P, Tsiantis M (2011) Model for the regulation of *Arabidopsis thaliana* leaf margin development. Proc Natl Acad Sci USA **108:** 3424-3429.

Kasprzewska A, Carter R, Swarup R, Bennett M, Monk N, Hobbs JK, Fleming A (2015) Auxin influx importers modulate serration along the leaf margin. Plant J **83**: 705-718.

Wilson-Sánchez D, Rubio-Díaz S, Muñoz-Viana R, Pérez-Pérez JM, Jover-Gil S, Ponce MR, Micol JL (2014) Leaf phenomics: a systematic reverse genetic screen for Arabidopsis leaf mutants. Plant J **79:** 878-891.

Mapping-by-sequencing to identify mutations: simulations, case studies, and outlooks

Wilson-Sánchez, D., Sarmiento-Mañús, R., Muñoz-Díaz, E., Ponce, M.R., and Micol, J.L.

Instituto de Bioingeniería, Universidad Miguel Hernández, Campus de Elche, 03202 Elche, Spain.

Forward genetic screens have identified many genes and continue to be powerful tools for the dissection of gene action and interactions in Arabidopsis and other plant species. Moreover, next-generation sequencing (NGS) has revitalized the time-consuming genetic approaches to identify the mutation causing a phenotype of interest. Mapping-by-sequencing combines NGS with classical mapping strategies and allows rapid identification of point mutations (Schneeberger et al., 2009). As in conventional linkage analyses, mapping-by-sequencing requires a phenotyped mapping population, but requires only a single round of crosses to define a very narrow candidate region and the position of the causal mutation itself. In addition, the mapping populations are pooled for NGS; mapping-by-sequencing does not require individual genotypes. The single-nucleotide polymorphisms (SNPs) caused by the chemical mutagenesis can be used as markers, enabling the use of a single backcross to obtain a mapping population and thus making polymorphic strains dispensable. Mapping-by-sequencing also does not require previous knowledge of the wild-type sequence, making this approach useful for non-model species.

We performed several simulations to facilitate the design of mapping-by-sequencing experiments for the identification of chemically induced point mutations. Through these simulations, we evaluated first which short-read NGS technology is best suited to Arabidopsis gene-rich genomic regions, and the minimum sequencing depth required to confidently call variants. Next, we simulated mapping-by-sequencing experiments for the identification of point mutations and determined how mapping population size and sequencing depth affect mapping resolution. We also performed virtual outcrosses and backcrosses in order to compare natural variations versus chemically induced SNPs as mapping-by-sequencing tools. We also evaluated the viability of crossing two chemically induced non-allelic mutants to obtain a mapping population to simultaneously map two recessive mutations. In addition, we compared different ways of identifying dominant mutations. Finally, using simulations, we tested a custom protocol to map T-DNA or transposon insertions with paired-end Illumina-like reads; we assessed its

reliability using low sequencing depths and pooling several mutants together. The results of these simulations proved useful for the design of real experiments (Figure 1).

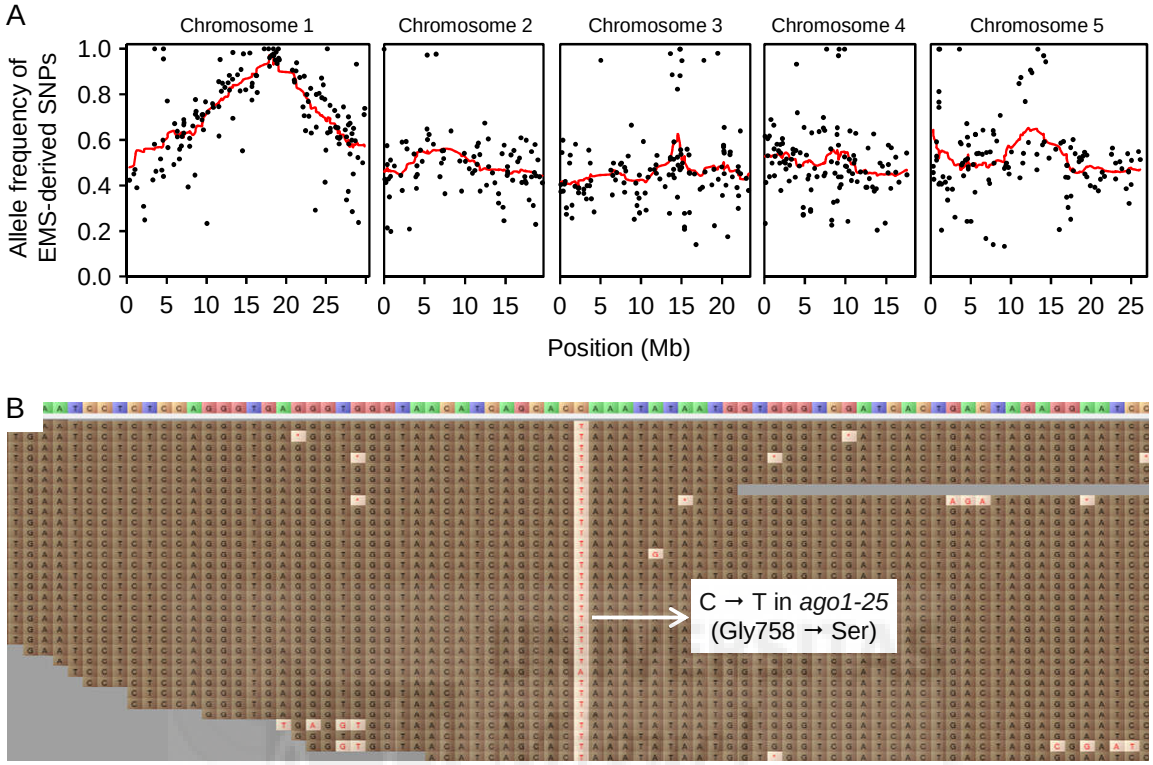

Figure 1. Mapping-by-sequencing of the *argonaute1-25* (*ago1-25*; Morel et al., 2002) mutation, whose position was already known. (A) Allele frequency of ethyl methanesulfonate-derived SNPs (black dots; the resulting mapping signal is shown as a red line) across the Arabidopsis genome. The DNA sample subjected to NGS was obtained from a pool of 100 phenotypically mutant F_2 plants derived from a single *ago1-25* × Col-0 backcross. (B) NGS reads aligned at the *AGO1* locus show a SNP at position 17,887,923 of chromosome 1 and the predicted amino acid change in the AGO1 protein. Whole-genome sequencing was performed with a Life Technologies Ion Proton and returned single-end reads with an average length of 180 nt. A reference-guided assembly of the clean reads and a SNP report were obtained with BWA-MEM (Li and Durbin, 2010) and GATK Unified Genotyper (DePristo et al., 2014), respectively.

This research was supported by grants from the Ministerio de Economía y Competitividad of Spain (BIO2014-53063-P to José Luis Micol and BIO2014-56889-R to María Rosa Ponce) and the Generalitat Valenciana (PROMETEOII/2014/006 to José Luis Micol and María Rosa Ponce). David Wilson-Sánchez held a predoctoral fellowship from the VALi+d program of the Generalitat Valenciana (ACIF/2012/137).

DePristo MA, Banks E, Poplin R, Garimella KV, Maguire JR, Hartl C, Philippakis AA, del Angel G, Rivas MA, Hanna M, McKenna A, Fennell TJ, Kernytsky AM, Sivachenko AY, Cibulskis K, Gabriel SB, Altshuler D, Daly MJ (2014) A framework for variation discovery and genotyping using next-generation DNA sequencing data. Nat Genet **43:** 491-498.

Li H, Durbin R (2010) Fast and accurate long-read alignment with Burrows-Wheeler transform. Bioinformatics **26:** 589-595.

Morel JB, Godon C, Mourrain P, Béclin C, Boutet S, Feuerbach F, Proux F, Vaucheret H (2002) Fertile hypomorphic *ARGONAUTE* (*ago1*) mutants impaired in post-transcriptional gene silencing and virus resistance. Plant Cell **14:** 629-639.

Schneeberger K, Ossowski S, Lanz C, Juul T, Petersen AH, Nielsen KL, Jørgensen JE, Weigel D, Andersen SU (2009) SHOREmap: simultaneous mapping and mutation identification by deep sequencing. Nat Methods **6:** 550-551.

VII.- AGRADECIMIENTOS

VII.- AGRADECIMIENTOS

La realización de esta Tesis ha sido posible gracias a la financiación de la investigación que se realiza en el laboratorio de José Luis Micol por la Comisión Europea (AGRON-OMICS, LSHG-CT-2006-037704), la Generalitat Valenciana (PROMETEOII/ 2014/006) y el Ministerio de Economía y Competitividad (BFU2011-22825 y BIO2014-53063-P). Durante parte de mi periodo predoctoral he sido beneficiario de un contrato del programa VALi+d (ACIF/2012/137) de la Generalitat Valenciana.

A mi director, José Luis Micol, por haberme permitido iniciar mi carrera investigadora en su laboratorio, y por dirigir mi Tesis con atención y apoyo.

A mi codirectora, Sara Jover, por todos los conocimientos que ha compartido conmigo y por ser tan agradable durante todos estos años.

A María Rosa Ponce, por prestarme su ayuda a lo largo de estos años y por proponer el nombre del gen *DESIGUAL1*.

A José Manuel Serrano, por ser el técnico de laboratorio perfecto.

A todos los profesores del área de Genética, por su cercanía y por aclararme tantas dudas sobre la Genética como ciencia y como profesión.

A todos los que pusieron sus manos para el proyecto AGRON-OMICS (Rafa, Silvia, Sara, Leila, José María y Diana), por ayudar a sacar adelante la ingente cantidad de trabajo.

A Sebastián Martínez, por implicarse tanto en esta Tesis como si fuera la suya.

A todos mis compañeros en el laboratorio durante estos años (José Manuel, Sara, Rafa, Silvia, Tania, Arantxa, Paqui, Raquel, Almudena Ferrández, Almudena Mollá, David, Leila, Bea, Rubén, Tamara, Ana Belén, Rosa, Edu, Rebeca, Zeynep, Diana, Amani, María José, Sergio y Juan), por hacer que siempre recuerde estos años como un tiempo increíble.

A mis padres, al resto de mi familia, a Esther y a Martín por ofrecerme el ambiente de amor, estabilidad y apoyo que me ha permitido ofrecer lo mejor de mí mismo para esta Tesis.

A Amando, Juanjo y Gabi por prestarse a discutir las cuestiones que les he planteado durante estos años acerca de muchos aspectos del trabajo de esta Tesis.

A toda la comunidad de programadores de PHP y MySQL en Internet, por enseñarme todo lo que he necesitado saber hacer con estos lenguajes, y por mostrarme el camino hacia otra forma de pensar más estructurada.

A todos lo que se han interesado por el desarrollo de esta Tesis.